THE LAGRANGE MULTIPLIER CONSTRAINT TECHNIQUE

IN THE FINITE ELEMENT ANALYSIS

OF COUPLED SHEAR WALLS AND FRAMES

Thesis submitted in accordance with the requirements of the University of Liverpool for the degree of Doctor in Philosophy

by

Christopher Brian LITTLER

September, 1985

ACKNOWLEDGEMENTS

The author is indebted to Mr C. Thomas M.Sc. for his invaluable assistance and encouragement. His guidance throughout this investigation is gratefully acknowledged.

The author also wishes to express his thanks to the other members of staff of the Civil Engineering Department and of the University, who have helped in many different ways.

SUMMARY

In this thesis the finite element method, as applied to the analysis of coupled shear walls and shear wall frame structures, is investigated.

Various finite element models, which have been employed for the static modelling of coupled shear walls, are compared by means of convergence tests. Lagrange multiplier schemes, which permit the combined use of the quadrilateral isoparametric element for the walls and the flexural line element for beams, are shown to be advantageous. These schemes connect the two types of element by means of constraint equations. A set of constraints are proposed and shown to be particularly advantageous in comparison with others previously used.

The efficacy of the proposed Lagrange multiplier scheme is verified by means of small-scale static model tests. These include coupled shear walls and shear walls fixed and pinned to a frame. The proposed scheme is shown to be capable of providing accurate deflection and coupling moment predictions.

The Lagrange multiplier method is developed to allow dynamic analysis. This includes both free vibration and forced response. The free vibration problem is solved by the bisection technique of eigenvalue extraction, the forced response problem by step-by-step numerical integration of the equations of motion using the Newmark beta method.

The results from the dynamic analysis procedure are compared with those from model tests conducted on a shaking table. These employ the same models as used previously for the static experiments. The proposed scheme is shown to give accurate

predictions for the mode shapes and natural frequencies.

The Lagrange multiplier method is developed to allow non-linear dynamic analysis. The non-linear behaviour is restricted to the constrainted joints between walls and beams. The method is therefore particularly suited to the analysis of structures subjected to earthquakes, where the walls are required to remian elastic to prevent structural instability and the beams are required to be ductile to dissipate the earthquake energy. It is shown to be particularly advantageous as it requires little additional computation above that required by the linear forced response analysis.

The predictions of the non-linear analysis technique are compared with results from shaking table tests of coupled walls pin jointed to a frame. Friction in these joints provides damping which is shown to be poorly represented by the usual assumption of equivalent viscous damping. The non-linear Lagrange multiplier technique is shown to be capable of giving accurate results when used to model these joints.

CONTENTS

NOTATION

A	=	Cross-section area
a	=	Overall response amplitude
[B]	=	Strain matrix
b	=	Base excitation amplitude
[C]	=	Damping matrix
[Co]	=	Nodal co-ordinate matrix
c	=	Relative response amplitude
D	=	Wall width
[D]	=	Elasticity matrix
d_b	=	Beam depth
E	=	Elastic modulus (Young's modulus)
EXM	=	Excess moment
f	=	Displacements at point
G	=	Constraint coefficients (Chapters 3, 4, 5)
	=	Shear modulus (Chapter 7)
g	=	Shear factor
I	=	2nd moment of area
[J]	=	Jacobian matrix
det[J]	=	Determinant of [J]
[K]	=	Stiffness matrix
k	=	Joint rotational stiffness
L	=	Distributed load (Chapters 2, 6)
	=	Length (Chapters 7, 8)
M	=	Moment (Chapters 6, 7)
[M]	=	Mass matrix (Chapters 4, 8)
MA	=	Yield moment
MF	=	Final moment

MI = Moment at end of time interval

MX = Excess moment

N = Shape function

P = Load

Ps = Percentage stiffness after yield

q = Nodal displacements

[R] = Co-ordinate function

{RHS} = Excess moment vector for yielding joints

{r} = Mode shape

S = Constrained displacement or acceleration (Chapters 3, 4, 5)

= Shear force (Chapter 6)

[SOL] = Moment reduction matrix for yielding joints

[STS] = Moment reduction matrix

t = Thickness (Chapters 2, 6)

= Time (Chapters, 4, 8)

U = Strain energy

u = x-direction displacements

v = y-direction displacements

W = Potential energy

Wi,Wj = Weighting factors

x = Global co-ordinate direction

y = Global co-ordinate direction

Z = Magnification factor

α = Polynomial constants (Chapter 2)

= Integration parameter (Chapter 4)

β = Integration parameter (Chapters 4, 5)

= Form factor (Chapter 7)

γ = Shear strain (Chapter 2)

= Modal amplitude (Chapter 8)

Δt = Time step

Δ_o = Centre line tip deflection

ε = Direct strain

η = Isoparametric element co-ordinate

θ = Rotation

λ = Lagrange multiplier

μ = Damping ratio

ν = Poisson's ratio

ξ = Isoparametric element co-ordinate

ρ = Density

σ = Direct stress

τ = Shear stress

ϕ = Total potential energy (Chapters 2, 3)

= Phase angle (Chapter 8)

ψ = Eigenvalue

ω_F = Forcing frequency

ω_i = Natural frequency in the ith mode

CHAPTER ONE - INTRODUCTION

1.1 GENERAL

Shear walls are a common feature among high-rise buildings. They are employed as an efficient means of providing stiffness and strength to resist lateral loadings and may often be used in conjunction with moment resisting frames. They may take many different forms. Usually they extend over the whole height of the building and are laid out as a series of walls connected by beams or slabs, or as a central core containing lifts and stairways. Whatever layout is used the walls will normally contain openings for services such as doors and windows.

Winds and earthquakes which cause the lateral loading of such structures are both dynamic in nature. Wind loads are regularly encountered and buildings are designed to respond elastically to them, with equivalent static loads normally being employed for design. However, to design a building to respond elastically to a large earthquake would be prohibitively expensive. The objective therefore, is to design a structure to respond elastically to a small earthquake, and to survive a large earthquake without collapse and loss of lives.

To this end it is necessary to be able to analyse the behaviour of both coupled shear walls and shear walls in combination with frames. The analysis must be able to deal with dynamic loadings and be able to take account of non-linear behaviour during large earthquakes.

1.2 REVIEW

Three categories of methods for the analysis of coupled shear walls have been prominent. They are the continuous laminae method, the equivalent frame method and the plane stress finite element method.

Of these, the laminae method introduced by Beck [1] and Rosman [2] requires the least calculation and may be used as a "hand" method. In this the coupling beams are replaced with a continuous lamina of equivalent properties which allows the problem to be formulated as a differential equation.

For static analysis Coull and Choudhury [3, 4] and Coull and Irwin [5] used this method to present graphical charts as a convenient method for evaluating deflections and stresses for a variety of geometries and load types. Tso and Biswas [6] calculated equivalent static loads and used the method for approximate seismic analysis. Coull and Pari [7] extended the method to look at the effect of shearing deformations of the walls and flexibility of the wall-beam connections.

Tso and Chan [8] and Coull and Mukherjee [9, 10] used the method for the analysis of the natural vibration frequencies of coupled walls. Rosman [11] analysed the natural frequencies of buildings of which shear walls were a major component.

The technique has also been employed for inelastic response by Winokur and Gluck [12] who assumed plastic hinges at the wall-beam joint and by Paulay [13] who used it to assess ductility requirements.

The principal disadvantage with this method is its inability to deal with discontinuities and irregularities in either the

structure or its loading. Non-linear behaviour in particular is difficult to model in detail.

The problem with irregularities may be overcome by the equivalent frame technique which is a computer method wherby the wall is replaced by equivalent wide column members. These, in combination with beam members may then be analysed by a "plane-frame" program. This method has been used by Schwaighofer and Microys [14] and MacLeod [15, 16] for the analysis of coupled shear walls. Smith and Girgis [17] have developed this method by using diagonal bracing members to improve the accuracy.

With the development of the finite element method from frame analysis methods, plane stress elements were used to analyse coupled shear walls. Girijavallabhan [18] used triangular and rectangular elements. Wee [19] used a rectangular element with bending characteristics improved by Wilson et.al. [20]. In these studies the same type of elements were used to model the connecting beams and the walls.

To allow the use of beam elements for the coupling beams, MacLeod [21] and Agrawal and Mufti [22] used plane stress elements with rotational degrees of freedom for the walls. This permitted the direct connection of the two types of element.

Al-Mahaidi and Nilson [23] proposed "imaginary" elements using the Lagrange multiplier technique to impose constraints. This linked plane stress elements for the walls to frame elements for the coupling beams. Antony and Geanesan [24] proposed alternative constraints using the same method. Both these studies covered elastic, static analysis only.

For the analysis of walls and frames together, the continous laminae method has been used. Basu and Dar [25] replaced the frame by an equivalent uniform shear beam for a simple regular structure. However, more widely employed is the equivalent frame technique as this readily permits the modelling of the combination. With the wall replaced by an equivalent frame, the addition of a frame becomes straightforward. Emori and Schnobrich [26, 27] and Fintel and Ghosh [28-30] have conducted inelastic dynamic analysis for the evaluation of ductility demands in this manner.

The finite element method has the advantage that it makes possible the modelling of complex non-linear behaviour, albeit with a large increase in the complexity of the solution. Many models for the inelastic behaviour of concrete have been developed.

For beams they range from a single component model employed by Giberson [31] which has inelastic rotational hinges at member ends, to mulit-component [32] and layering [33] models. A very popular moment - rotation hysteretic model is that of Takeda et.al. [34].

For dynamic problems Agrawal et.al. [35] have developed a non-linear plane stress element which models cracking and crushing of the concrete in walls and yielding of the reinforcing steel.

1.3 OBJECTIVE AND SCOPE

The Lagrange multiplier technique proposed by Al-Mahaidi and Nilson had only been developed for the static analysis of coupled shear walls but could equally well be applied to walls coupled to frames. In this thesis the first objective is to compare different sets of constraint equations and other finite element

schemes when used for static analysis. This allowed the selection of the most appropriate. In chapter 6 the different finite element schemes are compared and a Lagrange multiplier scheme shown to give good results. In chapter 7 this scheme is compared with static laboratory experiments using both coupled walls and coupled walls in combination with a frame.

However, for this scheme to be of significant use in analysing the resistence of structures to seismic loadings, it would also be necessary to be able to apply it to dynamic analysis.

The theory for this is developed in chapter 4. This chapter shows how it may be employed for the analysis of free vibration using an eigenvalue technique and develops the theory for a forced response analysis. Chapter 5 extends this to include non-linear behaviour.

Inelastic behaviour can be treated in the same manner as previous investigations by reforming the stiffness matrix for yielding elements. However, chapter 5 makes use of the Lagrange constraints to produce a much more economical method. This is restricted in that yielding may only take place at the wall-beam joints.

In view of the desirability of absorbing energy by hysteretic damping due to inelastic behaviour, a favoured design philosophy is the use of strong walls and weak beams. The beams are designed to be ductile to absorb the earthquake energy whilst the walls deform elastically and prevent structural instability. Hence, a method which permits modelling of a yielding beam with an elastic wall is ideally suited to this analysis.

In chapter 8 the Lagrange multiplier scheme is compared with the results from dynamic laboratory tests on coupled walls and coupled walls with a frame. These include free vibration, forced response and non-linear behaviour of the wall frame joints.

CHAPTER TWO - FINITE ELEMENT ANALYSIS

2.1 INTRODUCTION

The finite element method can be used to model analytically a continuous problem by subdividing it into a number of portions or elements. The behaviour of each element is described in terms of a finite number of nodal degrees of freedom which are interconnected to those of other elements. In this way a continuous problem with infinite degrees of freedom can be approximated by a system with a finite number of degrees of freedom. This is then suitable for solution by a digital computer.

In a structural context, the force-displacement (stiffness) relationships are calculated for the nodes of each element. The displacement degrees of freedom at the nodes of the elements are connected together at discrete joints. Equilibrium equations involving element and external forces are then used to solve for the unknown displacements.

The behaviour of the elements can be derived by assuming functions to describe either the displacement or the stress pattern within the elements. Of these, displacement functions have been more widely employed. They are used with the principle of minimum potential energy to calculate the element stiffness properties. The methods involved have been documented in many publications [36-39].

2.2 GENERAL PROCEDURE

Displacement function:

The displacement function represents the displacements within the element. It approximates the actual displacement field over the element.

The displacement function can be expressed in terms of the shape functions of the nodal parameters by

$$f = N_1(x,y)q_1 + N_2(x,y)q_2 + \ldots\ldots \qquad 2.1$$

in which f is the displacement at any point (x,y) in the element, q_i are the displacements at node i and Ni(x,y) the corresponding shape functions.

Strains:

The strains $\{\varepsilon\}$ at any point within the element can be obtained by differentiation of the displacement function with respect to the co-ordinate variables x and y.

$$\{\varepsilon\} = [B]\{q\} \qquad 2.2$$

[B] is termed the strain matrix.

For a plane stress element

$$\{\varepsilon\} = \begin{bmatrix} \varepsilon x \\ \varepsilon y \\ \gamma xy \end{bmatrix} = \begin{bmatrix} \partial u/\partial x \\ \partial v/\partial y \\ \partial u/\partial y + \partial v/\partial x \end{bmatrix} \qquad 2.3$$

where u and v are the displacements in the x and y directions. In this case

$$f = \begin{bmatrix} u \\ v \end{bmatrix} \qquad 2.4$$

Stresses:

The stresses $\{\sigma\}$ are related to the strains by

$$\{\dot{\sigma}\} = [D]\{\varepsilon\} = [D][B]\{q\} \qquad 2.5$$

The matrix [D] is referred to as the elasticity matrix.

Plane stress:

A wall acted on by in-plane forces can be considered to be free from normal components of stress. The stress at any point may then be described in terms of three components, σx, σy and τxy. This is known as a state of plane stress.

For a plane stress element with isotropic properties

$$[D] = \frac{E}{1-\nu^2} \begin{bmatrix} 1 & \nu & 0 \\ \nu & 1 & 0 \\ 0 & 0 & \frac{1-\nu}{2} \end{bmatrix} \qquad 2.6$$

where ν is Poissons ratio.

Minimization of total potential energy:

The strain of energy of a linear elastic body is given by

$$U = \frac{1}{2} \int \{\varepsilon\}^T \{\sigma\} \quad d(vol) \qquad 2.7$$

Substituting for $\{\varepsilon\}$ and $\{\sigma\}$ from equations 2.2 and 2.5 produces

$$U = \frac{1}{2} \int \{q\}^T [B]^T [D][B] \{q\} \quad d(vol) \qquad 2.8$$

The potential energy due to the distributed loads {L} may be written as

$$W = -\int \{f\}^T \{L\} \quad d(vol) \qquad 2.9$$

$$= -\int \{q\}[N]^T \{L\} \quad d(vol) \qquad 2.10$$

For concentrated loads $\{P\}$, integration is not necessary and the expression reduces to the loads multiplied by the corresponding displacements

$$W = -\{q\}^T\{P\} \qquad 2.11$$

The total potential energy is given by

$$\phi = U + W \qquad 2.12$$

$$= \frac{1}{2}\int \{q\}^T[B]^T[D][B]\{q\} \quad d(vol)$$

$$- \{q\}^T\{P\} \qquad 2.13$$

The total potential energy of a system in equilibrium is a minimum value. The potential energy is minimum when

$$\frac{\partial \phi}{\partial \{q\}} = 0 \qquad 2.14$$

Substituting equation 2.13 into this equation produces

$$\frac{\partial \phi}{\partial \{q\}} = \int [B]^T[D][B]\{q\} \quad d(vol) \quad - \quad P \quad = 0 \qquad 2.15$$

or

$$[K]\{q\} - \{P\} = 0 \qquad 2.16$$

in which the stiffness matrix

$$[K] = \int [B]^T[D][B] \quad d(vol) \qquad 2.17$$

For two dimensional problems this reduces to

$$[K] = t\int [B]^T[D][B] \quad d(area) \qquad 2.18$$

in which t is the element thickness.

2.3 Selection of Elements for Structural Idealisation

Shear walls:

The geometry of the regular rectangular shear wall suggests a division into rectangular elements.

The shape functions chosen to describe the displacements within the elements will then govern the accuracy of the elements. Elements with quadratic or cubic (high order) rather than simple linear shape functions will give a more accurate approximation. Such elements have been developed and employed to model shear walls [21,22]. However, their use is at the expense of greater effort in calculating their stiffness relationships. A greater number of degrees of freedom for each element also results in an increased solution cost. It is, therefore, desireable to use the lowest order element which gives suitably accurate solutions.

The quadrilateral isoparametric element with linear shape functions can be revised to improve bending behaviour. With the addition of non-conforming displacement modes it has been shown to give highly accurate results [19,20]. Thus, this element is preferred to model the walls.

Beams and columns:

The connecting beams of a coupled shear wall can be modelled using the same elements as for the wall. The accuracy of the approximations will improve with a larger number of elements to each beam. However, to model a frame in this way would lead to the use of a very large number of elements. This would make the solution prohibitively costly to complete.

Individual frame members can be accurately modelled using a single line element producing a much smaller set of equations. Thus, this element is preferred to model beams and columns.

Wall-frame structures:

The two preferred types of element for the analysis of walls and frames can not be used together directly. The quadrilateral isoparametric element with linear shape functions has two degrees of freedom at each node. The line element has three. The next chapter describes the Lagrange multiplier technique which allows them to be connected.

Agrawal and Mufti [22] report better results using a rectangular element with rotational, in addition to the translational, degrees of freedom. This element, which was developed by Sisodya et al. [40] for the analysis of box-girder bridges, allows a direct connection to be made between the wall and beam elements. The use of this element, therefore, is also investigated.

2.4 THE QUADRILATERAL ISOPARAMETRIC ELEMENT

A classical four noded quadrilateral element has two translational degrees at each of the four nodes (Fig 2.1).

The shape functions used for the linear element are

$$N_1 = \tfrac{1}{4}(1-\xi)(1-\eta)$$

$$N_2 = \tfrac{1}{4}(1+\xi)(1-\eta)$$

$$N_3 = \tfrac{1}{4}(1+\xi)(1+\eta)$$

$$N_4 = \tfrac{1}{4}(1-\xi)(1+\eta) \qquad 2.19$$

in terms of the local (element) co-ordinates ξ and η.

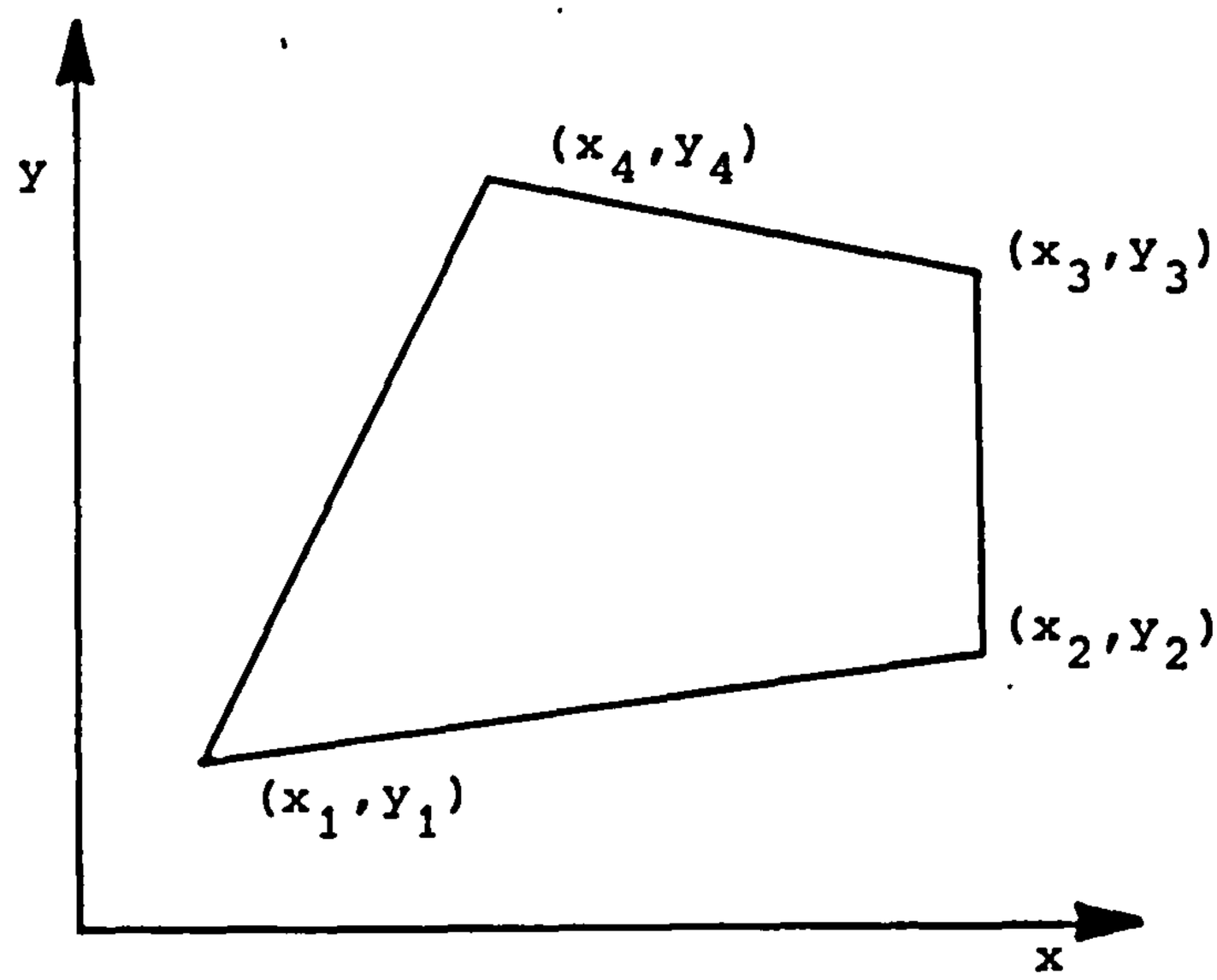

a) Global Co-ordinates

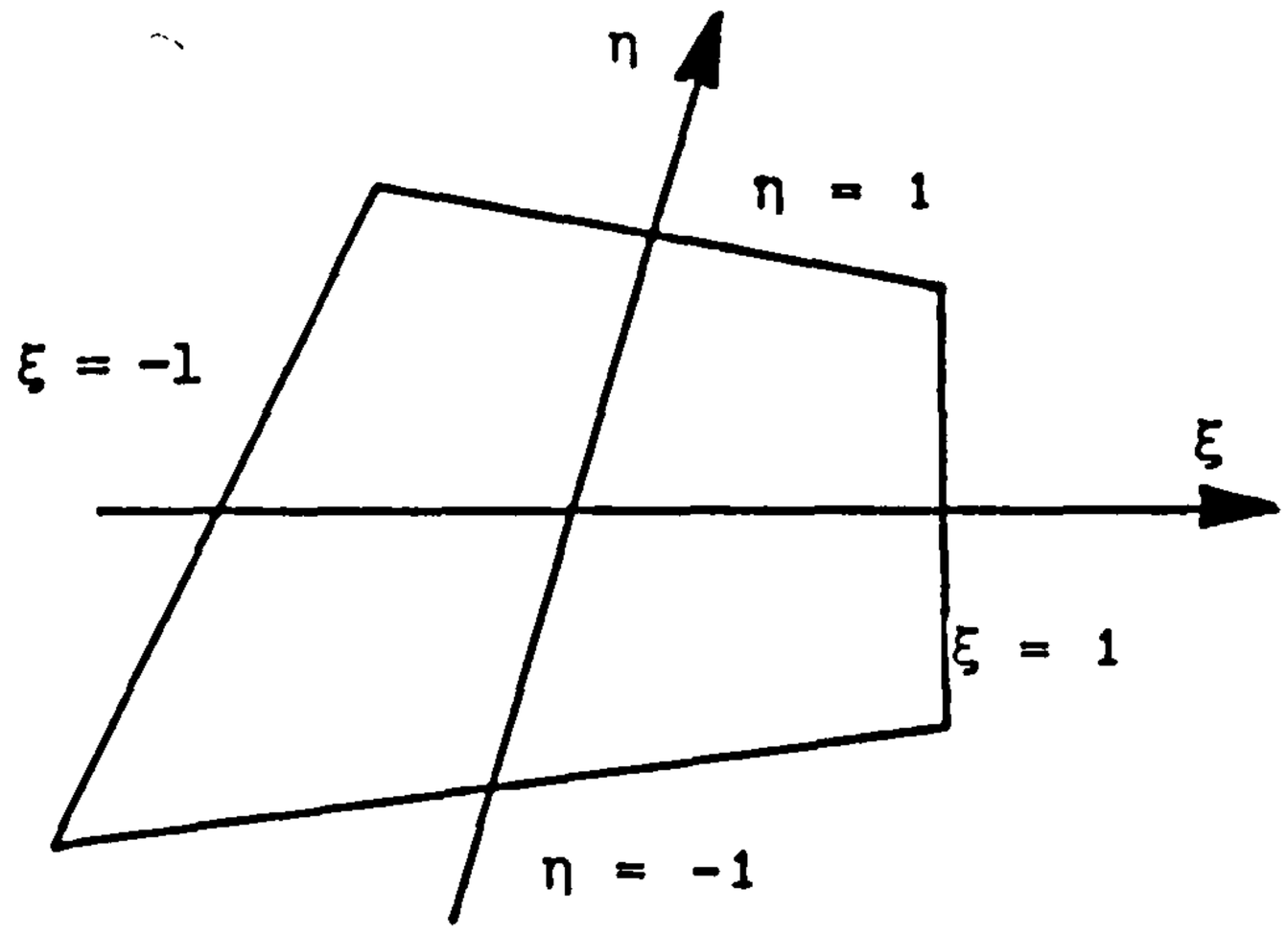

b) Local Co-ordinates

FIG. 2.1

Quadrilateral Isoparametric Element

These same functions are also used to transform from the local to the global co-ordinate system. The co-ordinate systems are related by

$$\begin{bmatrix} x \\ y \end{bmatrix} = \sum_{i=1}^{4} N_i(\xi, \eta) \begin{bmatrix} x_i \\ y_i \end{bmatrix} \qquad 2.20$$

Elements such as this, where the functions defining the displacement field and the geometry are identical, are termed isoparametric.

The shape functions of this element are defined in terms of the local co-ordinates ξ and η. Thus, they cannot be differentiated with respect to the global co-ordinates x and y to give the strain matric [B]. It is, therefore, necessary to obtain a relationship between the two sets of co-ordinate derivatives using the chain rule of partial differentiation.

$$\begin{bmatrix} \frac{\partial N}{\partial \xi} \\ \frac{\partial N}{\partial \eta} \end{bmatrix} = \begin{bmatrix} \frac{\partial x}{\partial \xi} & \frac{\partial y}{\partial \xi} \\ \frac{\partial x}{\partial \eta} & \frac{\partial y}{\partial \eta} \end{bmatrix} \begin{bmatrix} \frac{\partial N}{\partial x} \\ \frac{\partial N}{\partial y} \end{bmatrix} = [J] \begin{bmatrix} \frac{\partial N}{\partial x} \\ \frac{\partial N}{\partial y} \end{bmatrix} \qquad 2.21$$

The matrix [J] is called the Jacobian matrix and its coefficients may be evaluated by differentiating equation 2.20 with respect to ξ and η.

Now $\partial N/\partial x$ and $\partial N/\partial y$ may be expressed in terms of $\partial N/\partial \xi$ and $\partial N/\partial \eta$ through the inverse of [J].

$$\begin{bmatrix} \frac{\partial N}{\partial x} \\ \frac{\partial N}{\partial y} \end{bmatrix} = [J]^{-1} \begin{bmatrix} \frac{\partial N}{\partial \xi} \\ \frac{\partial N}{\partial \eta} \end{bmatrix} \qquad 2.22$$

To complete the transformation between the two systems it is also necessary to express the elemental area of equation 2.18 in terms of ξ and η. This produces

$$[K] = t \int_{-1}^{+1}\int_{-1}^{+1} [B]^T[D][B]\ \det[J]\ d\xi d\eta \qquad 2.23$$

This may be written as

$$[K] = t \sum_{j}\sum_{k} W_j W_k\ \det[J][B(\xi_j, \eta_k)]^T [D][B(\xi_j, \eta_k)] \qquad 2.24$$

for numerical integration by Guassian quadrature [37]. ξ_j and η_k are the integration points, W_j and W_k the weighting factors.

Addition of non-conforming modes:

The main source of inaccuracy with this element is its inability to represent a state of pure bending (Fig. 2.2). This may be overcome by the addition of non-conforming displacement modes [20]. Internal degrees of freedom are added at element level to remove the linear edge displacement constraints. These non-conforming modes give a more realistic displacement shape at the expense of the inter-element displacement compatibility. For the linear quadrilateral element, the shape functions to be added are

$$N_5 = 1 - \xi^2$$
$$N_6 = 1 - \eta^2 \qquad 2.25$$

The displacement field with non-conforming modes added may be expressed as

$$\begin{bmatrix} u \\ v \end{bmatrix} = \sum_{i=1}^{4} N_i \begin{bmatrix} u_i \\ v_i \end{bmatrix} + \begin{bmatrix} N_5 a_1 + N_6 a_2 \\ N_5 a_3 + N_6 a_4 \end{bmatrix} \qquad 2.26$$

This results in an element stiffness matrix of 12 x 12 terms. However, if the internal strain energy of the element is minimized with respect to the internal degrees of freedom a_i, then this may be reduced to 8 x 8 terms.

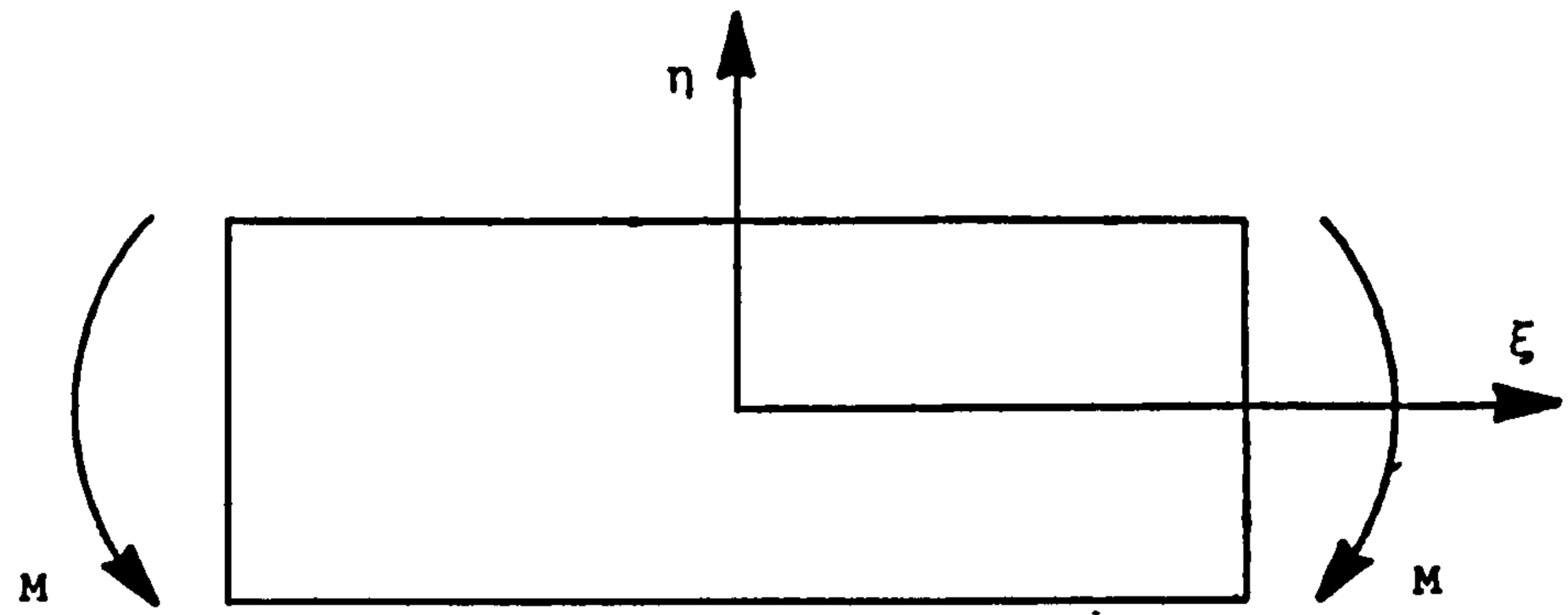

a) Element under pure bending

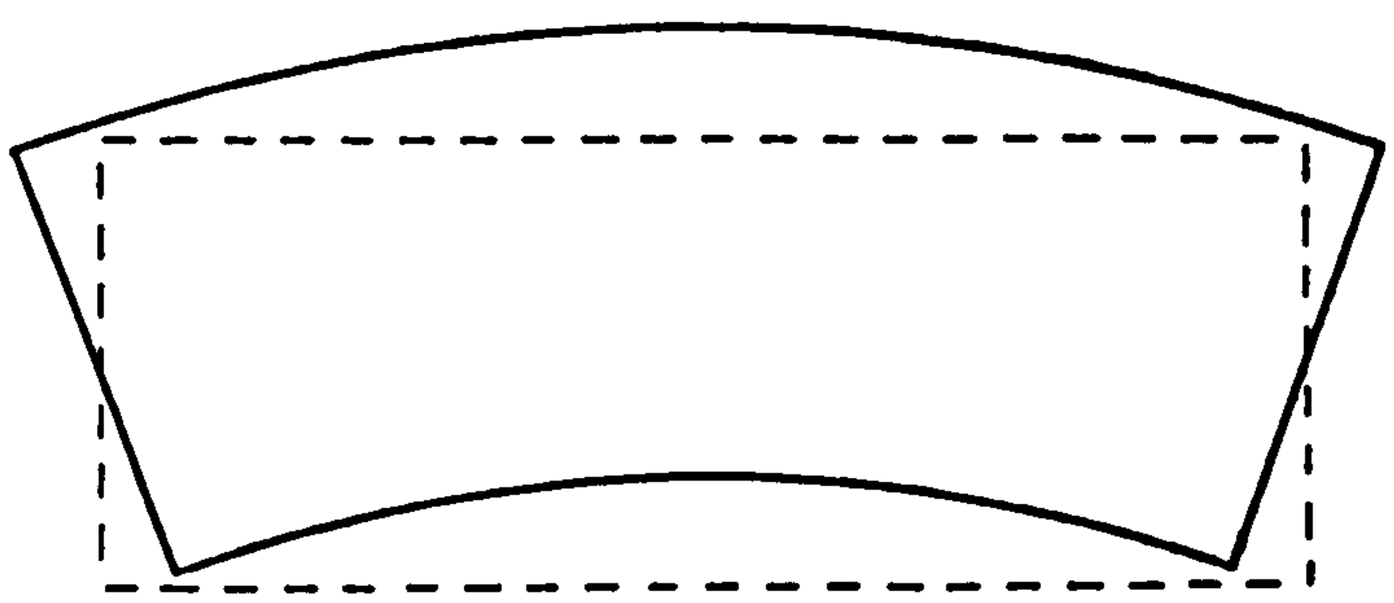

b) Exact displacements

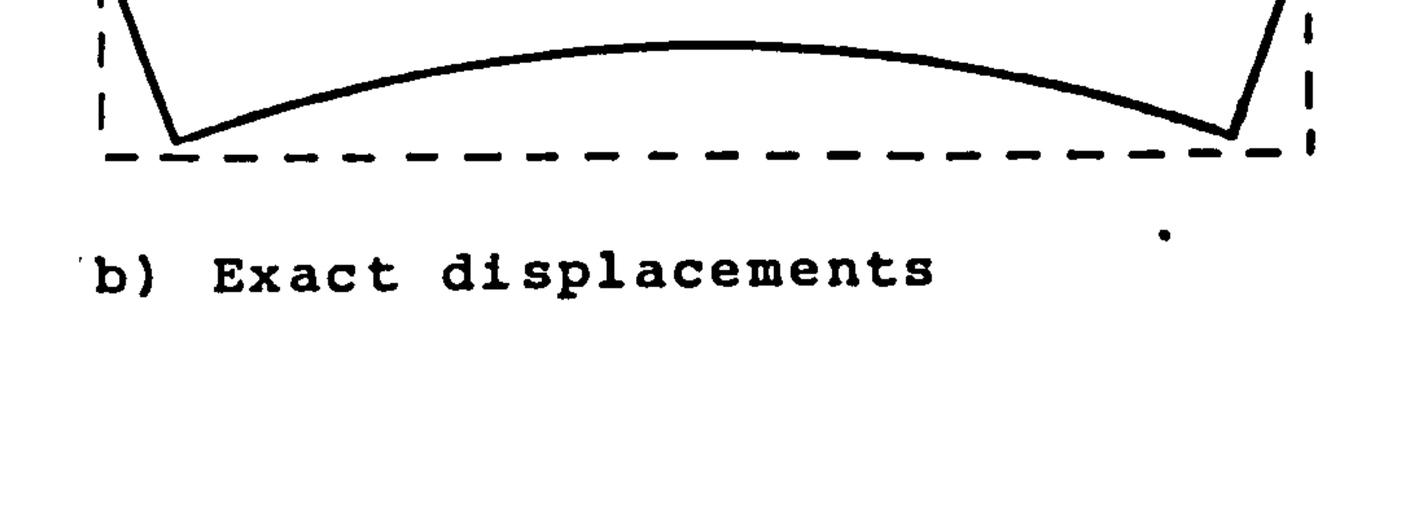

č) Displacements of the linear element

FIG. 2.2

Bending Behaviour of the Linear Element

This element has been shown to give highly accurate results when used in parallelogram or rectangular (which is a special case of the parallelogram) form [19, 20]. However, when distorted to a general quadrilateral form, it does not yield a convergent solution [41,42].

A remedy for this has been shown by Taylor et al. [43]. When the derivatives for the Jacobian matirx [J] are evaluated at the centre of the element (ξ=0, η=0), irrespective of the actual co-ordinates of the integration points, then convergence is restored. For the rectangular parallelogram elements, these derivatives are constant and hence the co-ordinates at which they are evaluated have no effect. The stiffness matrix for the modified element is identical to the original incompatible element for the rectangular and parallelogram cases and gives improved results for the general quadrilateral form.

2.5 RECTANGULAR PLANE STRESS ELEMENT WITH ROTATIONAL DEGREES OF FREEDOM

The element proposed by Agrawal and Mufti [22] assumes the following displacement functions

$$u = \alpha_1 + \alpha_2 x + \alpha_3 y + \alpha_4 xy \qquad 2.27$$

$$v = \alpha_5 + \alpha_6 x + \alpha_7 x^2 + \alpha_8 x^3 + \alpha_9 y + \alpha_{10} xy + \alpha_{11} x^2 y + \alpha_{12} x^2 y \qquad 2.28$$

$$\theta = \frac{\partial v}{\partial x} = \alpha_6 + 2\alpha_7 x + 3\alpha_8 x^2 + \alpha_{10} y + 2\alpha_{11} xy + 3\alpha_{12} x^2 y \qquad 2.29$$

which are biased towards one axis. With the element in the orientation of Fig. 2.3 the bias direction will be referred to as horizontal.

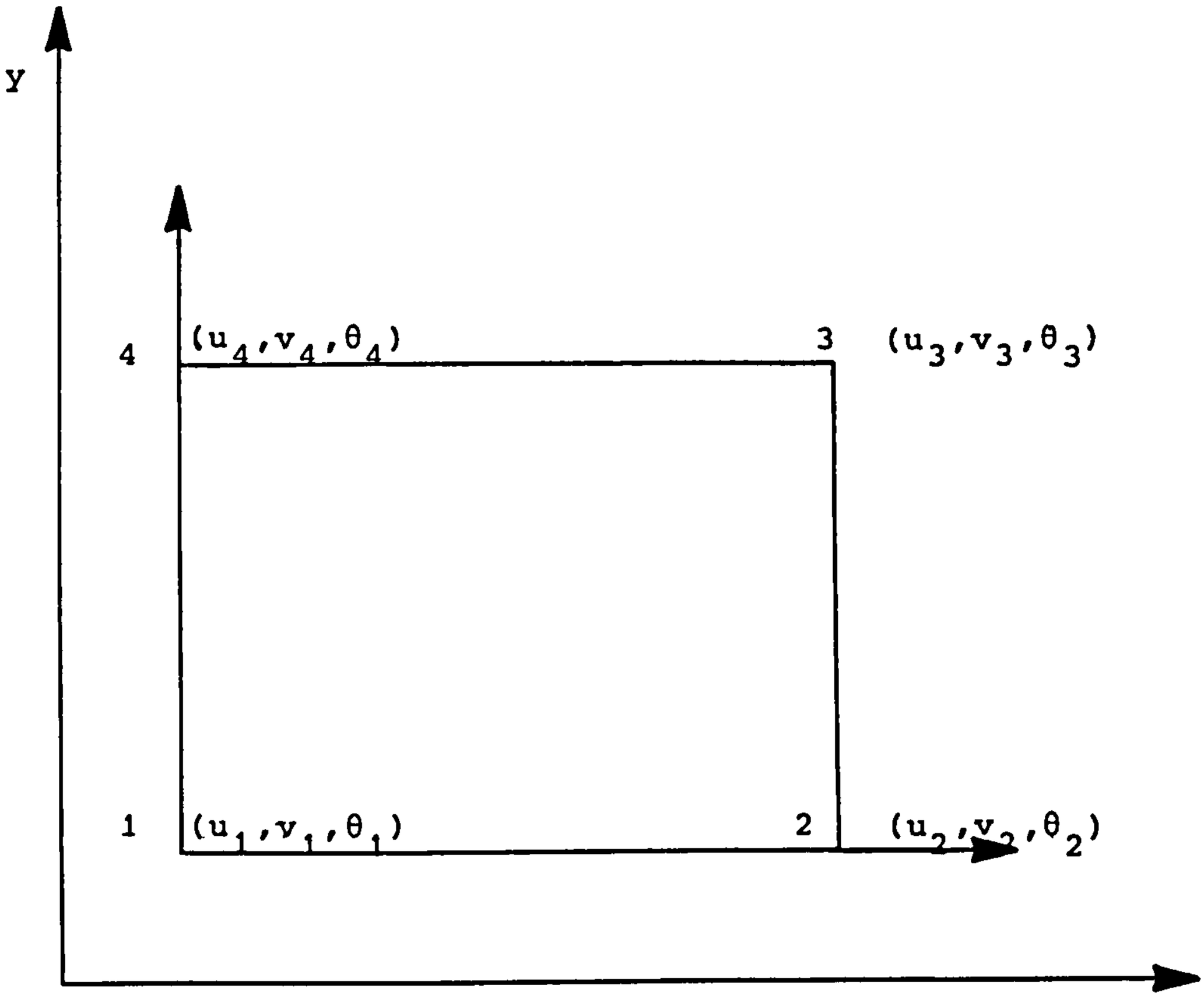

Bias Horizontal:

Local (element) x and y axes parallel to global (structure) x and y axes

FIG. 2.3

Rectangular Plane Stress Element with Rotational Degress of Freedom

The displacement may functions be written as

$$\{f\} = [R]\{\alpha\} \qquad 2.30$$

where [R] is a function of the co-ordinates and $\{\alpha\}$ is a vector of polynomial constants.

To express the displacement function in terms of the nodal displacement parameters $\{q\}$, the nodal co-ordinates are substituted into equation 2.30 producing

$$\{q\} = [Co]\{\alpha\} \qquad 2.31$$

where [Co] is a matrix of the nodal co-ordinates.

This may be rearranged to

$$\{\alpha\} = [Co]^{-1}\{q\} \qquad 2.32$$

Substituting into equation 2.30 produces

$$\{f\} = [R][Co]^{-1}\{q\} \qquad 2.33$$

or

$$\{f\} = [N]\{q\}$$

The displacements are now given in shape function form as in equation 2.1. The strain matrix [B] and hence the stiffness matrix [K] may now be calculated as described earlier in the chapter.

2.6 THE LINE ELEMENT

The line element idealises a beam or column in terms of the displacements at each of the two end nodes. The nodes have three degrees of freedom, two translational and one rotational.

The stiffness relationships for this element are derived from simple beam bending theory. They may be derived using displacement functions and the principle of minimum potential energy. Alternatively, Hooke's law and the slope-deflection equations may be used to relate the displacements to the moments shear and axial forces at the member ends.

This type of element is used in the stiffness method for skeletal structures which have real discrete joints, from which the finite element method developed. The derivations of the stiffness matrix for this element are given in many publication [37, 44, 45] and need not be presented here.

CHAPTER THREE - THE LAGARANGE MULTIPLIER TECHNIQUE

3.1 INTRODUCTION

The quadrilateral isoparametric element and the line element cannot be used directly together if a fixed joint is to modelled. The end rotation of the line element needs to be related to the rotation of the wall at the joint. However, the displacements of the wall elements are all in terms of translational degrees of freedom. A method whereby these translational displacements can be linked to the end rotations of the line elements must be introduced if these two element types are to be linked.

This link may be accomplished by means of constraint equations incorporated into the finite element system of equations. The technique employed is that of Lagrange multipliers [38,46-48]. It involves an extra Lagrange multiplier degree of freedom being added for each constraint equation used.

3.2 SELECTION OF CONSTRAINT EQUATIONS

Several different sets of constraint equations have been suggested.

Method 1:

Al-Mahaidi and Nilson [23,49] proposed the following conditions.

The rotation of the line element must be compatible with the x-direction displacements of the wall elements to which it is to be connected (Fig. 3.1). For small angles

$$\tan \theta_j \simeq \theta_j \qquad 3.1$$

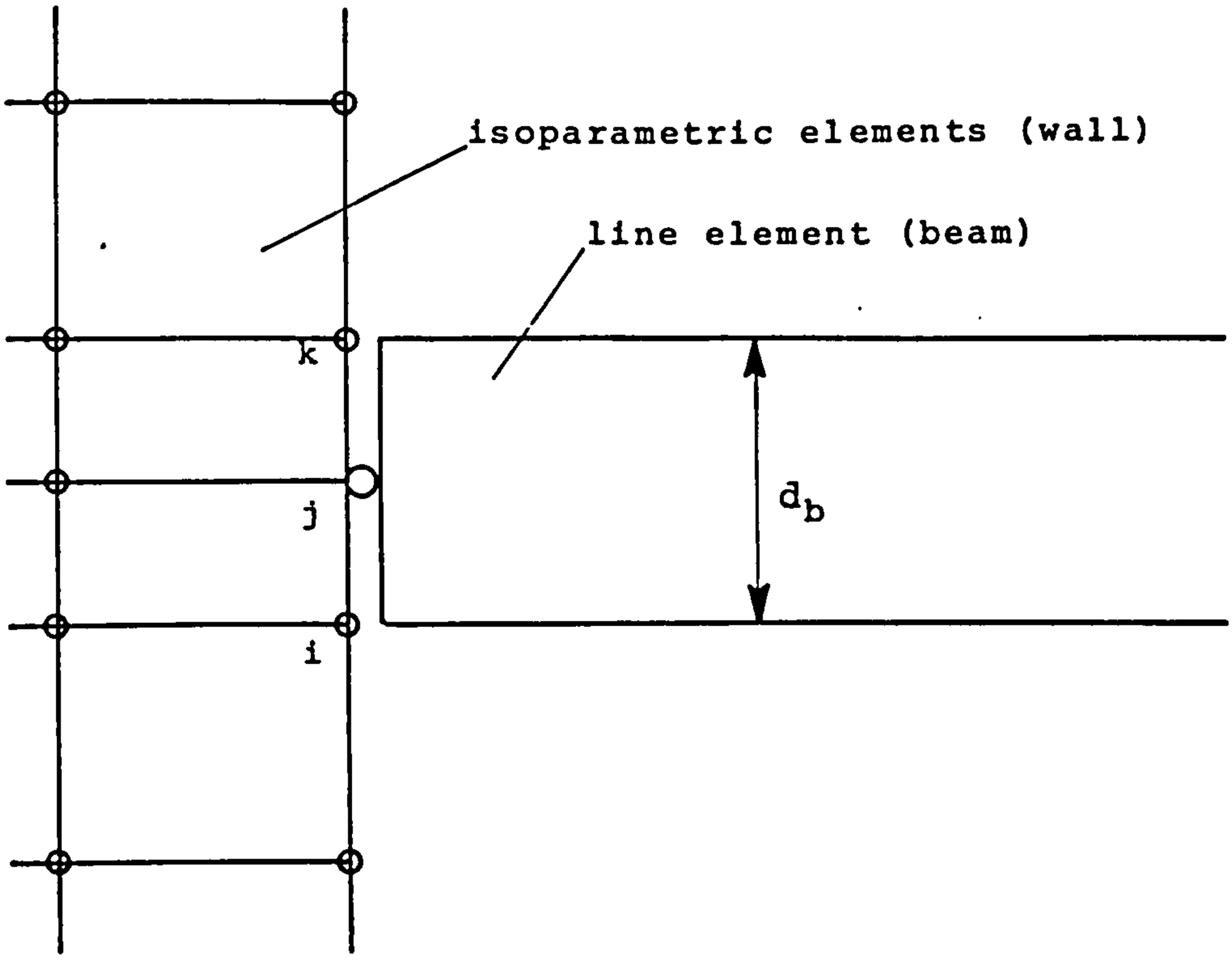

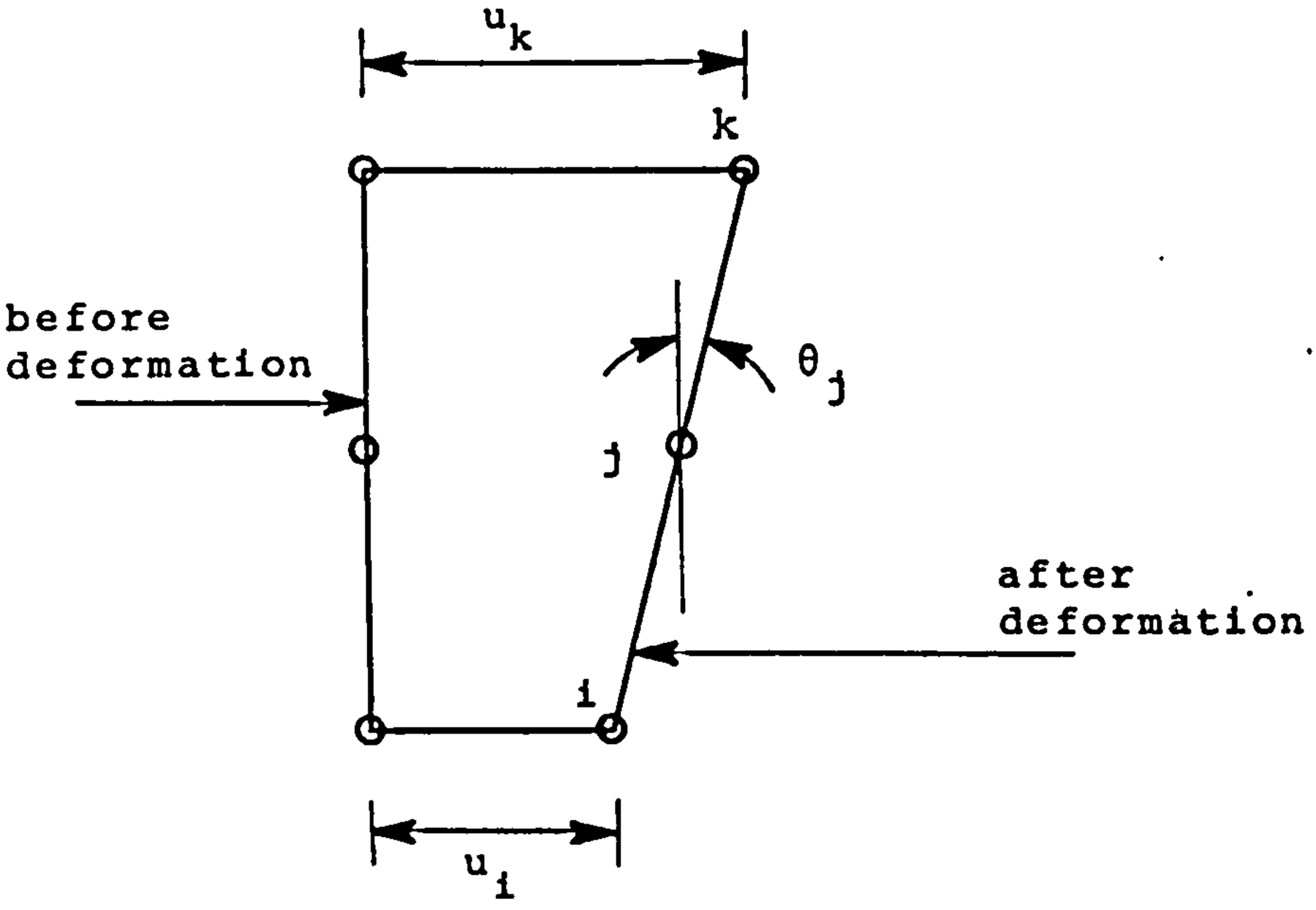

FIG. 3.1

Al-Mahaidi's Constraint Scheme

Thus this conditon may be written

$$\frac{1}{d_b}(u_k - u_i) + \theta_j = 0 \qquad 3.2$$

To comply with the Bernoulli-Navier hypothesis of plane sections remaining plane during bending, the nodes i, j and k must lie on a straight line. This condition may be expressed as

$$\frac{1}{2}(u_i + u_k) - u_j = 0 \qquad 3.3$$

Method 2:

A single constraint equation similar to equation 3.2 was proposed by Antony and Ganesan [24]. They allow nodes i and k to take any convenient position. This they refer to as a "wall face oriented connection" (Fig. 3.2 (a), (b)). Thus

$$\frac{1}{d_{ik}}(u_k - u_i) + \theta_j = 0 \qquad 3.4$$

Method 3:

Also proposed by Antony and Ganesan [24] is a "frame member oriented connection". They assume the relative rotation of the beam and the tangent to the beam to be zero. (Fig. 3.2 (a), (c)). This leads to the following constraint equation

$$\frac{1}{d_{jl}}(v_j - v_l) - \theta_j = 0 \qquad 3.5$$

However, for a wall to the right of the beam, this equation must be rearranged to

$$\frac{1}{d_{jl}}(v_l - v_j) - \theta_j = 0 \qquad 3.6$$

Proposed method:

The scheme proposed here is a wall face oriented connection to a single isoparametric element. The line element is connected

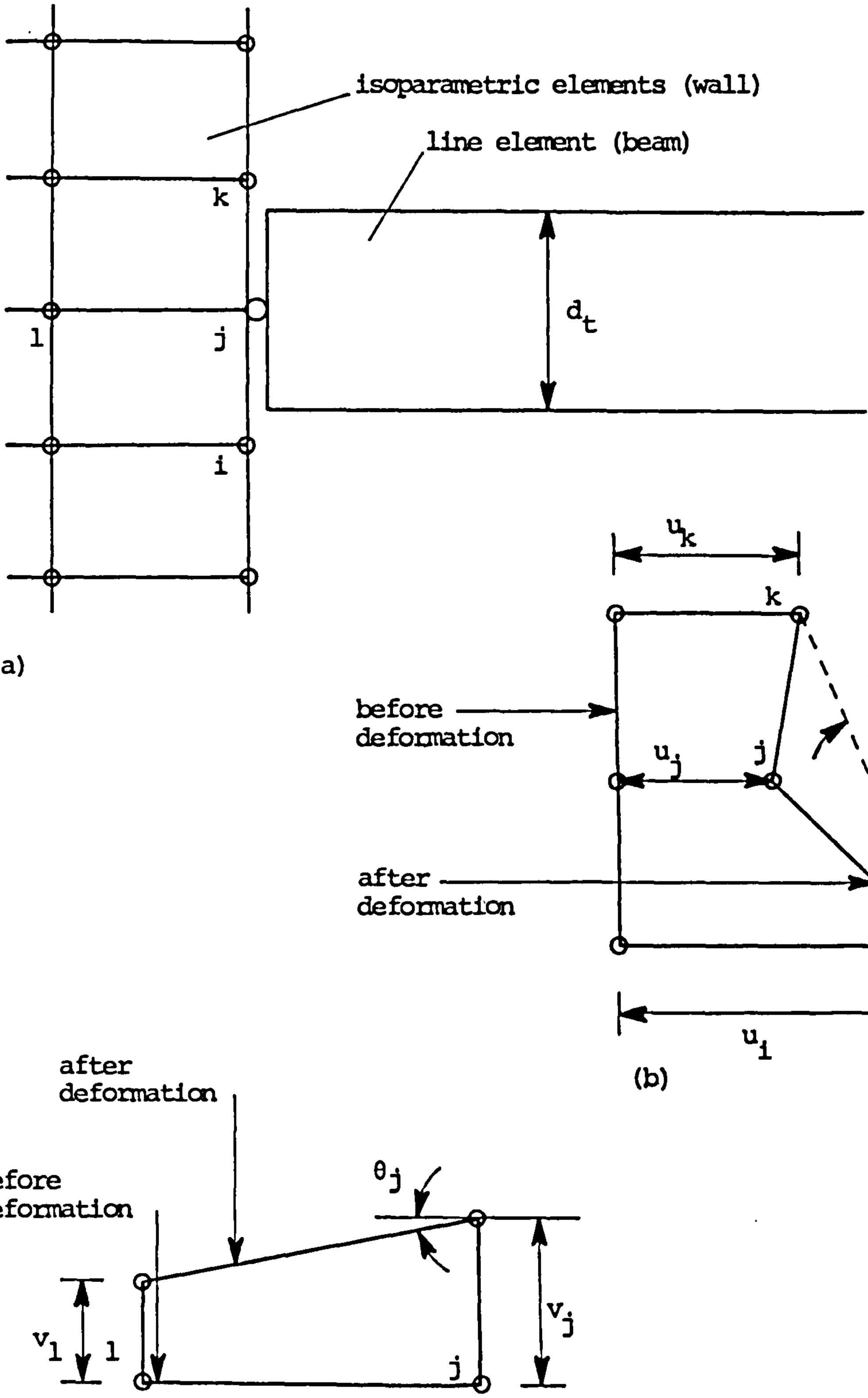

FIG. 3.2

Antony and Ganesan's constraint schemes

to the centre of an edge of the isoparametric element (Fig. 3.3). As there is no node at this point on the rectangular element, to achieve this, three constraining equations must be used at each joint. These link the rotational and translational displacements of the line element to the translational displacements of the isoparametric element.

The two translational displacements at the beam centre-line (node j) are assumed to be the average of those at the top and bottom (nodes i and k).

$$\frac{1}{2}(u_i + u_k) - u_j = 0 \qquad 3.7$$

$$\frac{1}{2}(v_i + v_k) - v_j = 0 \qquad 3.8$$

The end rotation of the beam element is made compatible with the x-direction displacements of the wall element such that

$$\frac{1}{d_b}(u_i - u_k) - \theta_j = 0 \qquad 3.9$$

These constraint equations may be written in matrix form as

$$\begin{bmatrix} \frac{1}{2} & 0 & \frac{1}{2} & 0 & -1 & 0 & 0 \\ 0 & \frac{1}{2} & 0 & \frac{1}{2} & 0 & -1 & 0 \\ 1/db & 0 & -1/db & 0 & 0 & 0 & -1 \end{bmatrix} \begin{bmatrix} u_i \\ v_i \\ u_k \\ v_k \\ u_j \\ v_j \\ \theta_j \end{bmatrix} = \begin{bmatrix} \\ 0 \\ \\ \end{bmatrix} \qquad 3.10$$

3.3 THE LAGRANGE MULTIPLIER TECHNIQUE

Constraint Equations:

The constraint equation 3.10 may be written more compactly as

$$[G]\{q\} = \{S\} \qquad 3.11$$

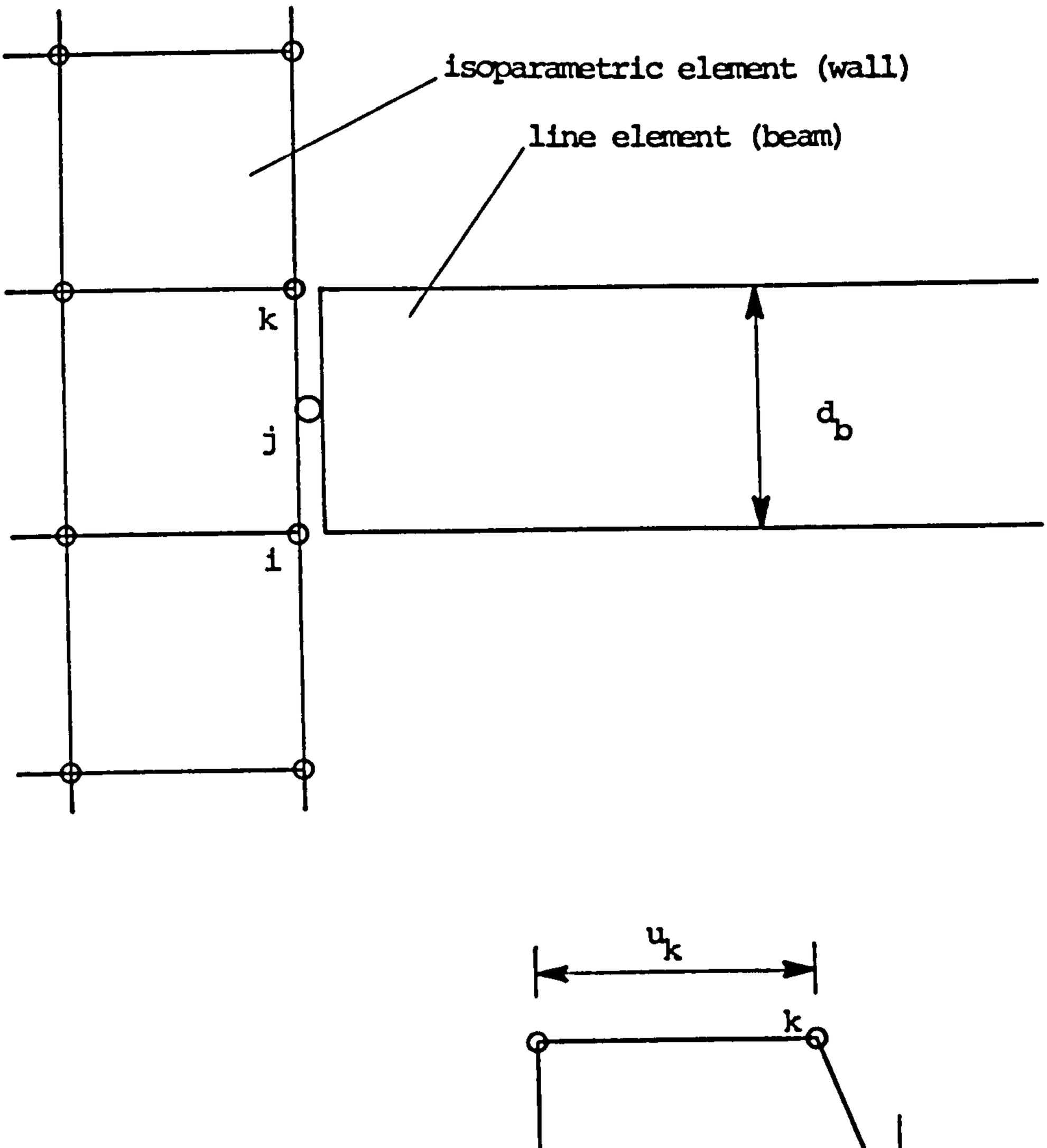

FIG. 3.3

Proposed constraint scheme

For a system with n degrees of freedom and m constraint conditions then

[G] is an m by n coefficient matrix

{S} is a vector of m constrained displacements

Potential Energy:

The total potential energy ϕ of the finite element model given by equation 2.13 may be rewritten as

$$\phi = \tfrac{1}{2} \{q\}^T[K]\{q\} - \{q\}^T\{P\} \qquad 3.12$$

Equilibrium:

By differentiating the total potential energy with respect to the independant variables {q}, the equilibrium condition may be found. With a set of constraint equations linking the displacements {q}, they are no longer independant.

To restore the independance, each constraint equation must be multiplied by a further variable λ_i.

$$\{\lambda\}[G]\{q\} - \{\lambda\}\{S\} = 0 \qquad 3.13$$

These new independant variables are termed Lagrange multipliers.

The constraint equations may now be added whilst maintaining the independance of the variables.

$$\bar{\phi} = \tfrac{1}{2}\{q\}^T[K]\{q\} - \{q\}^T\{P\} + \{\lambda\}[G]\{q\} - \{\lambda\}\{S\} \qquad 3.14$$

$\bar{\phi}$ is known as the augmented functional.

By taking the partial derivatives of $\bar{\phi}$ with respect to the independant variables {q} and {λ} and setting them simultaneously to zero, the equilibrium condition may now be found.

$$\frac{\partial \bar{\phi}}{\partial \{q\}} = [K]\{q\} - \{P\} + [G]^T\{\lambda\} = 0 \qquad 3.15$$

$$\frac{\partial \bar{\phi}}{\partial \{\lambda\}} = [G]\{q\} - \{S\} = 0$$

These equations may be written more compactly as

$$\begin{bmatrix} K & G^T \\ G & 0 \end{bmatrix} \begin{Bmatrix} q \\ \lambda \end{Bmatrix} = \begin{Bmatrix} P \\ S \end{Bmatrix} \qquad 3.16$$

3.4 RELATIVE MERITS OF DESCRIBED METHODS

The first method makes use of the Bernoulli-Navier hypothesis. This is an assumption made to simplify flexural bending theory and facilitate analysis. It would seem unnecessary to impose it upon the wall-beam joint. The other methods do not employ this constraint.

The first method also concentrates the isoparametric elements at the level of the joint. Two elements must be used for the depth of the beam across the full width of the wall. This increases the size of the problem to be solved.

Both of the first two methods link across a depth of two isoparametric elements. This leads to a large bandwidth with terms in the constraint equations widely spaced from the diagonal. With a larger set of equations to solve, computing costs are increased.

The third method does not have the previous disadvantages. However, it has the added complication that different equations must be used for a joint to a wall on the left or the right.

The proposed method suffers from none of these problems. Three Lagrange multiplier degrees of freedom are added at each joint which is more than for the other methods. This is useful when the forces in the line element are to be calculated, due to the physical identity of the mulipliers λ_i.

3.5 PHYSICAL INTERPRETATION OF THE LAGRANGE MULTIPLIERS

The augmented functional $\bar{\phi}$ of equation 3.14 has units of force multiplied by displacement. For dimensional consistency the multipliers $\{\lambda\}$, which are multiplied by displacements $\{q\}$, must have units of force.

For a single element, the nodal forces acting may be found by multiplying the stiffness [k] by the nodal displacement $\{q\}$. In the case of the line element these nodal forces are the moment, and shear and axial forces at the member ends.

Writing the augmented stiffness equations 3.16 for nodes i, j and k we have

$$\left[\begin{array}{cccc|ccc} K_{11} & K_{12} & & K_{17} & \frac{1}{2} & & 1/d_b \\ K_{21} & & & & & \frac{1}{2} & \\ & & & & \frac{1}{2} & & -/d_b \\ & & & & & \frac{1}{2} & \\ K_{51} & & \text{etc.} & K_{57} & -1 & & \\ & & & & & -1 & \\ K_{71} & & & K_{77} & & & -1 \\ \hline \frac{1}{2} & & \frac{1}{2} & & -1 & & \\ & \frac{1}{2} & & \frac{1}{2} & & -1 & \\ 1/d_b & & 1/d_b & & & & -1 \end{array}\right] \left[\begin{array}{c} u_i \\ v_i \\ u_k \\ v_k \\ u_j \\ v_j \\ \theta_j \\ \hline \lambda_1 \\ \lambda_2 \\ \lambda_3 \end{array}\right] = \left[\begin{array}{c} P_{xi} \\ P_{yi} \\ P_{xk} \\ P_{yk} \\ P_{xj} \\ P_{yj} \\ P\theta_j \\ \hline \\ 0 \\ \\ \end{array}\right] \qquad 3.17$$

Multiplying out equation 3.17 for the x-direction force at node j produces

$$\{K_{51}, K_{52} \ldots\ldots\ldots\ldots K_{57}\}\{q\} + (-1)\lambda_1 = P_{xj} \qquad 3.18$$

where Pxj is the x direction load at node j.

The stiffness coefficients in $\{K_{51} \ldots\ldots\ldots\ldots K_{57}\}$ are all contributed by the line element at node j. If no external load is imposed on node j then

$$\{K_{51} \ldots\ldots\ldots\ldots K_{57}\}\{q\} = \lambda_1 \qquad 3.19$$

Hence, when the system of equations 3.16 are solved for {q} and {λ}, λ_1 takes the value of the x-direction end force on the line element at node j.

Similarly it can be shown that λ_2 and λ_3 take the values of the y-direction force and the moment at node j.

This feature is very useful. The extra Lagrangian degrees of freedom, which must be solved for during analysis, take the values of the nodal forces at the joint. The moment, and shear and axial forces at the end of the beam are calculated automatically during the solution procedure. They need no longer be calculated subsequently.

3.6 ASSEMBLY OF THE CONSTRAINT EQUATION INTO THE STIFFNESS MATRIX

Al-Mahaidi and Nison [49] used a number of imaginary elements to represent the constraint equations for each joint. This was to allow different constraint equations to be used. Only connections to a vertical wall face are considered here and so this method is not employed.

The three Lagrange multipler degrees of freedom for each joint are assigned to a single node. The coefficients of the constraint equations in the form of equation 4.17 (with all K=0) can be considered as the stiffness coefficients of an imaginary element. This element has four nodes, two on an isoparametric element, one on a line element and the other with the multiplier degrees of freedom.

One subroutine is used to calculate the coefficients for this element. They are then assembled in the normal way. The

partitioning implied by equation 3.16 is not used as this would give a very large bandwidth. The equations are ordered by the node numbers.

The zeros on the leading diagonal can cause problems with standard solution procedures. However, with careful ordering of the equations this may be overcome. The solution methods used in this study were Guasian elimination and back substitution [50] for static and forced vibration analysis, and the bisection method [51] for free vibration. With these, no problems were encountered when the node with the Lagrange multiplier degrees of freedom was given a higher node number than the other nodes associated with the joint.

CHAPTER FOUR - DYNAMIC ANALYSIS

4.1 EQUATIONS OF MOTION

The equations of dynamic equibilibrium at any time t may be written as

$$[M]\{\ddot{q}\} + [C]\{\dot{q}\} + [K]\{q\} = \{P(t)\} \qquad 4.1$$

where

$\ddot{q}$ = nodal accelerations

$\dot{q}$ = nodal velocities

[M] = mass matrix

[C] = damping matrix

{P(t)} = nodal loads at time t

Mass matrix:

The mass matrix for the analysis may be derived by two different methods to give either a consistent or a lumped matrix.

When the shape functions used to describe the acceleration field over the element are the same as those used for the displacement field, then a consistent matrix results. This is populated in an identical manner to the stiffness matrix with many off-diagonal terms.

A simpler approach is to lump tributary areas to each node. This involves less computation and results in a diagonal matrix. For the analysis of a complete structure, a significant proportion of the mass may come from non-structural components. These external masses are also lumped to the nodes, usually at the floor levels.

Convergence studies [19,52] have shown that the lumped mass matrix is capable of producing accurate results. Particularly

when used with the non-conforming isoparametric element, a high degree of accuracy has been obtained [19]. Typical results for the natural frequencies of a plain wall are shown in Fig. 4.1 for both lumped and consistent mass matrices with conforming and non-conforming elements. It can be seen that the results remain accurate even when a small number of elements are used.

In view of the accuracy obtainable and the lesser computational effort required, the lumped mass matrix is used in this study.

Damping matrix:

The nature of damping present in a vibrating building is very difficult to characterize. To facilitate numerical analysis, equivalent viscous damping is usually assumed.

Studies on full scale building repsonse have supplied values for modal damping coefficients for the lower modes [53]. It is therefore desirable to specify a damping matrix whose properties are related to the known modal damping ratios of the physical system. This may be accomplished by evaluating the damping matrix as a linear combination of the mass and stiffness matrices [54].

$$[C] = C_1[M] + C_2[K] \qquad 4.2$$

The constants C_1 and C_2 are related to the damping ratio μ_i for any mode i by [55]

$$\mu i = \frac{C_1}{2\omega_i} + \frac{C_2\omega i}{2} \qquad 4.3$$

where ω_i is the natural frequency in the ith mode.

(a) First Mode

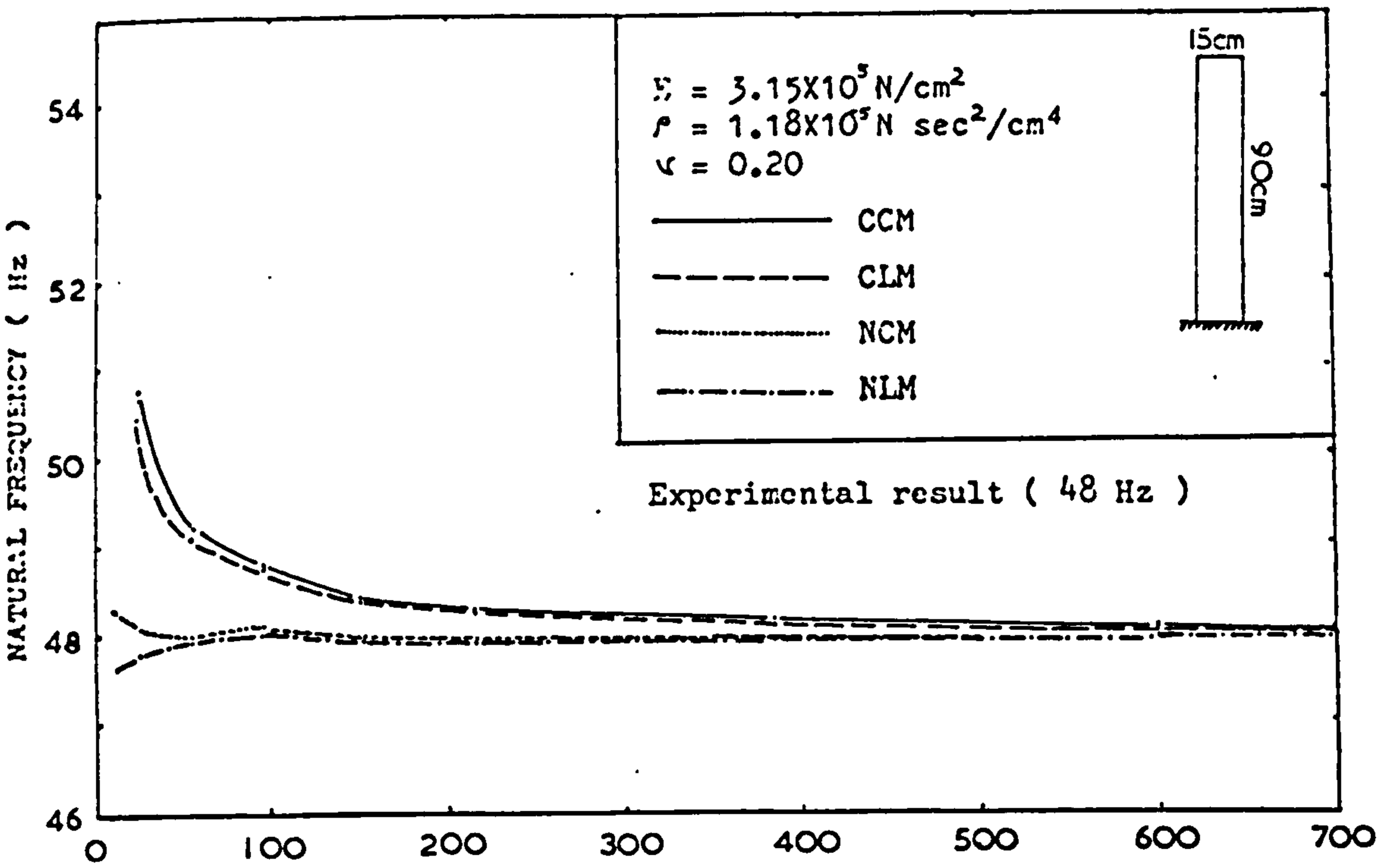

(b) Second Mode

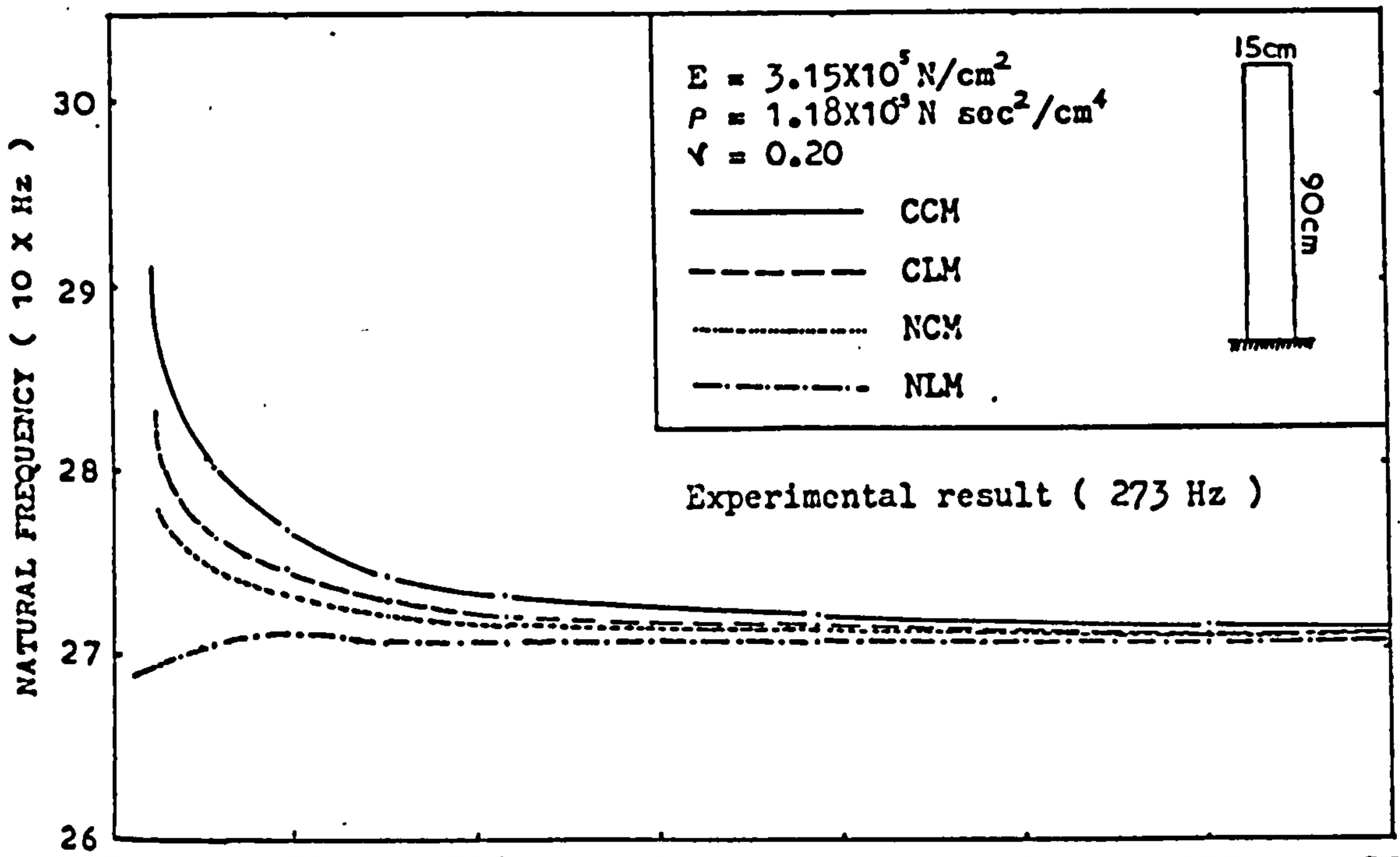

Fig 4.1

Effect of Lumped and Consistent Mass Matrices

Tests on existing structures [53] have shown that damping can range from 2% to 20% of critical in the first two modes. If suitable values are chosen for the anlysis then the constants C_1 and C_2 can be evaluated from

$$C_1 = \frac{2\omega_1\omega_2 \quad (\mu_2\omega_1 - \mu_1\omega_2)}{\omega_1^2 - \omega_2^2} \qquad 4.4$$

$$C_2 = \frac{2(\mu_1\omega_1 - \mu_2\omega_2)}{\omega_1^2 - \omega_2^2} \qquad 4.5$$

The damping in other modes may then be calculated from equation 4.3.

4.2 FREE VIBRATION

For the particular case of free vibration, no loads are applied and damping is not considered. Equation 4.1 reduces to

$$[M]\{\ddot{q}\} + [K]\{q\} = 0 \qquad 4.6$$

All the displacements are in phase and may be written as

$$\{q\} = \{r\}e^{i\omega t} \qquad 4.7$$

where

ω = natural frequency

$\{r\}$ = nodal displacements (mode shape)

t = time

Differentiating twice with respect to time produces:

$$\{\ddot{q}\} = -\omega^2\{r\}e^{i\omega t} \qquad 4.8$$

Substituting into equation 4.6 produces

$$[[K] - \omega^2[M]]\{q\} = 0 \qquad 4.9$$

This may be expressed as a standard eigenvalue problem.

$$[[K] - \psi[M]]\{q\} = 0 \qquad 4.10$$

where the eigenvalue $\Psi = \omega^2$.

A large number of solution techniques have been developed to solve this problem [56, 57]. However, no single method has been found suitable for all applications. For large, banded matrices where only the first few eigenvalues are required, the bisection method [51] has proved effective when a reasonable estimate can be made for the eigenvalues.

The required roots of equation 4.10 are solved for by calculating the eigenvalues Ψ for which

$$\left|[K] - \psi[M]\right| = 0 \qquad 4.11$$

An initial estimate is made for the eigenvalue and an increment is assumed. The sign of the determinant (equation 4.11) is calculated for the initial estimate and successive increments. The required root will lie between the values of Ψ for which the sign of the determinant changes. It may then be found by repeated bisection of the interval within which it lies.

Only the sign of the determinant is required with this method and thus the value is normalised as it is calculated to avoid possible numerical overflow problems. This has the disadvantage that when two roots lie close together, the sign may change twice during one increment, which will lead to the roots not being found.

This may be overcome by using a small increment but an accurate initial estimate is then needed if a large number of steps are to be avoided. If the logarithm of the value of the

determinant is calculated, overflow problems are readily avoided, whilst the values may be used to monitor convergence to the required root (Appendix A).

Constraint equations:

In equation 4.6 the inertial forces $[M]\{\ddot{q}\}$ are in equilibrium with the forces due to the deflections $[K]\{q\}$. With the inclusion of the constraint equations, the forces due to the deflections are given by equation 3.16. Equating these with the inertial forces produces

$$\begin{bmatrix} M & 0 \\ 0 & 0 \end{bmatrix} \begin{Bmatrix} \ddot{q} \\ \lambda \end{Bmatrix} + \begin{bmatrix} K & G^T \\ G & 0 \end{bmatrix} \begin{Bmatrix} q \\ \lambda \end{Bmatrix} = \begin{Bmatrix} 0 \\ \end{Bmatrix} \qquad 4.12$$

This equation may be solved for the natural frequencies and mode shapes in the same manner as equation 4.6. The subroutines presented by Raju et al. [51], modified to calculate the logarithm of the determinant, were used in this study.

4.3 FORCED VIBRATION

The equations of motion 4.1 may be solved by direct numerical integration. The response is evaluated for a series of short time increments Δt, at the beginning and end of which equilibrium is established.

Many different assumptions may be made as to the relationships between the acceleration, velocity and displacement for each interval [58]. Of these, one of the most popular is the Newmark-β method [59] which employs two parameters γ and β. These govern the proportions of the acceleration before and after the interval which enter into the equations for the velocity and displacement after the interval.

$$\{\dot{q}\}_{t+\Delta t} = \{\dot{q}\}_t + (1-\gamma)\Delta t\{\ddot{q}\}_t + \gamma\Delta t\{\ddot{q}\}_{t+\Delta t} \quad 4.13$$

$$\{q\}_{t+\Delta t} = \{q\}_t + \Delta t\{\dot{q}\}_t + (\tfrac{1}{2} - \beta)\Delta t^2\{\ddot{q}\}_t + \beta\Delta t^2\{\ddot{q}\}_{t+\Delta t} \quad 4.14$$

As the equations must be solved for each time step, it is advantageous to use a large increment Δt. This can be done only when the equations are unconditionally stable. Otherwise highly inaccurate, high frequency modes may predominate in the solution. The equations have been shown to be stable [60-62] when γ and β are chosen such that

$$\gamma = \tfrac{1}{2} + \alpha \quad 4.15$$

$$\beta = (1-\alpha)^2/4 \quad 4.16$$

where α is a parameter chosen between 0 and $1/3$. Hilber et al. [63] have proposed a method which also employs the parameter α directly in the equations of motion. This is to allow a greater degree of control over the numerical dissipation or damping in the higher modes. However, particularly widely employed is the assumption of constant acceleration during the interval. This has $\alpha = 0$ and hence $\gamma = \frac{1}{2}$ and $\beta = \frac{1}{4}$. In this case no artificial damping is introduced and the method of Hilber et al. is identical to the Newmark-β method, which is used in this study.

Solution procedure:

Substituting equations 4.13 and 4.14 into the equation of motion 4.1 at time $t + \Delta t$

$$[M]\{\ddot{q}\}_{t+\Delta t} + [C]\{\dot{q}\}_{t+\Delta t} + [K]\{q\}_{t+\Delta t} = \{P(t+\Delta t)\} \qquad 4.17$$

produces

$$[M]\{\ddot{q}\}_{t+\Delta t} + [C]\{\{\dot{q}\}_t + (1-\gamma)\Delta t\{\ddot{q}\}_t + \gamma\Delta t\{\ddot{q}\}_{t+\Delta t}\} +$$

$$[K]\{\{q\}_t + \Delta t\{\dot{q}\}_t + (\tfrac{1}{2}-\beta)\Delta t^2\{\ddot{q}\}_t + \beta\Delta t^2\{\ddot{q}\}_{t+\Delta t}\}$$

$$= \{P(t+\Delta t)\} \qquad 4.18$$

substituting equation 4.12 for [C] into equation 4.18

produces

$$[a[M] + b[K]]\{\ddot{q}\}_{t+\Delta t} = \{P(t+\Delta t)\}$$

$$- C_1[M]\{A\} - [K]\{C_2\{A\} + \{B\}\} \qquad 4.19$$

where

$$a = 1 + C_1\gamma\Delta t$$

$$b = C_2\gamma\Delta t + \beta\Delta t^2$$

$$\{A\} = \{\dot{q}\}_t + (1-\gamma)\Delta t\{\ddot{q}\}_t$$

$$\{B\} = \{q\}_t + \Delta t\{\dot{q}\}_t + (\tfrac{1}{2}-\beta)\Delta t^2\{\ddot{q}\}_t$$

This may be written more compactly as

$$[\overline{K}]\{\ddot{q}\}_{t+\Delta t} = \{\overline{F}\} \qquad 4.20$$

where

$$[\overline{K}] = a[M] + b[K]$$

$$\{\overline{F}\} = \{P(t+\Delta t)\} - C_1[M]\{A\} - [K]\{C_2\{A\} + \{B\}\}$$

Matrix $[\overline{K}]$ is a function of the mass and stiffness matrices. With conditions at the beginning of the interval known, $\{\overline{F}\}$ can be calculated. The accelerations at the end of the interval $\{\ddot{q}\}_{t+\Delta t}$ may then be calculated using equations 4.20. The velocities and displacements are calculated from equations 4.13

and 4.14 and these then form the initial conditions for the start of the next interval.

Constraint equations:

The dynamic equilibrium equation 4.20 is of the same form as the static equilibrium equation 2.16

$$[K]\{q\} = \{P\}$$

The constraint equations 3.11 used for the static equation may be employed in the same manner to constrain the accelerations in equation 4.20. With the constraint equations added we have

$$\begin{bmatrix} [\bar{K}] & G^T \\ G & 0 \end{bmatrix} \begin{bmatrix} \{\ddot{q}\}_{t+\Delta t} \\ \lambda \end{bmatrix} = \begin{bmatrix} \{\bar{F}\} \\ S \end{bmatrix} \qquad 4.21$$

which is of the same form as equation 3.16. Hence, the accelerations of equation 4.21 are constrained in the same manner as the displacement in equation 3.16. Using equations 4.13 and 4.14 for the velocities and displacements, it can be shown that, if the initial conditions are constrained, then the velocities and displacements are also constrained.

Using constraint equation 3.7, if at time t the initial conditons are

$$u_j(t) = \tfrac{1}{2}(u_i(t) + u_k(t)) \qquad 4.22$$

$$\dot{u}_j(t) = \tfrac{1}{2}(\dot{u}_i(t) + \dot{u}_k(t)) \qquad 4.23$$

$$\ddot{u}_j(t) = \tfrac{1}{2}(\ddot{u}_i(t) + \ddot{u}_k(t)) \qquad 4.24$$

then at the end of the interval the velocities can be calculated from equation 4.13 as

$$\dot{u}_j(t+\Delta t) = \dot{u}_j(t) + (1-\gamma)\Delta t\ddot{u}_j(t) + \gamma\Delta t\ddot{u}_j(t+\Delta t) \qquad 4.25$$

$$\dot{u}_i(t+\Delta t) = \dot{u}_i(t) + (1-\gamma)\Delta t\ddot{u}_i(t) + \gamma\Delta t\ddot{u}_i(t+\Delta t) \qquad 4.26$$

$$\dot{u}_k(t+\Delta t) = \dot{u}_k(t) + (1-\gamma)\Delta t\ddot{u}_k(t) + \gamma\Delta t\ddot{u}_k(t+\Delta t) \qquad 4.27$$

Substituting equations 4.23 and 4.24 into 4.25 produces

$$\dot{u}_j(t + \Delta t) = \tfrac{1}{2}(\dot{u}_i(t) + \dot{u}_k(t)) + (1 - \gamma)\Delta t\ \tfrac{1}{2}(\ddot{u}_i(t) + \ddot{u}_k(t) + \gamma\Delta t\ \ddot{u}_j(t+\Delta t) \quad 4.28$$

With the accelerations constrained

$$\ddot{u}_j\ (t+\ \Delta t) = \tfrac{1}{2}(\ddot{u}_i(t+\Delta\ t) + \ddot{u}_k(t+\Delta\ t)) \quad 4.29$$

Substituting into equation 4.28 produces

$$\ddot{u}_j\ (t+\Delta t) = \tfrac{1}{2}(\dot{u}_i(t) + \dot{u}_k(t)) + (1 - \gamma)\Delta t\ \tfrac{1}{2}\ (\ddot{u}_i(t) + \ddot{u}_k(t)) + \gamma\Delta t\ \tfrac{1}{2}\ (\ddot{u}_i(t+\Delta t) + \ddot{u}_k(t+\Delta\ t)) \quad 4.30$$

Comparing with equations 4.26 and 4.27 it can be seen that

$$\dot{u}_j(t+\ \Delta t) = \tfrac{1}{2}(\dot{u}_i(t+\Delta\ t) + \dot{u}_k(t+\ \Delta t)) \quad 4.31$$

and hence the velocities are constrained in the same manner as the accelerations. Using similar substitutions into equation 4.14 for the displacements, it can be shown that the displacements are also constrained.

The usual initial conditons before loads are applied are that all accelerations, velocities and displacements are zero. Thus equations 4.22 and 4.24 are simply satisfied.

Physical Interpretation of the Lagrange Multipliers:

Equation 4.14 can be written more compactly as

$$\{q\}_{t+\Delta t} = \{B\} + \beta\Delta t^2\{\ddot{q}\}_{t+\Delta t} \quad 4.32$$

By neglecting damping, equation 4.19 can be written as

$$[K]^*\{\dot{q}\}_{t+\Delta t} = \{P(t+\Delta t)\} - \{[K]\{B\}\} \quad 4.33$$

where $[K]^* = [M] + \beta\Delta t^2[K]$

With the addition of the constraint equations this becomes

$$\begin{bmatrix} [K]^* & G^T \\ G & 0 \end{bmatrix} \begin{bmatrix} \ddot{q} \\ \lambda \end{bmatrix} = \begin{bmatrix} P(t+\Delta t) - [K]\{B\} \\ S \end{bmatrix} \quad 4.34$$

Multiplying out this equation produces

$$[K]^*\{\ddot{q}\}_{t+\Delta t} + [G]^T\{\lambda\} = P(t+\Delta t) - [K]\{B\} \quad 4.35$$

which for nodes with no mass simplifies to

$$\beta\Delta t^2[K]\{\ddot{q}\}_{t+\Delta t} + [G]^T\{\lambda\} = -[K]\{B\} \quad 4.36$$

For earthquake loads, $P(t+\Delta t)$ is proportional to the mass at a node and hence is equal to zero at a node with no mass. For other types of loading, no load must be applied to the constrained beam end for this equation to be valid.

Expanding equation 4.36 in the same manner as equation 3.17 for the forces at the constrained end of the beam member produces

$$(-1)\{\lambda\} = -[K]\{\{B\} + \beta\Delta t^2\{\ddot{q}\}_{t+\Delta t} \quad 4.37$$

or using equation 4.32

$$\{\lambda\} = [K]\{q\}_{t+\Delta t} \quad 4.38$$

Two assumptions were made to derive this result. Damping and mass were both set to zero. This is only necessary at the constrained end of a beam member, the rest of the structure being treated in the normal manner. The mass from the end of the beam member may be lumped to adjacent nodes in the wall. The removal of damping at the constrained joint has very little effect on the overall solution.

With the imposition of these two restriction, the very useful equation 4.38 may be obtained. The variables $\{\lambda\}$ which are obtained during analysis, take the values of the nodal forces at the joint. This saves much subsequent calculation when these values are required for inelastic analysis, as will be demonstrated in the next chapter.

CHAPTER FIVE - NON-LINEAR DYNAMIC ANALYSIS

5.1 INTRODUCTION

The step by step numerical integration technique is a very powerful method for non-linear dynamic analysis. It is usually performed by assuming that the structural properties remain contant during each interval and then updating them using the deformation state at the end of the interval.

The change in material properties at the end of an interval generates unsupported stresses in the structural model. The assumption of a constant value of stiffness for each time increment during which plastic deformation takes place can lead to equilibrium as expressed by equation 4.1 not being satisfied. The accumulation of these errors can cause the divergence of the solution. A variety of methods have been employed to compensate for this.

The unsupported stresses can be converted into psuedo-loads [36,64]. These are then applied as corrective loads for the next time increment.

An additional incremental displacement can be calculated from the unbalanced loads. This may be repeated until equilibrium is established to the required tolerence [65].

Whenever non-linear behaviour occurs the time step may be reduced [66]. The stiffness changes at the end of each interval will then be smaller and the errors introduced correspondingly reduced.

All these methods of compensation involve considerable extra calculation. Also the stiffness matrix must be updated after any interval involving non-linear behaviour.

The equation of dynamic equilibrium 4.20 may be readily solved by Gaussian elimination and back substitution. With constant stiffness properties the elimination need only be performed once. However, when the stiffness changes and [K] is recalculated, then the elimination must also be performed again.

The described non-linear analysis method is very powerful and can accommodate many types of material non-linearity. However, it can be seen that it leads to a great increase in solution cost over the equivalent elastic analysis.

5.2 USE OF LAGRANGE MULTIPLIER

When the non-linear behaviour may be restricted to the joints between beams and walls, the Lagrange multiplier technique of chapter 4 may be modified to produce a more economic form of analysis. All the constraint equations presented have had their constrained displacements {S} equated to zero, giving a rigid joint. If these displacements are assigned values, depending upon the deformation state, then non-linear analysis can be performed without any change to the stiffness matrix. The amount of extra computation needed is thus greatly reduced.

The original constraint equation 3.9 makes the end rotation of the beam compatible with the x-direction displacement of the wall element.

$$\frac{1}{d_b} \quad (u_i - u_k) - \theta_j = 0$$

or

$$[G] \{q\} = \{S\}$$

For static problems, $\{S\}$ in this equation is the relative displacement between the beam and wall and is zero. If a non-zero relative displacement is specified then the solution will be modified and the forces in the structural model redistributed. Thus, by specifying the realtive displacements $\{S\}$, the end forces in the beam element may be controlled.

As shown in chapter 4 for forced vibration, the $\{S\}$ in equation 4.12 are relative accelerations at the end of the interval. From equation 4.14 it can be seen that for a joint with no relative acceleration or velocity at the beginning of the interval then the relative displacement during the interval is given by $\beta \Delta t^2 \{S\}$. Thus, for a particular analysis where β and Δt are selected constants, the relative displacement produced is proportional to the relative acceleration specified. Equation 4.21 is linear and thus applying the prinicple of superposition, a particular relative acceleration will always produce the same redistribution of forces.

This technique may be employed to regulate the forces at a beam wall junction. If for a particular time step the equations are solved for $\{S\} = 0$ and the forces in the beam calculated, a yield limit can be imposed upon them. This is done by calculating the relative acceleration at the joint to reduce the force to the required value. The equations are then re-solved using the calculated values for $\{S\}$.

5.3 IDEALISATION OF THE JOINT

For an initial study a simple model for the joint has been used. Yielding due to end moments only has been considered. The

beam behaves elastically up to a yield limit and then yields at this constant moment. This may be used as a first approximation to the real behaviour of a joint (Fig. 5.1).

5.4 SOLUTION PROCEDURE

The first stage is to calculate the moment reduction at the joints caused by a relative acceleration. A matrix [STS] can be built up where $STS_{i,j}$ is the moment reduction at joint j due to unit relative acceleration at joint i. The values for the matrix [STS] are calculated using equation 4.21. For each constrained joint i, the relative acceleration S_i is individually set to unity. Equation 4.21 is then solved for each of these cases. The forces due to the relative accelerations are immediatly available from the values of $\{\lambda\}$ as shown in the previous chapter. The matrix [STS] is symmetrical and thus for computational convenience, only terms on and above the leading diagonal need be used.

Solution then proceeds in the normal manner with all $\{S\}$ set to zero. At the end of each interval the forces at each constrained joint are given by the calculated values of $\{\lambda\}$. The moment MI_i at joint i can then be compared with the yield value MA_i.

For a structure with n constrained joints the method employed is shown in Fig. 5.2. The excess moment EXM_i at joint i is calculated. For any joint where the yield limit MA_i is exceeded a logical variable $SLIP_i$ is set to .TRUE. The absolute value of the moment MI_i is used to calculate the excess moment by comparison with a positive yield limit. The correct sign is then

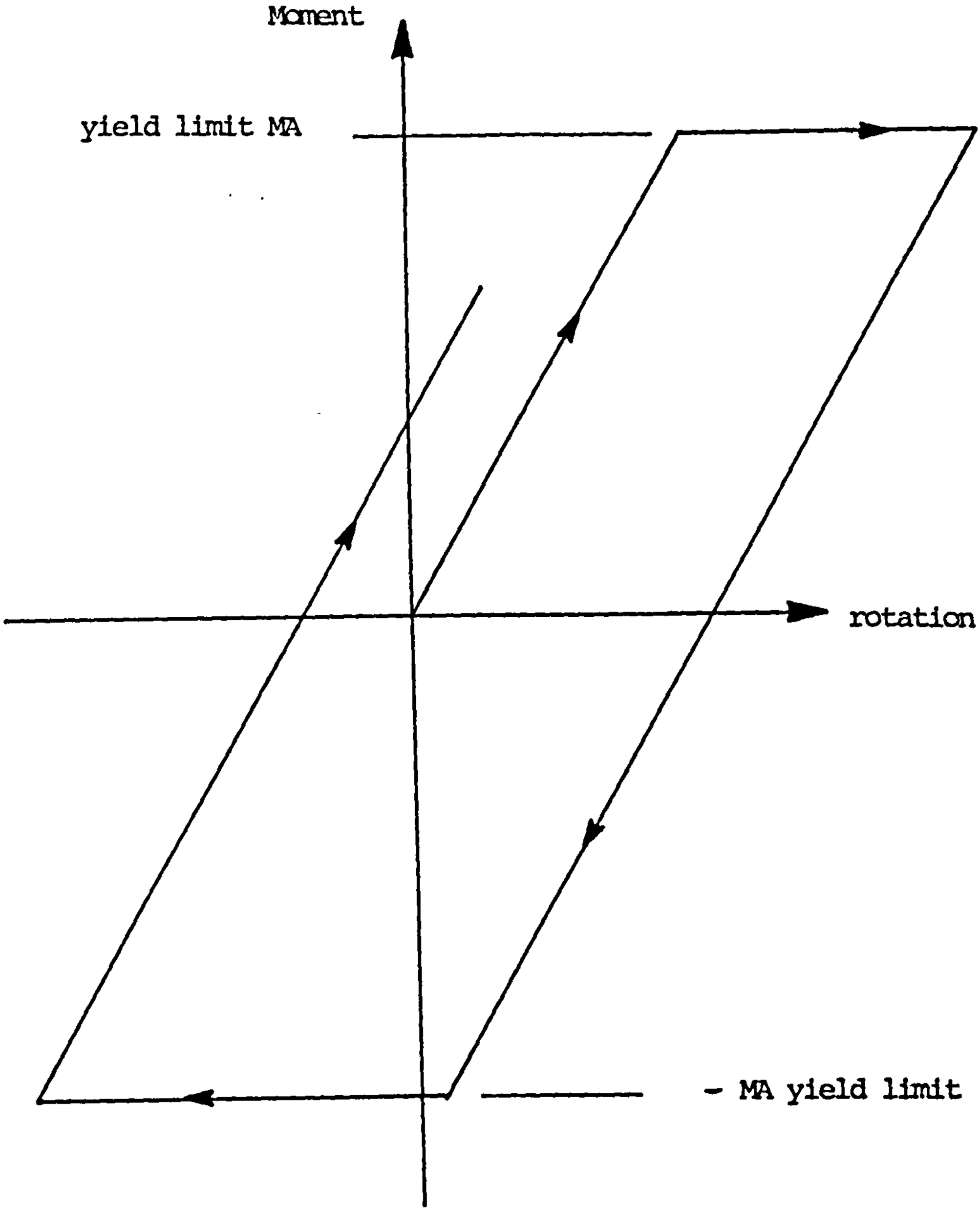

Fig 5.1

Joint Hysteresis

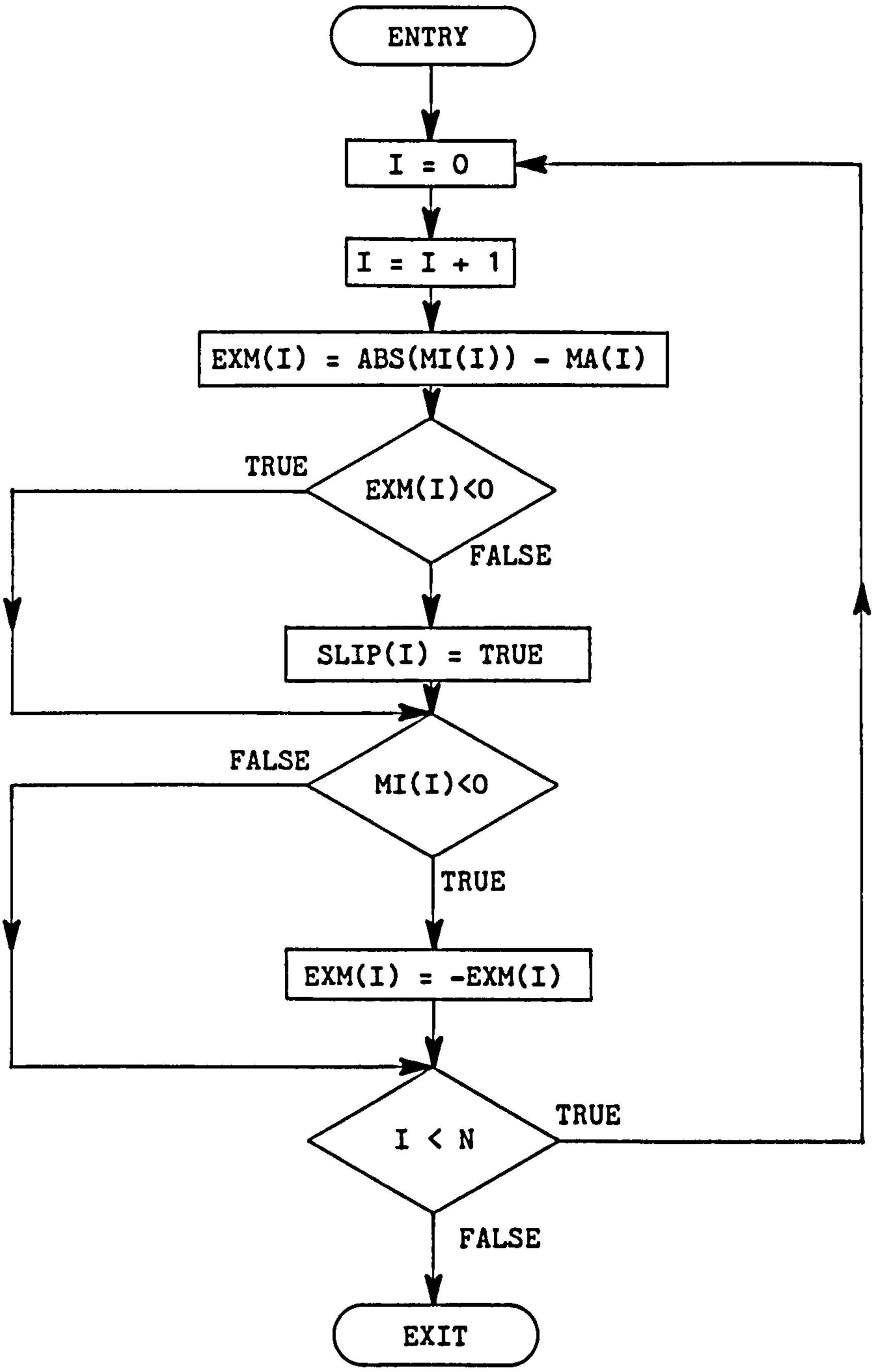

Fig. 5.2

Calculation of EXM

restored to the excess moment depending upon the sign of the moment MI_i.

The logical variables $SLIP_i$ may then be used to assemble a set of simultaneous equations for the yielding joints (Fig. 5.3). The excess moment at each joint is equated with the moment reduction caused by relative accelerations at these joints. They may then be solved to give the relative accelerations necessary to limit the moments to the yield values.

The coefficients from [STS] are assembled into a matrix [SOL] for the yielding joints only. The excess moments for these joints are assembled into an array {RHS} . The relative accelerations {S } may then be calculated from

$$[SOL]\ \{S\} = \{RHS\} \qquad 5.1$$

by Guassian elimintation and back substitution.

When all the joints are yielding this equation will be identical to

$$[STS]\ \{S\} = \{MI\} - \{MA\} \qquad 5.2$$

Equation 5.1 is a reduced form of this equation for yielding joints only.

At this stage two checks must be performed. The forces at non-yielding joints will have changed due to the redistribution of the stresses in the structure. The final moments MF at the non-yielding joints are calculated. These are then checked, to see if any other joints have reached the yield value. If so, SLIP must be set to .TRUE. for these joints and the procedure repeated from the assembly and solution of equation 5.1. The flow chart for this is shown in Fig. 5.4

The direction of yielding must be checked. Yielding at one

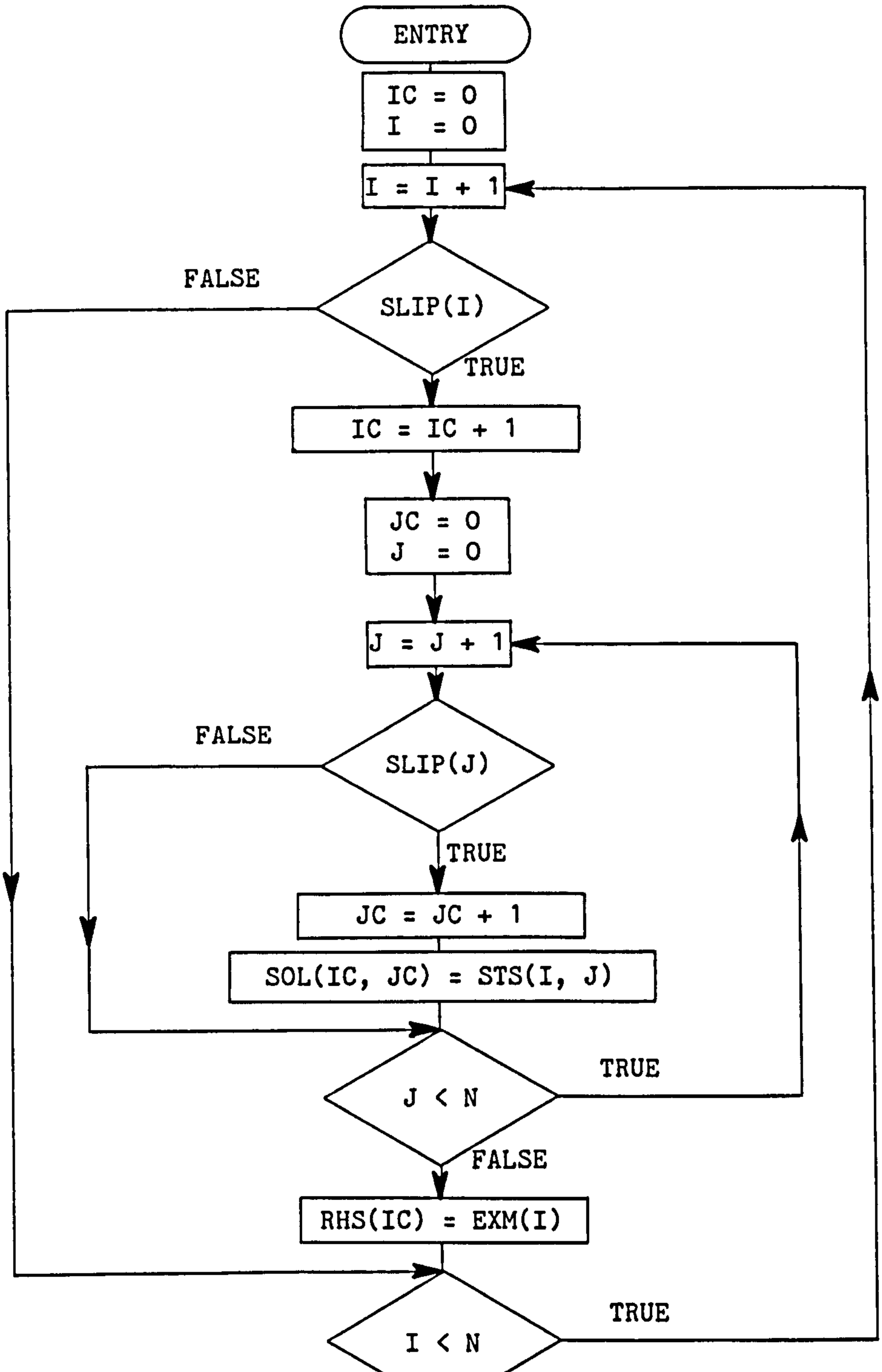

FIG. 5.3

Assembly of [SOL] matrix

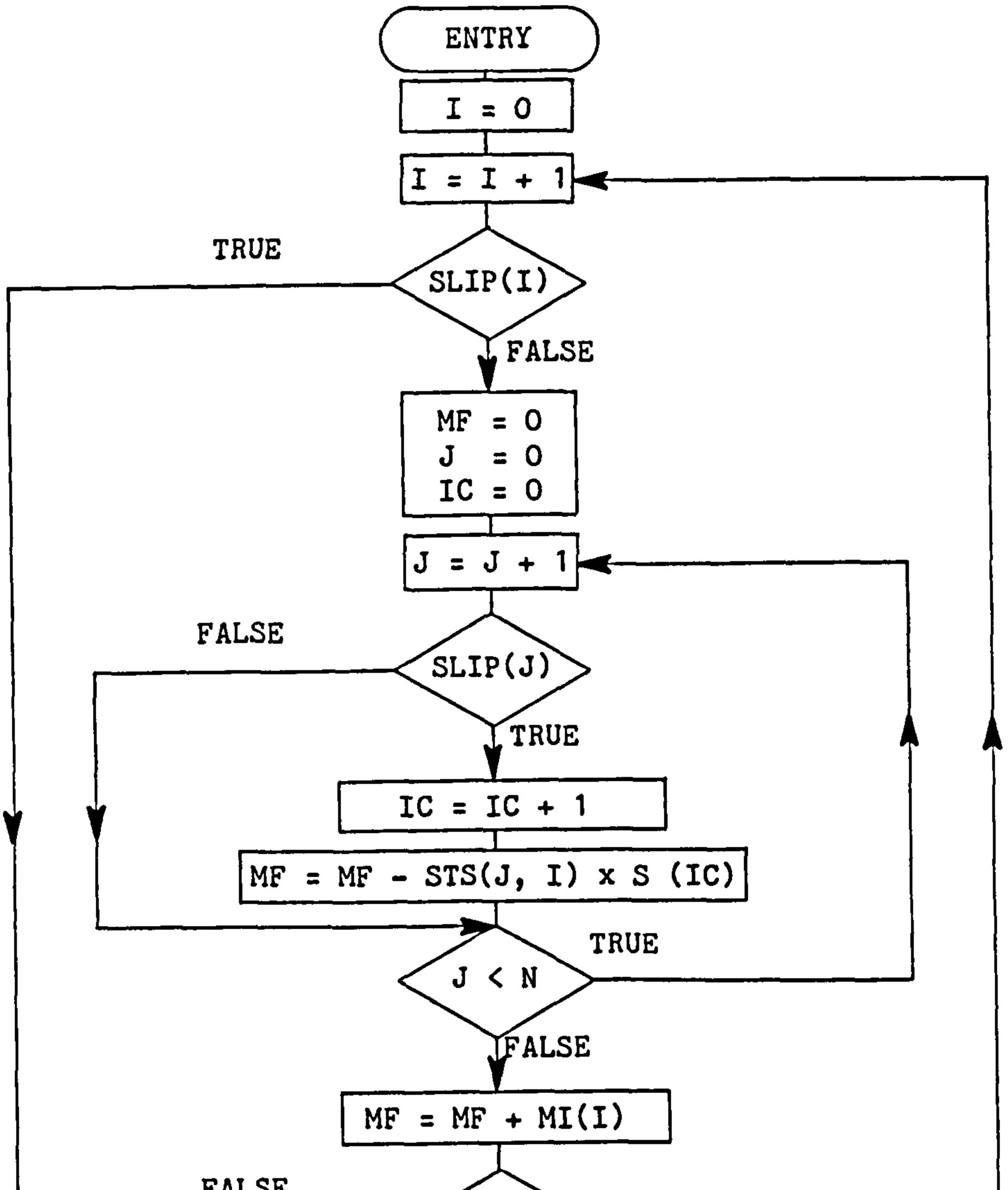

FIG. 5.4

Check for further yielding

joint may reduce the moment at another. This occurs when there is a joint at both ends of a beam such as a coupling beam in a shear wall system. Occasionaly, the yielding at one end i may reduce the moment at the other end j from above to below the yield value. When this happens equation 5.1 will still force the joint j to yield. However, this will now be in the wrong direction as it is increasing the moment there to the yield value. The equation for joint j must be removed from equation 5.1 and the procedure repeated from the assembly and solution of this equation. The direction of yielding may be checked from the product of STS_{jj}, S_j and MI_j which must be positive. If it is not positive $SLIP_j$ is set to .FALSE.

The values of {S} which satisfy these two checks may then be used to re-solve equation 4.21 for the time step. The velocities and displacements are then calculated for the step. The joints which have yielded during the step will now have relative accelerations, velocities and displacements. The relative displacements are the desired results but the accelerations and velocities will cause the joints to continue yielding during the next time step. This is prevented by calculating the acceleration and velocity of the beam end from the constraint equation 3.9. This produces

$$\dot{\theta}_j = \frac{1}{d_b} (\dot{u}_i - \dot{u}_k) \qquad 5.3$$

$$\ddot{\theta}_j = \frac{1}{d_b} (\ddot{u}_i - \ddot{u}_k) \qquad 5.4$$

when used for velocity and acceleration.

The solution may then continue to the next time step.

5.5 BILINEAR JOINT MODEL

Rather than yielding at a fixed moment, the joint may be modelled to yield at a reduced stiffness (Fig. 5.5). The moment at a yielding joint is given by MA plus an amount MX, proportional to the constrained relative displacement θ'. It can be seen (Fig. 5.6) that

$$\theta_1 = \frac{MX}{K_1} \qquad 5.5$$

$$\theta_2 = \frac{MX}{k_2} \qquad 5.6$$

Hence

$$\theta' = \frac{MX}{k_1} - \frac{MX}{k_2} \qquad 5.7$$

This may be rearranged to produce

$$MX = \frac{\theta'}{\frac{1}{k_2} - \frac{1}{k_1}} \qquad 5.8$$

The constrained relative displacement θ' can be calculated from the relative acceleration S using equation 4.14

$$\theta' = \beta . \Delta t^2 \; S \qquad 5.9$$

Substituting into equation 5.9 produces

$$MX = \frac{\beta \Delta t^2}{\frac{1}{k_2} - \frac{1}{k_1}} \; S \qquad 5.10$$

or more compactly

$$MX = Q \; S \qquad 5.11$$

Adding MX to MA in equation 5.1 produces

$$[STS] \{ S\} = \{MI\} - \{MA\} - [Q] \{S\} \qquad 5.12$$

in which [Q] is a diagonal matrix.

This may be rearranged for solution to produce

$$[[STS] + [Q]] \{S\} = \{MI\} - \{MA\} \qquad 5.13$$

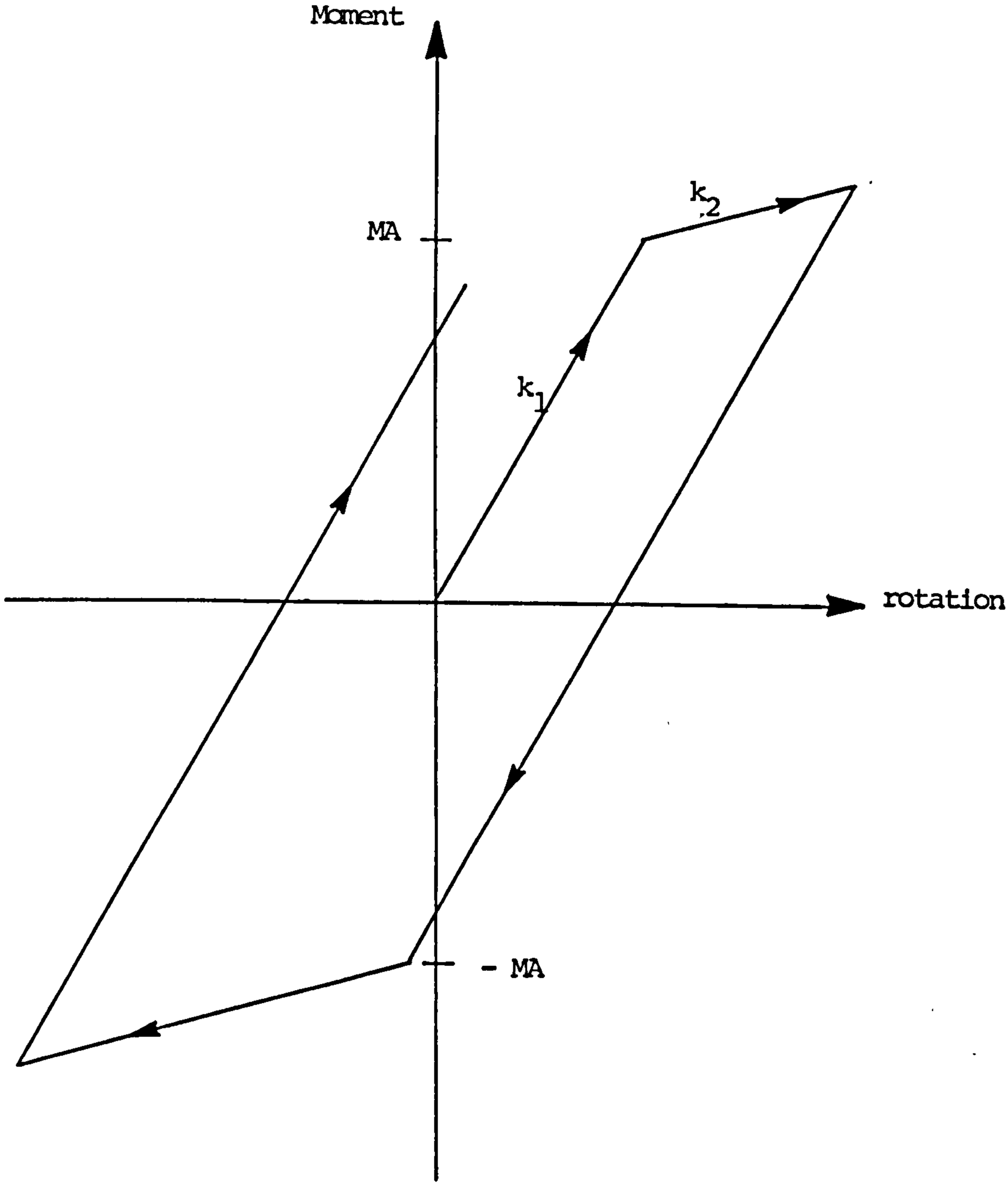

k_1 = stiffness before yielding

k_2 = stiffness after yielding

Fig 5.5

Bilinear Joint Model

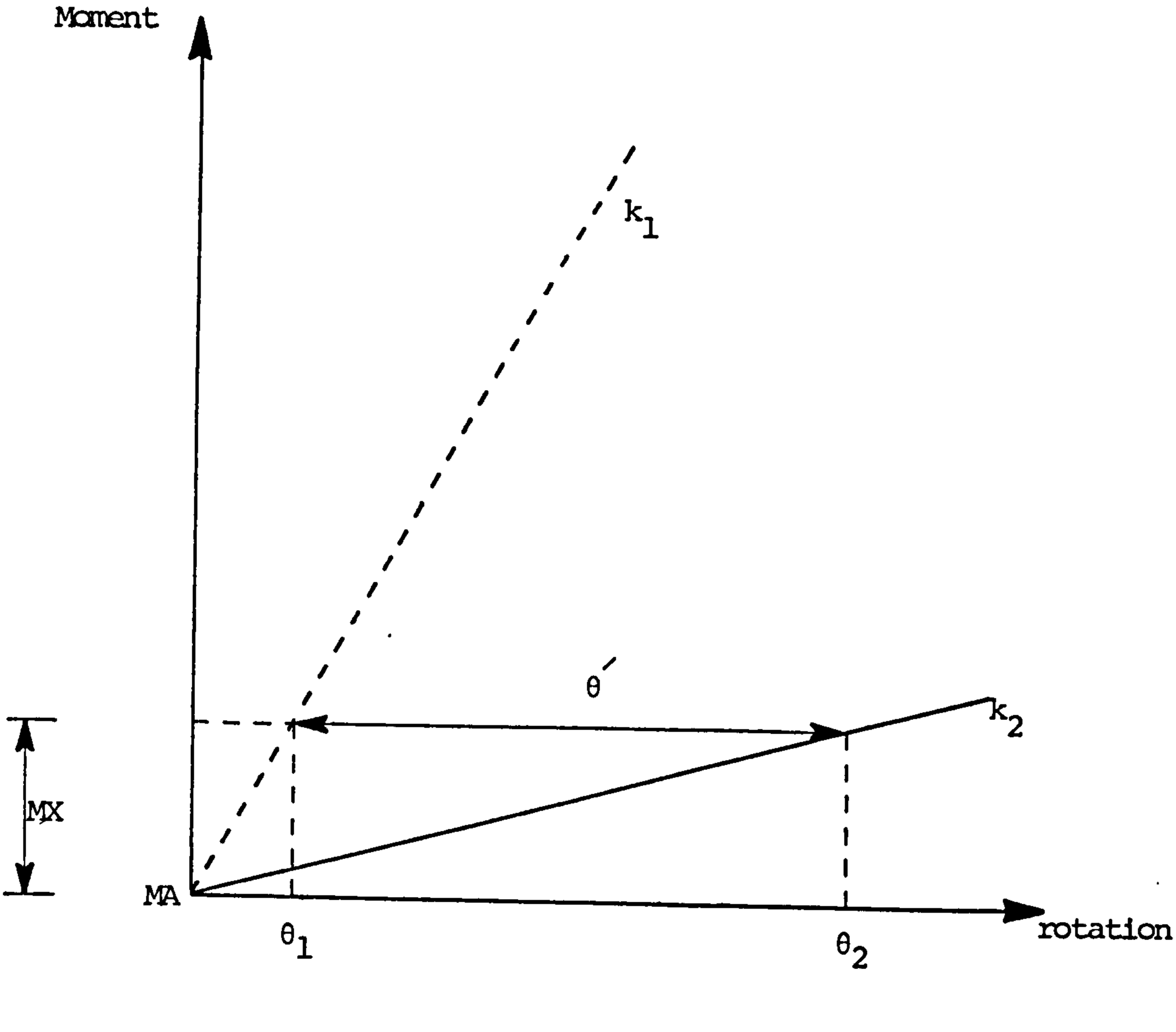

Fig 5.6

Relationship Between MX and θ'

which is identical to equation 5.2 except that the diagonal terms of [STS] are increased by the parameter Q. Exactly the same solution procedure may be used as previously for the constant moment yielding.

If the yielding stiffness k_2 is expressed as a percentage Ps of the initial stiffness k_1 then

$$k_2 = \frac{P_s}{100} k_1 \qquad 5.14$$

Substituting into equation 5.10 and rearranging produces

$$Q = \frac{\beta \Delta t^2 P_s k_1}{100 - P_s} \qquad 5.15$$

Using this equation the value of Q may be calculated to give the required stiffness.

CHAPTER SIX - COMPARISON OF THE FINITE ELEMENT SCHEMES

6.1 INTRODUCTION

The various finite element schemes described in chapters 2 and 3, for the analysis of coupled shear walls, are compared in this chapter. The method employed by Al-Mahaidi and Nilson [49] is discussed and used as a basis for this comparison. They compared the convergence of their Lagrange multiplier scheme to that of the quadrilateral isoparametric element, with increasing degrees of freedom. Their results, the behaviour of the rectangular element with rotational degrees of freedom and the Lagrange multiplier schemes are studied.

Al-Mahaidi and Nilson examined the convergence of their scheme using an eight storey, symmetrical coupled shear wall. The dimensions of the wall are shown in Fig. 6.1. The wall was subjected to a concentrated load P at the top and the tip deflection Δo plotted against the degrees of freedom employed. The tip deflection was plotted in the dimensionless form of a flexibility parameter

$$\frac{\Delta o \; E \; t}{P}$$

where

Δo = tip deflection at centre-line

E = modulus of elasticity

t = thickness

P = applied load

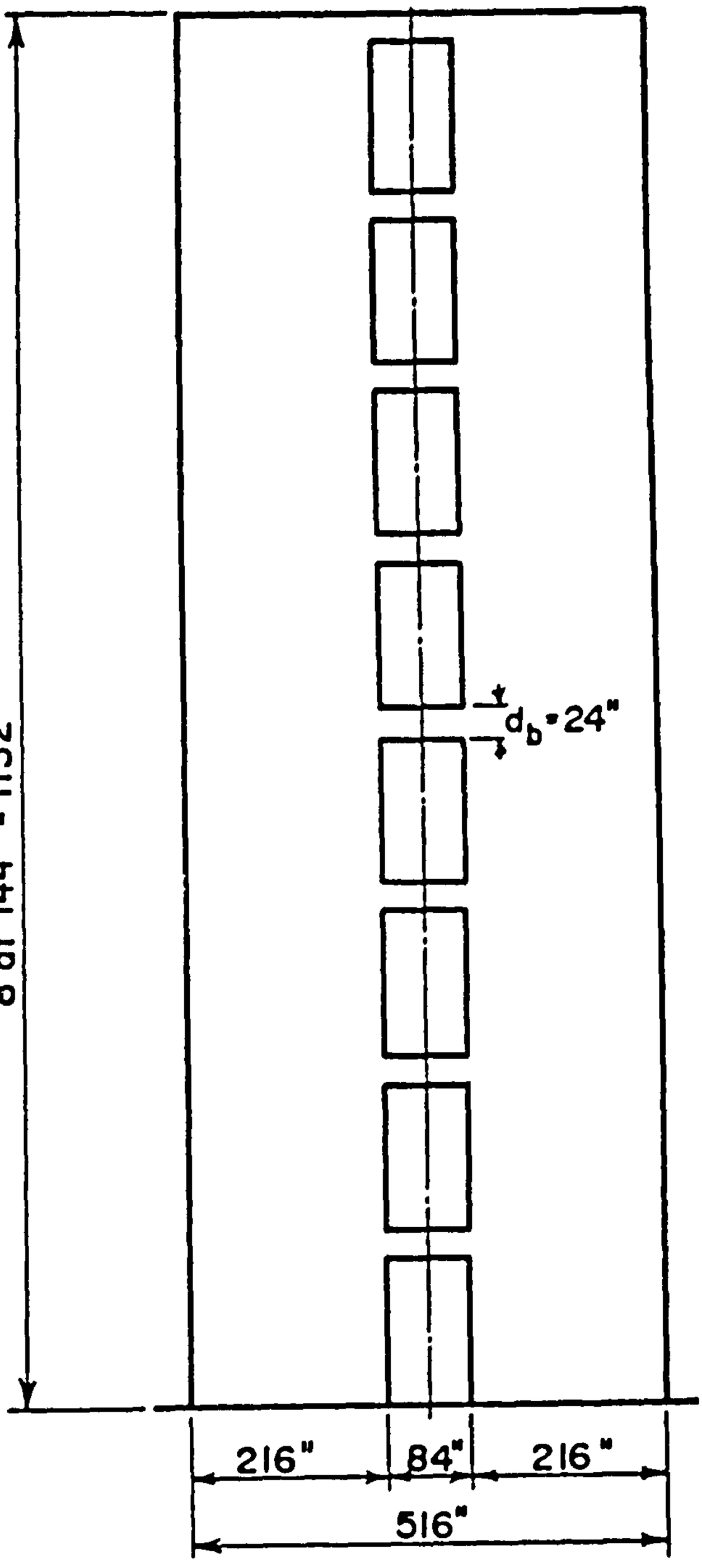

24" = 0.61m
84" = 2.13m
144" = 3.66m
216" = 5.49m
516" = 13.11m
1152" = 29.26m

Figure 6.1

Dimensions of Al-Mahaidi's Wall

For consistency, rotations and moments are treated in a similar manner in this chapter. Rotations θ are expressed as

$$\frac{\theta E t d_b}{P}$$

and the moments M as

$$\frac{M}{Pd_b}$$

where d_b = beam depth

This obviates the need to specify values for E, t and P.

6.2 METHOD OF LOAD APPLICATION

Forces from the floor slabs transmit to the shear walls as line loads. The distribution of these loads was assumed to be parabolic (Fig. 6.2) by Al Mahaidi et al. They must be converted to equivalent nodal loads for the finite element anlysis. This may be accomplished in two different ways.

Consistent loads:

The equivalent nodal loads $\{P\}$ are calculated from the distributed loads $\{L\}$ so that equality of work is established with the nodal forces and displacements.

$$\{P\} = \int [N]^T \{L\} \; d(vol) \qquad 6.1$$

The mesh shown in Fig. 6.2 is used to demonstrate this. The edge is subject to a parabolic shear load where the shear τ at any point is given by

$$\tau = \frac{3}{2} \frac{\overline{P}}{D} \left(1 - \frac{4x^2}{D^2}\right) \qquad 6.2$$

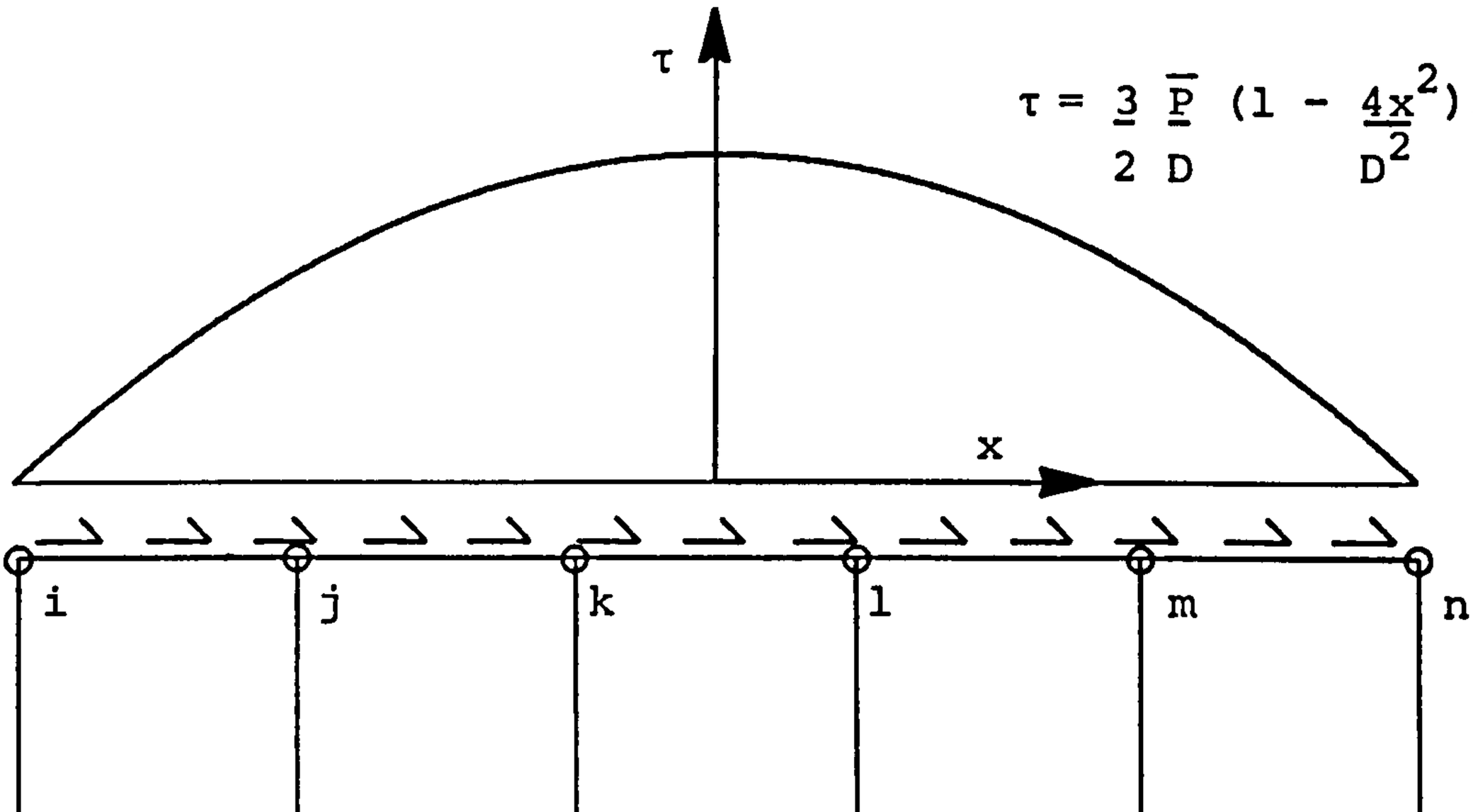

FIG. 6.2

Wall mesh subject to parabolic distribution shear load.

At the top of the element $\eta = 1$ (Fig. 2.1) and so the shape functions 2.19 become

$$N_1 = 0 \qquad 6.3$$

$$N_2 = 0$$

$$N_3 = \tfrac{1}{2}(1 + \xi)$$

$$N_4 = \tfrac{1}{2}(1 - \xi)$$

The shape function corresponding to the node n is N_3 and thus

$$Pn = \int_{3D/10}^{D/2} \frac{1}{2}(1 + \xi)\,\frac{3}{2}\,\frac{\overline{P}}{D}\left(1 - \frac{4x^2}{D^2}\right) dx \qquad 6.4$$

where

$$\xi = \frac{10x}{D} - 4 \qquad 6.5$$

which when evaluated produces

$$P_n = 0.036\,\overline{P}$$

Similar integrations are performed to give the loads at the other nodes.

<u>Lumped loads</u>:

A much simpler approach is to lump the load to the nearest node. For node n this tributary area method gives

$$P_n = \int_{4D/10}^{D/2} \frac{3}{2}\,\frac{\overline{P}}{D}\left(1 - \frac{4x^2}{D^2}\right) dx \qquad 6.6$$

$$= 0.028\,\overline{P}$$

with similar integrations producing the remaining nodal loads.

This differs from the result obtained by Al-Mahaidi et al. who based tributary area calculations on a rectangular load distribution instead of on the parabolic distribution used previously. The equivalent nodal loads for consistent and lumped formulations for the parabolic distribution and lumped formulation

for the rectangular distribution may be compared in table 6.1.

Al-Mahaidi el al. compared the results from the consistent load formulation with a parabolic distribution against those from the lumped formulation with a rectangular distribution. From this they concluded that the difference between the consistent and lumped formulation is significant and that the consistent formulation should be used. However, examining the results from the lumped formulation with a parabolic distribution, it can be seen that most of the difference is due to the change of distribution.

The mesh of Fig. 6.3 was used to compare the results of using the consistent and lumped formulations both with the parabolic distribution. With the consistent formulation, the tip deflection $\Delta o\ E\ t\ /P$ was 104.0308. Using the lumped formulation the deflection was 104.0342. The difference, being less than 0.004%, cannot be considered significant. It is therefore concluded that the simpler lumped formulation is to be prefered. However, for the purpose of comparison with Al-Mahaidi's results, the use of the consistent formulation is retained.

6.3 COMPARISON OF CONVERGENCE

The various schemes were compared using the shear wall shown in Fig 6.1. The following assumptions made by Al Mahaidi et al. are retained to enable comparison with their results.

1. The top coupling beam has half the stiffness of the others.
2. Each wall of the coupled system takes half the load, $\overline{P} = P/2$, distributed in a parabolic manner at the top.

		Nodal loads as a proportion of $\bar{P}$	
		Consistent formulation	Lumped formulation
Parabolic Distribution	$P_i = P_n$	0.036	0.028
	$P_j = P_m$	0.184	0.188
	$P_k = P_l$	0.280	0.284
Rectangular Distribution	$P_i = P_n$		0.1
	$P_j = P_m$		0.2
	$P_k = P_l$		0.2

Table 6.1

Nodal Load Distributions

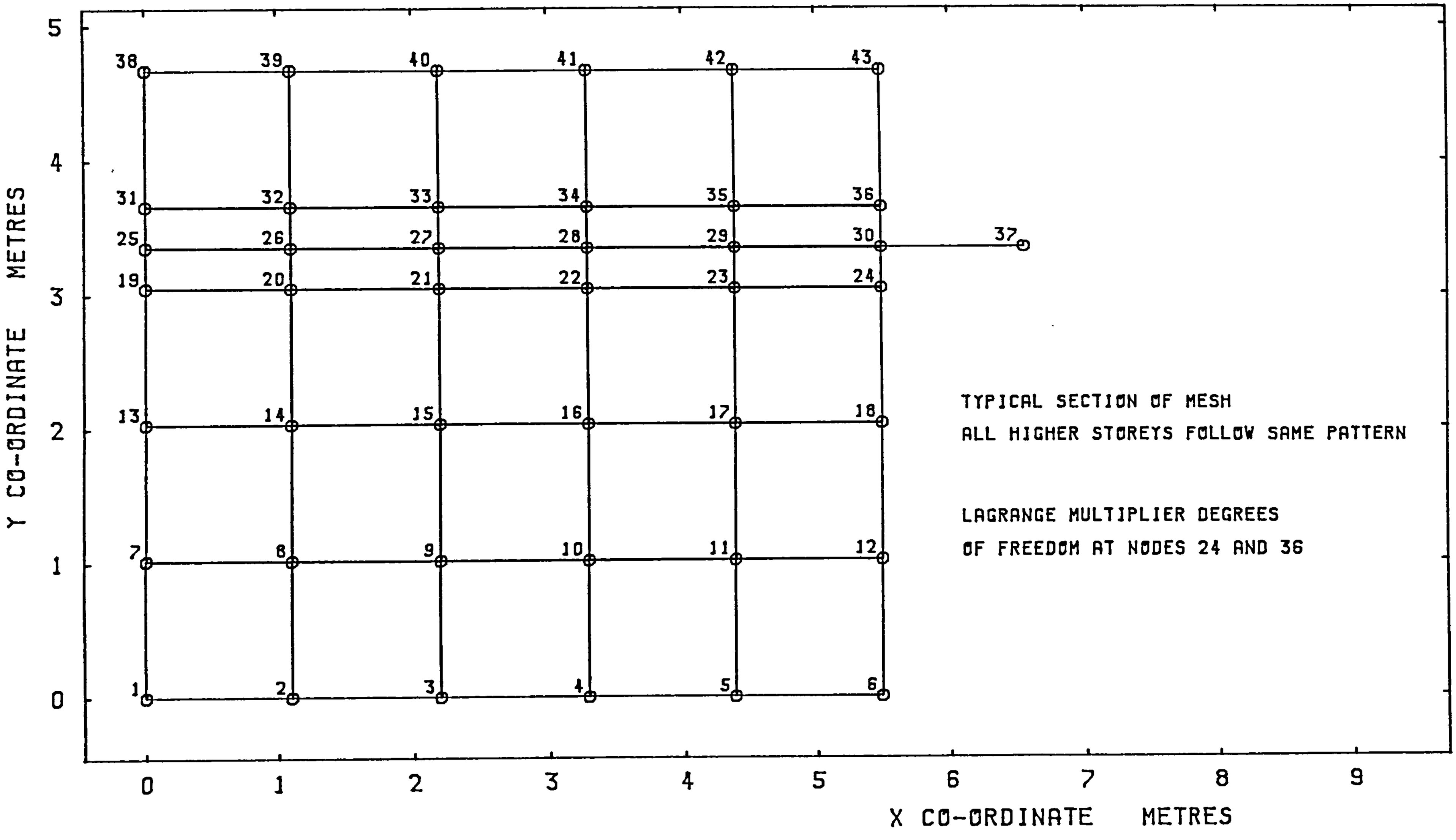

FIG 6.3

AL-MAHAIDI'S CONSTRAINT SCHEME 5 ELEMENT MESH

3. Owing to the symmetry of the structure, and the loading, it is possible to use only half the structure for analysis. This is accomplished by assuming a roller support at the mid-span of each coupling beam. This cannot be done when plane stress elements are used to model the beams as a roller support can not be placed at the beam centre line. In this case the whole structure is analysed and the number of degrees of freedom used is halved for comparison with the others.

Poisson's ratio:

Al-Mahaidi et al. do not state the value of Poisson's ratio used in their study. However, the value assumed does not greatly affect the results obtained and does not alter the relative stiffness of the schemes. A value of 0.2 gave results in agreement with those obtained by Al-Mahaidi et al. for the scheme with quadrilateral isoparametric elements only and is used in this study.

6.4 AL-MAHAIDI'S CONSTRAINT SCHEME

Al-Mahaidi et al. compared their Lagrange multiplier constrainted scheme against the use of quadrilateral isoparametric elements only. They found that their Lagrange multiplier scheme produced the more flexible results. The program written for this study produced stiffer results with Al-Mahaidi's Lagrange multiplier scheme as shown in Fig. 6.4. It is believed that the results of this study are correct.

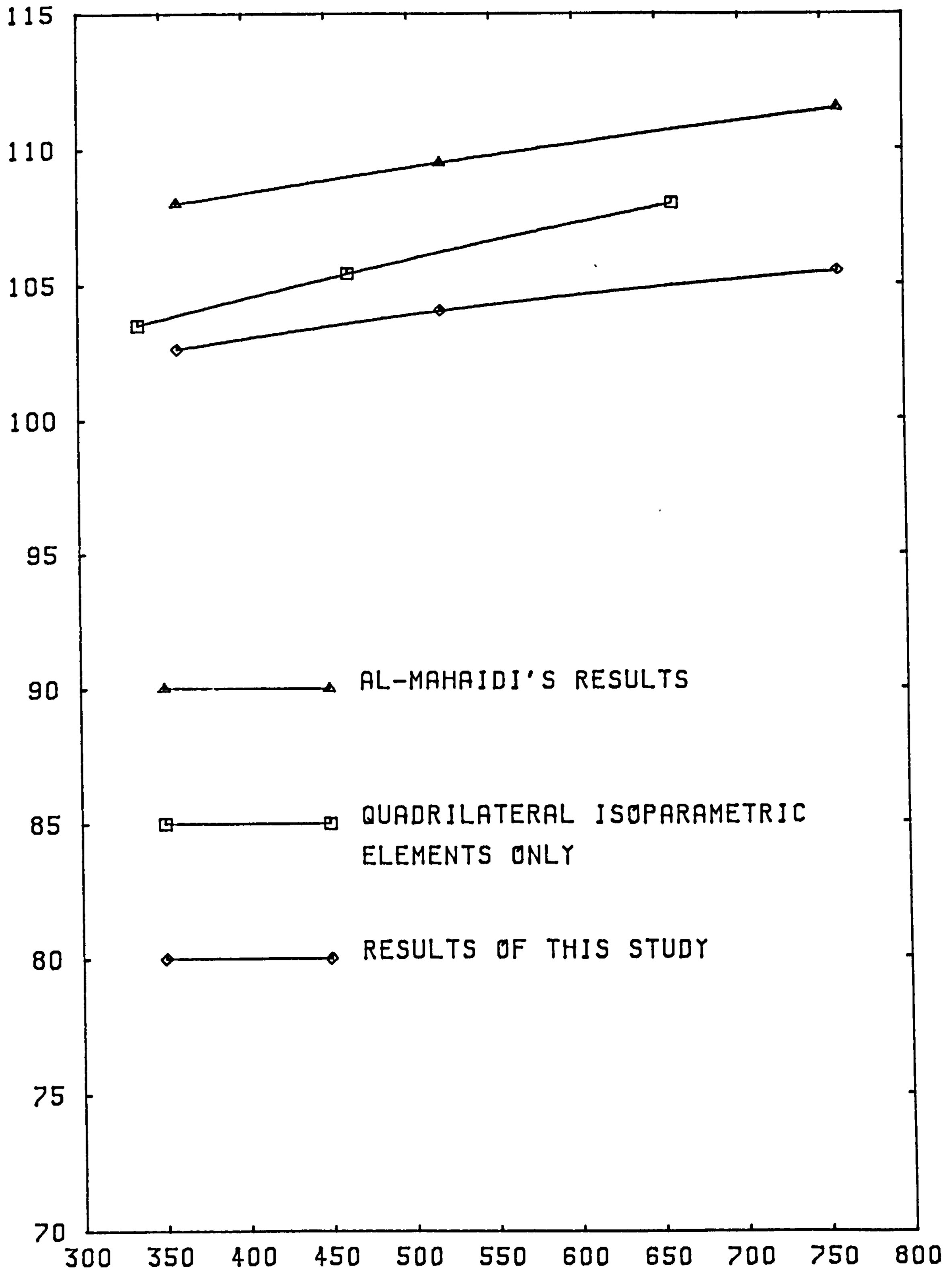

FIG 6.4

CONVERGENCE CURVES FOR AL-MAHAIDI'S CONSTRAINT SCHEME

Antony and Garesan [24] used Al-Mahaidi's Lagrange multiplier scheme to analyse a different coupled shear wall. This analysis was repeated and the results from the program were found to be in complete agreement with the results of Antony and Ganesan.

6.5 RECTANGULAR PLANE STRESS ELEMENT WITH ROTATIONAL DEGREES OF FREEDOM

Agrawal and Mufti [22] used a rectangluar plane stress element with a rotational degree of freedom at each node, and the flexural line element, to analyse the coupled shear wall. They found that they achieved the same tip deflection as Al-Mahaidi with a much lower number of degrees of freedom. From this they conclude that better accuracy can be obtained with their method. However, they used the corner deflection where Al-Mahaidi used the centre-line deflection to plot convergence curves. Their results are, therefore, not directly comparable.

The deflections obtained by Agrawal and Mufti are plotted in Fig. 6.5. For comparison the corner deflections obtained using Al-Mahaidi's constraint scheme and using an element MEM4 [67] in a commercial program are also shown. It can be seen that for Agrawal and Mufti's scheme thre is no significant convergence with increasing numbers of degrees of freedom. The results from the MEM4 element, which also employs a rotational degree of freedom at each of its four nodes, are very similar.

Two meshes, Fig. 6.6 and Fig. 6.7 were used to investigate further the behaviour of the element used by Agrawal and Mufti. Both meshes have the same number of degrees of freedom (400) but with different element layouts. Both horizontal and vertical bias

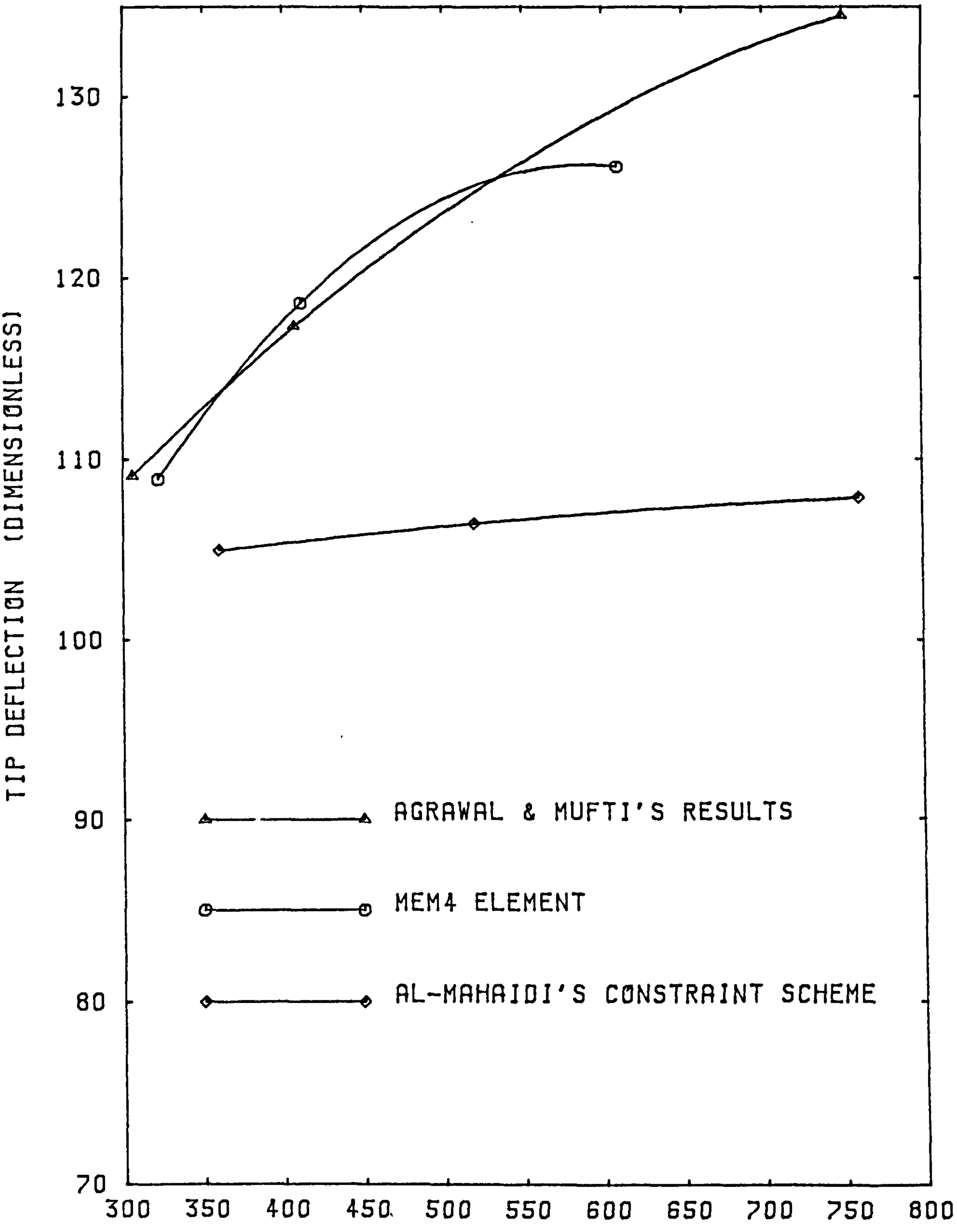

FIG 6.5

CONVERGENCE CURVES USING CORNER DEFLECTION

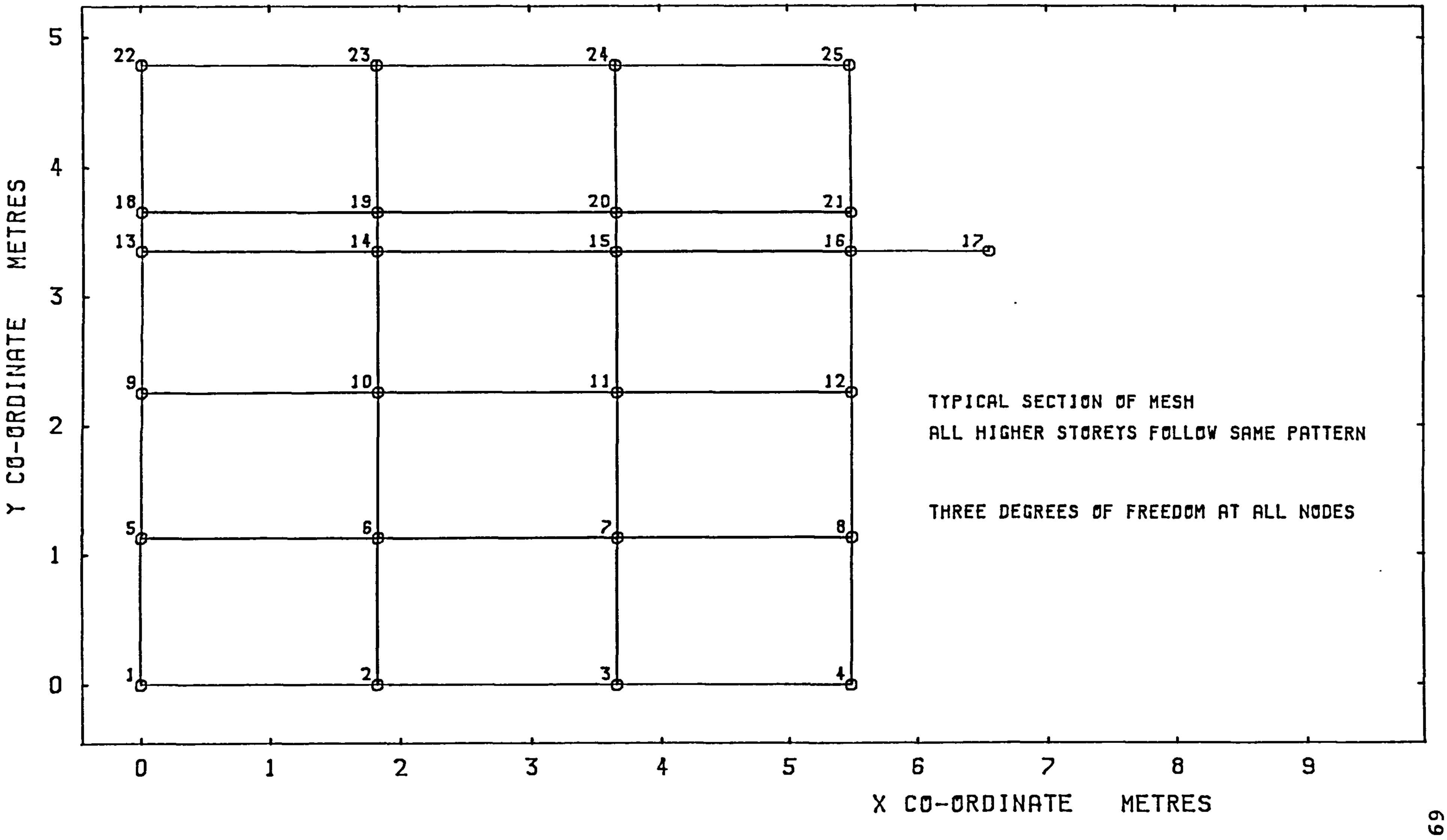

FIG 6.6

FIRST MESH FOR ELEMENT WITH ROTATIONAL FREEDOMS

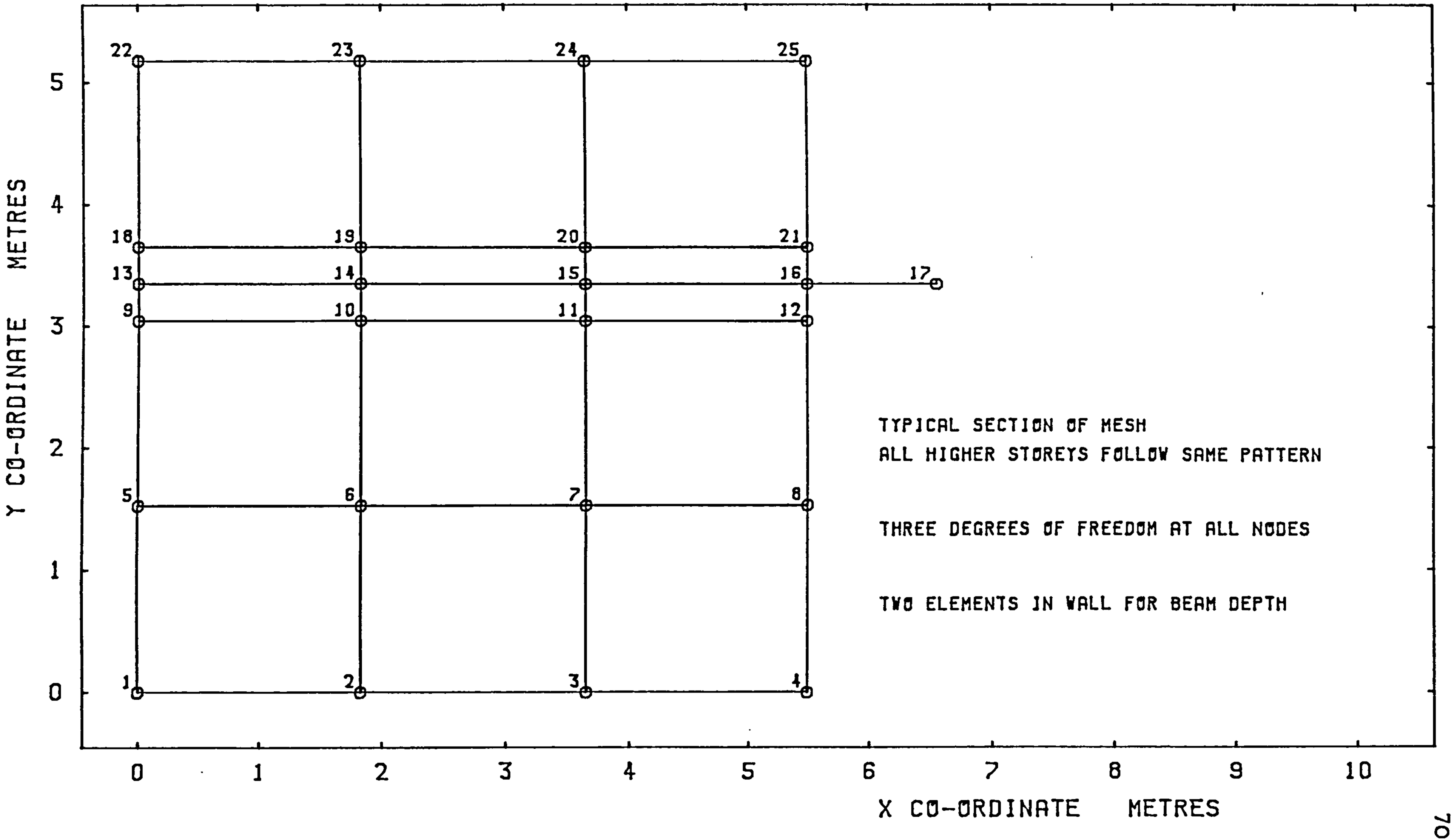

FIG 6.7

SECOND MESH FOR ELEMENT WITH ROTATIONAL FREEDOMS

directions were used with each mesh. The centre-line tip deflections and coupling beam moments obtained are shown in Fig. 6.8 and Fig. 6.9. All four analyses gave very large deflections, an explanation for which may be found in the modelling of the wall-beam junction.

The results for a typical connecting beam are presented in table 6.2 where the end rotation of the beam is compared with the rotation of the wall calculated from the x-direction displacements of the wall nodes. The seventh storey connecting beam was selected for this purpose as the rotations are largest towards the top of the wall. The eighth storey beam was not used as it is not typical, being of half the stiffness of the other beams.

The Lagrange multiplier technique makes the end rotation of the beam compatible with the rotation of the wall over the full depth of the beam. The use of the plane stress element with rotational degrees of freedom makes the beam rotation compatible with the wall rotation at a single point at the beam centre-line. This produces a connection which is much more flexible as the single node on the wall can rotate without significantly affecting the x-direction displacements of the wall nodes. This is illustrated in Fig. 6.10.

By substituting the nodal displacements into equation 2.33, the deflected shape at the face of the wall may be calculated. This is plotted in Fig. 6.10 for the seventh storey connecting beam of mesh Fig. 6.7 with a vertical bias. The end face of the connecting beam is also shown. It can be seen that at the beam centre-line the deflections are compatible but that within a very small distance of the centre line the displacements are quite

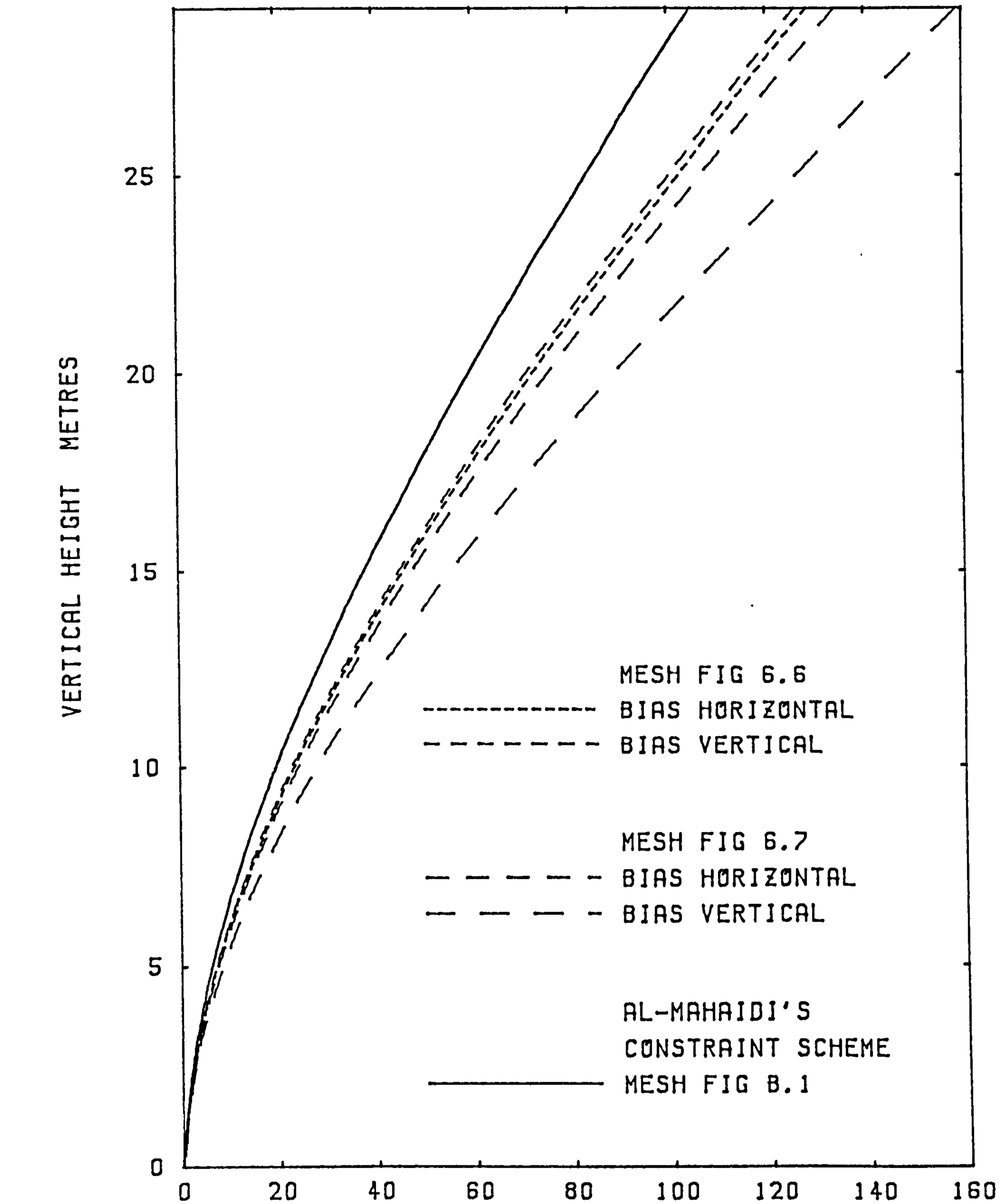

FIG 6.8

EDGE DEFLECTION OF MODELS USING ROTATIONAL FREEDOM ELEMENTS

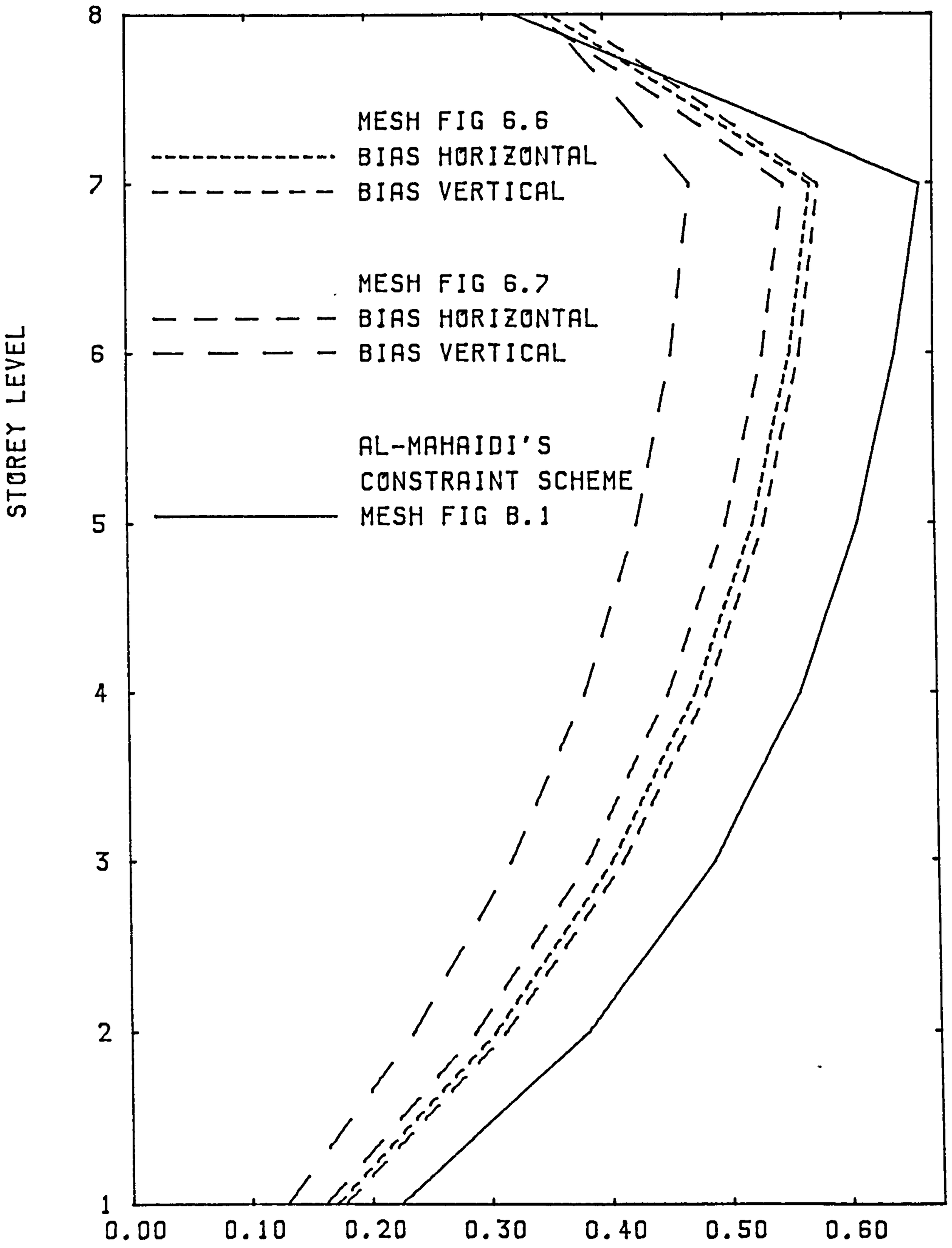

FIG 6.9

COUPLING BEAM END MOMENTS

Finite element model		Beam end rotation	Wall rotation	Beam end moment
Al-Mahaidi's constraints		-1.34	-1.34	-0.67
Wall face oriented connection		-1.34	-1.34	-0.67
Proposed constraints		-1.34	-1.34	-0.67
Rectangular element with rotational degrees of freedom	Fig 6.6 bias horizontal	0.78	-3.34	-0.57
	Fig 6.6 bias vertical	1.28	-3.48	-0.58
	Fig 6.7 bias horizontal	1.40	-3.22	-0.55
	Fig 6.7 bias vertical	5.30	-4.22	-0.47

Table 6.2

Beam End Rotations and Moments

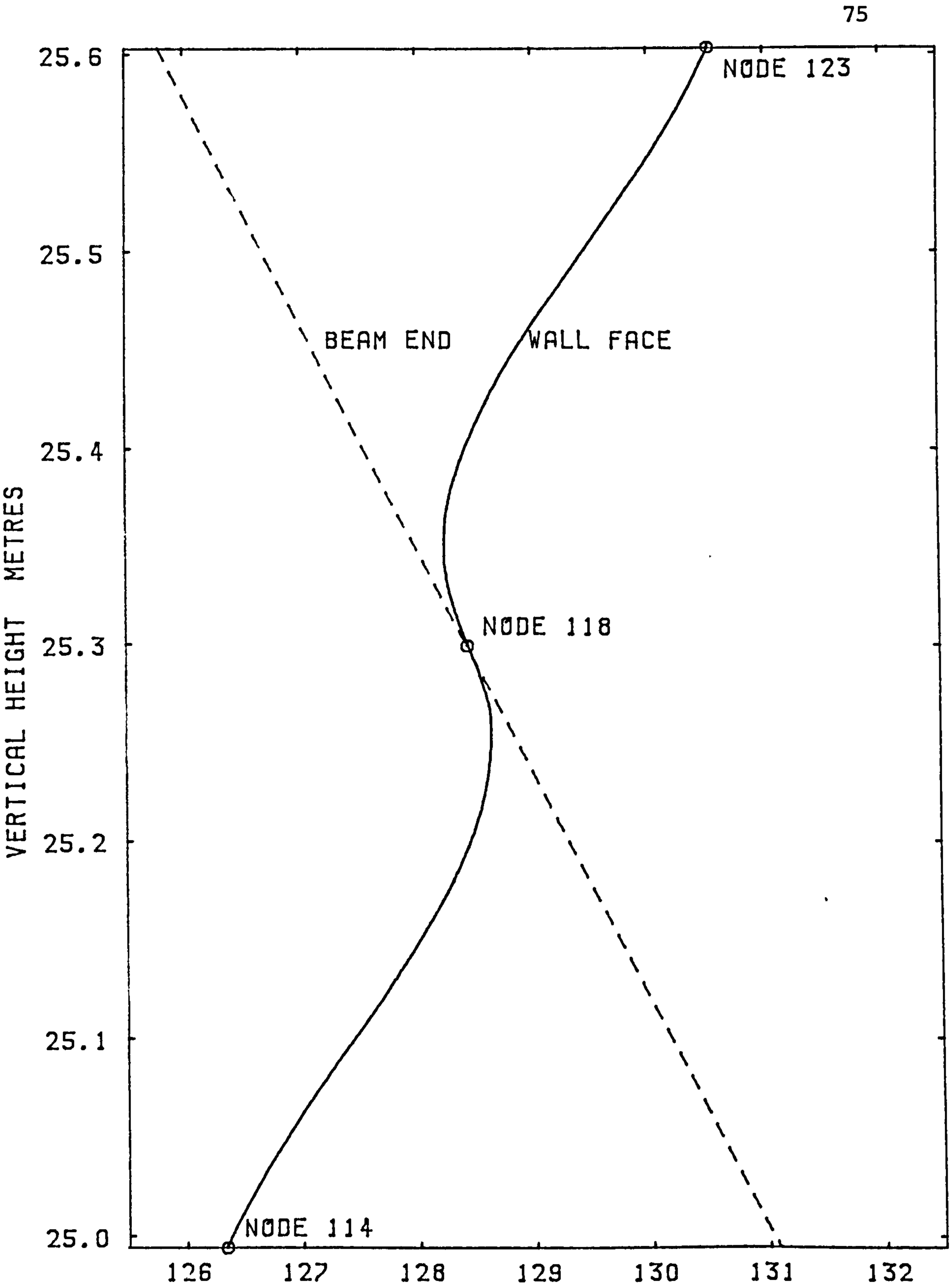

FIG 6.10

DEFLECTED SHAPE AT 7TH STOREY WALL-BEAM JOINT

incompatible and the rotations are in opposite directions.

The same wall without the coupling beams was analysed using the two types of plane stress element to compare their flexibility. The same mesh (Fig. 6.11) was used for each analysis and the results were found to be in very close agreement (table 6.3). However, the element scheme with rotational degrees of freedom used 50% more degrees of freedom to achieve this.

The plane stress element with rotational degrees of freedom, when used to model a coupled shear wall, achieves its greater flexibility through unrealistic modelling of the wall-beam joint. This produces a false distribution of the forces in the structure. The forces in the coupling beams are underestimated and the two halves of the wall behave with greater independence and less as a coupled system.

It can also be seen (Table 6.2 and Figs. 6.8, 6.9) that the results are sensitive to the direction of bias and the element layout when the place stress element with rotational degrees of freedom is used.

It is therefore concluded that this element is not suitable for use when modelling structures where beams are connected to shear walls as in a coupled shear wall or a shear wall-frame system.

The MEM4 element used with the flexural line element gave similar results. It can be concluded that the lack of displacement compatibility at the joint will always lead to an underestimate for joint stiffness. The wall will be able to deform locally instead of over the full depth of the beam.

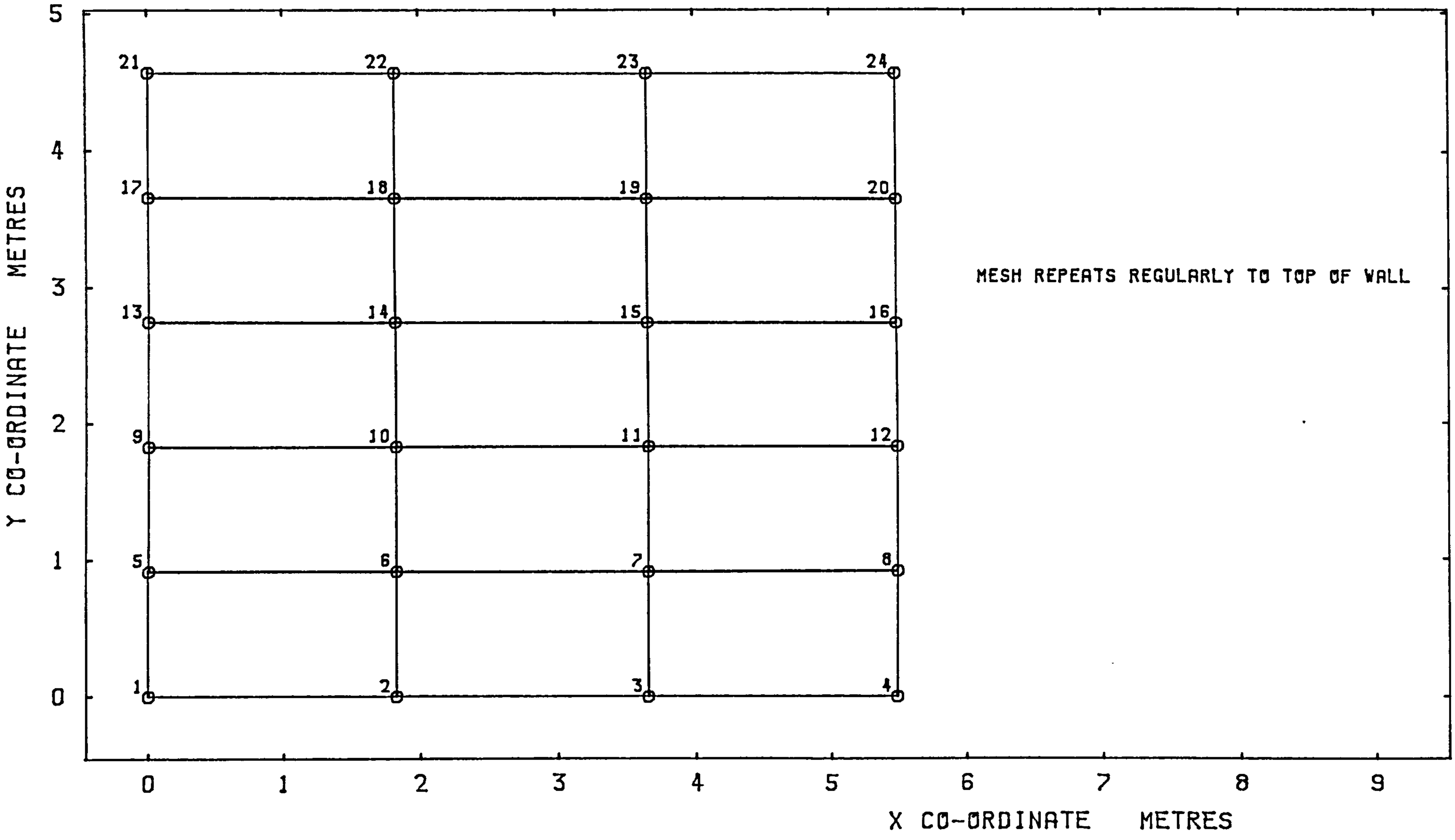

FIG 6.11

ELEMENT MESH FOR ANALYSIS OF PLAIN WALL

		Degrees of Freedom	Dimensionless Deflection
Quadrilateral Isoparametric Element		256	309.8
Rectangular Element with rotational degrees of Freedom	Bias Horizontal	384	305.5
	Bias Vertical	384	308.2

Table 6.3

Tip Deflection of Walls Without coupling beams

6.6 COMPARISON OF THE LAGRANGE MULTIPLIER CONSTRAINT SCHEMES

Three different schemes are compared for convergence using three different element meshes for each (Appendix B). For Al-Mahaidi's constraints, the wall face oriented connection of Antony and Ganesan and the proposed constraint scheme, the tip deflection $\Delta o\ E\ t\ /P$ is plotted against the number of degrees of freedom used in Fig. 6.12.

It can be seen that all three give very similar results. At no mesh refinement does the difference in tip deflection exceed 2%. With so small a difference, the relative accuracy is not an important criterion for the selection of a scheme to model shear wall systems.

Antony and Ganesan ignored Al-Mahaidi's second constraint (equation 3.3) to produce their wall face oriented connection. The flexural bending theory used to derive the line element assumes that plane sections remain plane. To give displacement compatibility between the end of the beam and the wall, the wall nodes are constrained to lie on a straight line. Non-conforming elements are in use for the wall and the further relaxation of displacement compatibility produced by ignoring this constraint would not be expected to have a great effect.

Antony and Ganesan found that this relaxation had very little effect on the analysis of the wall they used for comparison. This result was also found with the wall chosen by Al-Mahaidi et al. and used in this study. It is therefore concluded that the use of this second constraint equation offers no advantage and the simpler wall face oriented connection is to be preferred.

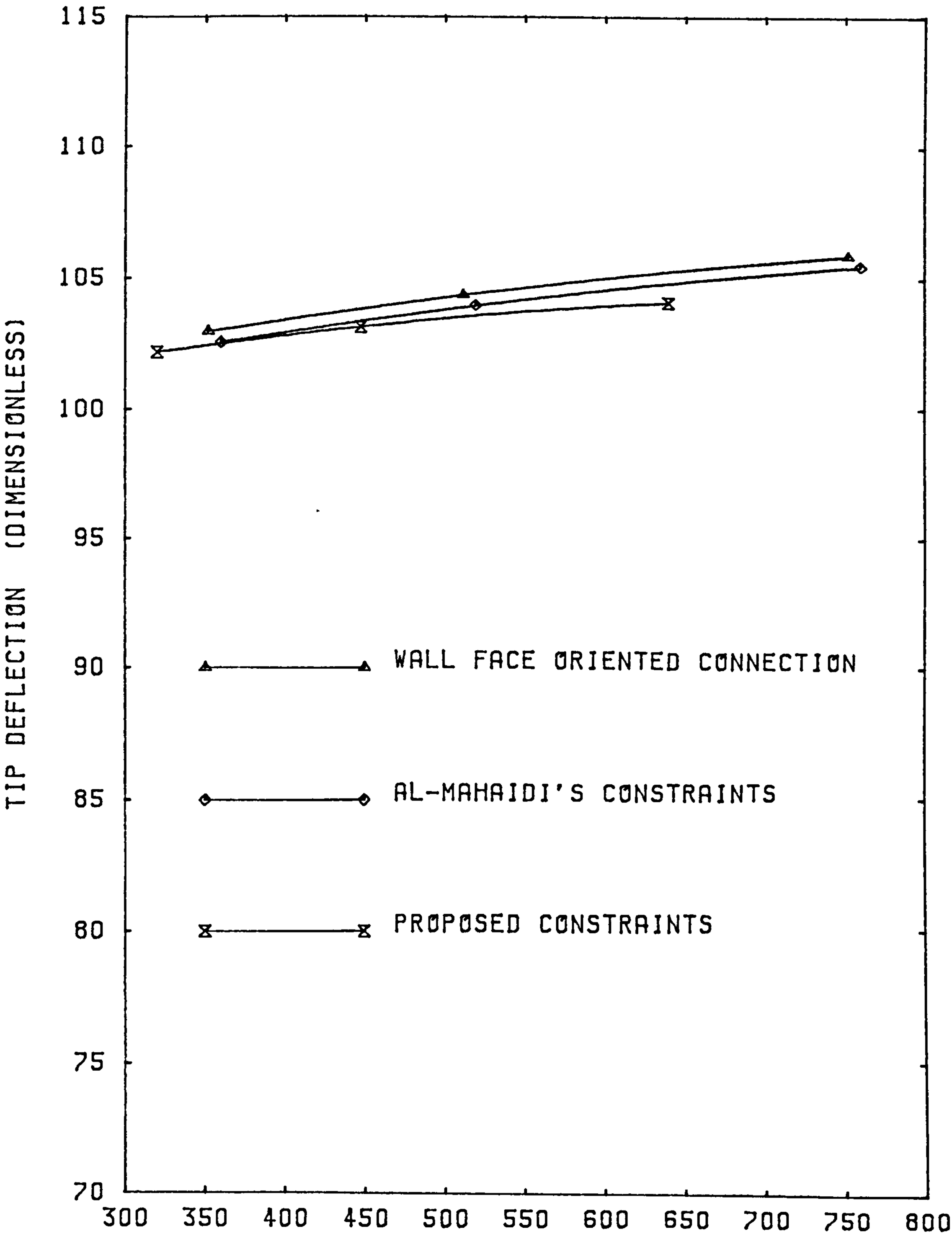

FIG 6.12

CONVERGENCE CURVES FOR LAGRANGE MULTIPLIER SCHEMES

The constraint equations proposed in this study use three Lagrange multiplier degrees of freedom at each joint compared with the one of the wall face oriented connection. The size of the problem to be solved depends upon the number of degrees of freedom with higher numbers producing a greater solution cost. It also depends upon the bandwidth of the equations. This is a function of the maximum node number difference for the elements [39]. A good measure of the size of the problem is given by the product of the degrees of freedom and the semiband width. This is given in table 6.4 for the meshes employed. Despite the greater degrees of freedom of the proposed constraint scheme, owing to its lower bandwidth it produces the smallest problem size.

Also, as shown in chapter 3, the beam end forces are automatically calculated with the proposed constraints. They are therefore the preferred constraints for the analysis of coupled shear walls and combined shear walls and frames.

	Scheme	Mesh		
		Coarse	Mid	Fine
Degrees of Freedom	Al-Mahaidi's	360	520	760
	Wall face oriented	352	512	752
	Proposed	320	448	640
Semiband Width	Al-Mahaidi's	24	29	41
	Wall face oriented	23	28	36
	Proposed	21	25	31
Product (Problem size)	Al-Mahaidi's	8640	15080	31160
	Wall face oriented	8096	14336	27072
	Proposed	6720	11200	19840

Table 6.4

Problem Size for the meshes employed

CHAPTER SEVEN - COMPARISON WITH STATIC EXPERIMENTS

7.1 INTRODUCTION

The proposed Lagrange multiplier scheme has been shown to compare favourably with other finite element methods for the analysis of coupled shear walls subject to static loading. In order to further validate its accuracy, experimental tests were carried out on model coupled shear walls both alone and connected to a frame. These provided data for comparison with the finite element analysis.

7.2 EXPERIMENTAL INVESTIGATION

Walls:

Perspex was chosen as the material used to model the shear walls, the principal advantage being the ease with which the complex shape of a coupled shear wall could be machined from a single sheet. The low modulus of elasticity when compared with metals gives readily measurable deflections at moderate loads. This allows simple apparatus to be used in performing the experiments.

The modulus of elasticity (Young's modulus) for the perspex used in the tests was determined from a cantilever bending test. A cantilever with a length to depth ratio of 10:1 was used as deflection due to shear stresses can be shown to be negligible (approximatley 1% [68]). It was loaded at the free end via a proving ring and the deflections were measured with dial gauges. The modulus of elasticity was then calculated from flexural bending theory as 0.31×10^{10} N/m^2.

Frames:

As the modulus of elasticity of perspex is quite low, aluminium was chosen to model the frames. It has a much lower modulus than steel, 7.0 x 10^{10} N/m^2 as opposed to 21.0 x 10^{10} N/m^2, and readily allowed the construction of frames of comparable stiffness with the walls.

Individual rectangular section bars were used for each of the frame members. To provide a full moment connection at each joint, aluminium disc flanges were used. A pair of these were bolted outside the members at each joint. Two bolts were used for each member. A typical joint is shown in Figure 7.1.

Effective length of members:

Owing to the stiffening effect of the discs at each joint, the use of the centre-line to centre-line lengths of the frame members for the finite element analysis produces a frame model which is too flexible. It is possible to rederive the stiffness matrix for a line element with stiffer lengths at each end [69] to give a better model. However, by taking the effective length of each member as the length between the extremes of the bolted connections, accurate results were obtained. This simpler method is therefore used in the analysis of the combined walls and frames. In a full scale structure this type of joint is not employed and the problem would not arise.

Experimental apparatus:

A heavy steel base was used for the experiments. The perspex walls were fastened to this by bolting to a steel angle on

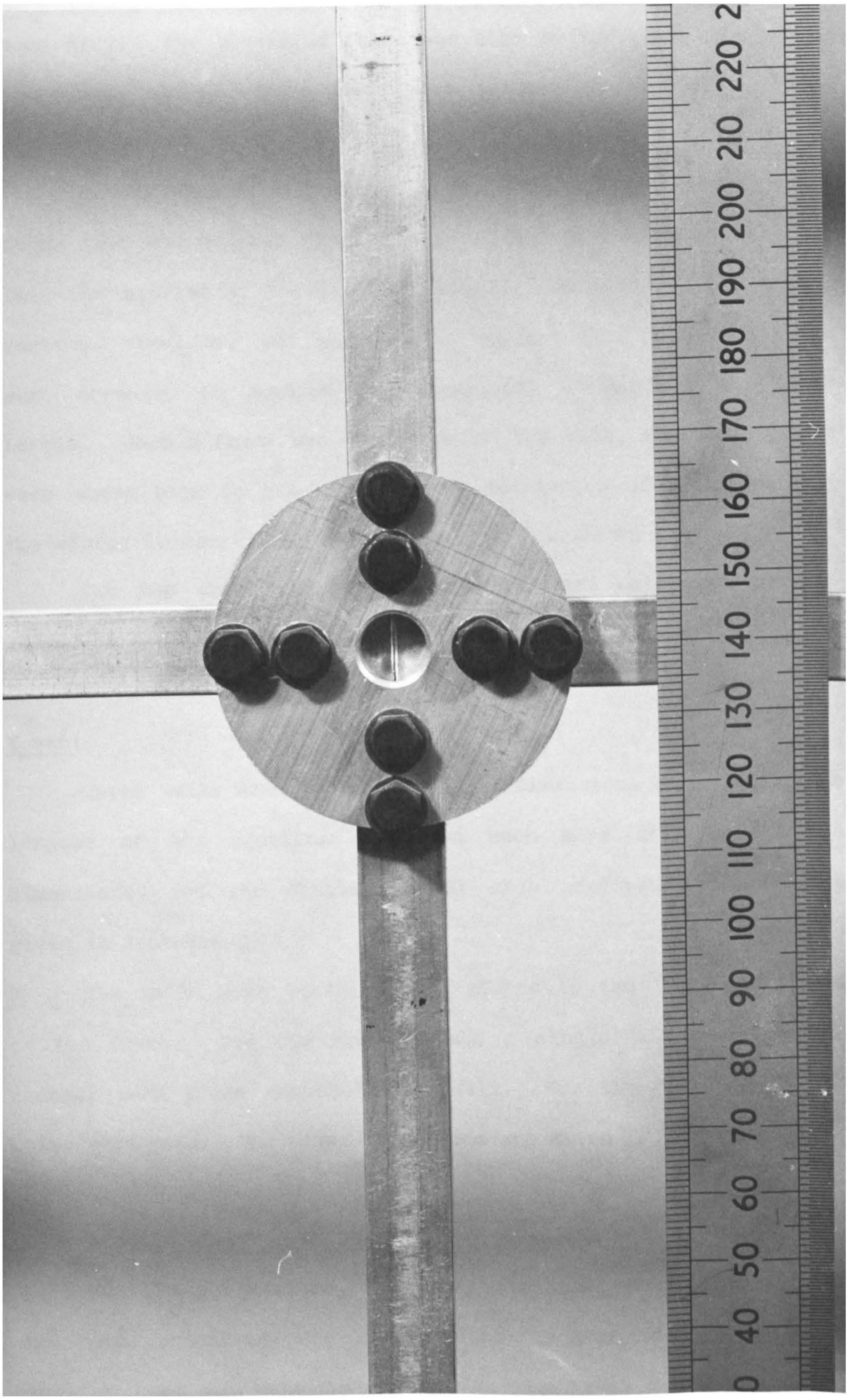

FIG. 7.1

Frame Joint

each side. The aluminium frame was also bolted down to a steel connecting plate. Both these were assumed to give fully fixed base conditions.

At one edge of the wall a steel frame was used to support a screw jack and proving ring to provide and measure a point load. This was applied at the top of the wall. At the opposite edge a vertical steel bar was employed to support dial gauges. These were arranged to measure the horizontal deflections at storey levels. When a frame was connected to the wall, the dial gauges were moved back to measure the edge deflection of the frame at the storey levels. This test apparatus is shown in Figure 7.2.

The top three connecting beams of each wall were strain-gauged to enable the calculation of the moments in them.

Tests:

Three walls with the same overall dimensions were used. The lengths of the coupling beams in each were different. The dimensions, and the finite element mesh employed for each are given in Appendix C.

The walls were tested alone, pinned to the frame and fixed to the frame. For the pinned tests a single bolt was used to connect each frame member to the wall. For the fixed tests two bolts were used. The frame dimensions are given in Appendix C.

7.3 RESULTS OF TESTS ON THE WALLS

For the walls alone, the results plotted in Figures 7.3-7.5 show the predicted and measured horizontal deflections and coupling beam end moments for an applied load of 100 N. The

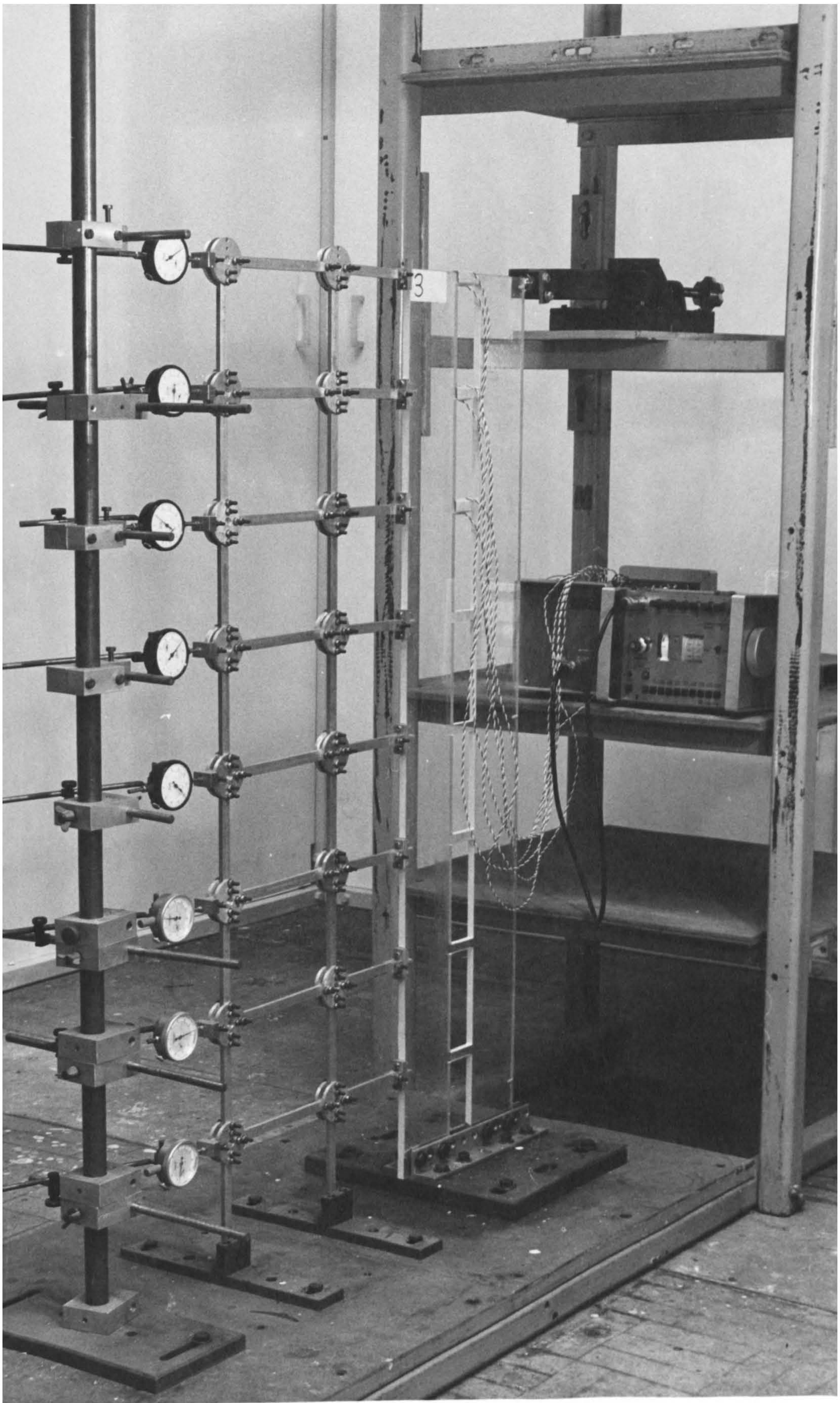

FIG. 7.2

Static Test Apparatus

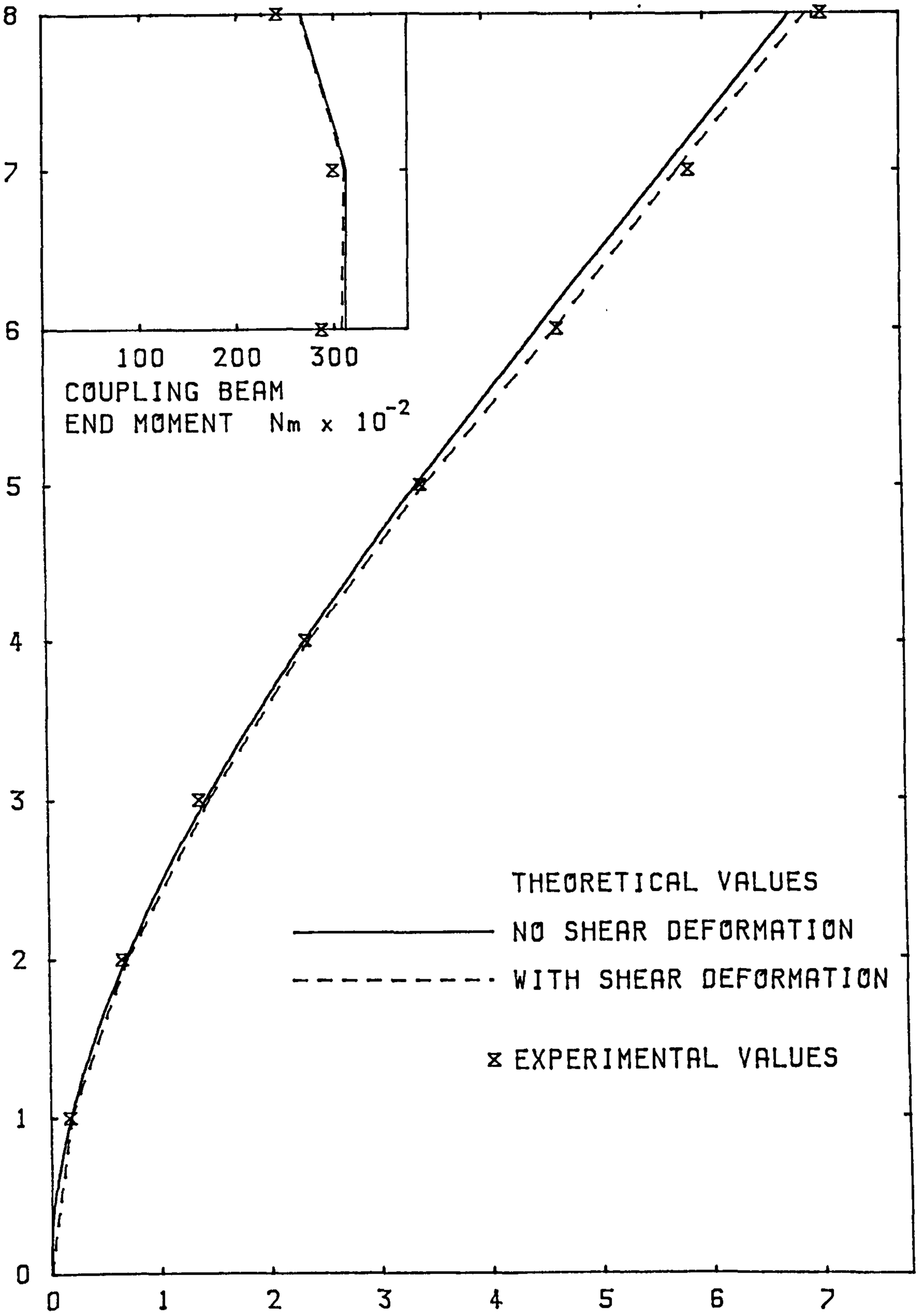

FIG 7.3

EDGE DEFLECTION AND COUPLING BEAM MOMENTS

WALL 1

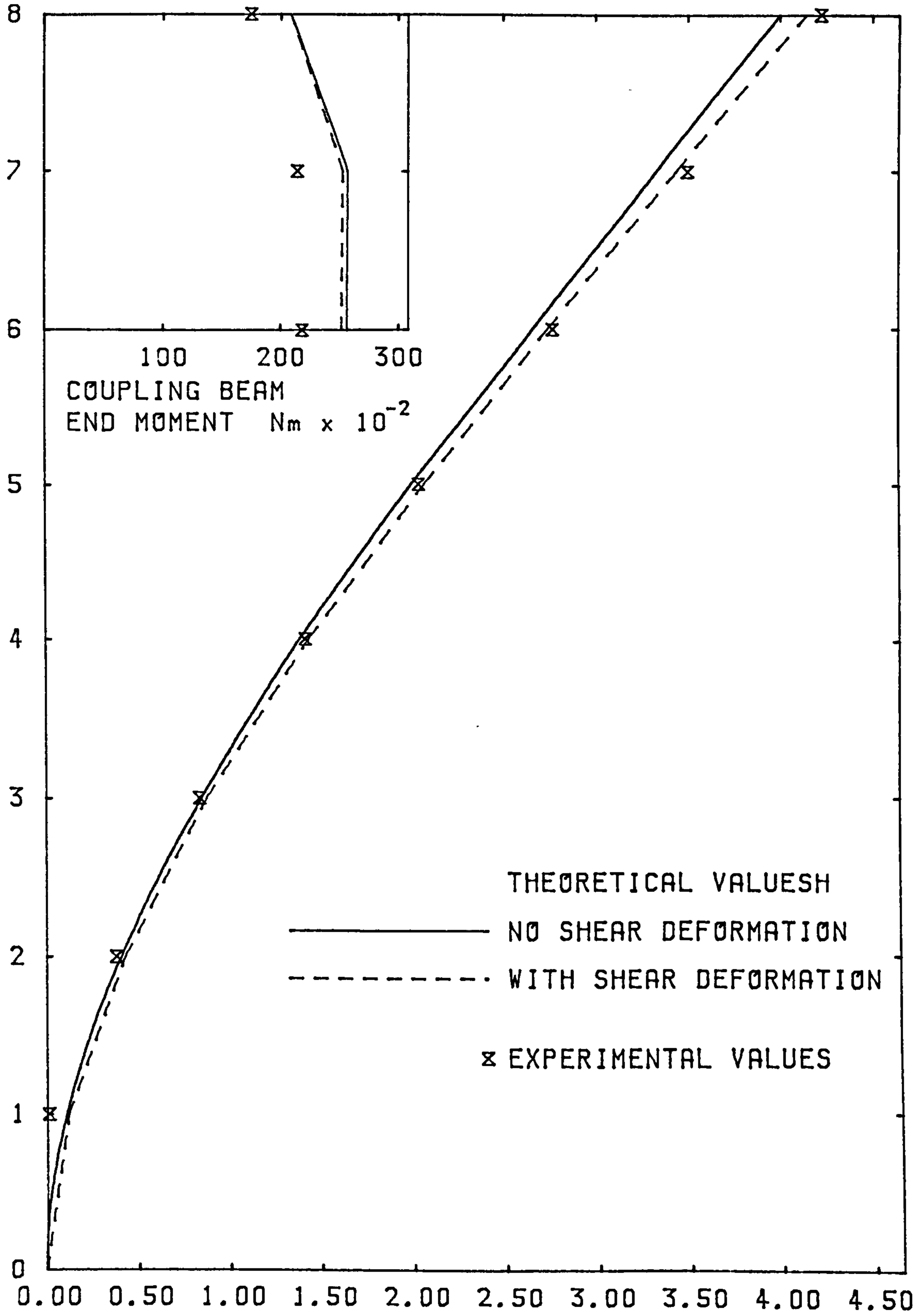

FIG 7.4

EDGE DEFLECTION AND COUPLING BEAM MOMENTS

WALL 2

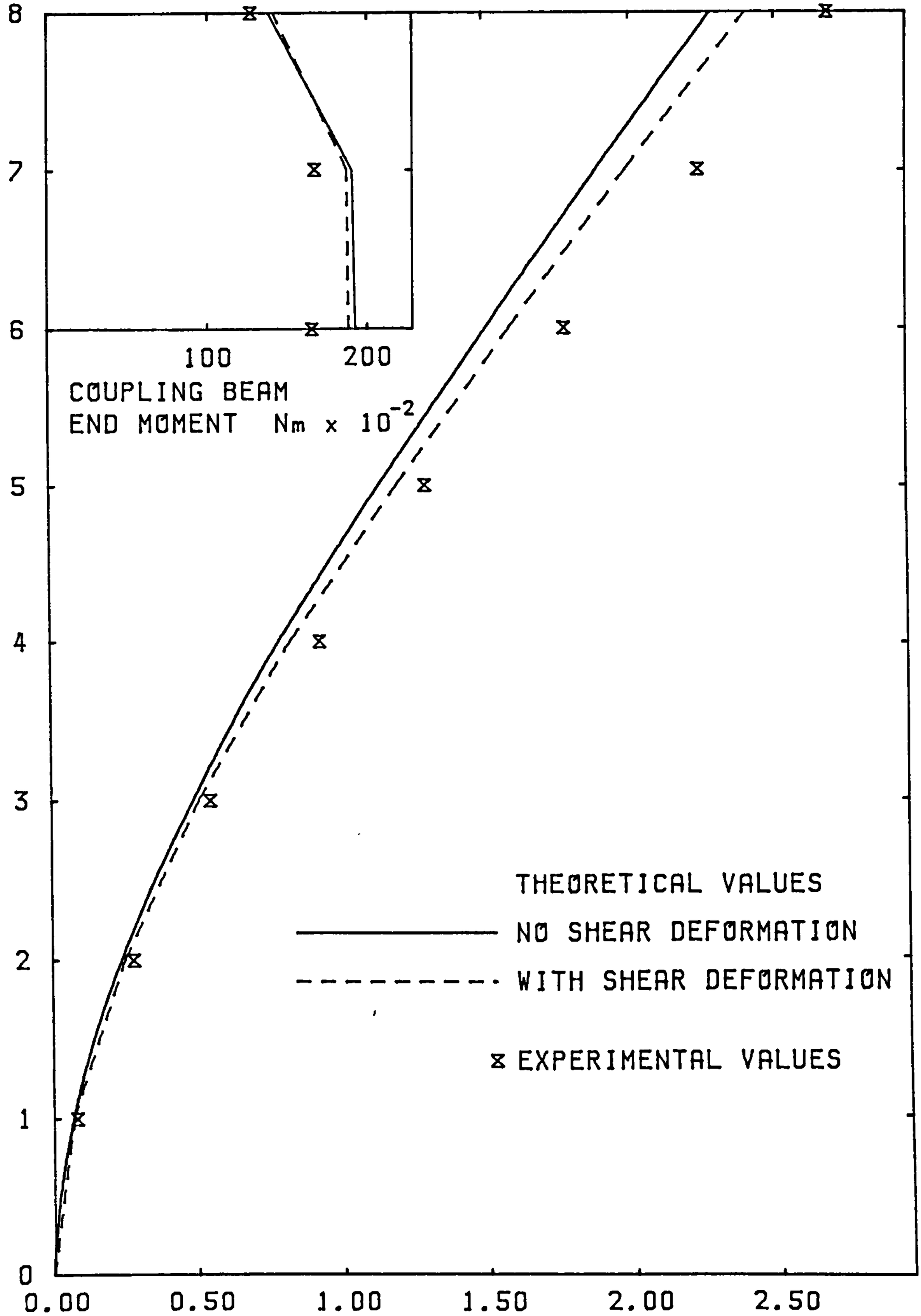

FIG 7.5

EDGE DEFLECTION AND COUPLING BEAM MOMENTS

WALL 3

theoretical result is labelled "NO SHEAR DEFORMATION" and is shown by a solid line.

From the graphs it can be seen that the results are most accurate for WALL 1 and least accurate for WALL 3. The length to depth ratio for the coupling beams of WALL 3 is 4:1. At this ratio, deflections due to shear strain can be shown to be approximately 6% [68].

Flexural bending theory was used to derive the stiffness matrix for the line elements employed to idealise these beams. This assumes that plane sections remain plane and hence no shear deflection takes place. For short deep beams the stiffness is overestimated, which is the result found from the experimental tests. It was therefore decided to modify the line element stiffness matrix to take account of shear deformation.

7.4 DERIVATION OF THE LINE ELEMENT STIFFNESS MATRIX

The stiffness coefficients may be derived from strain energy considerations using Castigliano's theorem [45]. The shear forces and moments at ends 1 and 2 of the beam are denoted by S_1, M_1, S_2 and M_2 and the corresponding displacements by V_1, θ_1, V_2 and θ_2.

The member is initially straight and given an end rotation θ_2 (Figure 7.6).

The bending moment at a distance x from end 1 is given by

$$M = - M_1 + S_1 x \qquad 7.1$$

but

$$M_1 + M_2 - S_1 L = 0 \qquad 7.2$$

then

$$M = - S_1 (L - x) + M_2 \qquad 7.3$$

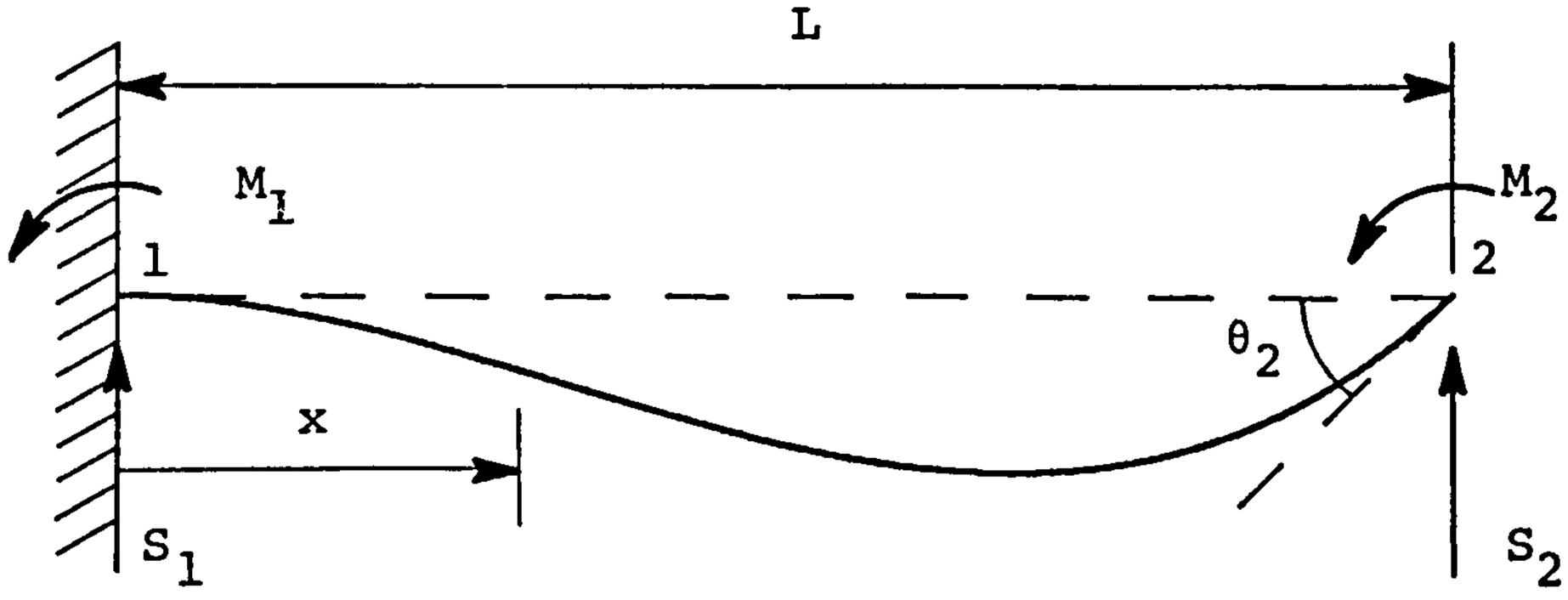

FIG. 7.6

Including shear strain as well as bending strain, the strain energy in the beam is given by

$$U = \int_0^L \frac{M^2}{2EI} \, dx + \int_0^L \frac{\beta S^2}{2GA} \, dx \qquad 7.4$$

in which

S = shear force

G = shear modulus

β = form factor

The form factor β depends upon the distribution of shear stress over the beam cross-section. For a rectangular beam $\beta = 1.2$ [68]. Substituting for M in equation 7.4 and integrating produces

$$U = \frac{1}{2EI}\left(S_1^2\frac{L^3}{3} + M_2^2 L - S_1 M_2 L^2\right) + \frac{\beta}{2GA}\left(S_1^2 L\right) \qquad 7.5$$

From Castigliano's theorem

$$\frac{\delta U}{\delta S_1} = V_1 = 0 \qquad 7.6$$

Thus

$$\frac{1}{2EI}\left(\frac{2L^3 S_1}{3} - M_2 L^2\right) + \frac{\beta}{2GA}\left(2S_1 L\right) = 0 \qquad 7.7$$

and

$$S_1 = \frac{M_2}{\frac{2L}{3} + \frac{2EI\beta}{GAL}} \qquad 7.8$$

From Catigliano's theorem

$$\frac{\delta U}{\delta M_2} = \theta 2 \qquad 7.9$$

then

$$\frac{1}{2EI}\left(2M_2 L - S_1 L^2\right) = \theta_2 \qquad 7.10$$

Substituting S_1 from equatioln 7.8 produces

$$\frac{1}{2EI}\left(2M_2 L - \frac{M_2 L^2}{\left(\frac{2L}{3} + \frac{2EI\beta}{GAL}\right)}\right) = \theta 2 \qquad 7.11$$

To simplify this equation we use

$$g = \frac{6\beta EI}{GAL^2} \qquad 7.12$$

which, rearranging produces

$$M_2 = \frac{EI}{(1 + 2g)}\,\frac{4}{L}\left(1 + \frac{g}{2}\right)\theta_2 \qquad 7.13$$

Substituting into equation 7.8 produces

$$S_1 = \frac{EI}{(1 + 2g)}\,\frac{6}{L^2}\,\theta_2 \qquad 7.14$$

The remaining stiffness relationships may be derived similarly to produce

$$\begin{bmatrix} S_1 \\ M_1 \\ \\ S2 \\ M_2 \end{bmatrix} \frac{EI}{(1+2g)} \quad [K] \quad \begin{bmatrix} V_1 \\ \theta_1 \\ \\ V2 \\ \theta_2 \end{bmatrix} \qquad 7.15$$

in which

$$[K] = \begin{bmatrix} \frac{12}{L^3} & \frac{6}{L^2} & -\frac{12}{L^3} & \frac{6}{L^2} \\ \\ \frac{6}{L^2} & \frac{4(1+g/2)}{L} & -\frac{6}{L^2} & \frac{2(1-g)}{L} \\ \\ -\frac{12}{L^3} & -\frac{6}{L^2} & \frac{12}{L^3} & -\frac{6}{L^2} \\ \\ \frac{6}{L^2} & \frac{2(1-g)}{L} & -\frac{6}{L^2} & \frac{4(1+g/2)}{L} \end{bmatrix} \qquad 7.16$$

Axial deformations produce no shear stress and the stiffness coefficients (not shown here) remain unchanged by the inclusion of shear strain energy. When the beam is slender, g is approximately zero, and the stiffness matrix reduces to the usual matrix for an element in pure bending.

7.5 EFFECT OF SHEAR DEFORMATION ON FINITE ELEMENT ANALYSIS

To test the performance of the model, including the effects of shear deformation, further computer analyses were performed

using the same wall as was employed in chapter 6 (Figure 6.1). The depth of the coupling beams was varied and the dimensionless tip deflection parameter $\Delta o\ Et\ /P$ was calculated for each depth.

Three models were compared, the proposed scheme both with and without the effects of shear deformation and the quadrilateral isoparametric element alone. This latter model was included as it is known to give accurate results with very deep beams whereas the Lagrange schemes have only been shown to give accurate results for slender beams.

The results are shown in Figure 7.7 as a plot of the dimensionless deflection parameter against coupling beam depth shown as a proportion of the storey height. It can be seen that the difference between the three schemes is very small. It was expected that the proposed scheme neglecting the effect of shear deformation would have given poor results for the very deep beams but this is not the case. The reason for this can also be seen from the graph. Once the beam depth is approximately one third of the storey height or more, there is very little change in the overall wall deflection. A large error in the coupling beam stiffness will produce a relatively small error in the wall deflection when the beams are deep.

The proposed Lagrange multiplier scheme can be seen to give accurate results even when the beams are deep. The inclusion of shear deformation produces a correction which, whilst not of major effect, is worthwhile as the extra computation is minimal. All further analyses use the corrected element.

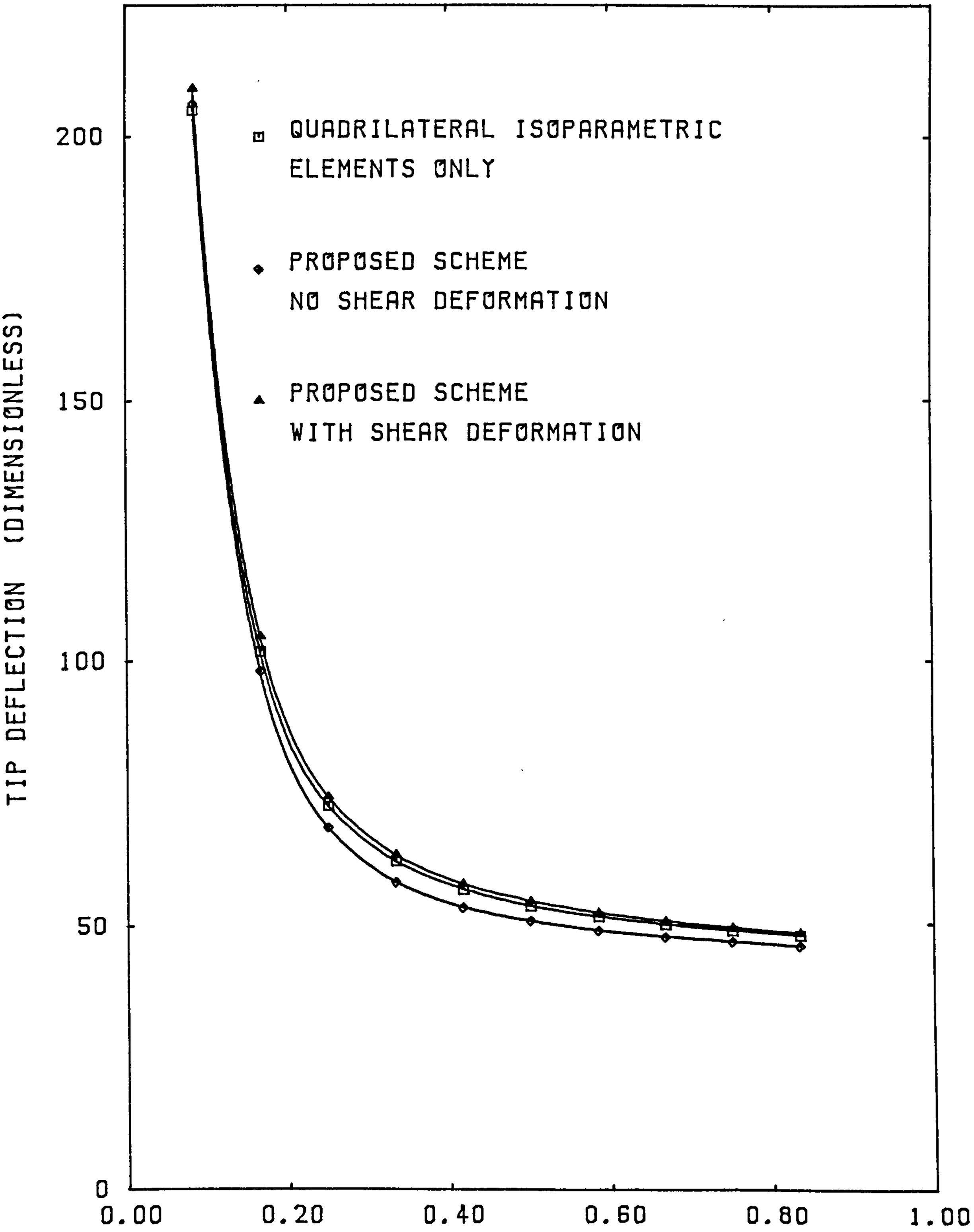

FIG 7.7

EFFECT OF SHEAR DEFLECTION WITH VARYING BEAM DEPTH

7.6 COMPARISON WITH EXPERIMENTAL RESULTS

The results for the walls were recalculated. The new theoretical predictions are shown in Figures 7.3-7.5 labelled "WITH SHEAR DEFORMATION" and shown by a broken line. It can be seen that the results are noticeably improved.

The results for the wall-frame combinations are shown in Figures 7.8-7.10. The theoretical results still become less accurate as the coupling beam becomes shorter. Also the end moment predictions are too high. This is the opposite of the result found using the rectangular element with rotational degrees of freedom in the previous chapter. There, the deflections were overestimated and the end moments were too low. This was found to be due to the wall elements twisting locally at the joint producing a very low rotational connection stiffness. This leads to the conclusion that, in the present scheme, the joint stiffness is too great.

The same number of elements were used for WALL 1 and WALL 3, hence the elements for WALL 3 are larger (Figures C.1, C.3). Thus it would be expected that the connection stiffness would be greater for WALL 3. In this case a reduction in the connection stiffness would be more significant. A more flexible connection would improve the results, especially for the shorter coupling beams where the error is greatest.

This may be accomplished by modifying the line element to produce an elastic connection [69], but this presents the difficulty of estimating the stiffness of this connection. It was seen in chapter 6, that as the number of degrees of freedom in the wall increased, the wall stiffness reduced. Hence the required

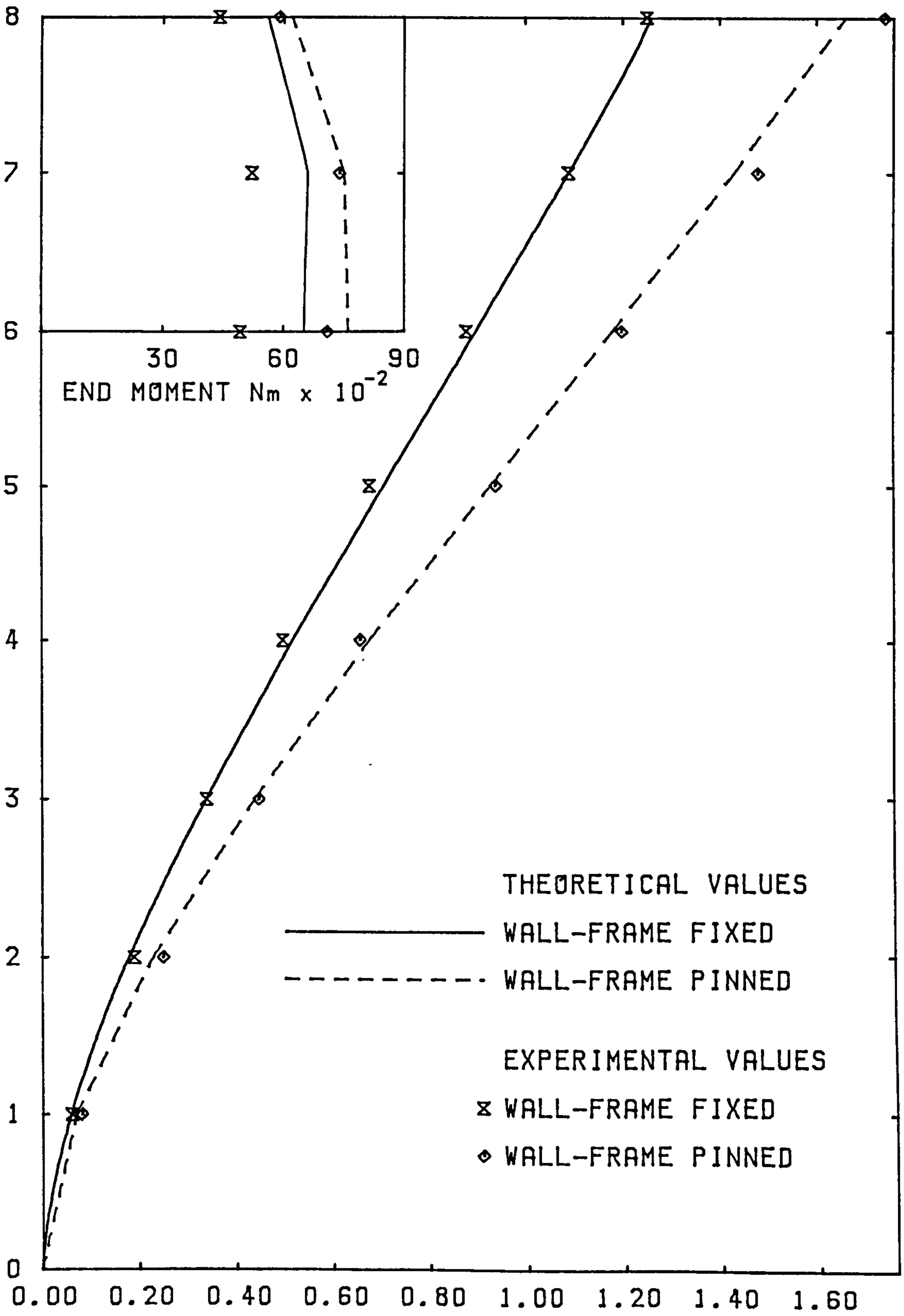

FIG 7.8

EDGE DEFLECTION AND COUPLING BEAM MOMENTS

WALL 1 AND FRAME WITH SHEAR DEFORMATION

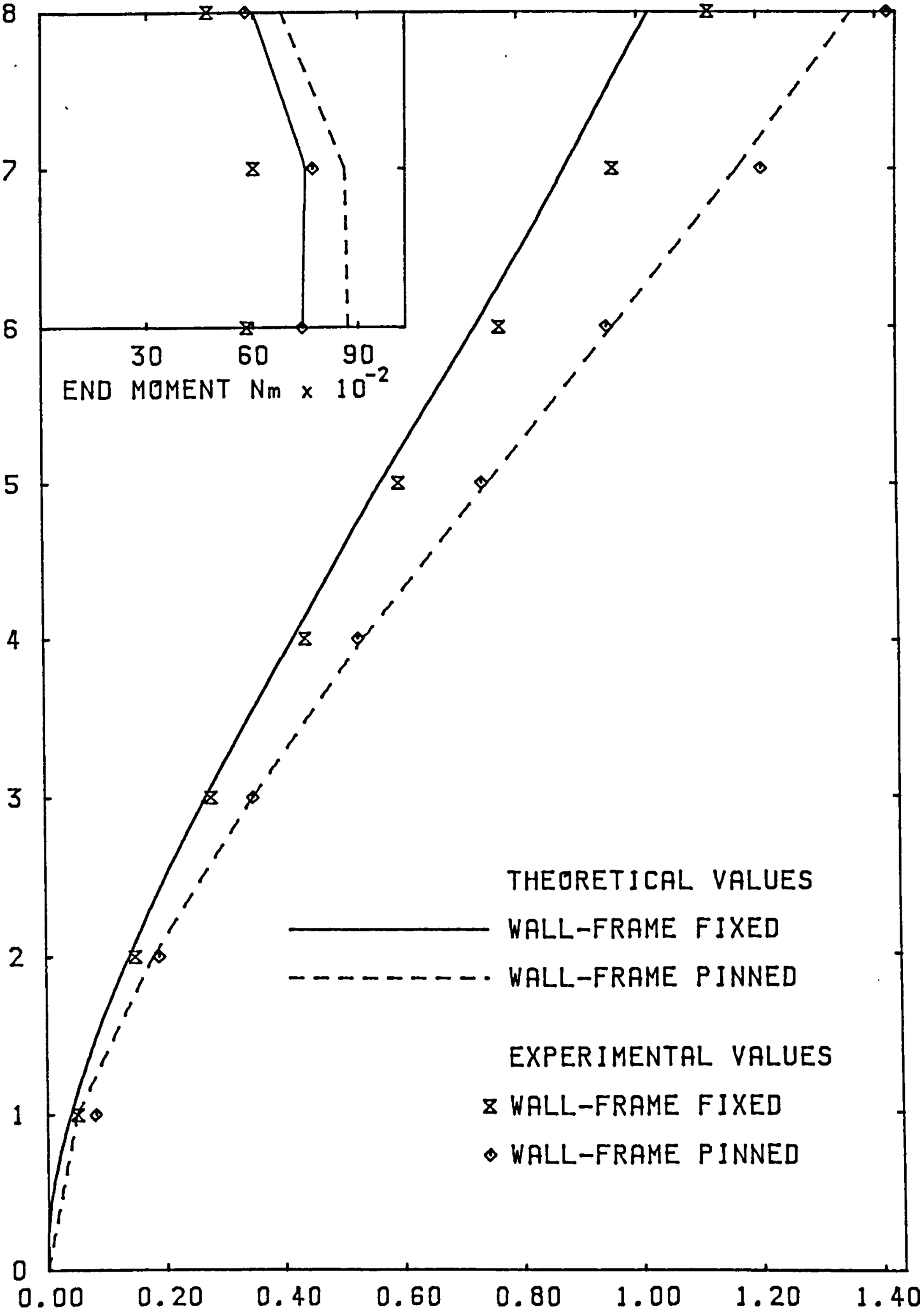

FIG 7.9

EDGE DEFLECTION AND COUPLING BEAM MOMENTS

WALL 2 AND FRAME WITH SHEAR DEFORMATION

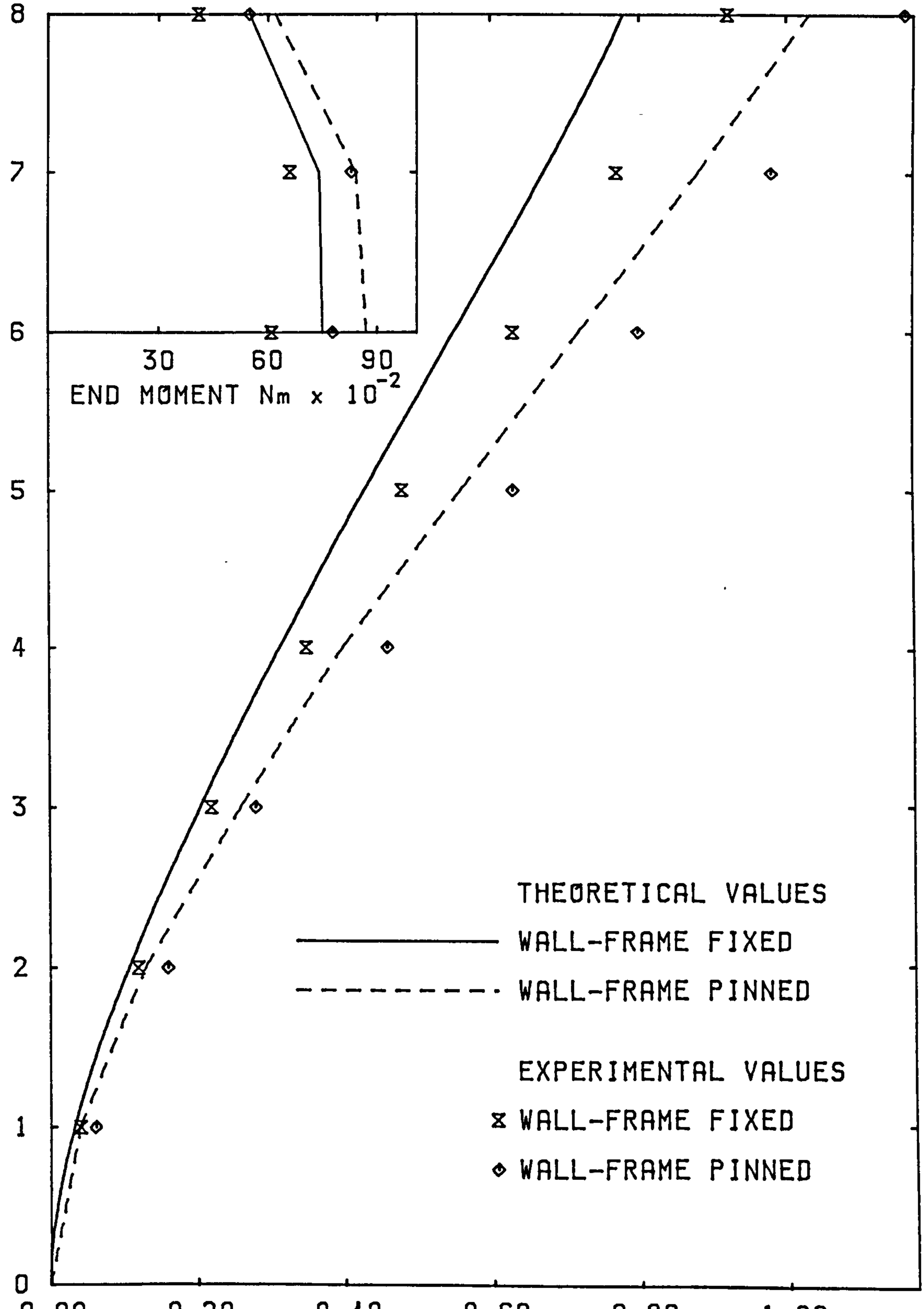

FIG 7.10

EDGE DEFLECTION AND COUPLING BEAM MOMENTS

WALL 3 AND FRAME WITH SHEAR DEFORMATION

joint stiffness will vary with the finite element mesh employed. In view of this, and with the present method giving good results, it was decided not to employ an elastic rotational connection.

Examining Figures 7.8-7.10 it can be seen that a pin joint between the wall and frame produces a marked reduction in stiffness with the finite element theory. This is matched by a reduction in the experimental results. To obtain accurate results for a fixed connection it is necessary to employ the constraint equations. The analysis assuming a pin joint, which may be accomplished without the use of these, would lead to large errors.

CHAPTER EIGHT - DYNAMIC EXPERIMENTS

8.1 INTRODUCTION

In this chapter the efficacy of the proposed finite element model when employed for dynamic analysis, is examined. The theory used for conducting small scale shaking table experiments is presented. The apparatus and methods employed for the experiments in this study are described. These experiments all employed steady-state harmonic excitation to evaluate natural frequencies mode shapes and damping. Finally, comparisons are made between experimental results and the theoretical predictions.

8.2 PEAK AMPLITUDE (RESONANCE) METHOD

Modal decoupling:

The mode shapes obtained by solving for the eigenvectors of equation 4.10 can be shown to be orthogonal and hence the equation of motion 4.6 may be decoupled. This allows the response of a structure to be calculated as the sum of the responses of each mode. This method is presented in many publications [48, 55, 70] and only a summary is given here.

The total displacement at any point may be obtained as the sum of all the modal components,

$$\{q\} = \{r\}_1 \gamma_1 + \{r\}_2 \gamma_2 + \ldots\ldots \{r\}_n \gamma_n \qquad 8.1$$

where $\{r\}_i$ is the mode shape

and γ_i the modal amplitude.

The response of each mode i may then be written as

$$M_i \ddot{\gamma}_i + C_i \dot{\gamma}_i + K_i \gamma_i = P_i(t) \qquad 8.2$$

or

$$\ddot{\gamma}_i + 2\mu_i \omega_i \dot{\gamma}_i + \omega_i^2 \gamma_i = \frac{P_i(t)}{M_i} \qquad 8.3$$

where $M_i = \{r\}_i^T [M] \{r\}_i$ 8.4

$C_i = \{r\}_i^T [C] \{r\}_i = 2 \mu_i \omega_i M_i$ 8.5

$K_i = \{r\}_i^T [K] \{r\}_i = \omega_i^2 M_i$ 8.6

$P_i(t) = \{r\}_i^T P(t)$ 8.7

Equivalent Single degree of freedom system:

Equation 8.2 is equivalent to the behaviour of a single degree of freedom system. The behaviour in response to steady-state harmonic loading may now be readily calculated from

$$M_i \ddot{\gamma}_i + C_i \dot{\gamma}_i + K_i \gamma_i = P_i \cos(\omega_F t) \qquad 8.8$$

where ω_F is the forcing frequency. The solution to this equation consists of two parts, the "Particular Integral" and the "Complementary Function". The response represented by the complementary function is damped out rapidly and after a few cycles only the particular integral

$$\gamma_i = \frac{P_i (\cos \omega_F t - \phi)}{[(K_i - M_i \omega_F^2)^2 + C_i^2 \omega_F^2]^{\frac{1}{2}}} \qquad 8.9$$

is significant. ϕ represents the phase angle between the response and the forcing function and is given by

$$\phi = \tan^{-1} \frac{C_i \omega_F}{K_i - M_i \omega_F^2} \qquad 8.10$$

The amplitude of the response is therefore given by

$$\frac{P_i}{[(K_i - M_i \omega_F^2)^2 + C_i^2 \omega_F^2]^{\frac{1}{2}}}$$

and the displacement under a static force Pi is given by

$$\frac{P_i}{K_i}$$

The ratio of these is known as the "dynamic magnifiction factor" Zi, which, using equations 8.4-8.7 may be expressed as

$$Zi = \frac{1}{[(1-\frac{\omega_F{}^2}{\omega_i{}^2})^2 + 4\ \mu i^2\ (\frac{\omega_F}{\omega i})^2]^{\frac{1}{2}}} \qquad 8.11$$

Hence, as the forcing frequency varies, the response amplitude varies with its maximum value when

$$\omega_F = \omega i\ \sqrt{1-\mu_i{}^2} \qquad 8.12$$

For most structures μ is small having a value from 2% to 20% (μ= 0.02 to 0.2) [53] and the maximum response is when $\omega_F \simeq \omega i$. This phenomenon is known as resonance. If a structure is subjected to harmonic loading over a range of frequencies, then the natural frequencies may be found from the resonances.

This method relies upon the response of the mode under investigation being much larger near resonance than the contributions of the other modes. When this is not the case, then more than one mode must be considered at a time [71]. However, in the tests performed in this study, the natural frequencies were well separated and the damping coefficients low and no problem of this nature was encountered.

8.3 EXPERIMENTAL INVESTIGATION

Models:

The same models were employed for the dynamic tests as were used for the static tests described in the previous chapter. The dynamic value of the elastic modulus (Youngs modulus) of the perspex was evaluated from a cantilever vibration test. Using flexural bending theory, the fundamental fequency for the vibration of a cantilever may be shown [70] to be given by

$$\omega i = \frac{3.516}{L^2}\ \left(\frac{EI}{\rho A}\right)^{\frac{1}{2}} \qquad 8.13$$

where E = Youngs modulus

I = 2nd moment of area

ρ = density

A = x - section area

L = length

The fundamental frequency was found from a resonance test and using equation 8.13 the dynamic modulus was calculated as 0.45 x 10^{10} N/m^2.

Apparatus:

The experiments in this study were performed using an aluminium shaking table driven by an electric vibrator.

The table was 1.2m by 1.2m and 0.025m thick. Earlier experiments had been carried out on a perspex table. This proved to be too flexible as significant vertical accelerations could be measured at the base of models. The table was "floated" on a film of oil supplied under pressure to the centre of the flat bed on which it rested. The continous oil flow was provided by a tank at a head of approximately 4m and was recirculated to this by a small electric pump.

The vibrator was driven by a power amplifier and a signal generator capable of operating at frequencies from $3H_z$ to $15kH_z$. The maximum possible acceleration of the unloaded table was approximately 10 m/sec^2.

The same base fastenings as were used for the static tests were again employed. These fastened the walls and frame to a steel base plate which was then bolted to the table. The intermediate steel base was used to minimize the number of holes

drilled into the shaking table for the mounting of models.

The response of the table and the models was monitored using electronic accelerometers. The signals from these were fed to conditioning and measuring units. These were capable of providing a direct reading of acceleration, velocity and displacement and of giving outputs suitable for measurement by other equipment. The phase angle between any acceleration or displacement signals was measured using a digital storage oscilloscope in conjunction with an x - y plotter.

The frequency of operation was measured using a digital frequency meter with a resolution of $1H_z$.

The table and vibrator with a model mounted are shown in Figure 8.1.

Technique:

The procedure used to measure the natural frequencies and damping coefficients of each model was as follows:

a) The frequency of the forcing (table vibration) was set.

b) The base acceleration was set at a level of $5m/sec^2$.

c) The response amplitude at the top of the model was recorded.

d) The phase angle between forcing and the response accelerations was measured.

e) The forcing frequency was increased by $1H_z$ and the procedure repeated from (b) above.

Using this method, response amplitudes were recorded either side of a resonance frequency. The base acceleration of $5m/sec^2$ was selected as it was found to produce a convenient spread of readings for the response amplitude.

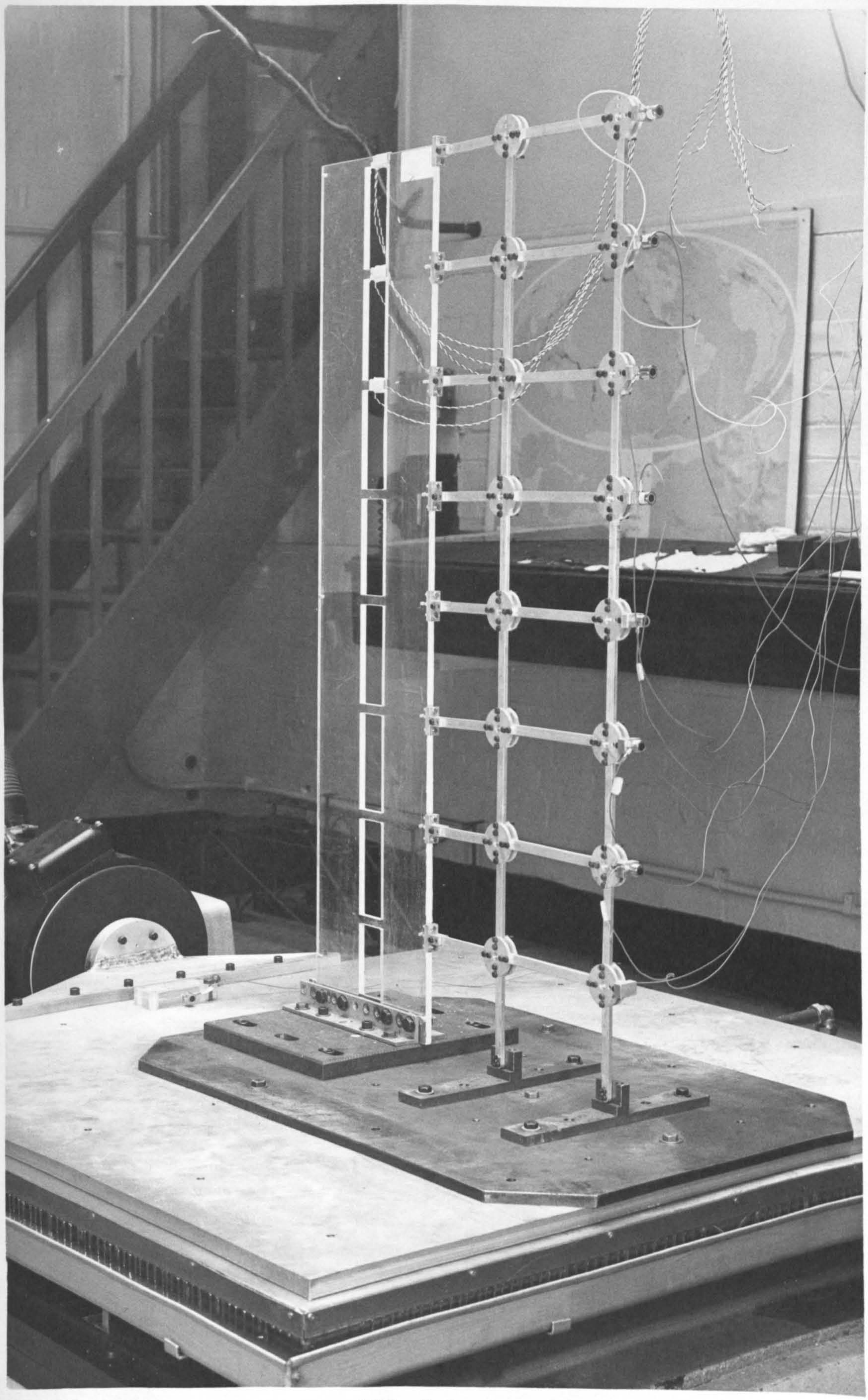

FIG. 8.1

Shaking Table

Having found the natural frequencies, the vibration mode shapes were also measured for the wall-frame models. The table was set to vibrate at the natural frequency of the model. The response amplitude at each of the top seven storey levels and the base acceleration were recorded and the phase angle between each response and the base measured.

8.4 EVALUATION OF THE NATURAL FREQUENCIES AND DAMPING

The response given by equation 8.11 is relative to the fixed base. In the experiments the accelerometers measure the overall response which includes the base acceleration. To allow for this, the response relative to the base is calculated using the measured phase angles. By plotting a phasor diagram [72] the relative response amplitude may be calculated from

$$c^2 = a^2 + b^2 - 2ab \cos \phi \qquad 8.14$$

where a = overall amplitude

b = base amplitude

c = relative response amplitude

ϕ = phase angle between a and b

This has very little effect upon the evaluation of the natural frequencies. The base acceleration is small compared with the response near resonance. However, if the response amplitude is plotted against forcing frequency, it can be seen from equation 8.11 that the shape of the curve is dependent upon the damping present (Figure 8.2). As it is desired to utilise this relationship to evaluate the damping, then for the greatest accuracy it is necessary to calculate the response relative to the base.

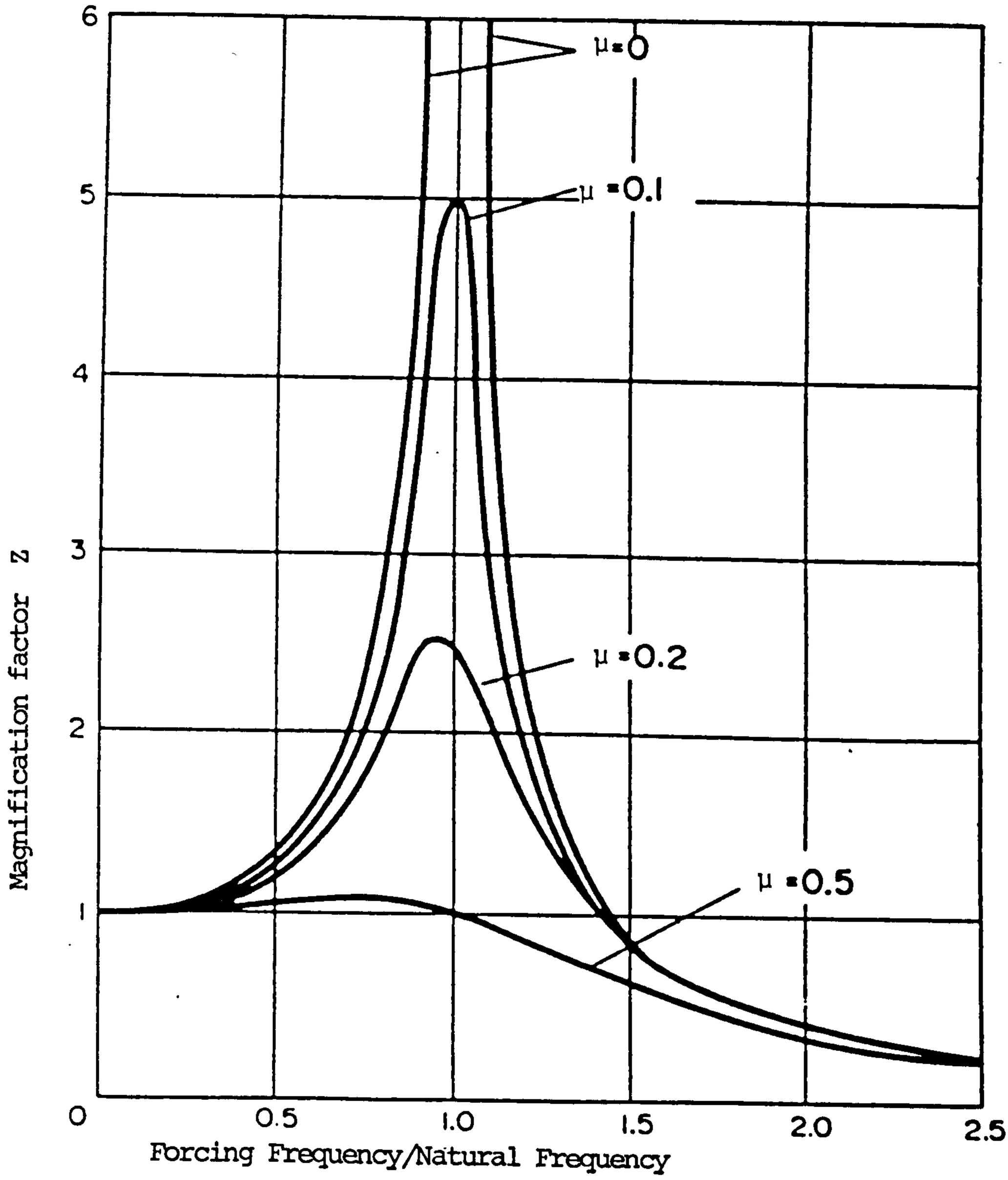

Figure 8.2

Resonance Curves

Various properties of the curve may be employed to evaluate the damping [55]. These commonly involve plotting a curve through the data points and then using this to calculate the damping. This can lead to errors if the data points do not lie exactly on a smooth curve.

To minimize the error involved a "least squares curve fitting technique" [73] was used in this study. This method regards the separation between a data point and the theoretical curve as a random error due to the nature of the experiment. Mistakes in the readings taken will be given undue weighting by this method and care was taken to avoid these. The total of the square of the error for each of the data points is minimized by selecting suitable values for the unknown parameters in the theoretical equation. By this means the theoretical curve which best fits the experimental data may be found.

The unknown parameters in equation 8.11 are ω_i and μ_i (the natural frequency and the damping coefficient). As the experiment measures the response amplitude as opposed to the dynamic magnification factor, a third parameter must be introduced to convert the amplitude to the magnification factor.

A program using a grid search method [74] was used to find the values of these parameters. A reasonable range for each of the parameters could be found from a simple inspection of the data. Small increments were used for each of these ranges. For every combination of the values of the parameters within the ranges, the program calculates the sum of the squares of the errors, allowing the minimum to be found. This is not a particularly efficient technique. However, with the simple nature

of the problem and reasonable estimates for the parameters it was found to be very effective. The program can also plot the data points and the theoretical curve to give a visual check of the accuracy obtained.

8.5 COMPARISONS WITH THE WALLS AND FRAME SEPARATELY

Effect of varying beam depth:

The first comparison carried out used results obtained by Tso and Chan [8] for the fundamental frequencies of their perspex models. They employed two coupled shear walls, one with equal piers and the second with unequal piers (Figs C.5, C.6). The beam depth of each was reduced in stages and the natural frequency evaluated at each.

The fundamental frequency (1st mode) is shown plotted against the beam depth as a proportion of the storey height in Figure 8.3. The theoretical predictions of the proposed finite element scheme are also plotted. It can be seen that the theoretical predictions agree very closely with the experimental results obtained for both walls.

It is also apparent that, once the coupling beams are deeper than approximately one third of the storey height, very little variation occurs in the fundamental frequency. This is in close agreement with the static analysis of the previous chapter (Figure 7.8) and with dynamic analysis of Wee [19].

Tests performed:

The walls and frame used for the static tests described in chapter 7 (Figs C.1-C.4) were tested to evaluate their natural

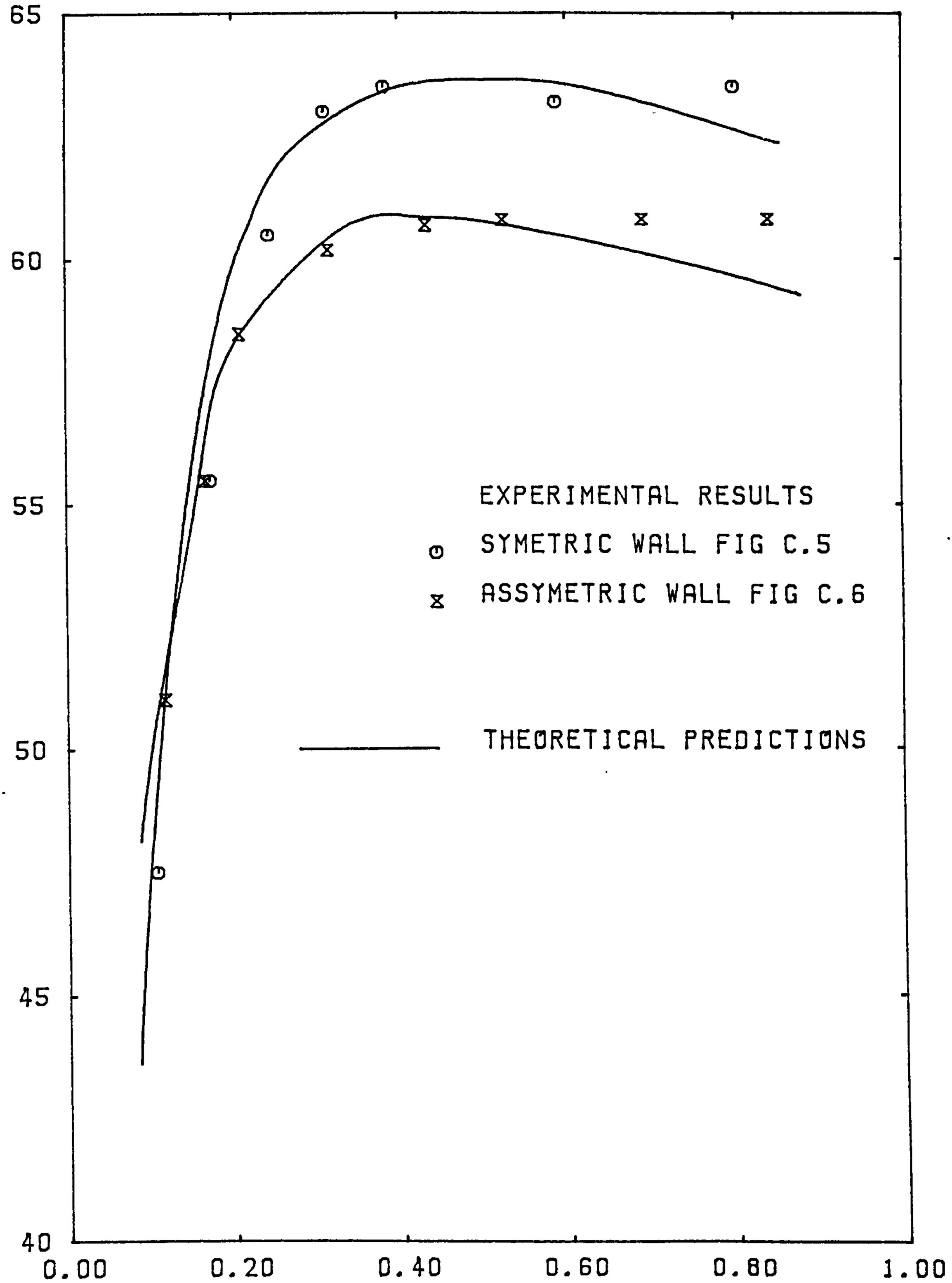

FIG 8.3

VARIATION OF FUNDAMENTAL FREQUENCY OF WALLS FIG C.5 & C.6

frequencies and damping. In the case of the walls the first two modes were found. Two accelerometers were used, one at the top and one at the 4th storey level. The lower one was used to determine which mode was being excited. When the frame was tested the top seven storey levels had accelerometers attached. The first three in-plane modes were found for the frame.

With the frame, some interference was experienced from torsional vibration modes. This was minimized by accurately aligning the frame with the vibration axis of the table.

When analysing the models by the finite element program, all the extra non-structural mass must be included. The masses of all the connections and of the accelerometers were lumped to the appropriate nodes. Details are given in Appendix C.

The natural frequencies found from the tests and the analyses are compared in table 8.1.

It can be seen that, for the frame, the theoretical and experimental natural frequencies are very similar. This is to be expected as the frame is made from aluminium which has very uniform properties and may be accurately modelled.

The values for the walls are not as accurate but the error still never exceeds 10%. The dynamic modulus of elasticity for the perspex was evaluated as 0.45×10^{10} N/m^2 as opposed to 0.31×10^{10} N/m^2 for the static value. It would be expected, therefore, that this value would be variable and would depend upon the frequency of loading. The experimental natural frequency was slightly low for all the walls in the first mode and slightly high in the second. This would be explained by a rise in modulus as

		Natural Frequency Hz		
		1st Mode	2nd Mode	3rd Mode
Frame	Theoretical	26.5	82.3	147
	Experimental	26.5	85.0	154
Wall 1	Theoretical	28.4	121	
	Experimental	28.0	130	
Wall 2	Theoretical	34.5	145	
	Experimental	33.5	158	
Wall 3	Theoretical	42.7	176	
	Experimental	39.5	189	

Table 8.1

Natural Frequencies of the Walls and Frame

the loading frequency increased. The cantilever which was tested to determine the modulus, had a natural frequency of $48H_z$. This is between the natural frequencies obtained for the first and second modes of each of the walls and would tend to support this conclusion.

It can be seen that, for the first mode, the theoretical natural frequency is greater than the experimental by a larger margin as we move from WALL 1 to WALL 3. Natural frequency increases with increasing stiffness, so this is in agreement with the results for the theoretical stiffness of the walls in chapter 7.

The damping was evaluated by fitting resonance curves. All three walls had the same values of 4% critical damping in the first mode and 2.5% in the second. The curves for WALL 1 are shown in Figs 8.4, 8.5.

The frame damping was much lower, being 1% in the first mode and less than 0.5% in the second. The damping for the third mode was lower still but was not accurately evaluated as the program employed worked to the nearest 0.5%. The resonance curves for the first two modes are shown in Figs 8.6, 8.7.

8.6 COMPARISONS WITH THE WALLS AND FRAME FIXED TOGETHER

The walls were tested fixed to the frame. For each, the first two natural frequencies were found, the mode shapes measured and the damping evaluated. The results for the natural frequencies are compared to the theoretical values in table 8.2.

It can be seen by comparing table 8.1 for the walls alone with table 8.2 for the walls fixed to the frames, that fixing a

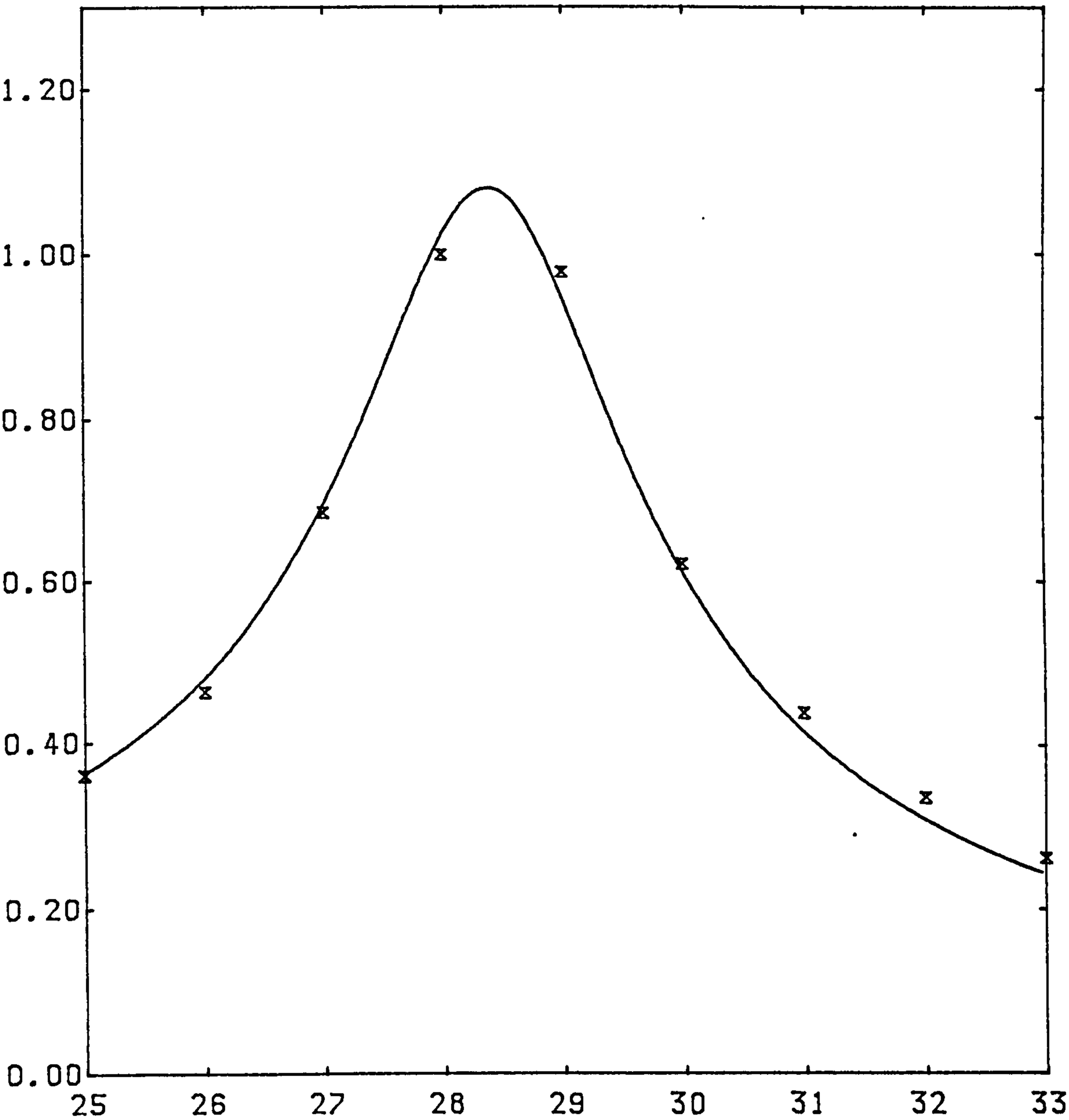

BEST FIT RESONANCE CURVE FOR EXPERIMENTAL DATA

NATURAL FREQUENCY 28.4 HERTZ

PERCENTAGE DAMPING 4.0

FIG 8.4

WALL 1 FIRST MODE

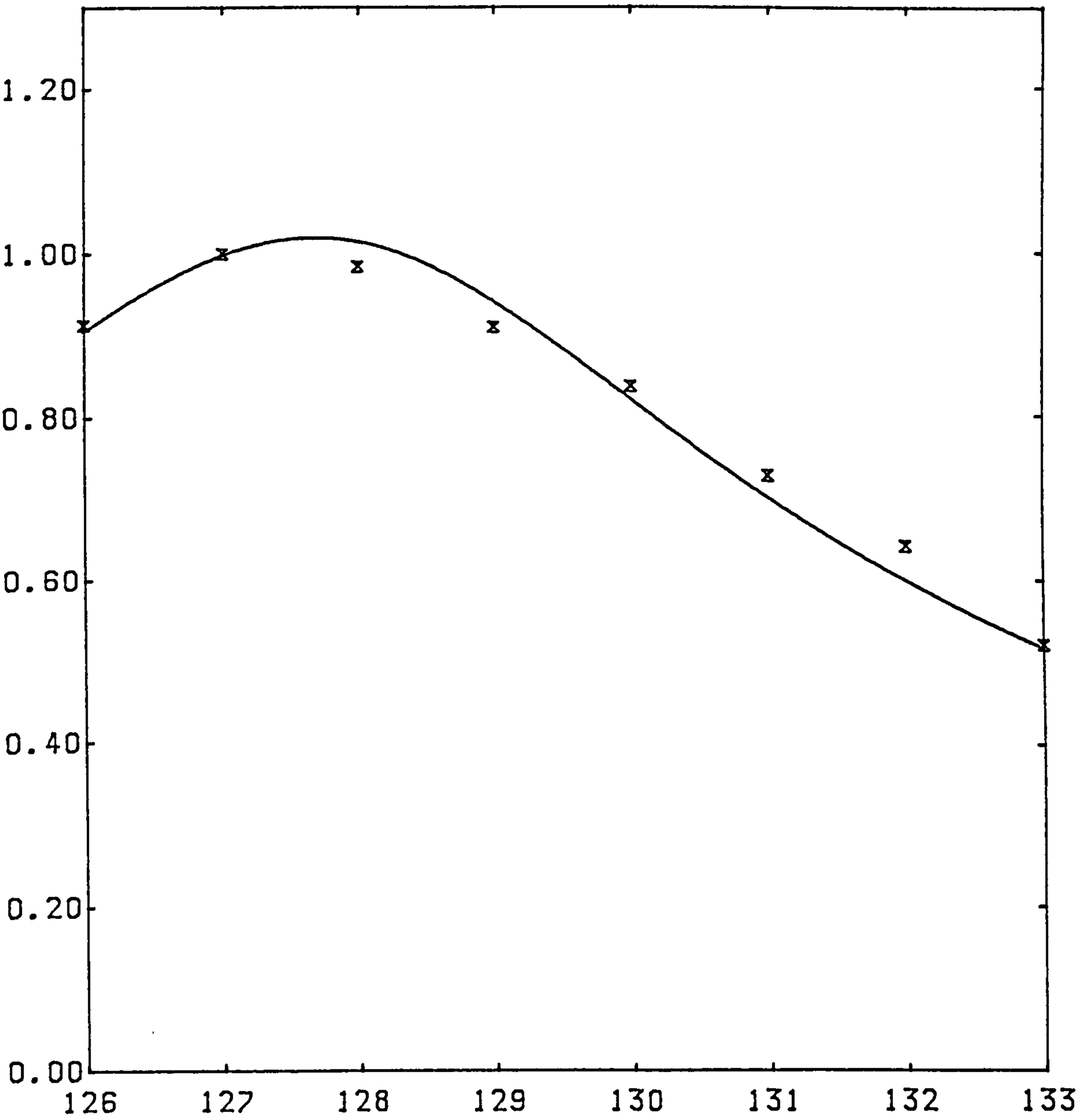

BEST FIT RESONANCE CURVE FOR EXPERIMENTAL DATA

NATURAL FREQUENCY 127.8 HERTZ

PERCENTAGE DAMPING 2.5

FIG 8.5

WALL 1 SECOND MODE

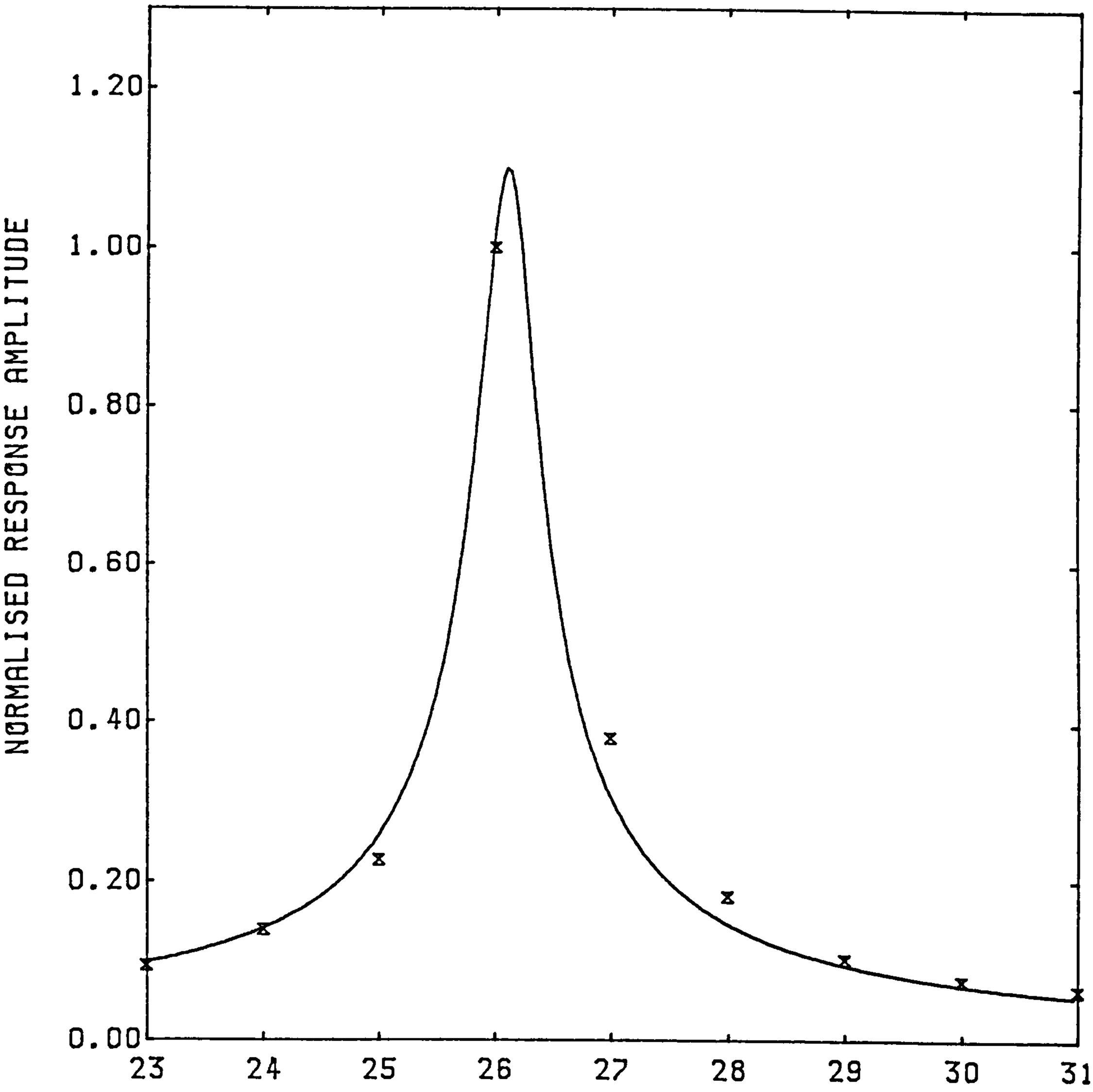

BEST FIT RESONANCE CURVE FOR EXPERIMENTAL DATA

NATURAL FREQUENCY 26.1 HERTZ

PERCENTAGE DAMPING 1.0

FIG 8.6

FRAME FIRST MODE

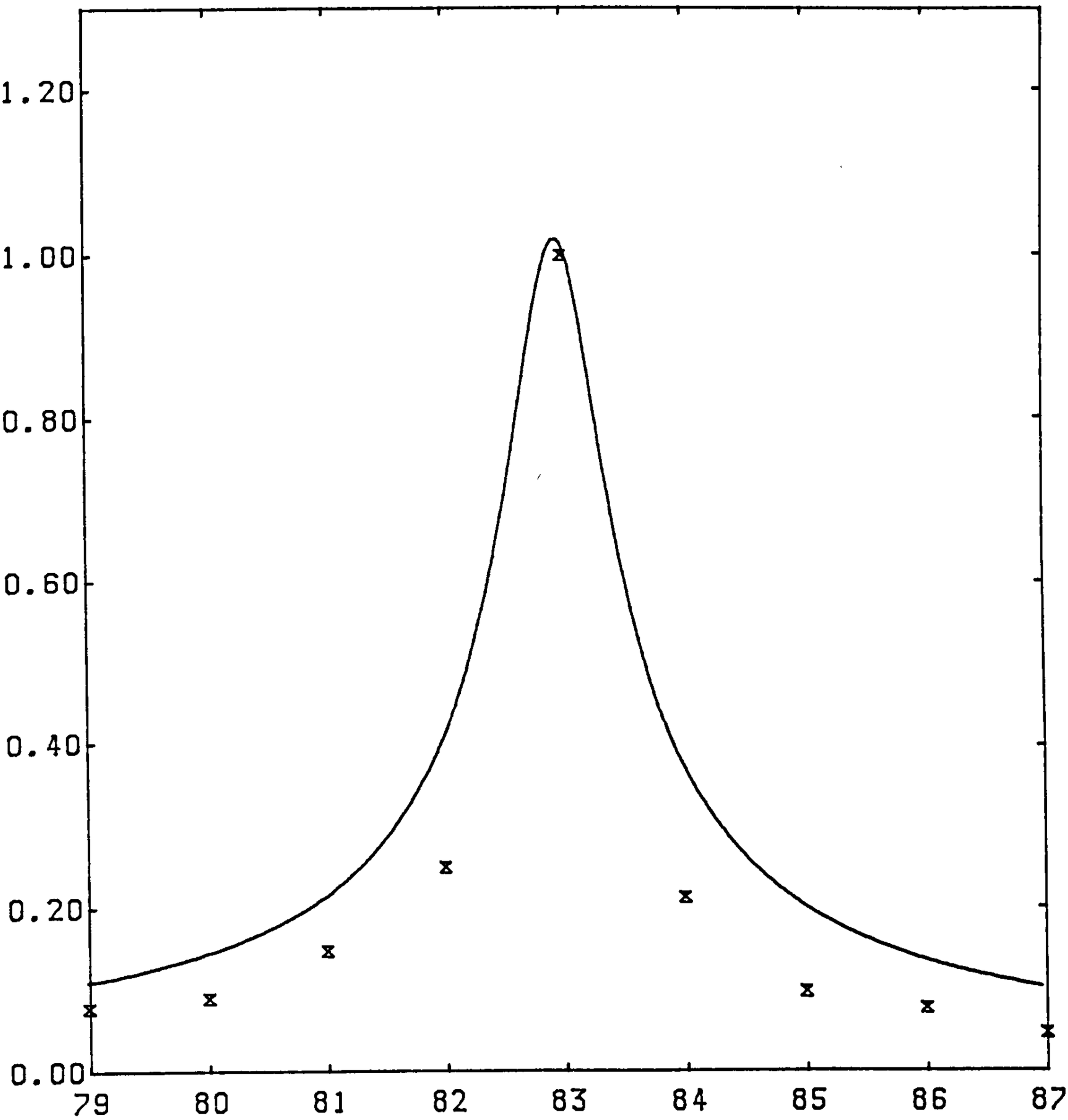

BEST FIT RESONANCE CURVE FOR EXPERIMENTAL DATA

NATURAL FREQUENCY 83.0 HERTZ

PERCENTAGE DAMPING 0.5

FIG 8.7

FRAME SECOND MODE

		Natural Frequency Hz	
		1st Mode	2nd Mode
Wall 1 and Frame	Theoretical	35.5	121
	Experimental	38.5	133
Wall 2 and Frame	Theoretical	39.0	135
	Experimental	41.0	147
Wall 3 and Frame	Theoretical	44.4	155
	Experimental	45.0	168

Table 8.2

Natural Frequencies of the Walls and Frame Fixed Together

frame to the walls increased the natural frequency in each case. This is despite the fact that the frame natural frequencies were lower than those for the walls. However, this is to be expected as the interaction of the frame and the wall produces a greatly stiffened structure owing to their different natural deflected shapes. This stiffening effect can be seen in the static results of the previous chapter.

Again, the theoretical predictions are accurate for the first two modes with the error never exceeding 10%.

The theoretical and experimental mode shapes are shown in Figs 8.8-8.10. Examining these, the agreement can be seen to be very close for all three walls for both modes. The proposed theoretical scheme is capable of accurately representing the fixed joints between the wall and frame.

Resonance curves for the first two modes of WALL 1 fixed to the frame are shown in Figs 8.11, 8.12. The proportions of critical damping are 2.5% for the first mode and 1.5% for the second mode. These values are as expected, lying between the values found for the walls and frame individually. Similar results were found for the other two walls fixed to the frame.

8.7 COMPARISON WITH THE WALLS AND FRAME PINNED TOGETHER

As in the static analyses, a single bolt was used at the joint between the frame and the wall to give a pinned joint (Figure 8.13). The resonance tests were repeated to measure the natural frequencies, mode shapes and damping.

The theoretical and experimental natural frequencies are shown in table 8.3. It can be seen that the theoretical values

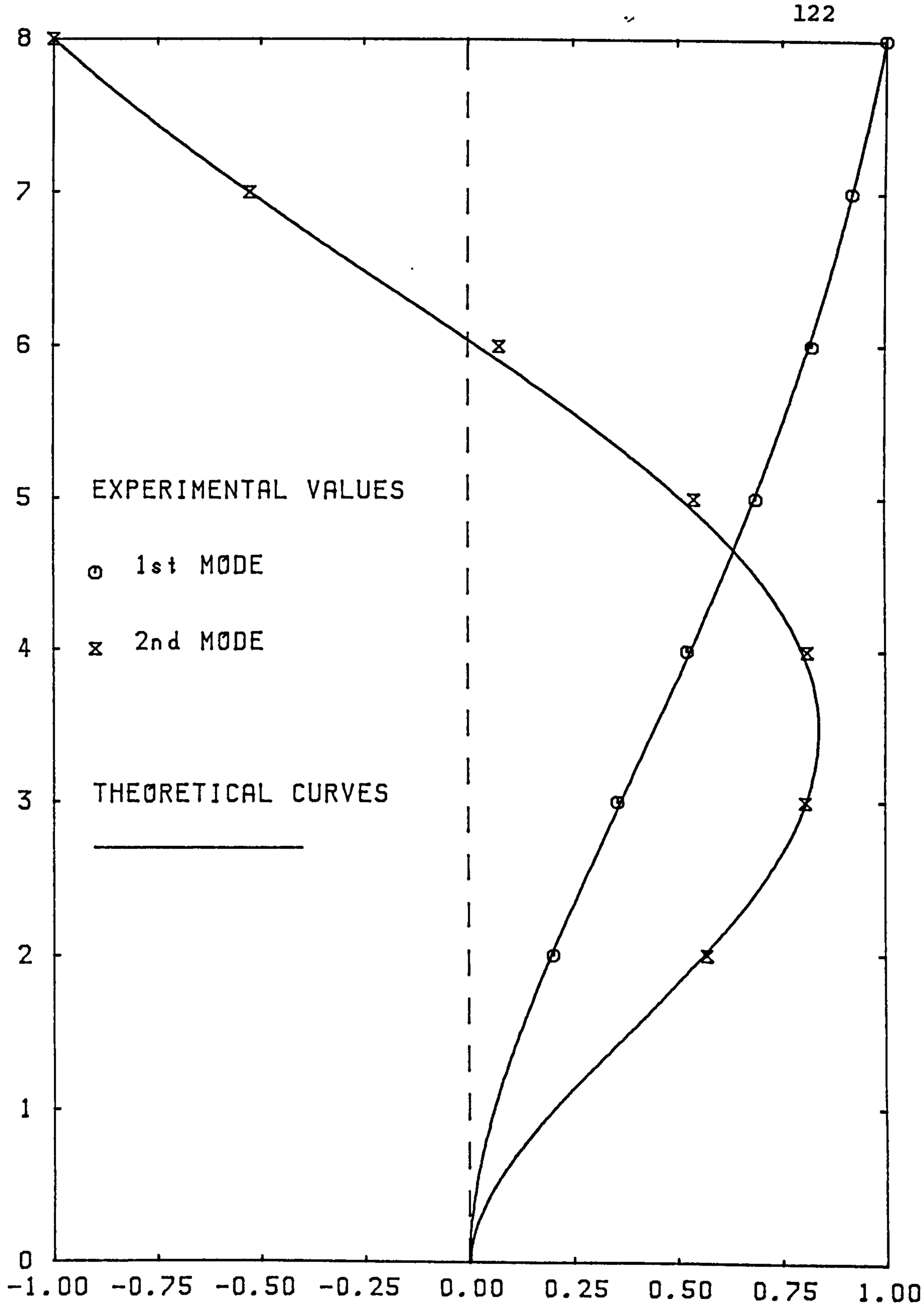

LATERAL DEFLECTION
FOR FIRST AND SECOND VIBRATION MODES

FIG 8.8

WALL 1 FIXED TO FRAME

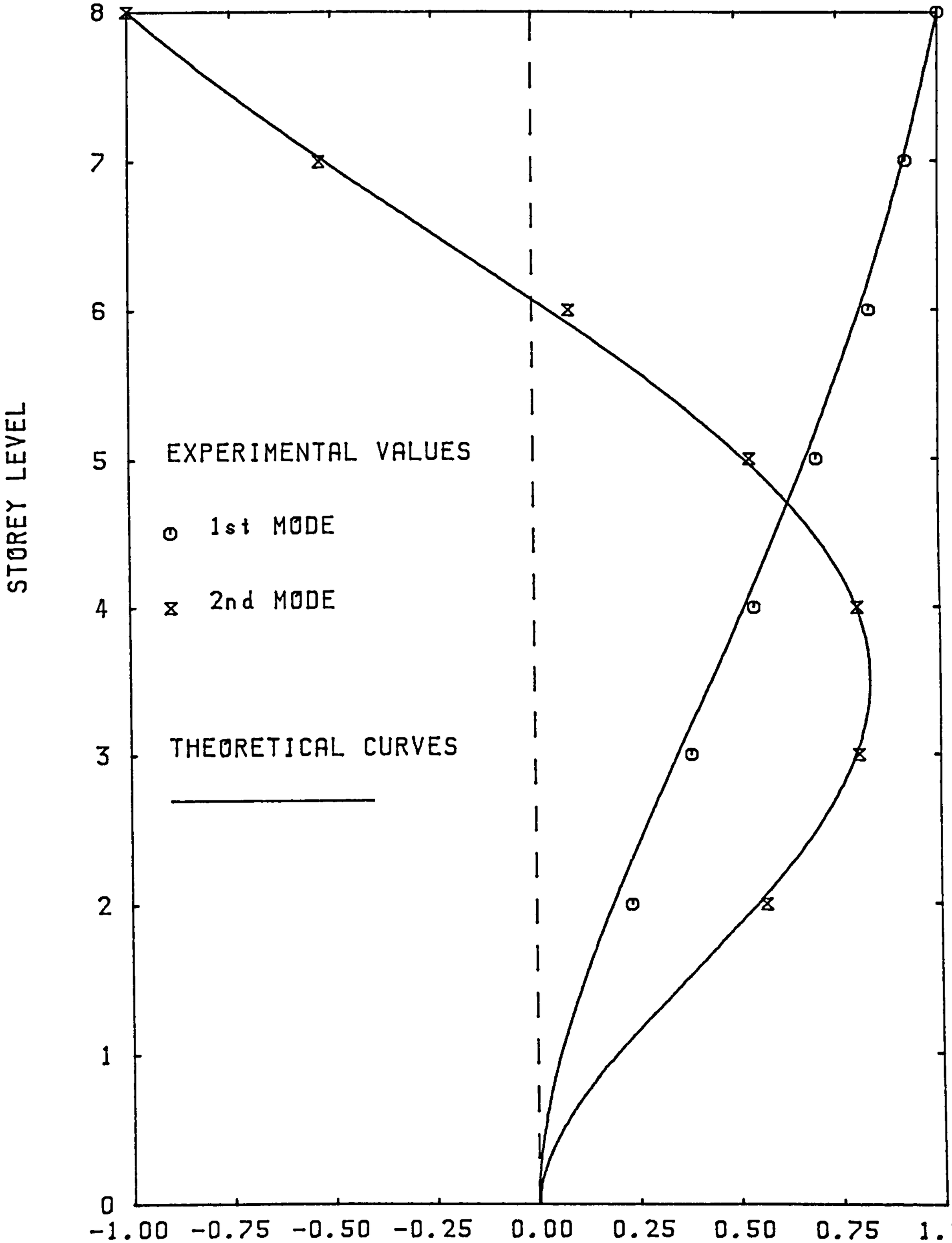

FOR FIRST AND SECOND VIBRATION MODES

FIG 8.9

WALL 2 FIXED TO FRAME

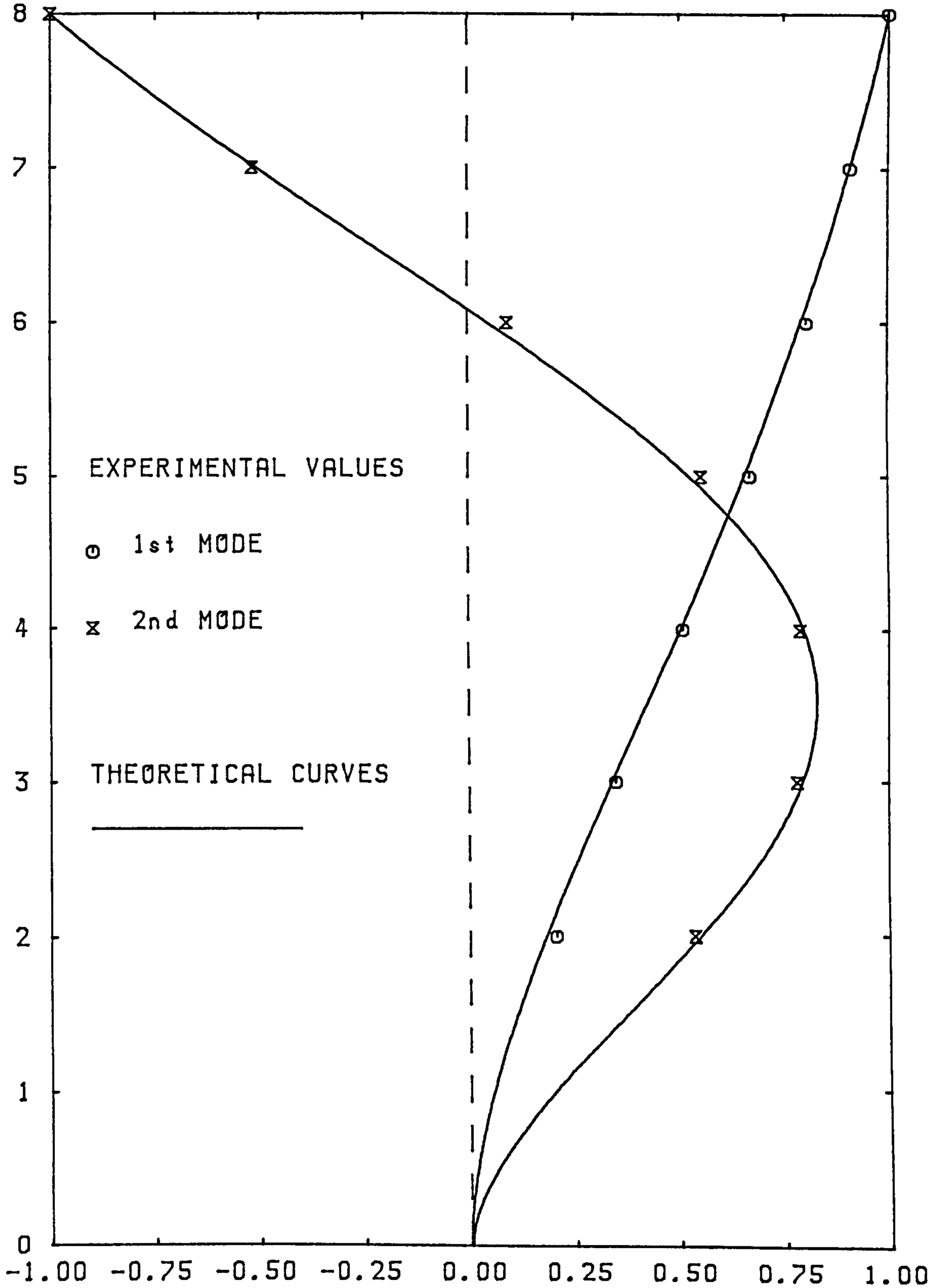

LATERAL DEFLECTION
FOR FIRST AND SECOND VIBRATION MODES

FIG 8.10

WALL 3 FIXED TO FRAME

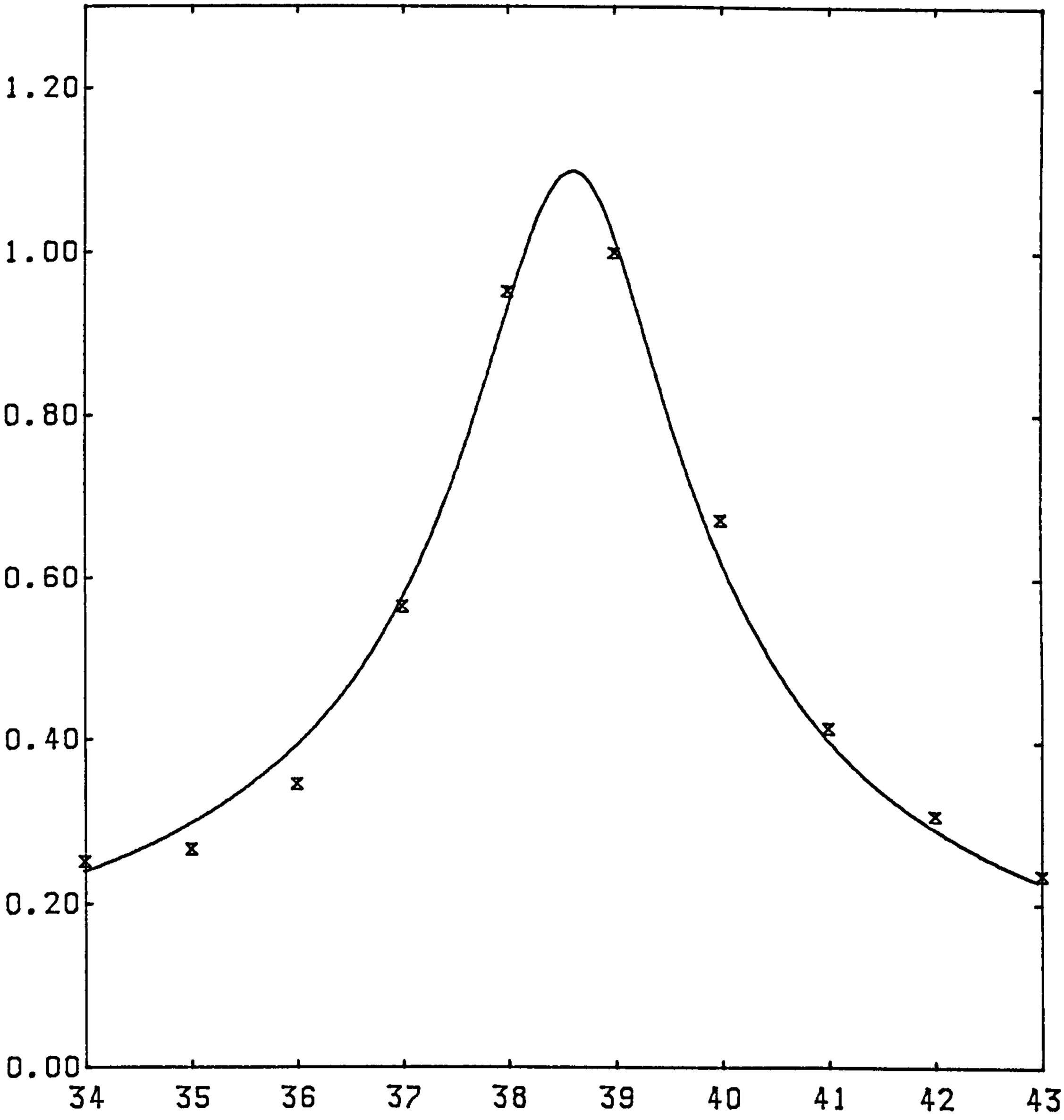

BEST FIT RESONANCE CURVE FOR EXPERIMENTAL DATA

NATURAL FREQUENCY 38.6 HERTZ

PERCENTAGE DAMPING 2.5

FIG8.11

WALL 1 FIXED TO FRAME FIRST MODE

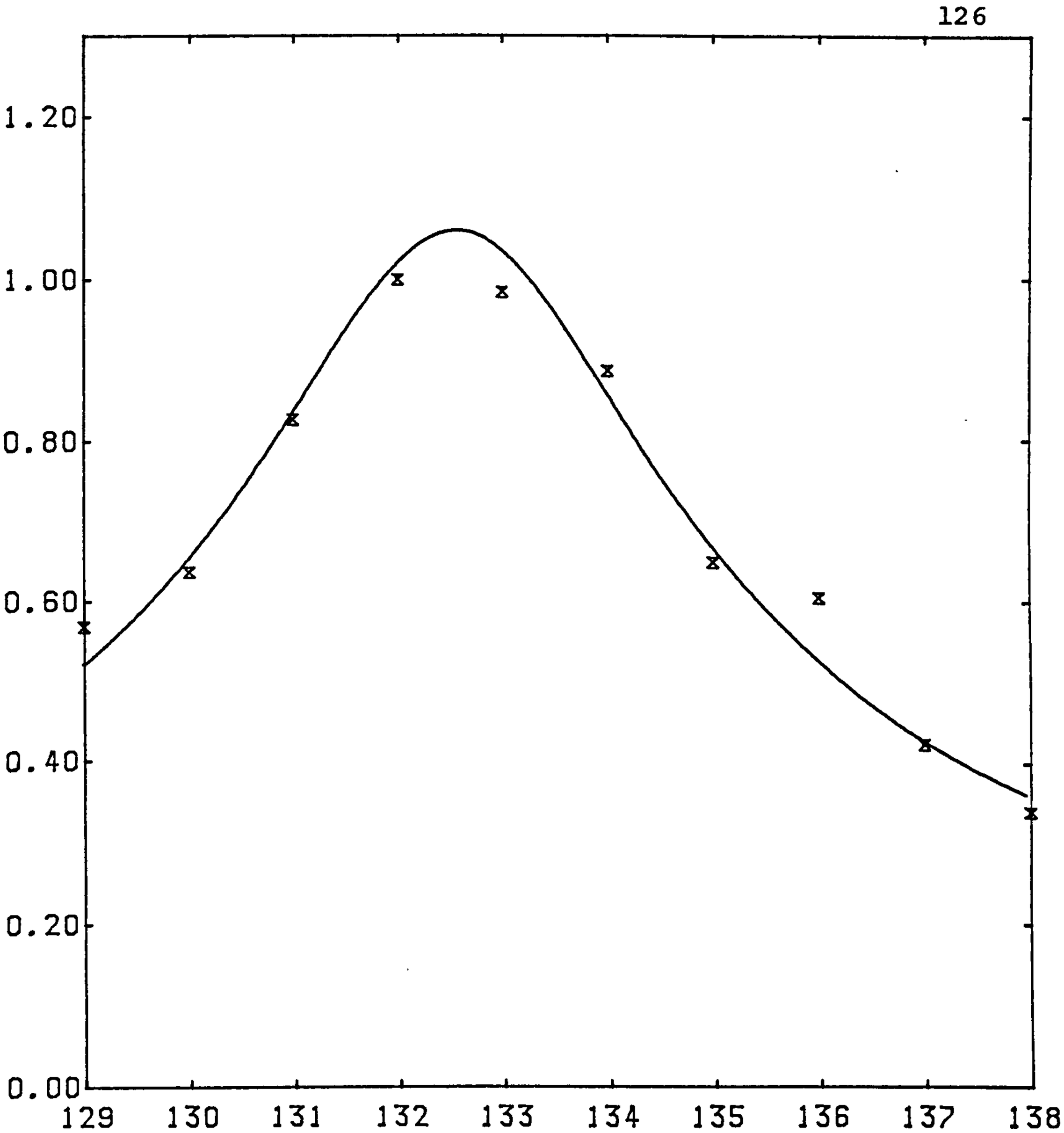

BEST FIT RESONANCE CURVE FOR EXPERIMENTAL DATA

NATURAL FREQUENCY 132.6 HERTZ

PERCENTAGE DAMPING 1.5

FIG 8.12

WALL 1 FIXED TO FRAME SECOND MODE

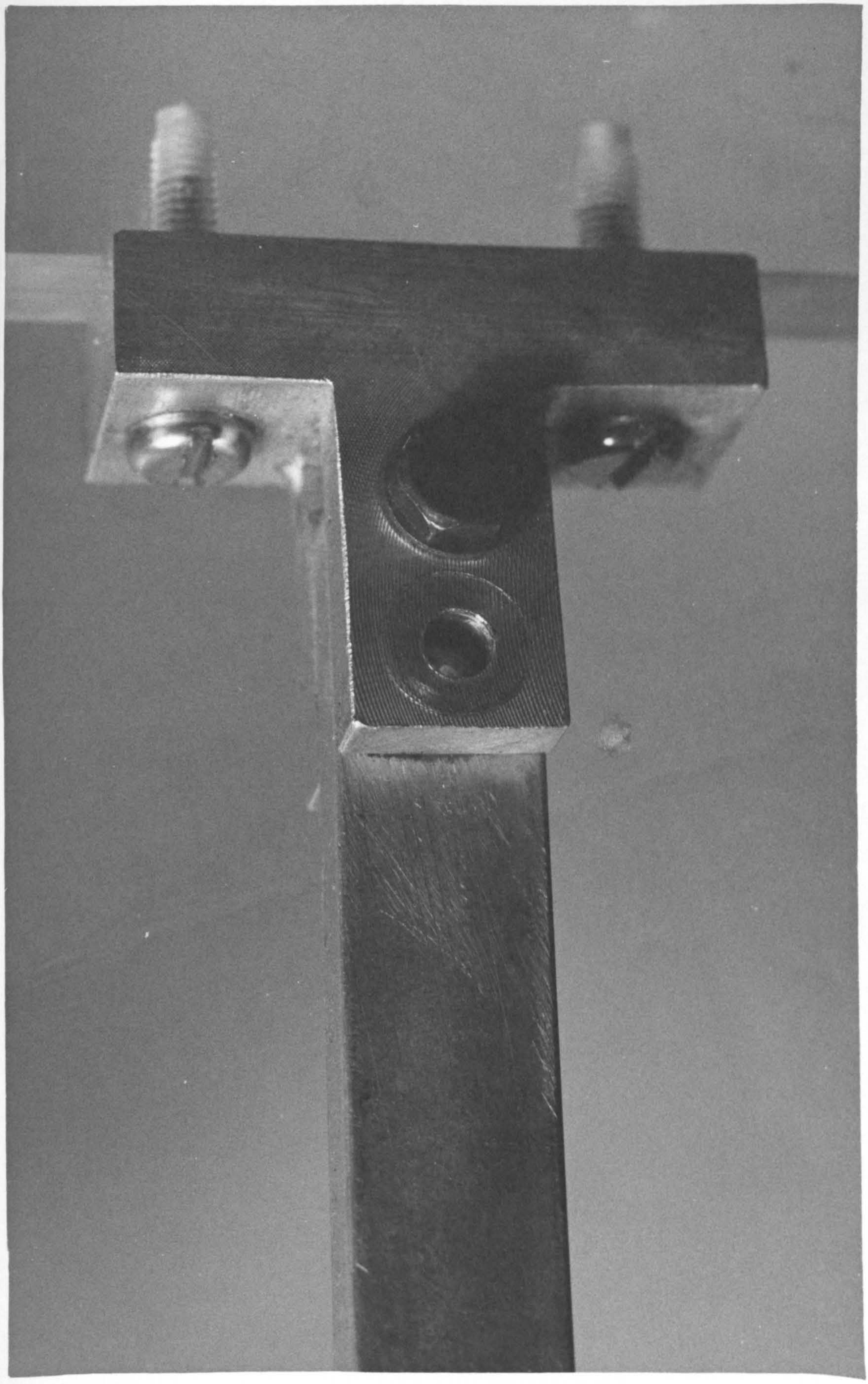

FIG. 8.13

Wall-Frame Joint Pinned

		Natural Frequency Hz	
		1st Mode	2nd Mode
Wall 1 and Frame	Theoretical	30.9	109
	Experimental	37.0	127
Wall 2 and Frame	Theoretical	34.2	123
	Experimental	39.0	146
Wall 3 and Frame	Theoretical	39.3	144
	Experimental	42.0	165

Table 8.3

Natural Freqencies of the Walls and Frame Pinned Together

are rather low when compared to the experimental frequencies.

The theory assumes that the wall-frame joint is perfectly pinned and produces no moments. In practice, friction in these joints was effectively fixing them at low moment values. This partial fixity produced natural frequencies only slighly lower than those for the fully fixed joint.

The friction in these joints was measured by a simple technique. Most of the frame was removed leaving only the members pinned to the wall as cantilevers. The moment at which these started to slip and rotate was then measured. This was accomplished by hanging weights from the cantilever beams and gradually increasing the distance between the "pin" joint and the weight hanger. The distance at which the joint began to move enabled calculation of the moment. The moment measured varied from zero, with the joint unable to support the weight of the beam, to a value of approximately 0.3 Nm. This variation was attributed to small differences in the manufacture of the joints.

To try to improve the consistency of the experiments, the bolts at the joints were tightened to produce a resisting moment of 0.5 Nm at each. This value was only obtained approximately as the surfaces were not very smooth and tended to slip and stick. All the results for a pinned joint presented here were obtained with the joints adjusted in this manner.

The theoretical and experimental mode shapes are shwon in Figs 8.14-8.16. It can be seen that the agreement is not as close as for the fixed joint mode shapes shown in Figs 8.8-8.10. This may be attributed to the friction in the joints producing partial fixity. The theoretical predictions are, however, still close,

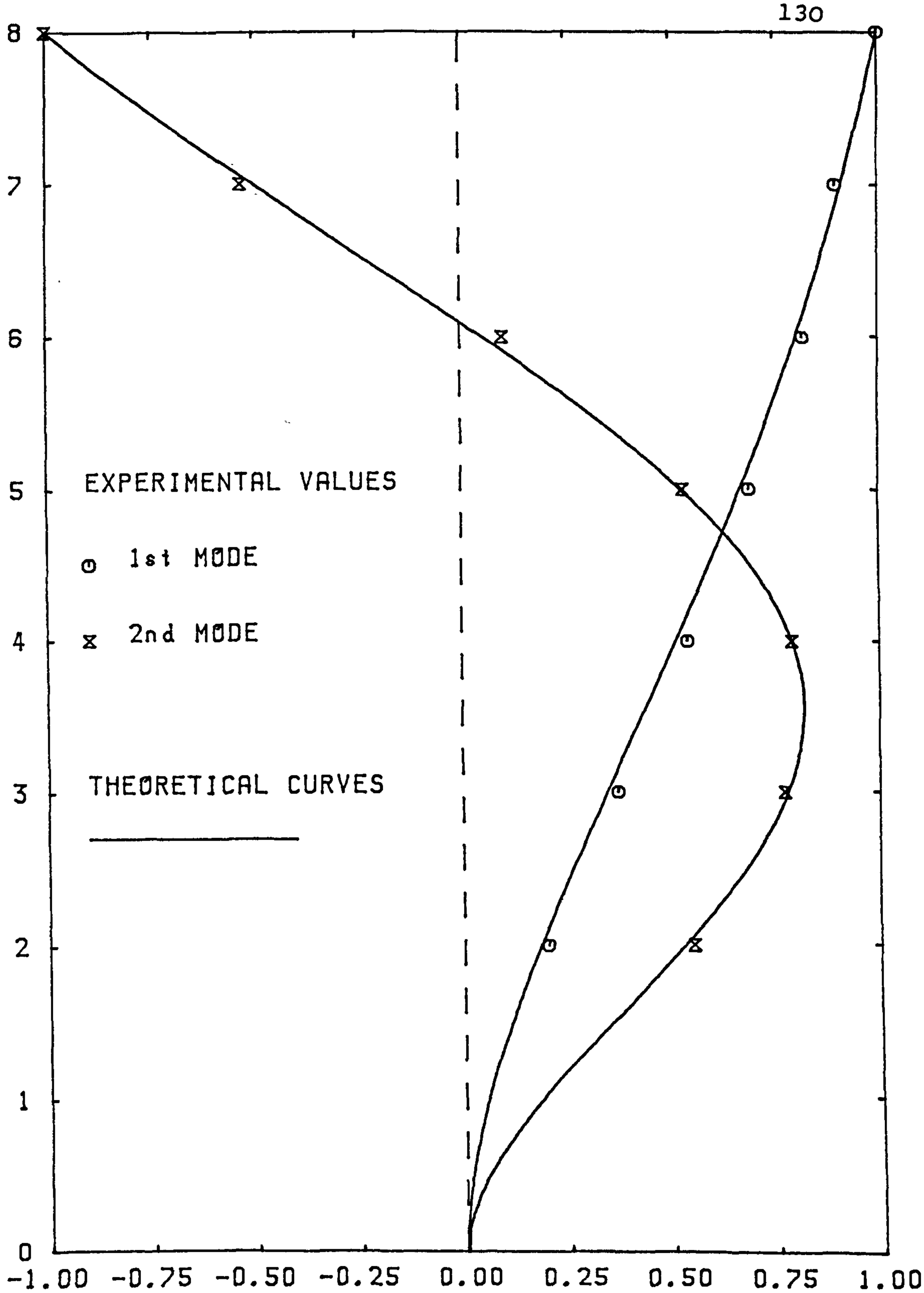

LATERAL DEFLECTION
FOR FIRST AND SECOND VIBRATION MODES

FIG 8.14

WALL 1 PINNED TO FRAME

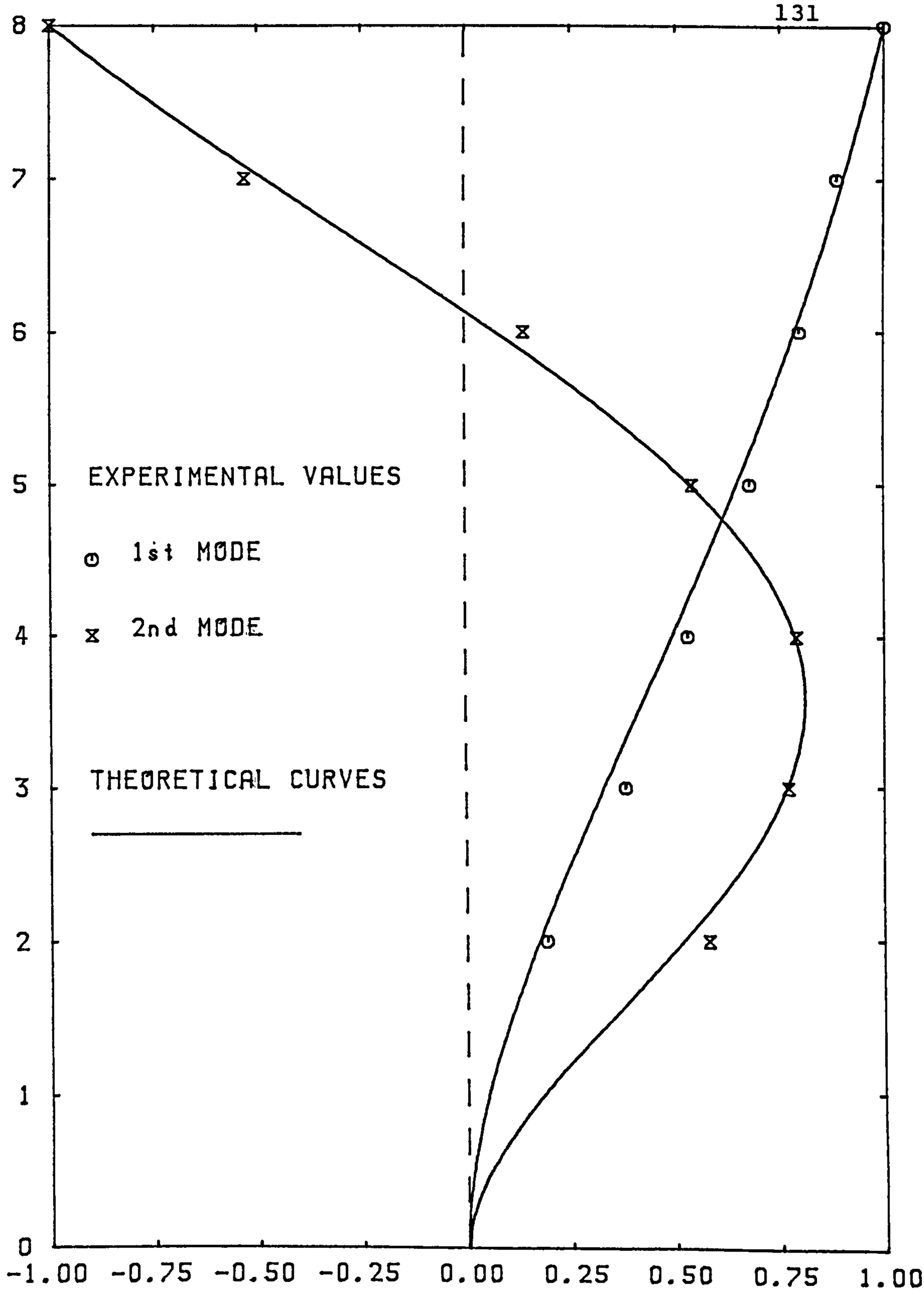

LATERAL DEFLECTION
FOR FIRST AND SECOND VIBRATION MODES

FIG 8.15

WALL 2 PINNED TO FRAME

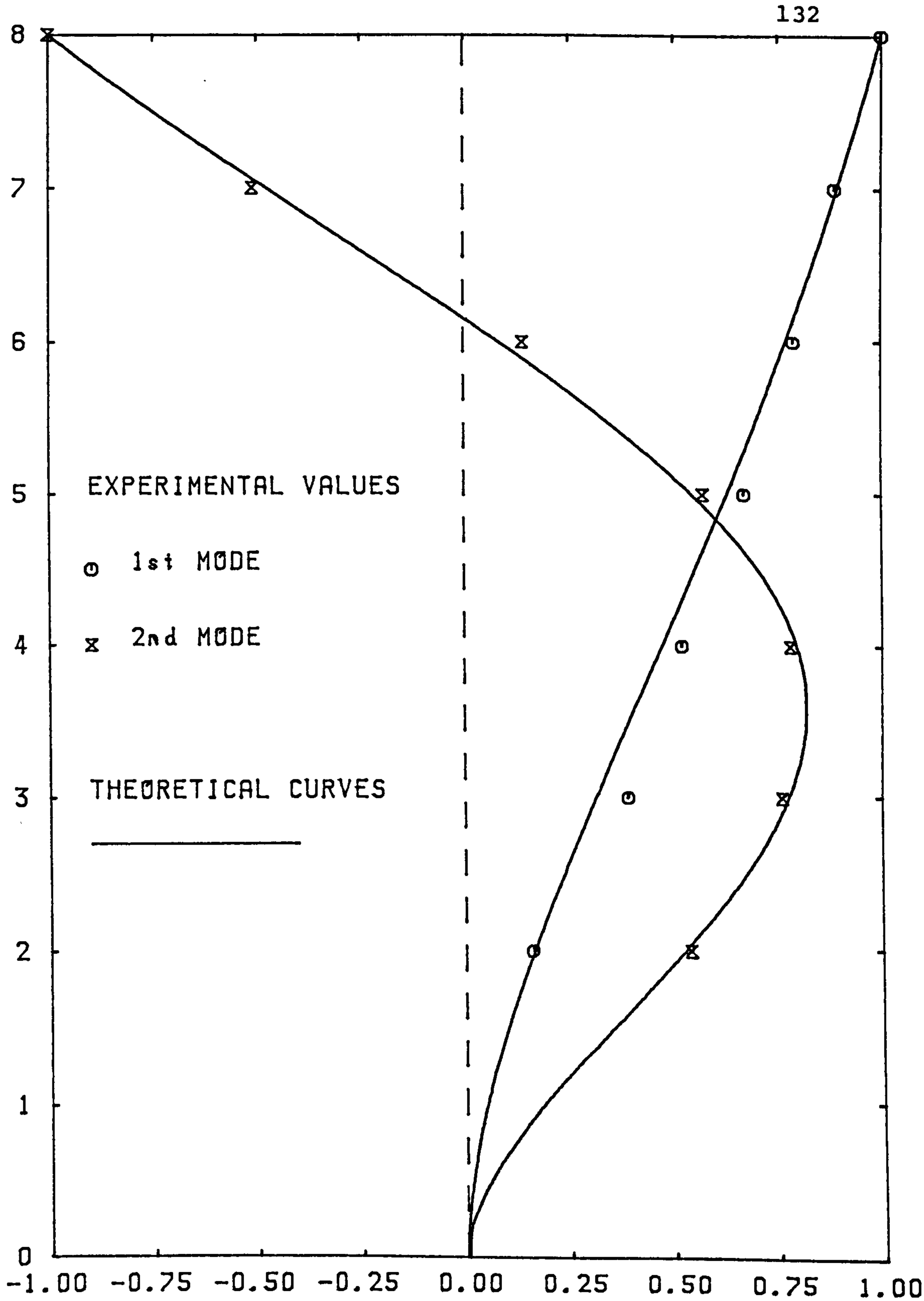

LATERAL DEFLECTION
FOR FIRST AND SECOND VIBRATION MODES

FIG 8.16

WALL 3 PINNED TO FRAME

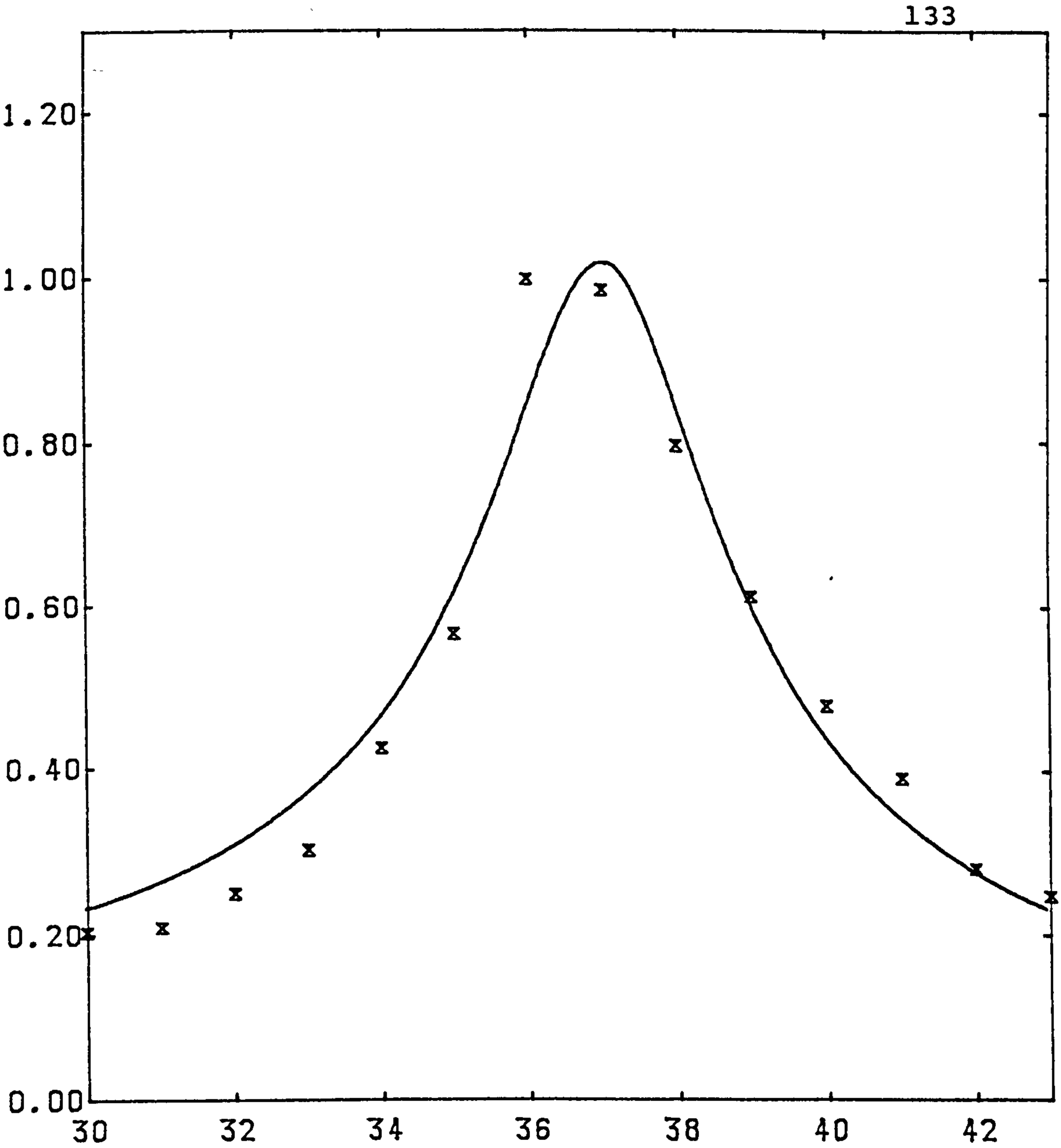

BEST FIT RESONANCE CURVE FOR EXPERIMENTAL DATA

NATURAL FREQUENCY 37.1 HERTZ

PERCENTAGE DAMPING 4.0

FIG 8.17

WALL 1 PINNED TO FRAME ALL DATA PLOTTED

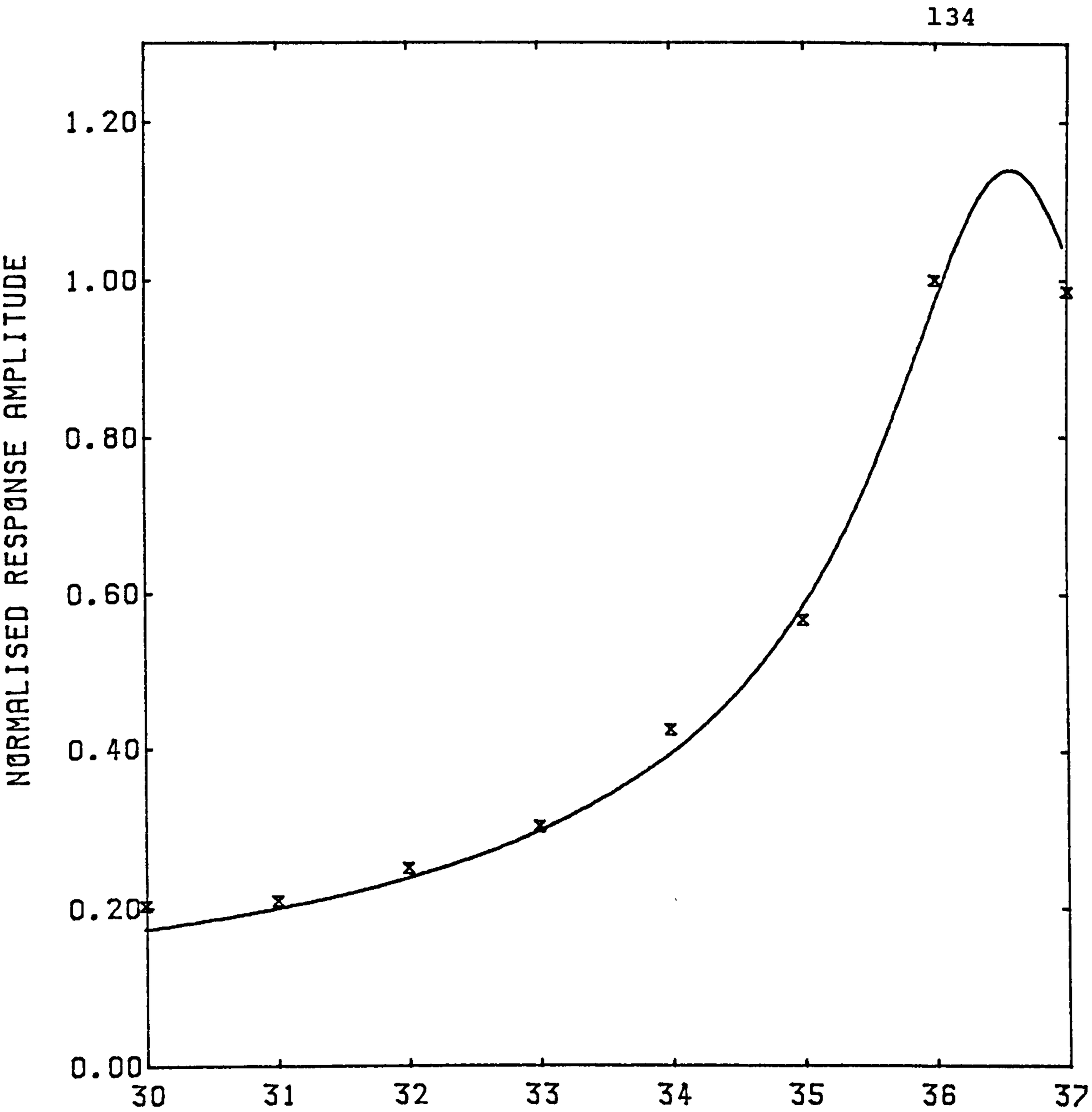

BEST FIT RESONANCE CURVE FOR EXPERIMENTAL DATA

NATURAL FREQUENCY 36.6 HERTZ

PERCENTAGE DAMPING 2.5

FIG 8.18

WALL 1 PINNED TO FRAME BELOW RESONANCE

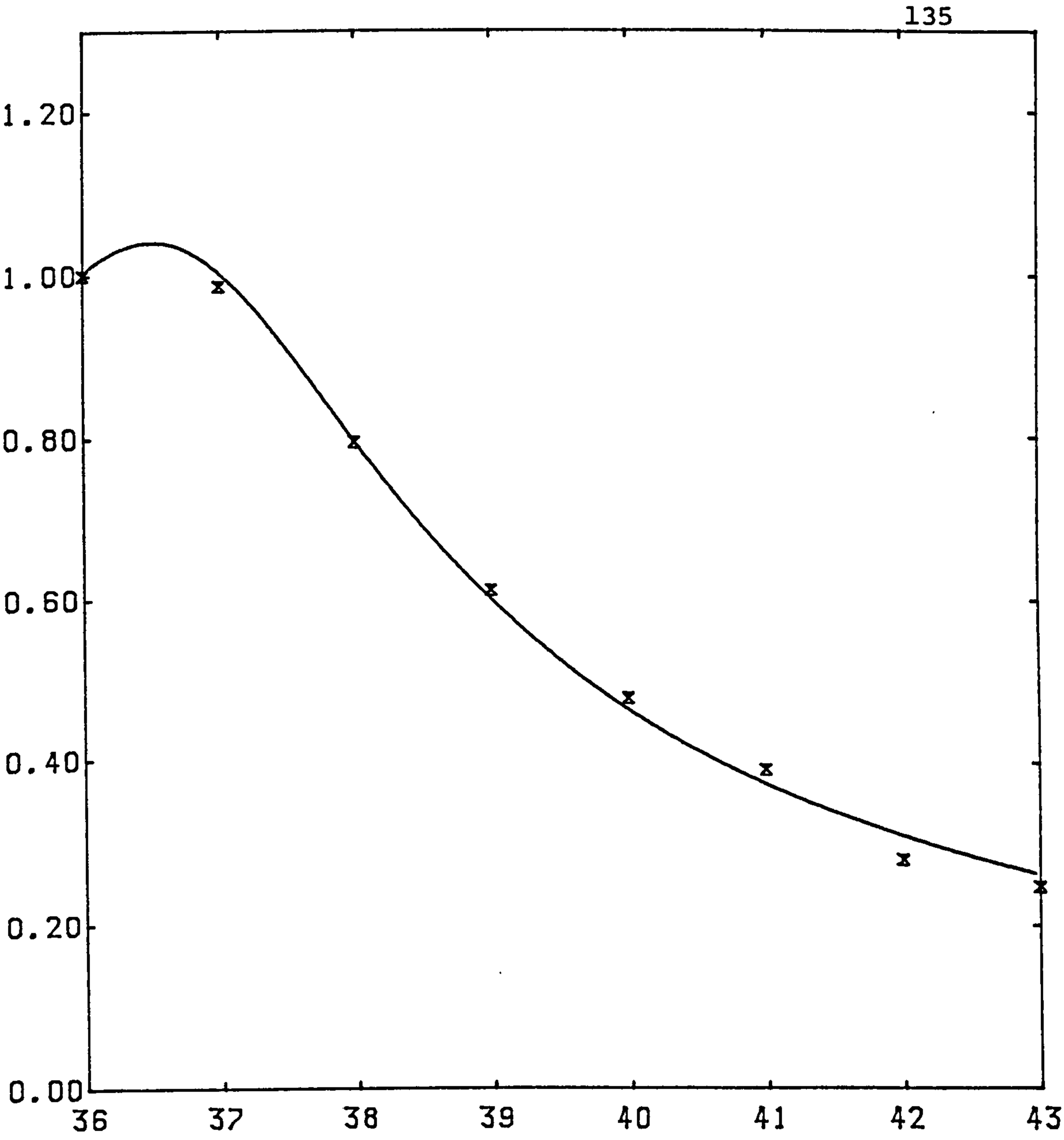

BEST FIT RESONANCE CURVE FOR EXPERIMENTAL DATA

NATURAL FREQUENCY 36.6 HERTZ

PERCENTAGE DAMPING 5.0

FIG 8.19

WALL 1 PINNED TO FRAME ABOVE RESONANCE

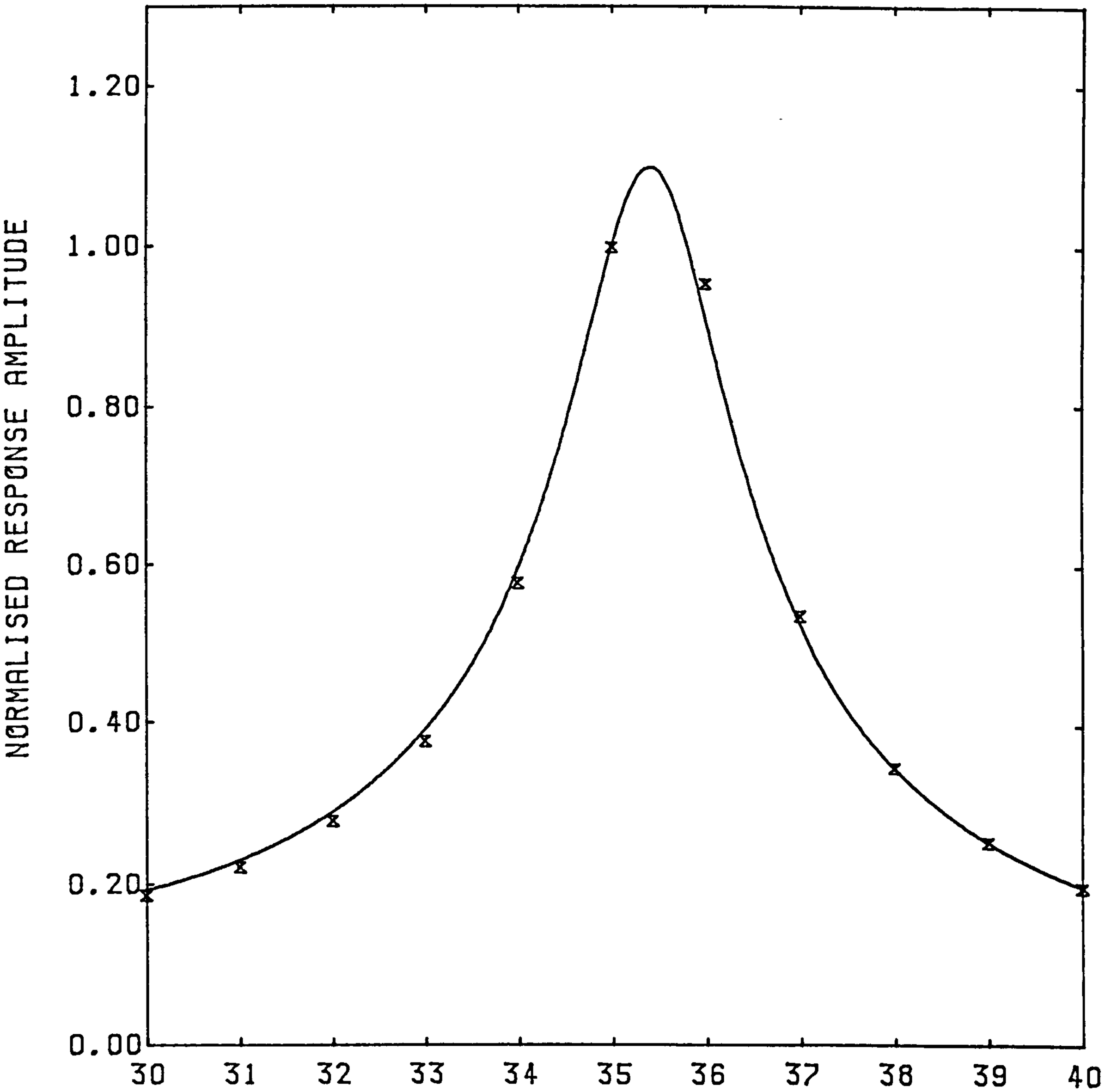

BEST FIT RESONANCE CURVE FOR EXPERIMENTAL DATA

NATURAL FREQUENCY 35.4 HERTZ

PERCENTAGE DAMPING 2.5

FIG 8.20

LINEAR COMPUTED DATA WALL 1 PINNED TO FRAME

owing to the similarity between the mode shapes for the fixed and pin jointed connections.

Damping:

The damping for the first mode of WALL 1 pinned to the frame was evaluated from the resonance curve Figure 8.17. The value of 4% was higher than for the wall and frame fixed together. This could again be attributed to the friction in the joints. However, it can be seen that the curve is not a good fit for the data points. The curve is based upon the assumption of viscous damping whilst the real mechanism is frictional damping. By plotting the points either side of resonance separately (Figs 8.18, 8.19), it can be seen that below resonance the best fit gives a value of 2.5% critical damping. Above resonance the best fit curve is 5% critical damping. Equivalent viscous damping does not provide a good model for the friction in the joints.

To try to overcome this, the forced response analysis procedure was employed to model the wall and frame. The frame was modelled as fixed to the wall and 2.5% equivalent viscous damping was employed. The analysis was then performed for a range of sinusoidal forcing frequencies to obtain the steady-state response amplitude for each. This allowed the plotting of the response curve Figure 8.20. As would be expected, the natural frequency is $35.4H_3$ which is almost identical to the value predicted by the free vibration analysis. Also, the data points are an excellent fit to the resonance curve.

To model the behaviour of the pinned joints, the yield value was then set to 0.5 Nm for non-linear analysis. For this analysis

the mass and damping at the constrained joints must be zero as shown in chapter 5. To achieve this, the mass at the joint was lumped to adjacent wall nodes. Mass proportional damping was then used. In this case the amount of damping in only one mode may be controlled. As the response in only the first mode was being studied, this provided a convenient means of controlling the damping in this mode whilst removing it at the joints. Equation 4.3, with $C_2 = 0$, may be rearranged to produce

$$C_1 = 2 \ \mu i \ \omega i \qquad 8.15$$

for the damping constant C_1.

The analyses were then performed again for a range of sinusoidal forcing frequencies. The steady state response at each was then plotted to produce the response curve of Figure 8.21. Again, by plotting the values below and above resonance (Figs 8.22, 8.23), it can be seen that the damping produced is of the same form as that obtained experimentally. A low value of equivalement viscous damping is obtained below resonance and a higher value above. The theoretical values obtained for the damping are higher than those found experimentally. This is probably due to the poor control obtained over the friction in the joints. These were not designed to provide friction damping and their adjustment was only approximate.

However, it can be seen that the forced response analysis technique, using Lagrange multiplier constraints, gives accurate predictions when employed for both linear and non-linear analysis.

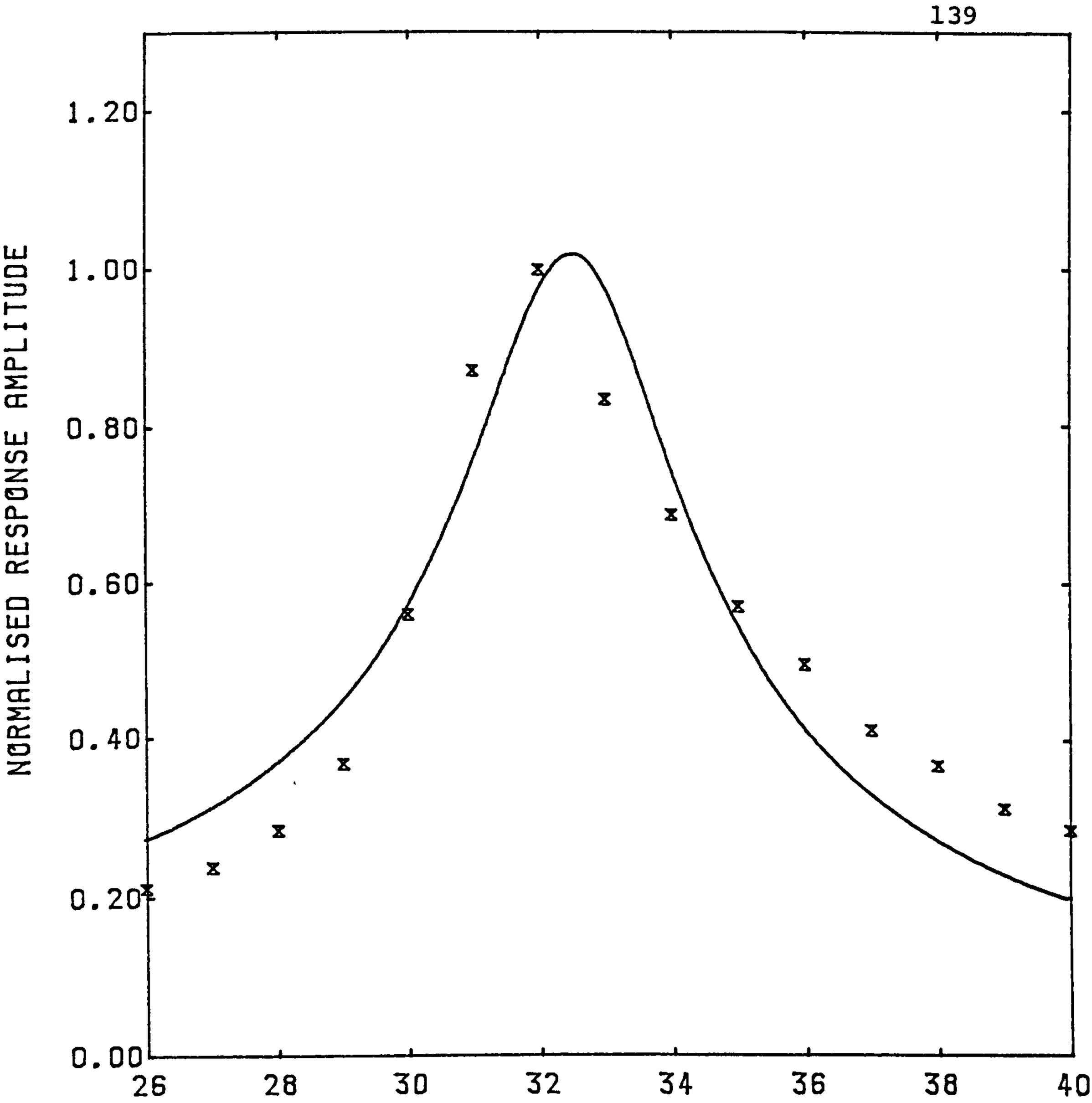

BEST FIT RESONANCE CURVE FOR EXPERIMENTAL DATA

NATURAL FREQUENCY 32.6 HERTZ

PERCENTAGE DAMPING 5.0

FIG 8.21

NON-LINEAR COMPUTED DATA ALL POINTS PLOTTED

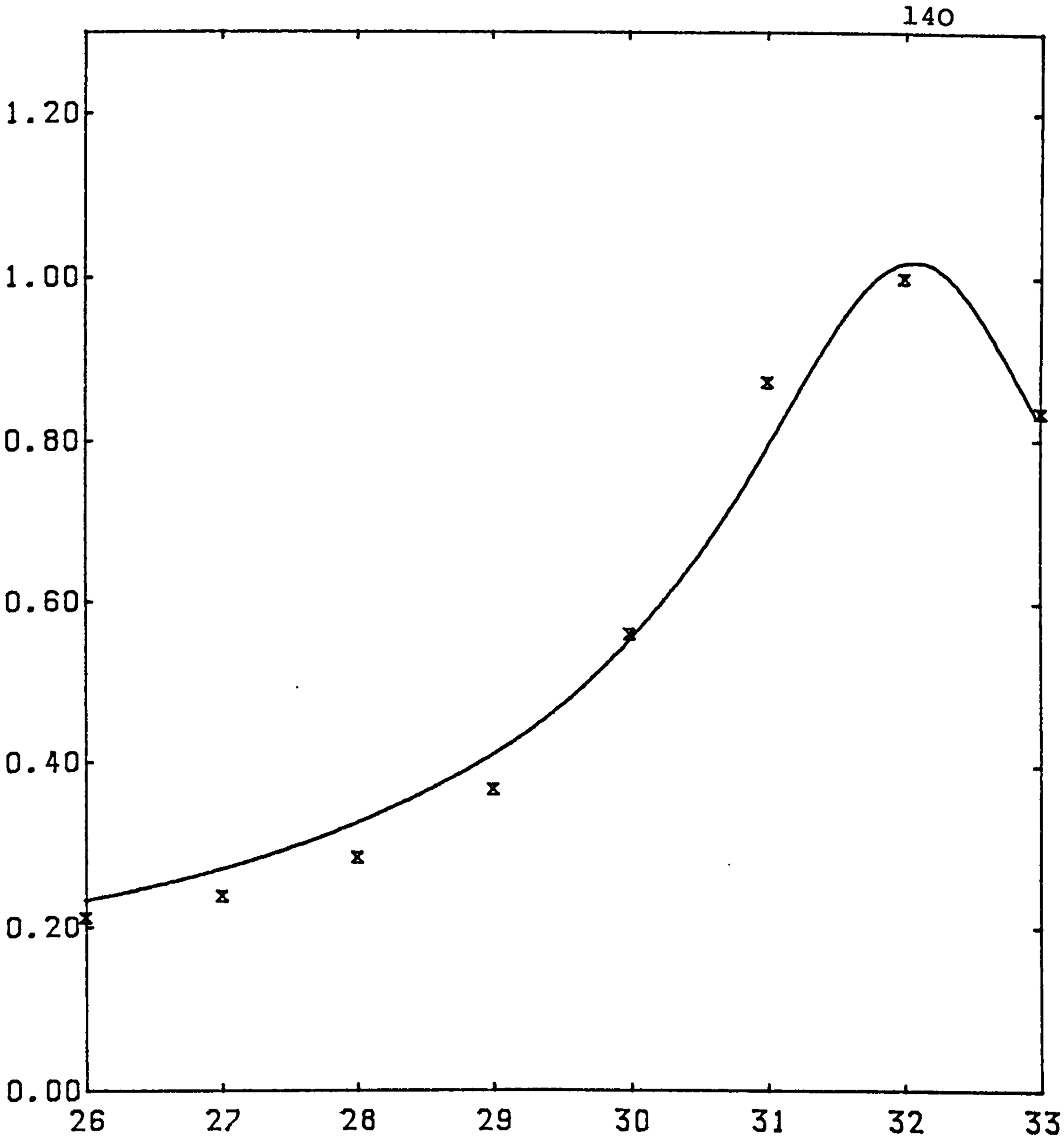

BEST FIT RESONANCE CURVE FOR EXPERIMENTAL DATA

NATURAL FREQUENCY 32.1 HERTZ

PERCENTAGE DAMPING 4.0

FIG 8.22

NON-LINEAR COMPUTED DATA BELOW RESONANCE

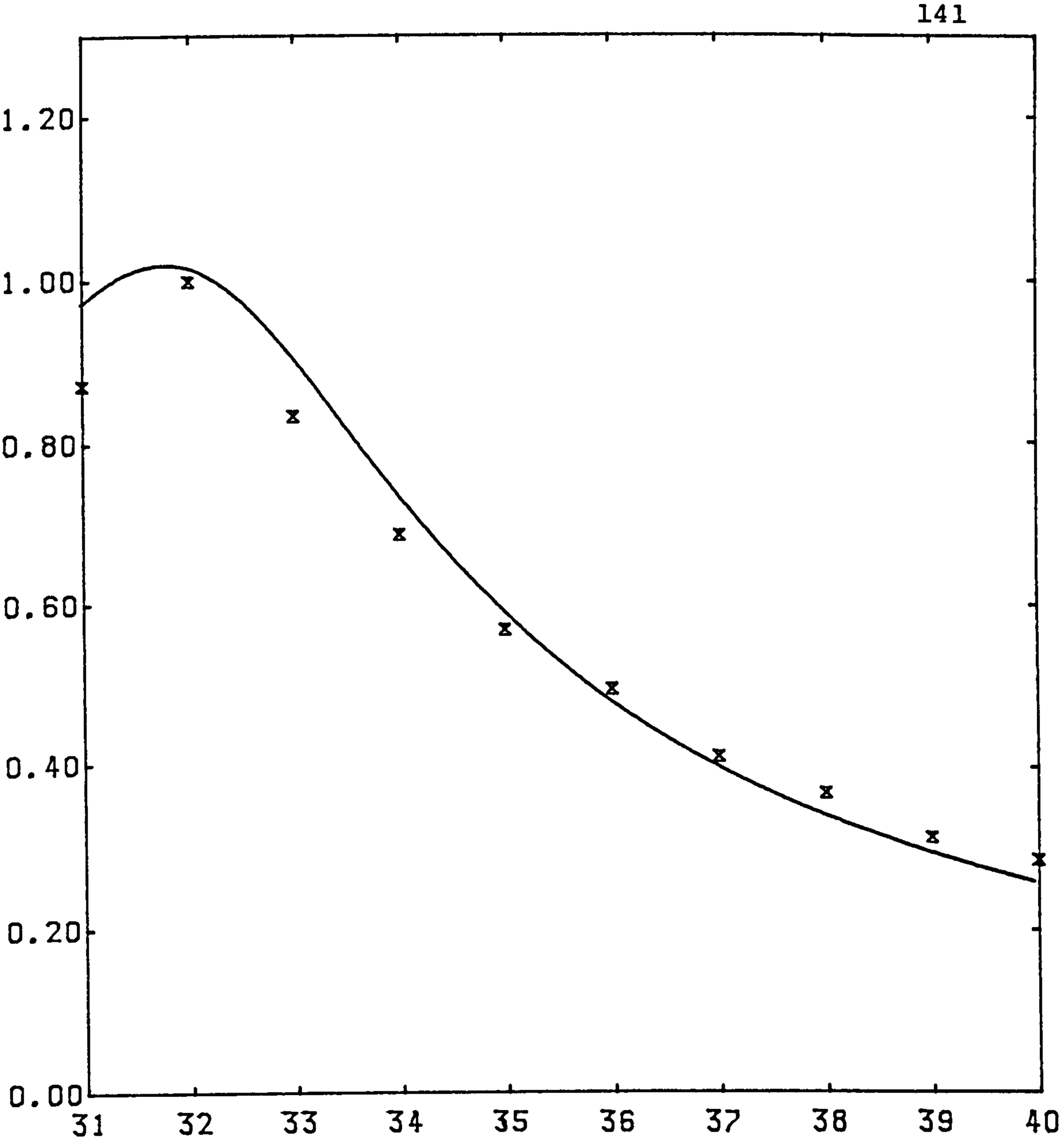

BEST FIT RESONANCE CURVE FOR EXPERIMENTAL DATA

NATURAL FREQUENCY 32.0 HERTZ

PERCENTAGE DAMPING 7.5

FIG 8.23

NON-LINEAR COMPUTED DATA ABOVE RESONANCE

CHAPTER NINE - CONCLUSIONS

9.1 CONCLUSIONS OF THIS STUDY

The finite element method is the most versatile technique that has been used for the analysis of coupled shear walls or shear wall-frame combinations. It can readily deal with discontinuities and irregularities in the structure and can model non-linear behaviour in detail.

From the studies made here of the various finite element schemes which have been proposed for static analysis, the following conclusions may be drawn.

1. For coupled shear walls, the Lagrange multiplier schemes produce very similar results to the use of quadrilateral isoparametric elements only. This may be seen from the results presented in chapter 6.4 and 6.6.
2. As discussed in chapter 2.3, the Lagrange multiplier technique is preferable to the use of quadrilateral isoparametric elements only, as it reduces the number of degrees of freedom required for beams and columns.
3. From comparisons with the test results presented in chapter 7, it can be seen that the Lagrange multiplier technique allows the accurate analysis of a wall and frame fixed together.
4. The use of the plane stress element with rotational degrees of freedom produces highly inaccurate results owing to the low rotational connection stiffness at the wall-beam joint. The joint at a single point can rotate without significantly

affecting the x-direction displacements of the wall face. This may be seen from the results in chapter 6.5.

5. From the results presented in chapter 6.6, it may be seen that the second constraint equation proposed by Al-Mahaidi et al. for the Lagrange multiplier technique does not improve the accuracy of the analysis. Its omission to produce the "wall face oriented connection" of Antony and Ganesan is to be preferred.

6. Also from chapter 6.6 it may be seen that the Lagrange multiplier scheme proposed in this thesis, is advantageous in comparison with the others as it produces the lowest problem bandwidth and gives automatic calculation of the forces at a constrained joint.

7. The results presented in chapter 7.5 show that the results from the proposed scheme are accurate even when the coupling beams are deep.

8. More accurate results may be obtained when shear deformation effects are included for the line elements. The effect is not great but the amount of extra computation involved is very small. This may be seen from the results in chapter 7.5 and 7.6.

Having selected the most suitable finite element model for static analysis (the proposed Lagrange multiplier scheme), it was then developed to allow dynamic analysis. The Lagrange multiplier technique was also developed to model non-linear behaviour at the constrained joints. From the comparison between the finite element analysis and small scale dynamic model tests the following conclusions were drawn.

1. From the results presented in chapter 8, it can be seen that the proposed scheme gives accurate natural frequencies and mode shapes, when used for the free vibration analysis of coupled walls and wall-frame combinations.

2. The linear forced response analysis, when used to evaluate steady state response amplitudes, gives results in close agreement with the free vibration analysis. This may be seen from chapter 8.7.

3. As discussed in chapter 5.1, the non-linear Lagrange multiplier technique is very economical, as no changes have to be made to the stiffness matrix. Very little extra computation, above that required for linear forced response analysis, is required.

4. From the results presented in chapter 8.7, it can be seen that the non-linear joint model produces accurate results when used to model friction in the wall-frame joints.

5. Equivalent viscous damping does not give an accurate model of the damping produced by the friction in the wall-frame joints. This can also be seen from the results in chapter 8.7.

During the dynamic tests, two techniques were developed which proved to be of great use.

1. The bisection method for eigenvalue evaluation was improved by the calculation of the logarithm of the value of the determinant. This permits less accurate initial estimates to be used for the eigenvalues. It also prevents

eigenvalues being missed when they lie close together. This is shown in chapter 4.2 and appendix A.

2. The least squares curve fitting technique, used to fit resonance curves to experimental data, has several advantages when employed to calculate equivalent damping ratios. It uses all of the data points and not just those near resonance; it does not require accurate hand plotting of a curve through data points which may not lie on a smooth curve owing to experimental errors; and most useful of all, it allows a check to be made on whether equivalent viscous damping produces an accurate model of the actual damping mechanism present. This is shown in chapter 8.4.

9.2 SCOPE FOR FURTHER WORK

A finite element model has been developed which allows the accurate modelling of coupled shear walls and shear wall-frame combinations. A technique for modelling the joints between beams and walls, when they are non-linear, has been shown. This opens up the possibility of two lines of work.

The analytical model could be developed further. Including conventional non-linear element methods would allow the analysis of more complex non-linear behaviour. Alternatively, the simple non-linear constrained joint could be developed to model more complex behaviour. This might be accomplished by calculating the constrained accelerations and displacements by linear programming methods [75]. In this technique the equations, for which a solution is required, are expressed as inequalities. Hence these would be suitable for expressing yield moment limits.

The second direction which work could take, would be to use the finite element model developed to investigate the possibilities of friction as a useful damping mechanism in resisting earthquakes. Friction has been employed as a base isolation technique [76], however, the model tests suggest that useful damping may be obtained from bolted joints. These have been employed as static load controld devices [77]. The non-linear Lagrange multiplier technique could be used to investigate their dynamic use at the connection between beams and walls in both coupled shear walls and wall frame combinations. This could be in conjunction with model component tests on a shaking table to accurately determine frictional joint behaviour.

REFERENCES

1. BECK, H.,
"Contribution to the Analysis of Coupled Shear Walls"
J. ACI, Vol. 59, No. 8, Aug. 1962, pp.1055-1069.

2. ROSMAN, R.,
"Approximate Analysis of Shear Walls Subject to Lateral Loads" J. ACI, Vol. 61, No. 6, June 1964, pp.717-732.

3. COULL, A., CHOUDHURY, J. R.,
"Stress and Deflections in Coupled Shear Walls" J. ACI, Vol. 64, No. 2, Feb. 1967, pp.65-72.

4. COULL, A., CHOUDHURY, J. R.,
"Analysis of Coupled Shear Walls" J. ACI, Vol. 64, No. 9, Sept. 1967, pp.587-593.

5. COULL, A., IRWIN, A. W.,
"Design of Connecting Beams in Coupled Shear Walls" J. ACI, Vol. 66, No. 3, March 1969, pp.205-209.

6. TSO, W. K., BISWAS, J. K.,
"An Approximate Seismic Analysis of Coupled Shear Walls" Build. Sci. Vol. 7, 1972, pp.249-256.

7. COULL, A., PARI, R. D.,
"Analysis of Pierced Shear Walls" J. Struct. Div. ASCE, Vol. 94, No. ST1, 5710, Jan. 1968, pp.71-82.

8. TSO, W. K., CHAN, H. B.,
"Dynamic Analysis of Plane Coupled Shear Walls" J. Eng. Mech. Div. ASCE, Vol. 97, No. EM1, 7899, Feb. 1971, pp.33-48.

9. COULL, A., MUKHERJEE, P. R.,
"Free Vibrations of Coupled Shear Walls" J. Earth. Eng. and Struct. Dyn. Vol. 1, 1973, pp.377-386.

10. COULL, A., MUKHERJEE, P. R.,
"Approximate Analysis of Natural Vibrations of Coupled Shear Walls" J. Earth. Eng. and Struct. Dyn. Vol. 2, 1973, pp.171-183.

11. ROSMAN, R.
"Dynamics and Stability of Shear Wall Building Structures"
J. ICE Proc. Part 2, June 1973, Vol. 55.

12. WINOKUR, A., GLUCK, J.,
"Ultimate Strength Analysis of Coupled Shear Walls" J. ACI, Vol. 65, No. 12, Dec. 1968, pp.1029-1036.

13. PAULAY, T.,
"An Elasto-Plastic Analysis of Coupled Shear Walls" J. ACI, Vol. 67, No. 11, Nov. 1970, pp.915-922.

14. SCHWAIGHOFER, J., MICROYS, H. F.,
"Analysis of Shear Walls Using Standard Computer Programs" J. ACI, Vol. 66, No. 12, Dec. 1969, pp.1005-1007.

15. MACLEOD, I. A.,
"Connected Shear Walls of Unequal Width" J. ACI, Vol. 67, No. 5, May 1970, pp.408-412.

16. MACLEOD, I. A.,
"Analysis of Shear Wall Buildings by the Frame Method" Proc. ICE Part 2, Sept. 1973, Vol. 55, pp.593-603.

17. SMITH, B. S., GIRGIS, A.,
"Simple Analogous Frames for Shear Wall Analysis" J. Struct. Eng. ASCE, Vol. 110, No. 11, Nov. 1984, pp.2655-2666.

18. GIRIJAVALLABHAN, C. V.,
"Analysis of Shear Walls with Openings" J. Struct. Div. ASCE, Vol. 95, No. ST10, Oct. 1969, pp.2093-2103.

19. WEE, H. J.,
"Free Vibration and Transient Response of Shear Wall Structures by Finite Element Method" M. Eng. Thesis, University of Liverpool 1976.

20. WILSON, E. L., TAYLOR, R. L., DOHERTY, W. P., GHABOUSSI, J.,
"Incompatible Displacement Models" International Symposium on Numerical Computer Methods in Structural Mechanics, University of Illinois, Urbana, Sept. 1971.

21. MACLEOD, I. A.,
"New Rectangular Finite Element for Shear Wall Analysis" J. Struct. Div. ASCE, Vol. 95, No. ST3, March 1969, pp.399-409.

22. AGRAWAL, A. B., MUFTI, A. A.,
Discussion paper "Coupled Shear Wall Analysis by Lagrange Multipliers" J. Struct. Div. ASCE, Vol. 102, No. ST7, July 1976, pp.1527-1528.

23. AL-MAHAIDI, R. S., NILSON, A. H.,
"Coupled Shear Wall Analysis by Lagrange Multipliers" J. Struct. Div. ASCE, Vol. 101, No. ST11, Nov. 1975, pp.2359-2366.

24. ANTONY, Y. G., GANESAN, T. P.,
"Analysis of Wall-Frames by Lagrangian Multipliers" J. Struct. Div. ASCE, Vol. 109, No. ST2, Feb. 1983, pp.580-585.

25. BASU, A. K., DAR, G. Q.,
"Dynamic Characteristics of Coupled Wall-Frame Systems" Earth. Eng. Struct. Dyn., Vol. 10, 1982, pp.615-631.

26. EMORI, K., SCHNOBRICH, W.,
"Dynamic Analysis of Reinforced Concrete Frame-Wall Structures" Eng. Struct., Vol. 2, April 1980, pp.103-112.

27. EMORI, K., SCHNOBRICH, W.,
"Inelastic Behaviour of Concrete Frame-Wall Structures" J. Struct. Div. ASCE, Vol. 107, No. ST1, Jan. 1981, pp.145-164.

28. FINTEL, M., GHOSH, S. K.,
"Application of Inelastic Response History Analysis in the Aseismic Design of a 31-Storey Frame-Wall Building" Earth. Eng. Struct. Dyn., Vol. 1981, pp.543-556.

29. FINTEL, M., GHOSH, S. K.,
"Explicit Inelastic Dynamic Design Procedure for Aseismic Structures" J. ACI, Vol. 79, No. 2, March-April 1982, pp.110-118.

30. FINTEL, M., GHOSH, S. K.,
"Case Study of Areismic Design of a 16-Storey Coupled Wall Structure Using Inleastic Dynamic Analysis" J. ACI, Vol. 79, No. 32, May-June 1982, pp.171-179.

31. GIBERSON, M. F.,
"The Response of Nonlinear Multi-Storey Structures Subjected to Earthquake Excitations" Earthquake Research Laboratory, California Insitute of Technology, Pasadena 1967.

32. CLOUGH, R. W., BENUSKA, K. L., WILSON, E. L.,
"Inelastic Earthquake Response of Tall Buildings" Proceedings of the Third World Conference on Earthquake Engineering, Vol. 2, New Zealand 1965, pp.68-84.

33. KENT, D. C., PARK, R.,
"Flexural Members with Confined Concrete" J. Struct. Div. ASCE, Vol. 97, No. ST7, July 1971, pp.1969-1990.

34. TAKEDA, T., SOZEN, M. A., NIELSEN, N.,
"R/C Response to Simulated Earthquakes" J. Struct. Div. ASCE, Vol. 96, No. ST12, Dec. 1970, pp.2557-2573.

35. AGRAWAL, A. B., JAEGER, L. G., MUFTI, A. A.,
"Response of R/C Shear Wall Under Ground Motions" J. Struct. Div. ASCE, Vol. 107, No. ST2, Feb. 1981, pp.395-411.

36. ZIENKIEWICZ, O. C.,
"The Finite Element Method" McGraw-Hill Book Co. (U.K.) Ltd 1977.

37. CHEUNG, Y. K., YEO, M. F.,
"A Practical Introduction to Finite Element Analysis" Pitman Publishing Ltd 1979.

38. GALLAGHER, R. H.,
"Finite Element Analysis Fundamentals" Prentice-Hall Inc., Englewood Cliffs N. J., 1975.

39. DESAI, C. S., ABEL, J. F.,
"Introduction to the Finite Element Method: A Numerical Method for Engineering Analysis" Van Nostrand Reinhold N. Y. 1972.

40. SISODIYA, R. G., CHEUNG, Y. K., GHALI, A.
"New Finite Elements with Application to Box Girder Bridges" Proc. ICE, Supplmental Paper No. 74795, 1972, pp.207-225.

41. COOK, R. D.,
"Improved Two-dimensional Finite Element" J. Struct. Div. ASCE, Vol. 100, No. ST9, Sept. 1974, pp.1851-1863.

42. COOK, R. D.,
"Avoidance of Parasitic Shear in Plane Element" J. Struct. Div. ASCE, Vol. 101, No. ST6, June 1975, pp.1239-1253.

43. TAYLOR, R. L., BERESFORD, P. J., WILSON, E. L.,
"A Non-Conforming Element for Stress Analysis" Int. J. Num. Meth. Eng., Vol. 10, 1976, pp.1211-1219.

44. TODD, J. D.,
"Structural Theory and Analysis" The MacMillan Press Ltd 1979.

45. COATES, R. C., COUTIE M. G., KONG, F. K.,
"Structural Analysis" Thomas Nelson and Sons Ltd 1980.

46. SOKOLNIKOFF, I. S., REDHEFFER, R. M.,
"Mathematics of Physics and Modern Engineering" McGraw-Hill Book Co. Inc., 1966.

47. SCHECHTER, R. S.,
"The Variational Method in Engineering" McGraw-Hill Book Co. Inc., 1967.

48. CRAIG, R. R.,
"Structural Dynamics - An Introduction to Computer Methods" John Wiley and Sons Inc., 1981.

49. AL-MAHAIDI, R. S., NILSON, A. H.,
"Coupled Shear-Walls: Improved Methods for Elastic Analysis" Research Report No. 355, Department of Structural Engineering, Cornell University, Ithaca, N. Y., Feb. 1974.

50. FADDEEVA, V. N.,
"Computational Methods of Linear Algebra" Dover Publications Inc. N. Y., 1959.

51. RAJU, I. S., RAO, G. V., MURTHY, T. V. G. K.,
"Eigenvalues and Eigenvectors of Large Order Banded Matrices" Computers and Structures, Vol. 4, 1974, pp.549-558.

52. TONG, P., PIAN, T. H. H., BUCCIARELLI, L. L.,
"Mode Shapes and Frequencies by Finite Element Method Using Consistent and Lumped Masses" Computers and Structures, Vol. 1, 1971, pp.623-638.

53. HART, G. C., RAMASWAMI, V.,
"Earthquake Design of Buildings: Damping" J. Struct. Div. ASCE, Vol. 101, No. ST1, Jan. 1975, pp.11-30.

54. WILSON, E. L., PENZIEN, J.,
"Evaluation of Orthogonal Damping Matrices" Int. J. Num. Meth. Eng., Vol. 4, 1972, pp.5-10.

55. CLOUGH, R. W., PENZIEDN, J.,
"Dynamics of Structures" McGraw-Hill Book Co. Inc. 1982.

56. WILKINSON, J. H.,
"The Algebraic Eigenvalue Problem" Clarendon Press 1965.

57. BATHE, K. J., WILSON, E. L.,
"Solution Methods for Eigenvalue Problems in Structural Mechanics" Int. J. Num. Meth. Eng., Vol. 6, 1973, pp.213-226.

58. KEY, S. W.,
"Transient Response by Time Integration: Review of Implicit and Explicit Operators", "Advanced Structural Dynamics" edited by DONEA, J., Applied Science Publishers Ltd, London, 1980.

59. NEWMARK, N. M.,
"A Method of Computation for Structural Dynamics" J. Eng. Mech. Div. ASCE, Vol. 85, No. EM3, 1959, pp.67-94.

60. GOUDREAU, G. L., TAYLOR, R. L.,
"Evaluation of Numerical Integration Methods in Elastodynamics" Computer methods in applied Mechanics and Engineering, Vol. 2, 1972, pp.69-97.

61. BATHE, K. J., WILSON, E. L.,
"Stability and Accuracy of Direct Integration Methods" Earth. Eng. Struct. Dyn., Vol. 1, 1973, pp.283-291.

62. GLADWELL, I., THOMAS, R.,
"Stability Properties of the Newmark Houbolt and Wilson θ Methods" International journal for numerical and analytical methods in geomechanics, Vol. 4, 1980, pp.143-158.

63. HILBER, H. M., HUGHES, T. J. R., TAYLOR, R. L.,
"Improved Numerical Dissipation for Time Integration Algorithms in Structural Dynamics" Earth. Eng. Struct. Dyn., Vol. 5, 1977, pp.283-292.

64. ZIENKIEWICZ, O. C., VALLIAPPAN, S., KING, I. P.,
"Elasto-Plastic Solution of Engineering Problems, Initial Stress Finite Element Approach" Int. J. Num. Meth. Eng., Vol. 1, Jan. 1969, pp.75-100.

65. BERGAN, P. G., CLOUGH, R. W.,
"Technical Notes, Convergence Criteria for Iterative Processes" AIAA Journal, Vol. 10, No. 8, Aug. 1972, pp.1107-1108.

66. PORTER, F. L., POWELL, G. H.,
"Static and Dynamic Analysis of Inelastic Frame Structures" Report No. EERC 71-3, Earthquake Eng. Meeting, Baltimore, April 1971.

67. LYONS, L. P. R.,
"Elastic Plane-Stress Analysis of Two-Dimensional Pierced Shear Walls by Finite Element Idealisation" C.I.R.I.A. Report 1970.

68. MEGSON, T. H. G.,
"Strength of Materials for Civil Engineers" Thomas Nelson and Sons Ltd. 1980.

69. GERE, J. M., WEAVER, W.,
"Analysis of Framed Structures" D. Van Nostrand Co. Inc., Princeton, New Jersey, 1965.

70. WARBURTON, G. B.
"The Dynamical Behaviour of Structures" Pergamon Press, 1976.

71. HOERNER, J. B., JENNINGS, P. C.
"Modal Interference in Vibration Tests" J. Eng. Mech. Div. ASCE, No. EM4, Aug. 1969.

72. WILLIAMS, G.
"An Introduction to Electrical Circuit Theory" The MacMillan Press Limited, 1973.

73. SPENCER, A. J. M. et al.
"Engineering Mathematics Vol. 2" Van Nostrand Reinhold, 1979.

74. TEMPLEMAN, A. B.
"Civil Engineering Systems" The MacMillan Press Limited, 1982.

75. ANDERSON, D R., SWEENEY, D. J., WILLIAMS, T. A.
"Linear Programming for Decision Making, an Applications Approach" West Publishing Co., 1974.

76. KELLY, J. M., BEUCKE, K. E.
"A Friction Damped Base Isolation System with Fail-Safe Characteristics" J. Earth. Eng. and Struct. Dyn., Vol. 11, 1983, pp.33-36.

77. CLARK, P. J., BASSETT, R. H., BRADSHAW, J. B.
"Plate Friction Load Control Devices - Their Application and Potential" J. ICE Proc. Part 2, June 1973, Vol. 55.

APPENDIX A

To illustrate the use of the logarithm of the value of the determinant $|[K] - \Psi[M]|$ in locating eigenvalues.

A three storey, four bay frame was selected as an example as this type of structure can readily have vertical and horizontal vibration modes of similar frequency.

As explained in chapter 4, the bisection method can miss roots which lie close together in frequency. With this example an initial estimate of 100 was made for the first eigenvalue and an increment of 50 chosen. The first eigenvalue found by a change of sign of the determinant occurs at Ψ = 10195. However, examining the logarithm of the value of the determinant (Fig. A.1) it can be seen that a pronounced dip in values occurs at approximately Ψ = 1850.

Now by using an initial estimate of 1800 and a smaller increment of 10, two eigenvalues can be found at 1833 and 1842. Using the increment 10 from the initial estimate of 100 would have needed over 170 steps to reach the first eigenvalue. By using the values of the logarithm of the determinant to provide an initial estimate of 1800, this can be reduced to four steps.

The values of log $|[K] - \Psi [M]|$ close to the two eigenvalues are shown in Fig. A.2.

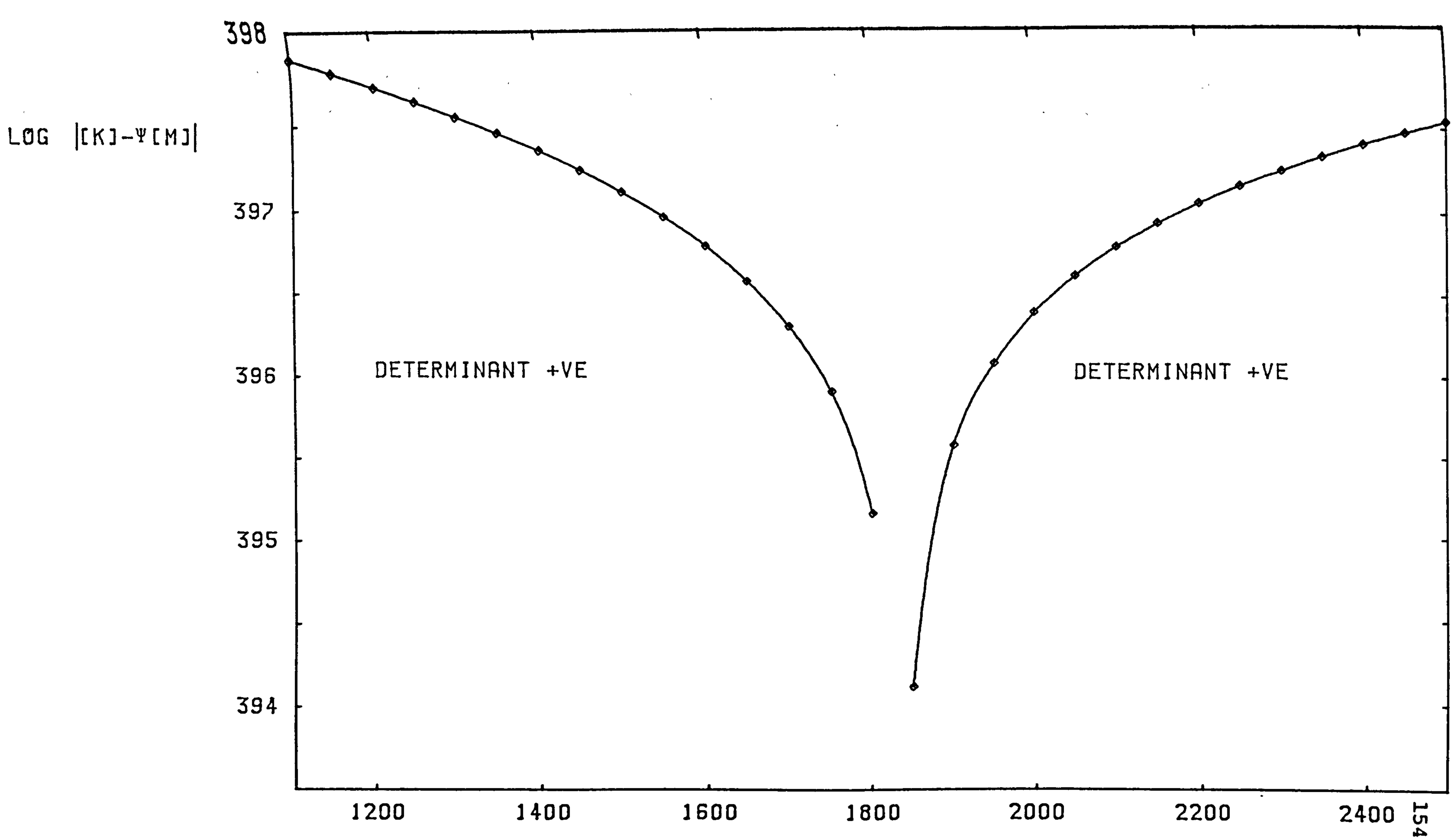
LOG |[K]-Ψ[M]|
398
397
396
395
394
DETERMINANT +VE
DETERMINANT +VE
1200
1400
1600
1800
2000
2200
2400
EIGENVALUE ESTIMATE

FIG 8.1

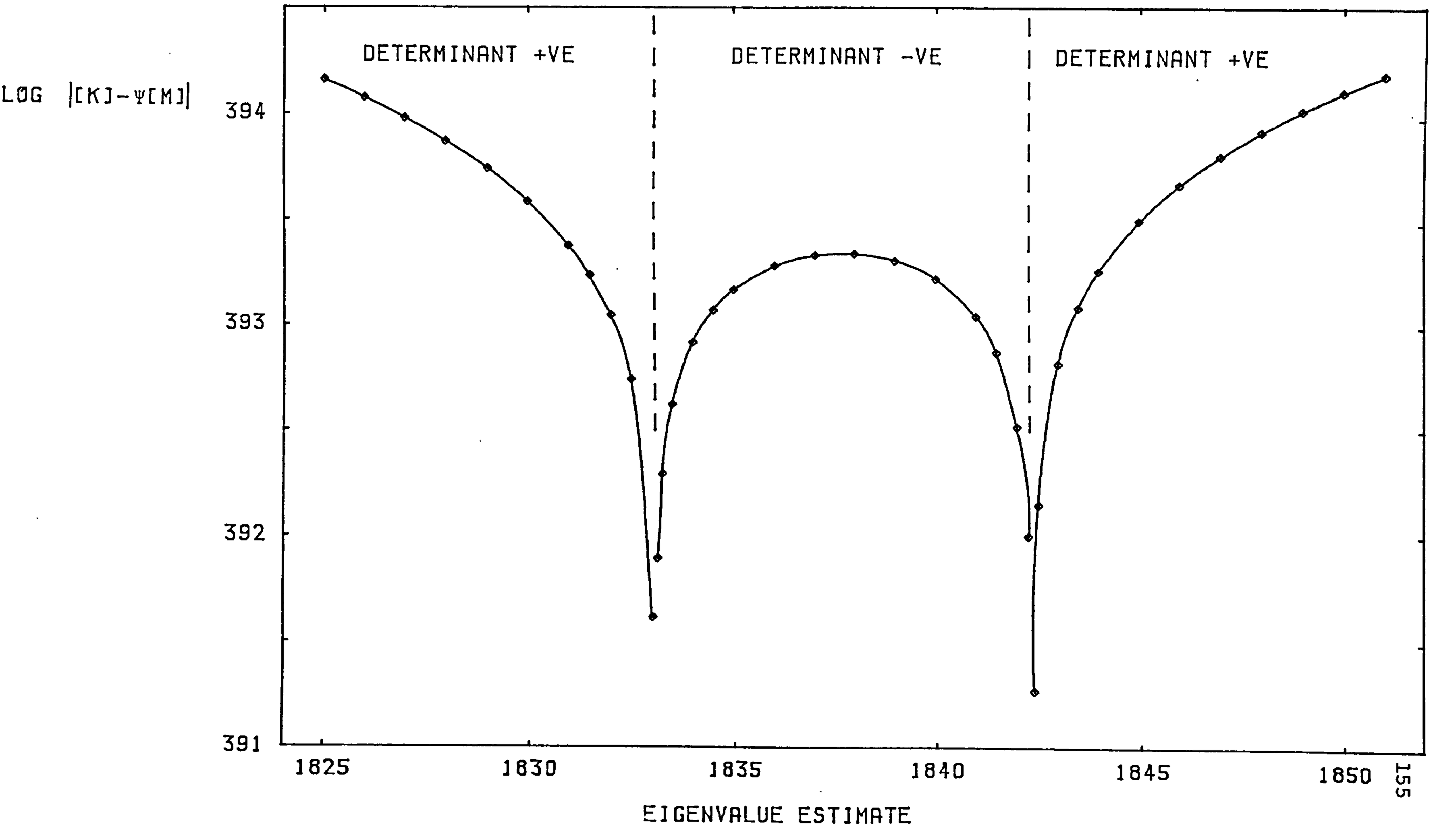
LOG |[K]-Ψ[M]|
DETERMINANT +VE
DETERMINANT -VE
DETERMINANT +VE
394
393
392
391
1825
1830
1835
1840
1845
1850
EIGENVALUE ESTIMATE

APPENDIX B

The finite element meshes used for the comparison of convergence in chapter 6 are shown here.

The elements for the first storey plus one level of elements for the second storey are shown in each case. All the higher storeys follow exactly the same pattern and node numbering sequence.

The co-ordinates of the nodes with the Lagrange multiplier degrees of freedom have no physical significance for the proposed scheme (figs. B.4-B.6). They are drawn on the element mesh close to the beam - wall connection with which they are associated.

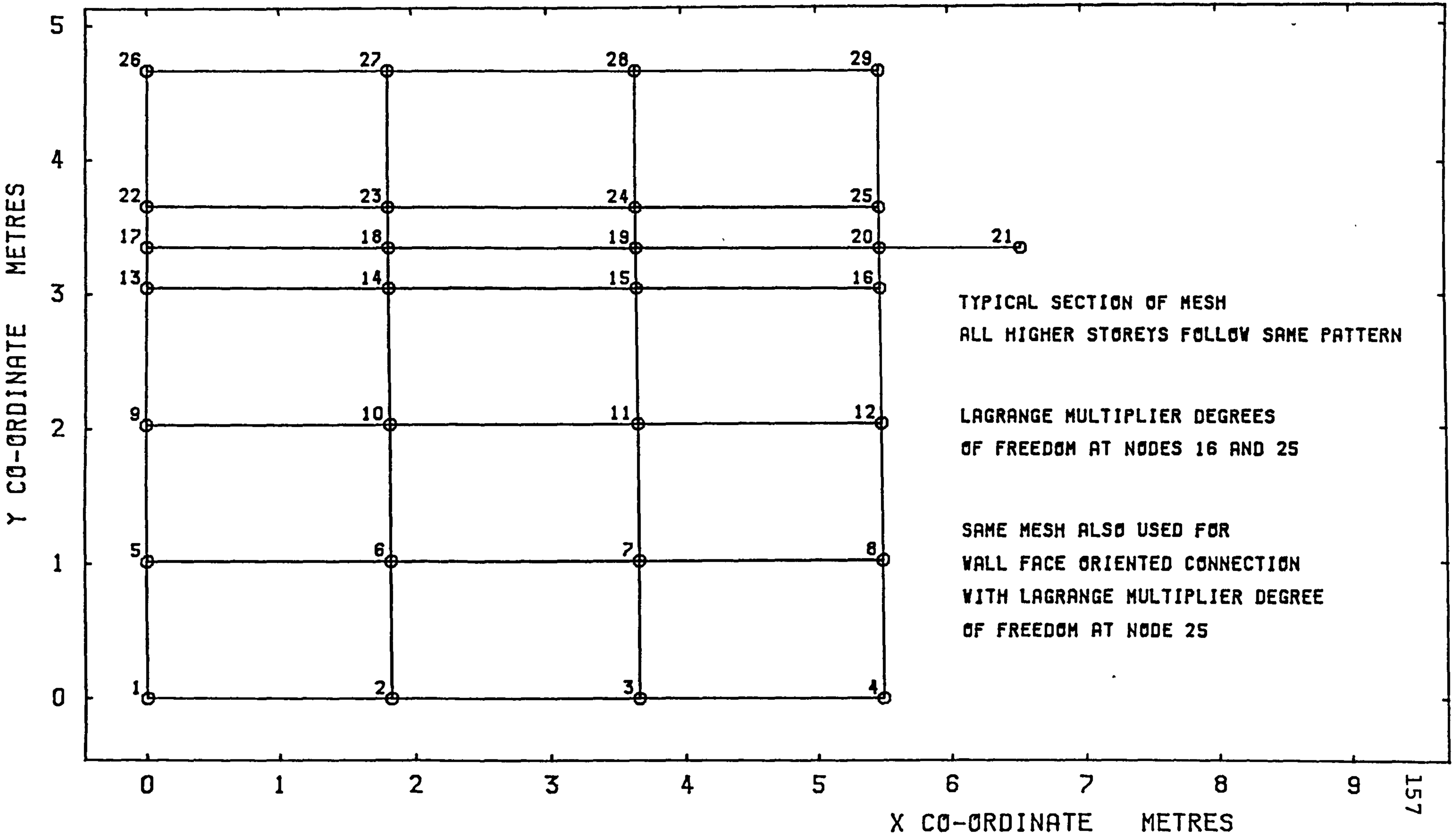

FIG B.1

AL-MAHAIDI'S CONSTRAINT SCHEME 3 ELEMENT MESH

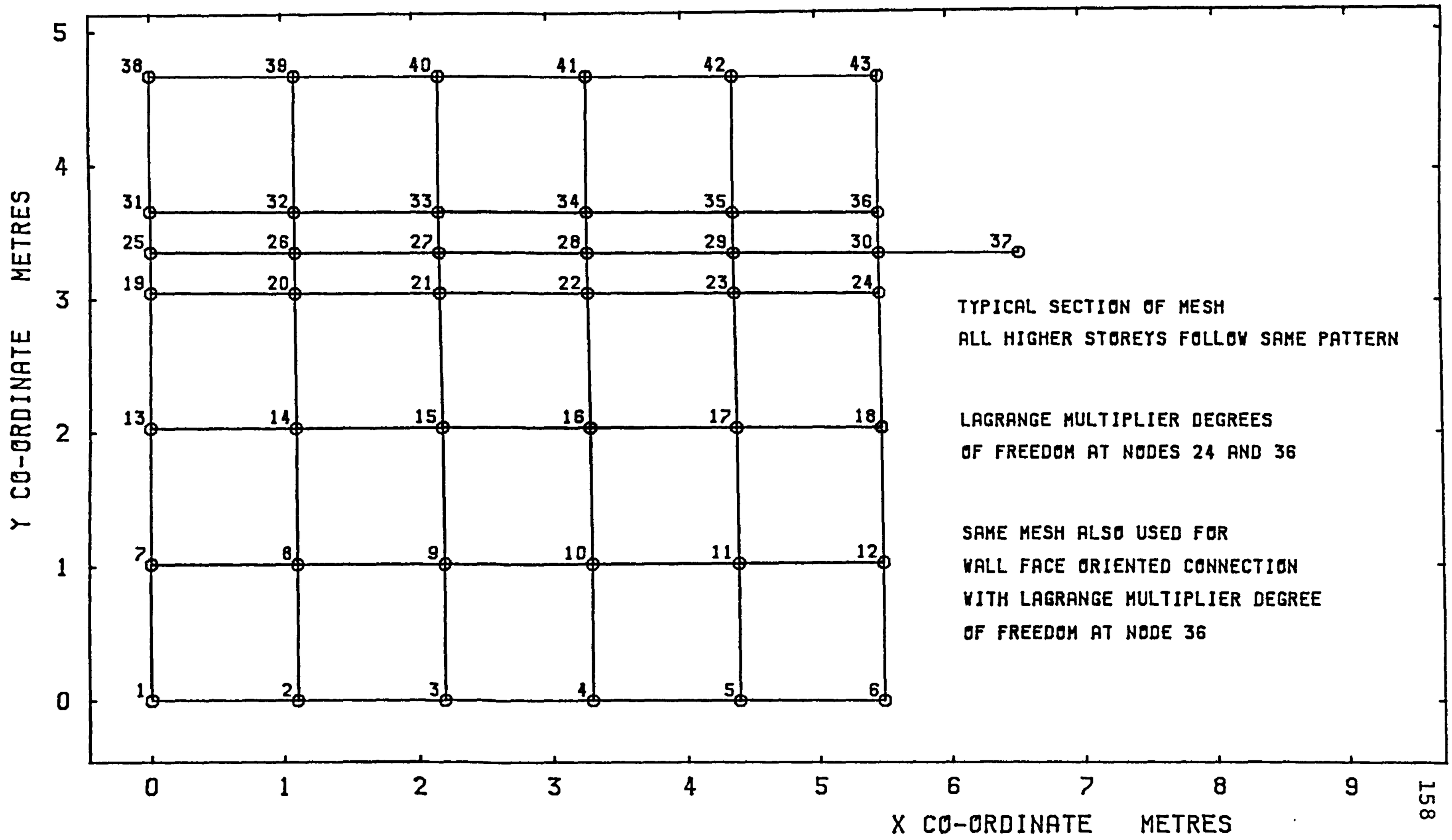

FIG B.2

AL-MAHAIDI'S CONSTRAINT SCHEME 5 ELEMENT MESH

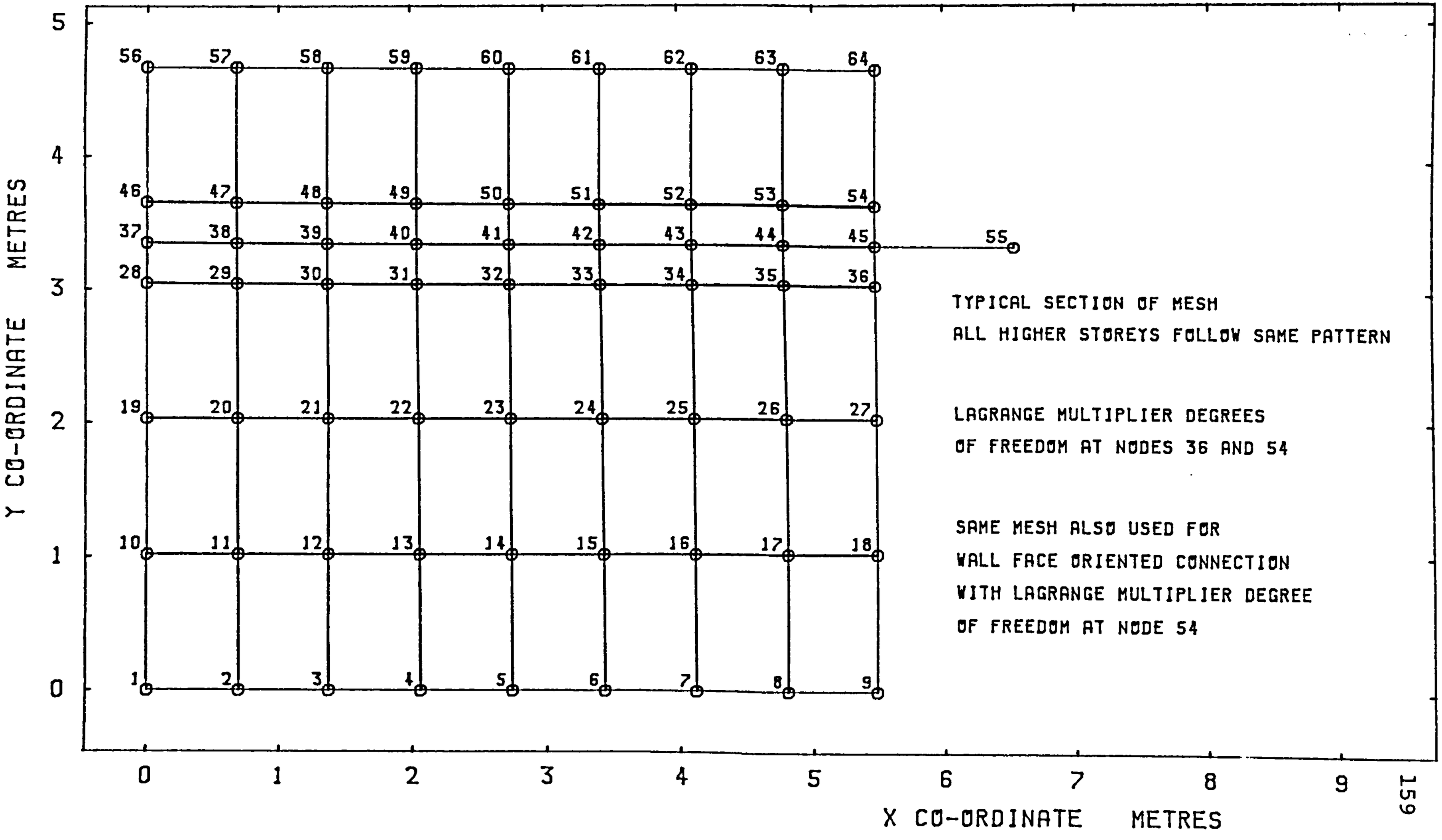

FIG B.3

AL MAHAIDI'S CONSTRAINT SCHEME 8 ELEMENT MESH

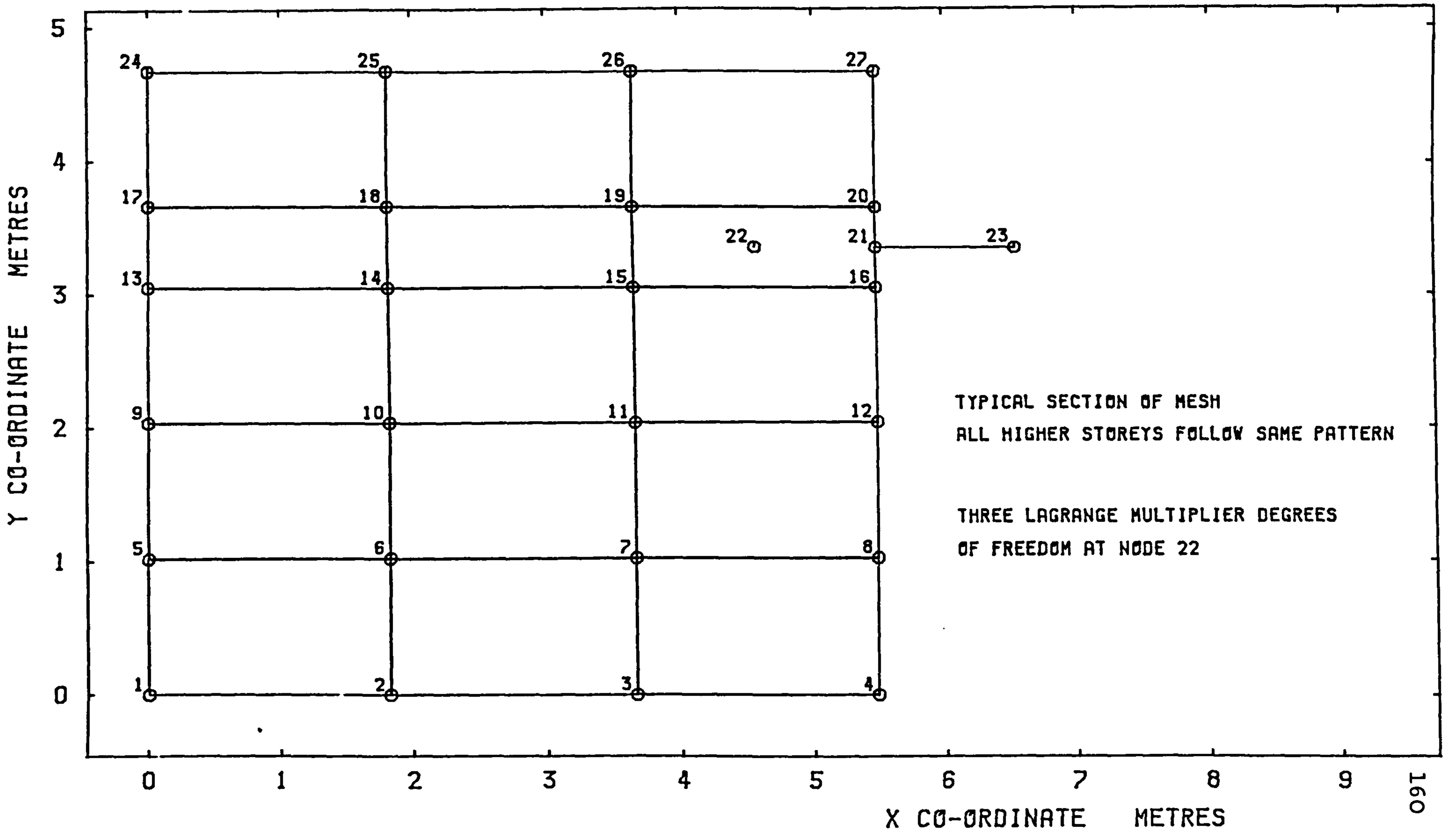

FIG B.4

PROPOSED CONSTRAINT SCHEME 3 ELEMENT MESH

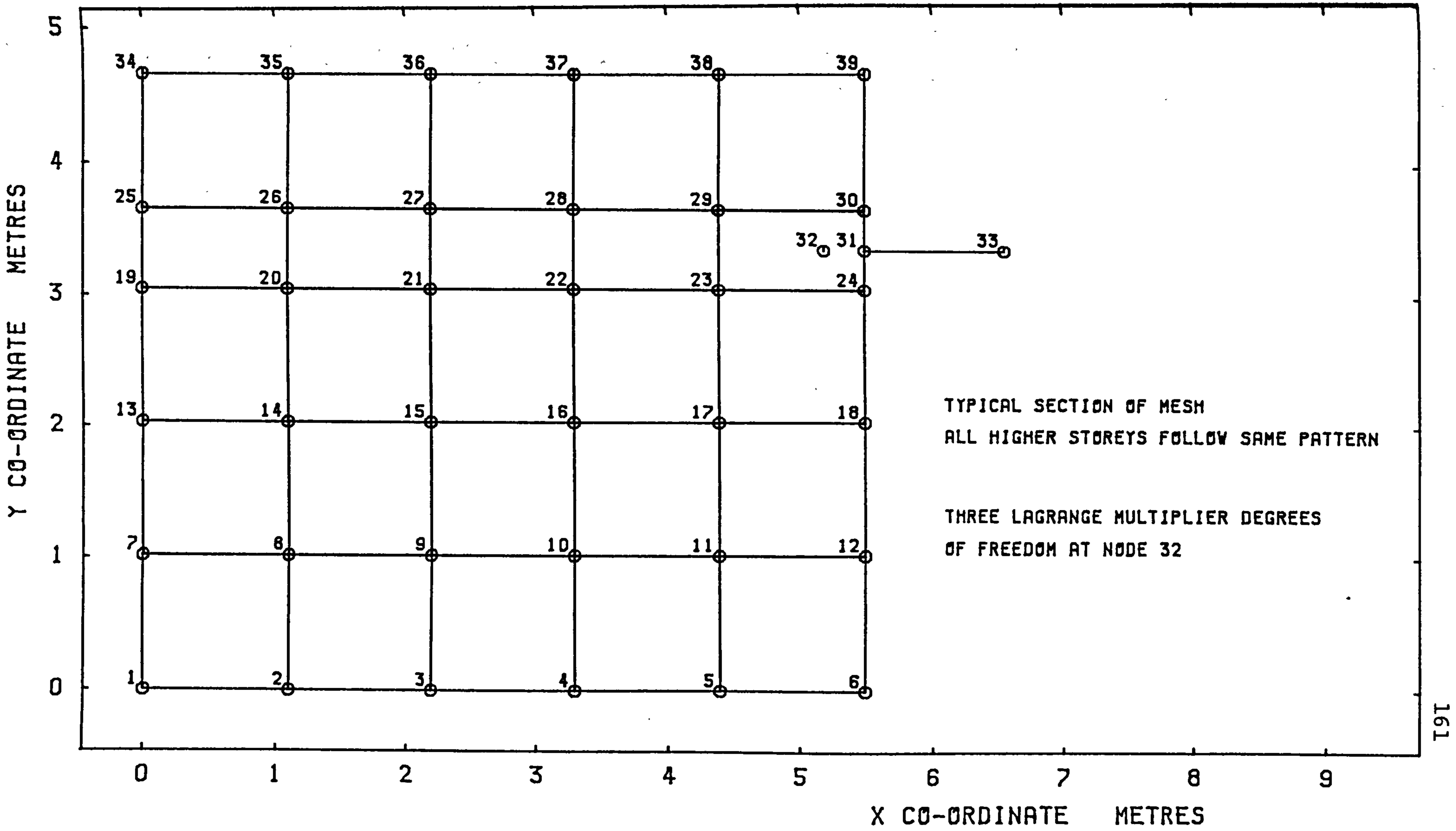

FIG B.5

PROPOSED CONSTRAINT SCHEME 5 ELEMENT MESH

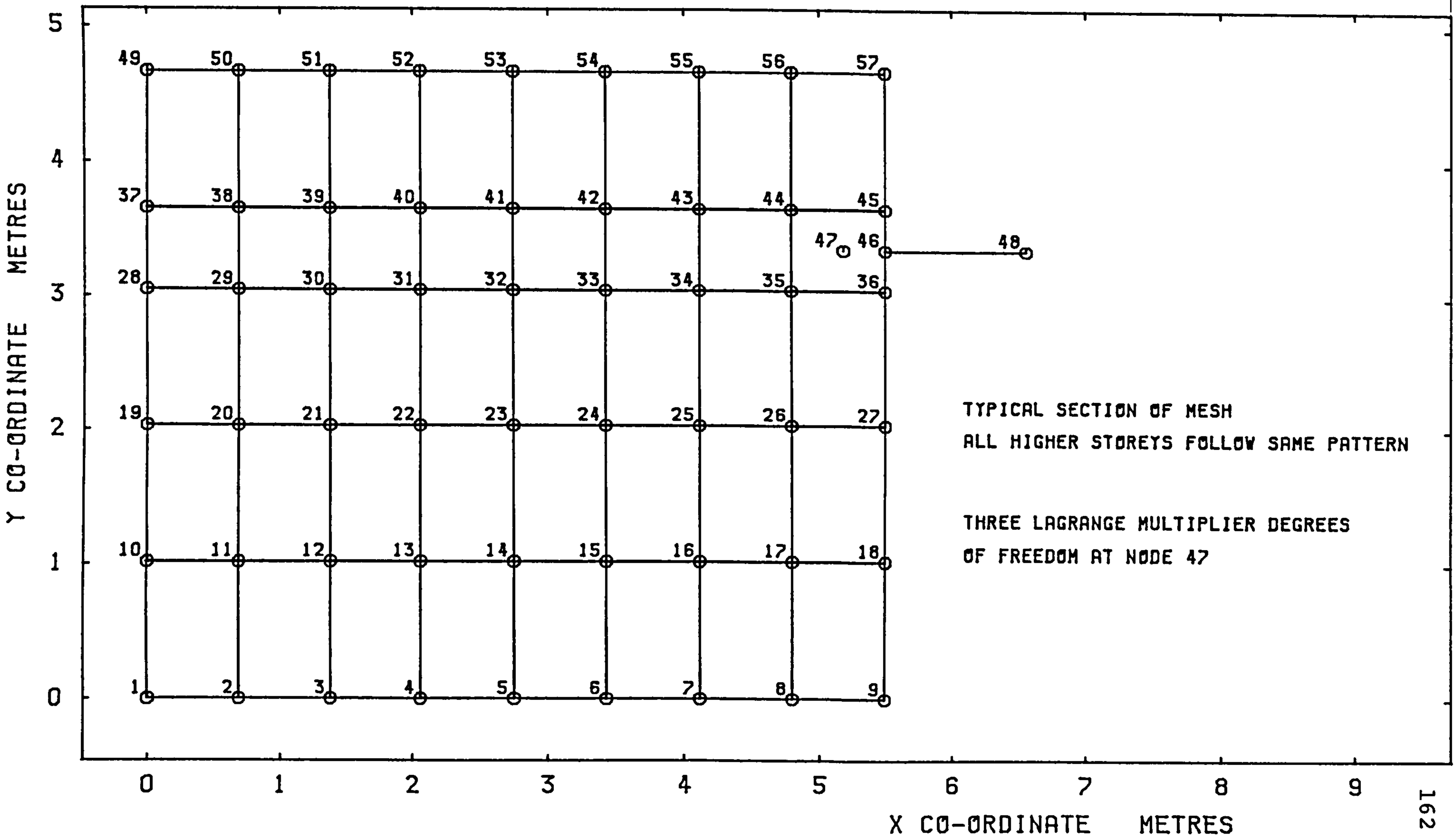

FIG B.6

PROPOSED CONSTRAINT SCHEME 8 ELEMENT MESH

APPENDIX C

This appendix gives details of the model walls and frame used as a basis for comparison with the finite element analysis.

The finite element meshes used for walls 1 to 3 are shown in Figs C.1-C.3 and that for the frame in Fig. C.4. The details of the walls tested by Tso and Chan [8] are given in Figs C.5 and C.6.

Properties of the Perspex Walls (C.1-C.3)

Poisson's ratio	= 0.2
Static modulus of elasticity	= 0.31 x 10^{10} N/m^2
Dynamic modulus of elasticity	= 0.45 x 10^{10} N/m^2
Density	= 1180 kg/m^3
Overall height, 8 storeys of 0.146m	= 1.168m
Overall width	= 0.254m
Thickness	= 0.010m
Beam depth, d_b	= 0.0125m

	Wall 1	Wall 2	Wall 3
Opening width, m	0.102	0.076	0.050

Properties of the Aluminium Frame (C.4)

Modulus of elasticity = 7.0×10^{10} N/m^2

Density = 2710 kg/m^3

Member cross-section

width = 0.0062m

depth = 0.0125m

member nodes	centre-line to centre-line length, m x 10^{-2}	effective length m x 10^{-2}
1-3 2-4	13.98	11.68
3-6 4-7	14.60	12.30
3-4 6-7	20.20	17.90
4-5 7-8	13.30	12.10

node	Mass of joints and accelerometers, kg x 10^{-3}		
	Frame alone	Frame fixed to wall	Frame pinned to wall
3	98	98	98
4	84	84	84
5	-	39	35
6	98	119	119
7	84	84	84
8	-	39	35
9	98	119	119
10	84	84	84
11	-	39	35
12	98	119	119
13	84	84	84
14	-	39	35
15	98	124	124
16	84	84	84
17	-	39	35
18	98	124	124
19	84	84	84
20	-	39	39
21	98	124	124
22	84	84	84
23	-	39	35
24	115	115	115
25	75	75	75
26	-	39	35

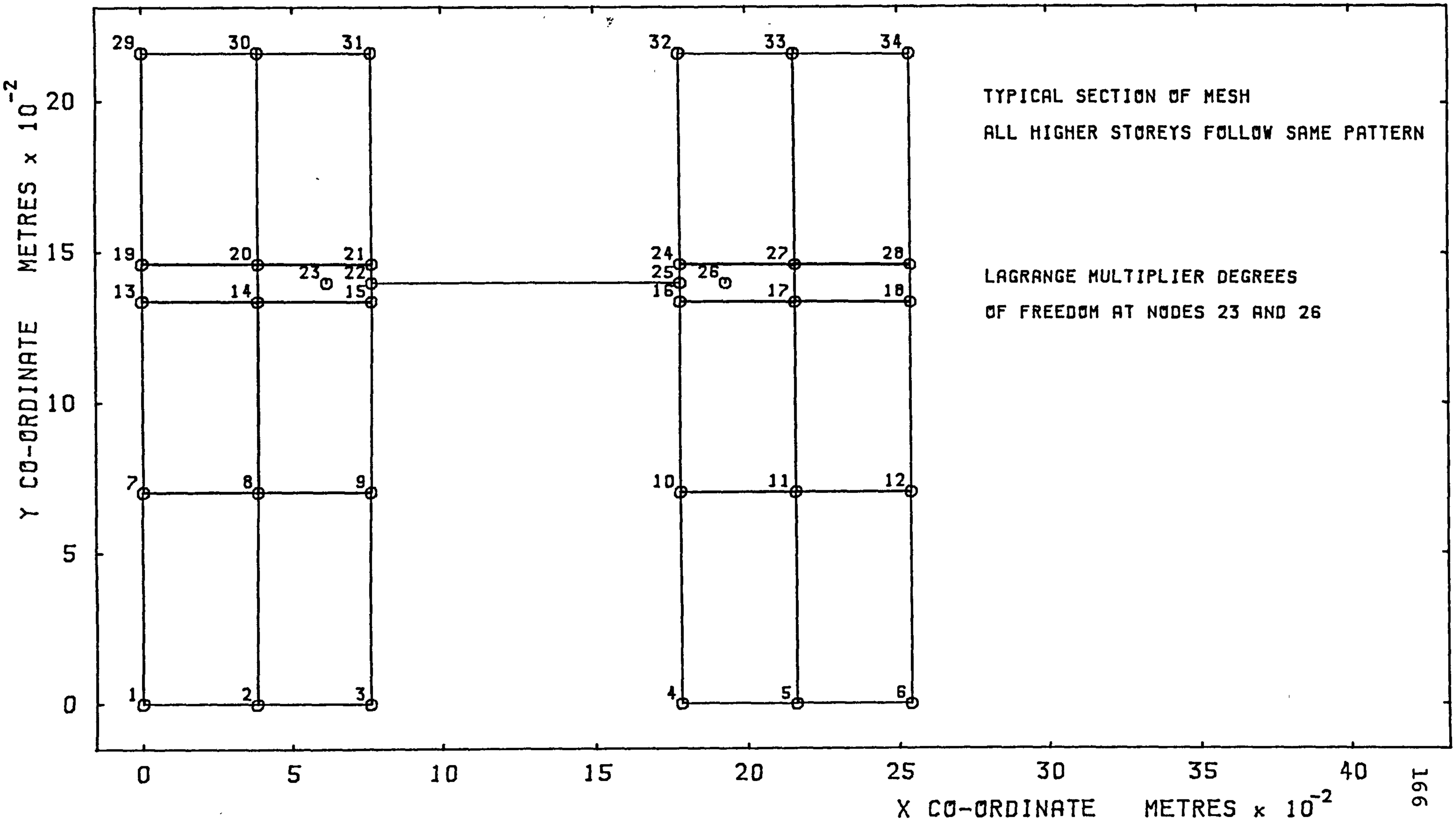

FIG C.1

MESH EMPLOYED FOR MODEL WALL 1

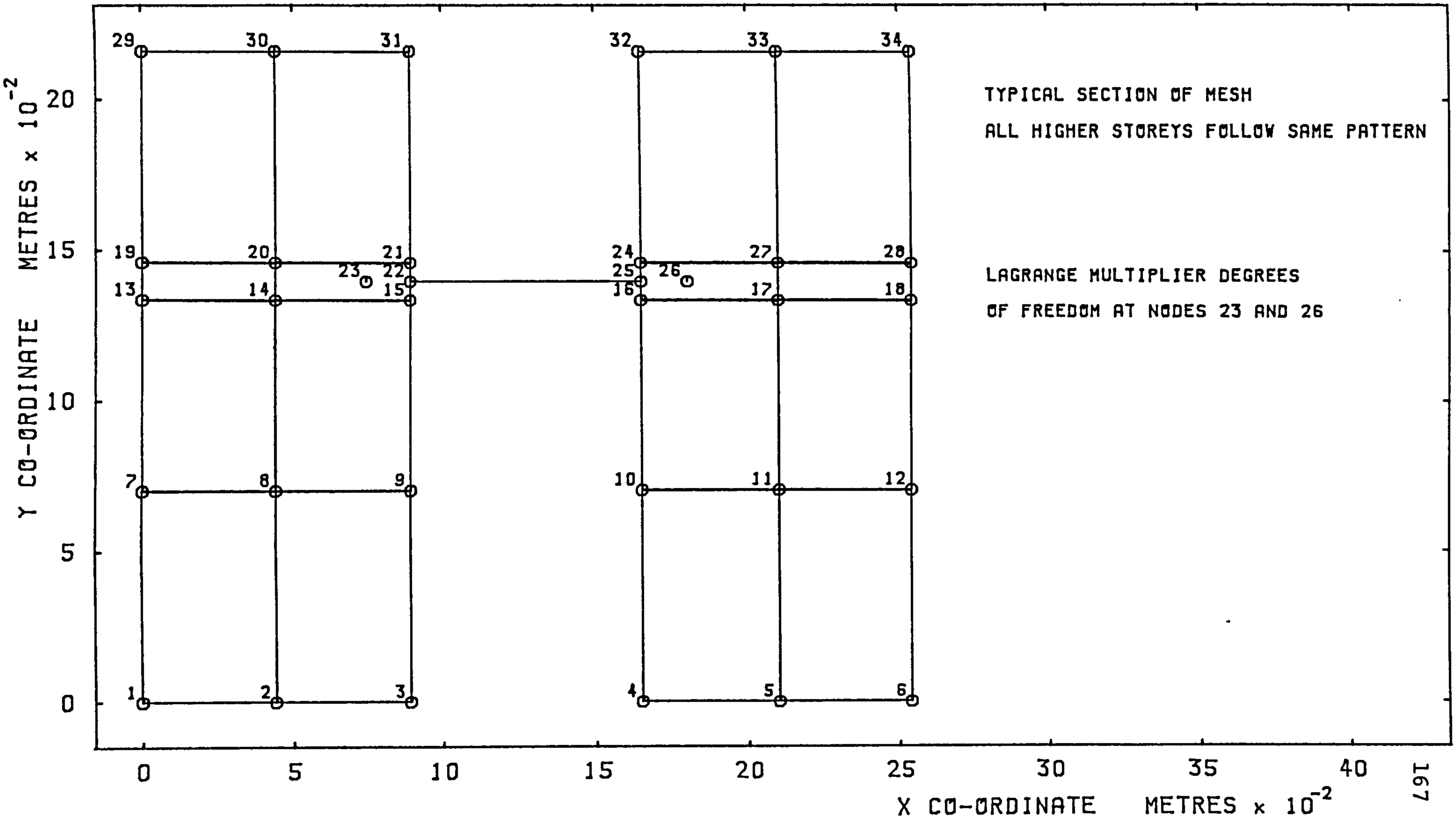

FIG C.2

MESH EMPLOYED FOR MODEL WALL 2

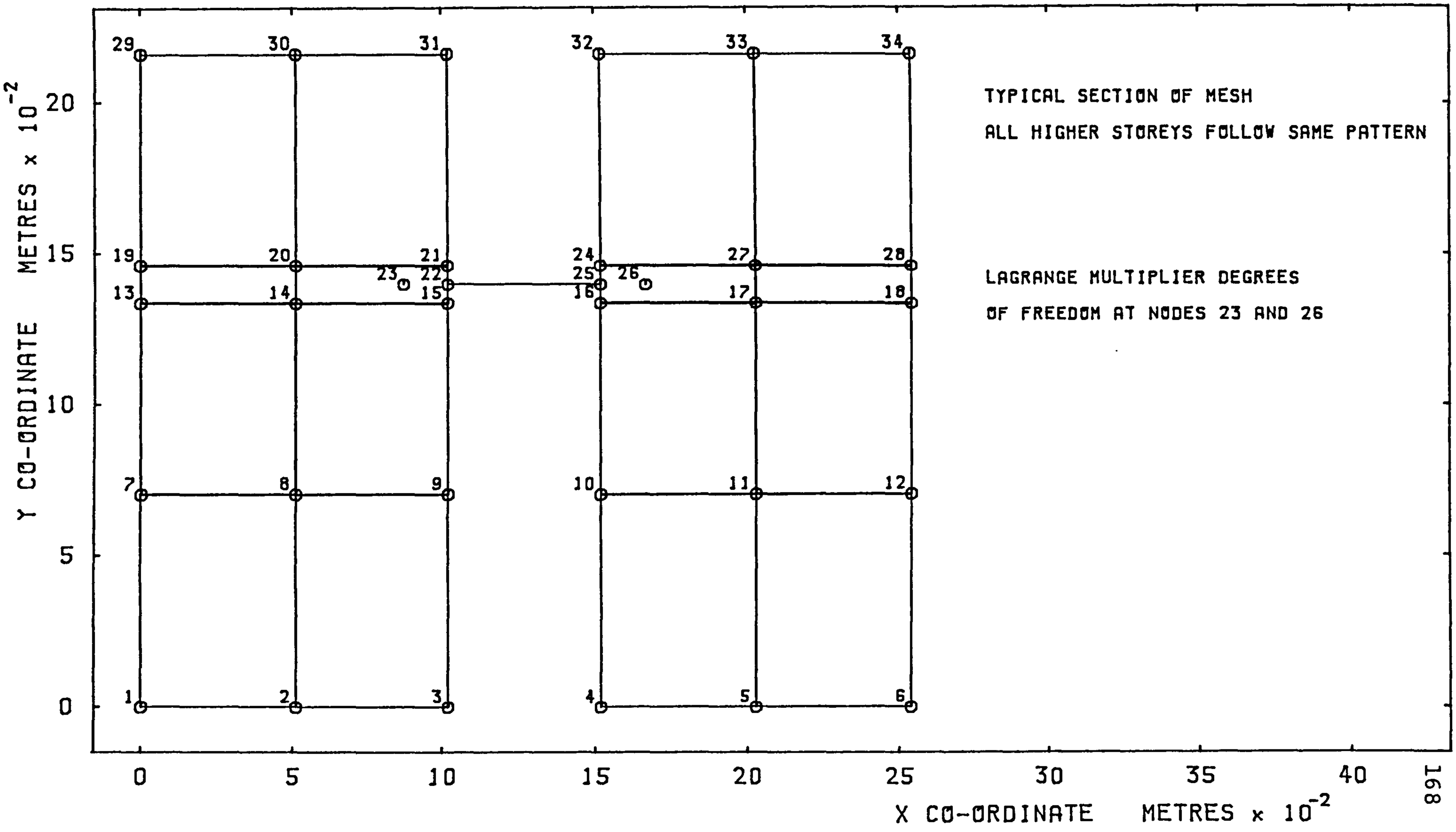

FIG C.3

MESH EMPLOYED FOR MODEL WALL 3

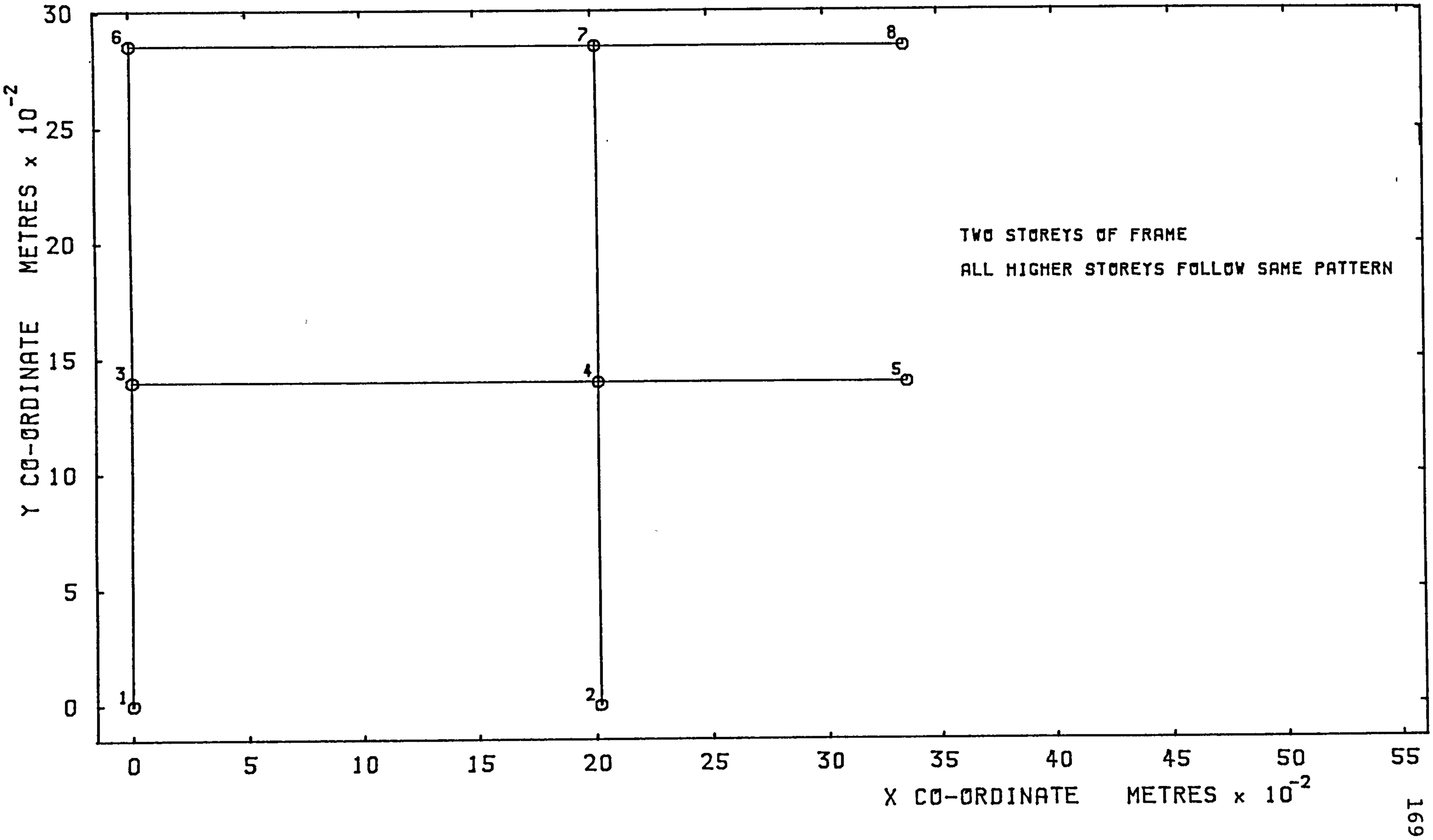

FIG C.4

CENTRE-LINE FRAME DIMENSIONS

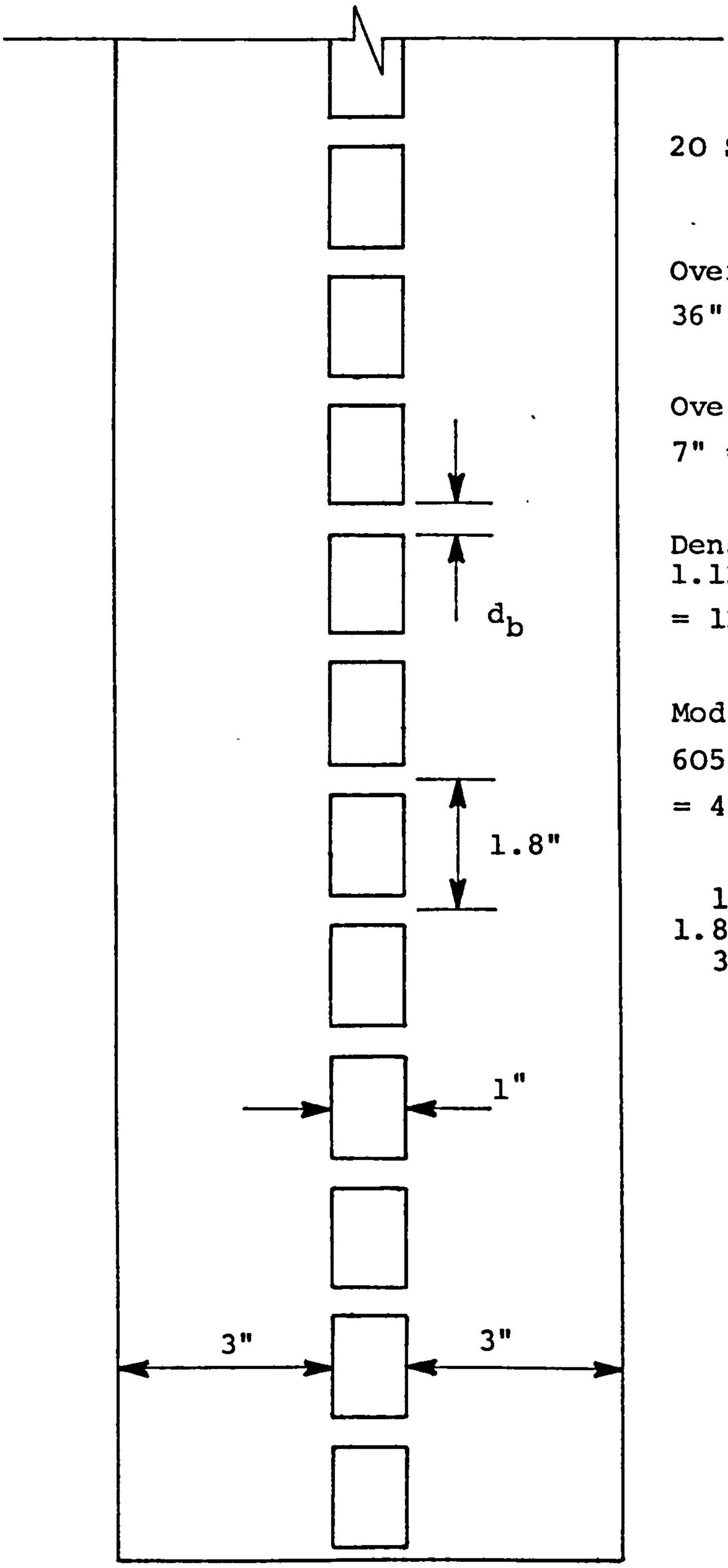

20 Storey Wall

Overall height
36" = 0.914m

Overall width
7" = 0.178m

Density
1.12×10^{-4} lb sec^2/in^4
= 1200 kg/m^3

Modulus of elasticity
605,000 psi
= 4.17×10^{-9} N/m^2

1" = 0.025m
1.8" = 0.045m
3" = 0.076m

FIG. C.5

Dimensions and Properties of Symmetric Wall

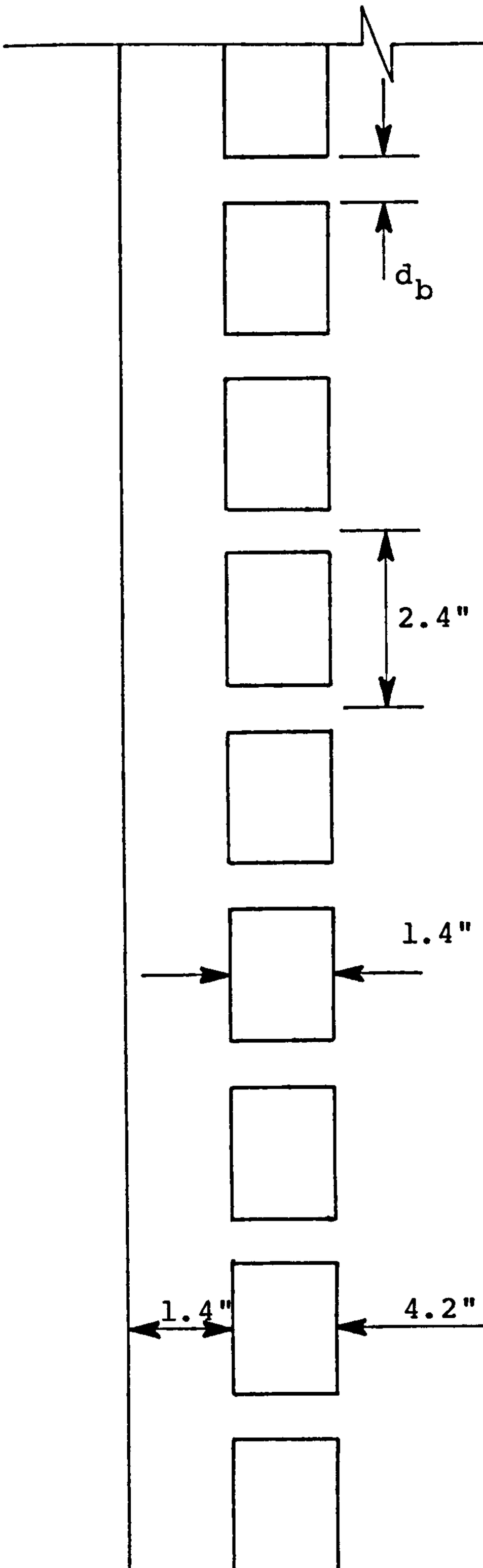

15 Storey Wall

Overall height
36" = 0.914m

Overall width
7" = 0.178m

Density
1.12×10^{-4} lb sec^2/in^4
= 1200 kg/m^3

Modulus of elasticity
605,000 psi
= 4.17×10^9 N/m^2

1.4" = 0.035m
2.4" = 0.061m
4.2" = 0.107m

FIG. C.6

Dimensions and Properties of Asymmetric Wall

APPENDIX D

Finite Element Program

Description of the data:

Card 1 (I5, 3X, 9, 8)

NPROB	problem number, 0 to stop
TITLE	problem title

Card 2 (F)

GACC	acceleration due to gravity

Card 3 (3I)

IPRINT	0 = none 1 = print mass and stiffness matrices
NDYNAN	0 = static problem 1 = free vibration
NDFORS	0 = none 1 = calculate line element forces 2 = line and isoparametric element forces and stresses

Card 4 (3I)

NNP	number of nodes
NBOUN	number of boundary nodes
NBODY	self weight, 0 = no, 1 = yes

Card 5 (6I) **Number of elements of each type**

NEL1(1)	Isoparametric
NEL1(2)	Line
NEL1(3)	Al-Mahaidi's constraints, to vertical face
NEL1(4)	Al-Mahaidi's constraints, to horizontal face
NEL1(5)	proposed constraints
NEL1(6)	rectangular with rotational freedoms

Card 6	(6I)	
	NMAT(1) . . NMAT(6)	number of material types for each of the above element types
Card 7	(I, 4F, I)	**One card for each node**
	NODE	node number
	X	x co-ordinate
	Y	y co-ordinate
	ULX	x direction load
	VLY	y direction load
	NT	node type 1 = 2 degrees of freedom 2 = 3 degrees of freedom 3 = wall-beam joint 4 = Lagrange multiplier degrees of freedom
Card 8	(2I)	**For isoparametric elements**
	MODIF	0 = conforming 1 = non-conforming
	NOPT	1 = plane strain 2 = plane stress
Card 9	(5I)	**For each isoparametric element**
	1E(M,1)	1st node number
	1E(M,2)	2nd
	1E(M,3)	3rd
	1E(M,4)	4th
	1E(M,5)	material property number

Card 10	(I, 4F)	**For each material type**
	I	material property number
	E	modulus of elasticity
	PR	Poisson's ratio
	RO	density
	TH	thickness
Card 11	(I)	**For line elements**
	IGSH	include shear deformations 0 = no, 1 = yes
Card 12	(3I)	**For each line element**
	1E(M,1)	1st node number
	1E(M,2)	2nd
	1E(M,5)	material property number
Card 13	(I, 5F)	**For each material type**
	I	material property number
	E	modulus of elasticity
	PR	2nd moment of area
	RO	density
	TH	X-section area
	ALEN	added length for stiffness
Card 14	(I)	**For Al-Mahaidi's constraints**
	NBN	use 2nd constraint 0 = no, 1 = yes
Card 15	(3I)	**For each Al-Mahaidi's constraint joint**
	1E(M,1)	1st node number
	1E(M,2)	2nd
	1E(M,3)	3rd

Card 16	(5I)	**For each proposed constraints joint**
	1E(M,1)	1st node number
	1E(M,2)	2nd
	1E(M,3)	3rd
	1E(M,4)	4th
	1E(M,5)	material property number
Card 17	(I, F, I, F)	**For each material type**
	I	material property number
	E	yield limit
	IP	yielding allowed, 0 = no, 1 = yes
	PR	percentage stiffness after yield
Card 18	(5I)	**For each rotational freedoms element**
	1E(M,1)	1st node number
	1E(M,2)	2nd
	1E(M,3)	3rd
	1E(M,4)	4th
	1E(M,5)	material property number
Card 19	(I, 4F)	**For each material type**
	I	material property number
	E	modulus of elasticity
	PR	Poisson's ratio
	RO	density
	TH	thickness
Card 20	(2I)	**For each boundary node**
	I	node number
	KODE	fixity 1 = roller 2 = pinned 3 = fixed

Card 21	(2I)	**For dynamic problems**
	KMAS	0 = lumped mass 1 = cosistent mass
	NSEC	number of external mass groups
Card 22	(2I, 2F)	**For ech external mass group**
	LUM (I,1)	first node in group
	LUM (I,2)	total number of nodes in group
	EXMAS	mass
	RMAS	rotational inertia
Card 23	(2I)	**For free vibration problems**
	NEIG	number of eigenvalues
	NSPUM	response spectrum analysis 0 = no, 1 = yes
Card 24	(3F, I)	**For each eigenvalue**
	W	approximate eigenvalue
	DW	step length
	EPS	accuracy
	NDEG	degree of freedom set equal to zero for mode shape

The remaining data is for forced vibration analysis only.

Card 25	(6I5)	
	INT	0 = initial conditions all zero 1 = displacements and velocity given 2 = acceleration also given
	NPRINT	the number of time steps between printing of results
	NSTEP	the total number of steps
	MAXSTP	the step at which initial conditions are saved
	NTYP	0 = 1 forcing function 1 = ground acceleration
	NP	number of data points describing forcing function or acceleration

Card 26	(5F10.6, F10.7)	
	C1	damping coefficient
	C2	damping coefficient
	DELT	integration parameter, usually = 0
	DT	time step
	TIME	initial time
	SF	scale factor
Card 27	(5I5)	
	NFIX	number of fixed nodes or = NNP to read force vector
	NVEC	horizontal or vertical forcing 10 = horizontal 01 = vertical 11 = both
	MSPAC	nodal spacing of printed results
	MSTRS	0 = no forces calculated 1 = line element forces 2 = and isoparametric element forces
	NEED	number of intervals for calculating forces
CARD 28	(6F10.4)	**For each NEED**
	TNED(I,1)	start of time interval
	TNED(I,2)	end of time interval for calculation of forces
CARD 29	(I5)	**If NFIX = NNP**
	NVC	number of nodes on which force vector acts
Card 30	(I5, 2F10.5)	**For each NVC**
	II	node
	CH	horizontal force
	CV	vertical force

Card 31 (3F10.4) For each NP

	NTYP = 1	NTYP = 0	NTYP = 0, NP = 1
P(1,J)	time	time	frequency
P(2,J)	horizontal acceleration	horizontal force	horizontal force
P(3,J)	vertical acceleration	vertical force	vertical force

The program then returns to the first data card.

A listing of the program follows.

```
      IMPLICIT REAL*8(A-H,O-Z)
      COMMON/DATA/ NEL,NMAT(6),NEL1(6),NOPT,NBODY,KMAS,MODIF,NBN,NELT
      COMMON/THREE/R(1400),AK(1400,40)
      COMMON/DISP/X(700),Y(700),ULX(700),VLY(700),KODE(700),NBOUN
      COMMON/NODE/IE(600,5)
      COMMON/PROTY/ALEN(30),E(30),PR(30),RO(30),TH(30),IP(30),IGSH
      COMMON/TWO/IBAND,NEQ
      COMMON/FRE/NT(700)
      COMMON/TEMP/IDF(700),NNP
      DIMENSION TITLE(18)
      DATA MAXEL,MAXNP,MAXMAT,MAXBW / 600,700,30,40 /
      NELT=6
   10 READ(5,1000) NPROB,(TITLE(I),I=1,18)
 1000 FORMAT(I5,3X,18A4)
      IF(NPROB.LE.0) GOTO 180
      WRITE(9,1010) NPROB,(TITLE(I),I=1,18)
 1010 FORMAT(/8H1PROBLEM,I5,3H...,18A4)
      READ(5,*)GACC
      READ(5,*) IPRINT,NDYNAN,NDPOBS
      WRITE(9,1020)
 1020 FORMAT(/1H ,90(1H*)////)
C
C INPUT ALL THE STRUCTURE INFORMATION
C
      CALL DATAIN (MAXEL,MAXNP,MAXMAT,ISTOP)
C
C CALCULATE NO OF EQUATIONS AND BANDWIDTH
C
      MAXDOF=2*MAXNP
      IDF(1)=0
      NNN=NNP+1
      DO 20 I=2,NNN
      IDF(I)=IDF(I-1)+2
   20 IF(NT(I-1).GT.1)IDF(I)=IDF(I)+1
      NEQ=IDF(NNN)
      IDOF=NEQ
      IBAND=0
      M=0
      DO 50 I=1,NELT
      IF(NEL1(I).LE.0)GOTO 50
      NUM=2
      GOTO(30,32,31,31,30,30),I
   30 NUM=NUM+1
   31 NUM=NUM+1
   32 CONTINUE
      DO 40 L=1,NEL1(I)
      M=M+1
      DO 40 J=1,NUM
      DO 40 K=1,NUM
      LL=IDF(IE(M,J)+1)-IDF(IE(M,K))
      IF(LL.GT.IBAND)IBAND=LL
   40 CONTINUE
   50 CONTINUE
      IF(IBAND.GT.MAXBW) GOTO 170
      WRITE(9,1030)IBAND
 1030 FORMAT(///13X,12HBANDWIDTH = ,I2)
      IF(ISTOP.GT.0) GOTO 180
C
C FORM STIFFNESS MATRIX
C
      CALL ASEMBL(ISTOP,MAXEL,MAXNP,MAXDOF,MAXBW,IDOF,GACC,NDYNAN)
      WRITE(9,1040)NEQ,IDOF
 1040 FORMAT(/3X,21HNUMBER OF EQUATIONS =,I4//4X,23HDEGREES OF FREEDOM =
     1,I4)
      IF(ISTOP.GT.0) GOTO 180
      IF(IPRINT.LE.0) GOTO 70
      WRITE(9,1070)
      DO 60 I=1,NEQ
      WRITE(9,1050) I
      WRITE(9,1060) (AK(I,J),J=1,IBAND)
   60 CONTINUE
   70 CONTINUE
      IF(NDYNAN.EQ.0) GOTO90
C
C FORM MASS MATRIX
C
      CALL ASEMAS(ISTOP,MAXDOF,MAXBW)
      IF(ISTOP.GT.0) GOTO 180
      IF(IPRINT.LE.0) GOTO 90
      WRITE(9,1080)
      DO 80 I=1,NEQ
      WRITE(9,1050) I
      WRITE(9,1060) (AK(I,J),J=1,IBAND)
   80 CONTINUE
 1050 FORMAT( I5,'XXXX NEW LINE ****************************************
     ************************************************')
 1060 FORMAT( 5X,10E10.3)
 1070 FORMAT( //10X,'***** STIFFNESS MATRIX *****' // )
 1080 FORMAT( //10X,'XXXXX MASS MATRIX *****'//)
   90 CONTINUE
C STATIC,FREE VIBRATION,DYNAMIC RESPONSE
      IF(NDYNAN.EQ.0) CALL BANSOL(0,AK,R,NEQ,IBAND,MAXDOF,MAXBW)
      IF(NDYNAN.EQ.1) CALL EIGEN(AK,R,MAXDOF,MAXBW,KMAS,GACC)
      IF(NDYNAN.EQ.2) CALL RESPON(MAXDOF,MAXEL,MAXNP,NEQ,IBAND
     *,GACC,MAXBW,NDYNAN)
      IF(IPRINT.LE.1)GOTO 110
      WRITE(9,1070)
      DO 100 I=1,NEQ
      WRITE(9,1050)I
      WRITE(9,1060)(AK(I,J),J=1,IBAND)
  100 CONTINUE
  110 CONTINUE
C
C PRINT DISPLACEMENT
C
      WRITE(9,1090)
      CONT=0.0D0
      AVDIS=0.0D0
      DO 160 IK=1,NNP
      I=NNP+1-IK
```

```
      J=IDF(I)+1
      CONT=CONT+1.0D0
      AVDIS=AVDIS+R(J)
      GOTO(120,130,130,140)NI(I)
  120 WRITE(9,1110) I,R(J),R(J+1)
      GOTO 150
  130 WRITE(9,1120)I,R(J),R(J+1),R(J+2)
      GOTO 150
  140 WRITE(9,1130)I,R(J),R(J+1),R(J+2)
  150 IF(X(I).NE.0.0D0) GOTO 160
      AVDIS=AVDIS/CONT
      WRITE(9,1140) AVDIS
      CONT=0.0D0
      AVDIS=0.0D0
      WRITE(9,1100)
  160 CONTINUE
 1090 FORMAT(1H1,/15X,'**** OUTPUT TABLE 1. NODAL DISPLACEMENT ****'//
     *3X,4HNODE,9X,10HU=X-DISP.   ,9X,11HV= Y-DISP. / )
 1100 FORMAT(4X,'*********************************************')
 1110 FORMAT(I7,3X,2E20.8)
 1120 FORMAT(I7,3X,3E20.8)
 1130 FORMAT(I7,3X,2E20.8,3H LL,E14.7,2HLI)
 1140 FORMAT(5X,39HAVERAGE DISPLACEMENT AT THIS SECTION = ,F15.5)
      IF(NDFORS.EQ.0) GOTO 10
C
C COMPUTE FORCES AND STRESSES
C
      CALL ENDFOR(R,MAXDOF)
      IF(NDFORS.EQ.1)GOTO10
      CALL FORCE(R,IE,MAXEL,MAXDOF,MAXNP,ULX,VLY,X,Y)
      CALL STRESS(R,IE,X,Y,ULX,VLY,MAXDOF,MAXEL,MAXNP,KODE)
      GOTO 10
  170 WRITE(9,1150) IBAND,MAXBW
 1150 FORMAT(///12H BANDWIDTH= ,I4,24H EXCEEDS MAX.ALLOWABLE  ,I4,//
     124H GO ON TO NEXT PROBLEM  )
      GOTO10
  180 IF(ISTOP.GT.0) WRITE(9,1160) ISTOP
 1160 FORMAT(////42H SOLUTION WILL NOT BE PERFORMED BECAUSE OF ,I5,15H
     1DATA ERRORS  /)
      STOP
      END
      SUBROUTINE ASEMBL(ISTOP,MAXEL,MAXNP,MAXNEQ,MAXBW,IDOF,GACC,NDYNAN)
      IMPLICIT REAL*8 (A-H,O-Z)
      COMMON/DATA/ NEL,NMAT(6),NEL1(6),NOPT,NBODY,KMAS,NODIF,NBB,NELI
      COMMON/THREE/ R(1400),AK(1400,40)
      COMMON/DISP/X(700),Y(700),ULX(700),VLY(700),KODE(700),NBOUN
      COMMON/NODE/IE(600,5)
      COMMON/PROTY/ALEN(30),E(30),PR(30),RO(30),TH(30),IP(30),IGSH
      COMMON/TWO/IBAND,NEQ
      COMMON/TEMP/IDF(700),NNP
      DIMENSION QK(12,12),Q(12)
      REWIND 7
      REWIND 8
      ISTOP=0
      NNP=NP
      DO 1 I=1,MAXNEQ
      R(I)=0.0D0
      DO2J=1,IBAND
    2 AK(I,J)=0.0D0
      TAREA=0.0D0
C
C     CALCULATES STIFFNESS FOR QUADRILATERAL ELEMENTS
C
      M=0
      IF(NEL1(1).LE.0)GOTO 15
      DO 10 I=1,NEL1(1)
      M=M+1
      CALL QUAD(M,AREA,QK,Q,MAXEL,MAXNP,IE,X,Y,GACC)
      TAREA=TAREA+AREA
      CALL ADDS(2,8,M,QK,Q)
   10 CONTINUE
      WRITE(9,110)TAREA
  110 FORMAT(/25H AREA OF QUAD ELEMENTS = ,E20.14)
C
C     CALCULATES STIFFNESS FOR LINE ELEMENTS
C
   15 IF(NEL1(2).LE.0)GOTO 25
      DO 20 I=1,NEL1(2)
      M=M+1
      CALL LINE(M,QK,Q,GACC)
      CALL ADDS(3,6,M,QK,Q)
   20 CONTINUE
C
C     CALCULATES STIFFNESS FOR HORIZONTAL JOINT ELEMENTS
C
   25 IF(NEL1(3).LE.0)GOTO 35
      DO 30 I=1,NEL1(3)
      M=M+1
      IF(NDYNAN.EQ.2)GOTO 30
      ZZ=Y(IE(M,3))-Y(IE(M,1))
      CALL JOINTH(QK,Q,ZZ,NBN)
      CALL ADDS(3,9,M,QK,Q)
   30 CONTINUE
C
C     CALCULATES STIFFNESS FOR VERTICAL JOINT ELEMENTS
C
   35 IF(NEL1(4).LE.0)GOTO 45
      DO 40 I=1,NEL1(4)
      M=M+1
      IF(NDYNAN.EQ.2)GOTO 40
      ZZ=X(IE(M,3))-X(IE(M,1))
      CALL JOINTV(QK,Q,ZZ,NBN)
      CALL ADDS(3,9,M,QK,Q)
   40 CONTINUE
C
C     CALCULATES STIFFNESS FOR TYPE 2 JOINT
C
   45 IF(NEL1(5).LE.0)GOTO 55
      DO 50 I=1,NEL1(5)
      M=M+1
      IF(NDYNAN.EQ.2)GOTO 50
```

```
      CALL CONECT(M,NDYNAN)
   50 CONTINUE
C
C     CALCULATES STIFFNESS FOR RECTANGULAR BEAM ELEMENT
C
   55 IF(NEL1(6).LE.0)GOTO 65
      TAREA=0.0D0
      DO 60 I=1,NEL1(6)
      M=M+1
      CALL BQUAD(M,AREA,QK,Q)
      TAREA=TAREA+AREA
      CALL ADDS(3,12,M,QK,Q)
   60 CONTINUE
      WRITE(9,120)TAREA
  120 FORMAT(///25H AREA OF BEAM ELEMENTS = ,F10.4)
   65 CONTINUE
C
C     SET UP LOAD VECTOR
C
      DO58N=1,NNP
      K=IDF(N)+2
      R(K-1)=R(K-1)+ULX(N)
      R(K)=R(K)+VLY(N)
   58 CONTINUE
C
C     ADJUSTS MATRICES FOR FIXED NODES
C
      DO70M=1,NNP
      IF(KODE(M).GE.0.AND.KODE(M).LE.3) GO TO 72
      ISTOP=ISTOP+1
      GOTO 70
   72 K=KODE(M)+1
      GOTO(70,69,68,67),K
   67 CALL GEOME(0.0D0,IDF(M)+3,R,AK,MAXNEQ,MAXBW,1)
      IDOF=IDOF-1
   68 CALL GEOME(ULX(M),IDF(M)+1,R,AK,MAXNEQ,MAXBW,1)
      IDOF=IDOF-1
   69 CALL GEOME(VLY(M),IDF(M)+2,R,AK,MAXNEQ,MAXBW,1)
      IDOF=IDOF-1
   70 CONTINUE
      REWIND 1
      WRITE(1)   ((AK(I,J),J=1,IBAND),I=1,NEQ)
   81 RETURN
      END
      SUBROUTINE ADDS(NF,LIM,M,QK,Q)
      IMPLICIT REAL*8 (A-H,O-Z)
      COMMON/THREE/R(1400),AK(1400,40)
      COMMON/NODE/IE(600,5)
      COMMON/TEMP/IDF(700),NNP
      DIMENSION LP(12),QK(12,12),Q(12)
C
C     FINDS POSITION OF ELEMENT MATRIX IN STIFFNESS MATRIX
C
      DO 10 I=NF,LIM,NF
      IJ=I/NF
      J=IDF(IE(M,IJ))
      DO 10 K=1,NF
      KK=I-NF+K
      LP(KK)=J+K
   10 CONTINUE
C
C     ADDS IN ELEMENT STIFFNESS AND SELF WEIGHT
C
      DO 20 LL=1,LIM
      I=LP(LL)
      R(I)=R(I)+Q(LL)
      DO 20 MM=1,LIM
      J=LP(MM)-I+1
      IF(J.LE.0)GOTO 20
      AK(I,J)=AK(I,J)+QK(LL,MM)
   20 CONTINUE
      RETURN
      END
      SUBROUTINE BQUAD(M,AREA,QK,Q)
      IMPLICIT REAL*8 (A-H,O-Z)
      COMMON/DATA/NEL,NMAT(6),NEL1(6),NOPT,NBODY,KMAS,MODIF,NBN,NELT
      COMMON/DISP/X(700),Y(700),ULX(700),VLY(700),KODE(700),NBCON
      COMMON/NODE/IE(600,5)
      COMMON/PROTY/ALEN(30),E(30),PR(30),RO(30),TH(30),IP(30),IGSH
      COMMON/GAUSS/CORD(5,5),WEIGHT(5,5)
      DIMENSION QK(12,12),Q(12),BM(3,12),BT(12,3)
      DIMENSION D(3,3),TDB(3,12),TQK(12,12),DUM(12,12),TDUM(12,12)
      DO 20 I=1,12
      DO 10 J=1,3
   10 BM(J,I)=0.0
      DO 20 J=1,12
   20 QK(I,J)=0.0
C
C  CALCULATE SIZE & ORIENTATION OF ELEMENT
C
      XS=X(IE(M,2))-X(IE(M,1))
      YS=Y(IE(M,2))-Y(IE(M,1))
      A=(SQRT(XS**2+YS**2))/2.0
      S=YS/(A*2.0)
      C=XS/(A*2.0)
      B=(SQRT((X(IE(M,4))-X(IE(M,1)))**2+(Y(IE(M,4))-Y(IE(M,1)))**2))
     1/2.0
      DET=A*B
      AREA=DET*4.0
      AFB=A/B
      MTYP=IE(M,5)
C
C  PLANE STRESS MATRIX
C
      DF=(E(MTYP)/(1.0-PR(MTYP)**2))*TH(MTYP)*DET
      D(1,1)=DF
      D(1,2)=PR(MTYP)*DF
      D(1,3)=0.0
      D(2,1)=D(1,2)
      D(2,2)=DF
```

```
      D(2,3)=0.0
      D(3,1)=0.0
      D(3,2)=0.0
      D(3,3)=DF*(1.0-PR(MTYP))/2.0
C
C  INTEGRATION ORDER,COORDINATES & WEIGHTING
C
      NH=3
      NV=2
      DO 40 I2=1,NV
      YC=CORD(I2,NV)
      WEIG1=WEIGHT(I2,NV)
      DO 40 J2=1,NH
      XC=CORD(J2,NH)
      WEIG2=WEIGHT(J2,NH)
      FACT=WEIG1*WEIG2
C
C     [B] MATRIX
C
      X4=XC/4.0
      Y4=YC/4.0
      X8=XC/8.0
      Y8=YC/8.0
      X83=X8*3.0
      Y83=Y8*3.0
      X2=(XC**2)/8.0
      X23=X2*3.0
      X3=(XC**3)/8.0
      XY=(XC*YC)/4.0
      X2Y=((XC**2)*YC*3.0)/8.0
      BM(1,1)=(-0.25+Y4)/A
      BM(3,1)=(-0.25+X4)/B
      BM(2,2)=(-0.25+X83-X3)/B
      BM(3,2)=(-0.375+X23+Y83-X2Y)/A
      BM(2,3)=(-0.125+X8+X2-X3)*APB
      BM(3,3)=-0.125-X4+X23+Y8+XY-X2Y
      BM(1,4)=(0.25-Y4)/A
      BM(3,4)=(-0.25-X4)/B
      BM(2,5)=(-0.25-X83+X3)/B
      BM(3,5)=(0.375-X23-Y83+X2Y)/A
      BM(2,6)=(0.125+X8-X2-X3)*APB
      BM(3,6)=-0.125+X4+X23+Y8-XY-X2Y
      BM(1,7)=(0.25+Y4)/A
      BM(3,7)=(0.25+X4)/B
      BM(2,8)=(0.25+X83-X3)/B
      BM(3,8)=(0.375-X23+Y83-X2Y)/A
      BM(2,9)=(-0.125-X8+X2+X3)*APB
      BM(3,9)=-0.125+X4+X23-Y8+XY+X2Y
      BM(1,10)=(-0.25-Y4)/A
      BM(3,10)=(0.25-X4)/B
      BM(2,11)=(0.25-X83+X3)/B
      BM(3,11)=(-0.375+X23-Y83+X2Y)/A
      BM(2,12)=(0.125-X8-X2+X3)*APB
      BM(3,12)=-0.125-X4+X23-Y8-XY+X2Y
C
C  CALCULATE STIFFNESS MATRIX
C
      CALL TRANS(3,12,BM,BT)
      CALL MATMUL(3,3,12,D,BM,TDB)
      CALL MATMUL(12,3,12,BT,TDB,TQK)
      DO 40 I=1,12
      DO 40 J=1,12
      QK(I,J)=QK(I,J)+(TQK(I,J)*FACT)
   40 CONTINUE
C
C  ROTATE TO GLOBAL COORDINATES
C
      DO 50 I=1,12
      DO 50 J=1,12
   50 TQK(I,J)=0.0
      TQK(1,1)=C
      TQK(1,2)=S
      TQK(2,1)=-S
      TQK(2,2)=C
      TQK(3,3)=1.0
      TQK(4,4)=C
      TQK(4,5)=S
      TQK(5,4)=-S
      TQK(5,5)=C
      TQK(6,6)=1.0
      TQK(7,7)=C
      TQK(7,8)=S
      TQK(8,7)=-S
      TQK(8,8)=C
      TQK(9,9)=1.0
      TQK(10,10)=C
      TQK(10,11)=S
      TQK(11,10)=-S
      TQK(11,11)=C
      TQK(12,12)=1.0
      CALL MATMUL(12,12,12,QK,TQK,DUM)
      CALL TRANS(12,12,TQK,TDUM)
      CALL MATMUL(12,12,12,TDUM,DUM,QK)
      RETURN
      END
      SUBROUTINE CONECT(M,NDYNAM)
      IMPLICIT REAL*8 (A-H,O-Z)
      COMMON/DISP/X(700),Y(700),ULX(700),VLY(700),KODE(700),NBCON
      COMMON/NODE/IE(600,5)
      COMMON/PROTY/ALEN(30),E(30),EB(30),EO(30),TH(30),IP(30),IGSH
      DIMENSION QK(12,12),Q(12)
      DO 10 I=1,12
      Q(I)=0.0D0
      DO 10 J=1,12
   10 QK(I,J)=0.0D0
      QK(1,10)=0.5D0
      QK(2,11)=0.5D0
      QK(4,10)=-1.0D0
      QK(5,11)=-1.0D0
      QK(7,10)=0.5D0
```

```
      QK(8,11)=0.5D0
      QK(10,1)=0.5D0
      QK(10,4)=-1.0D0
      QK(10,7)=0.5D0
      QK(11,2)=0.5D0
      QK(11,5)=-1.0D0
      QK(11,8)=0.5D0
      IF(NDYNAN.LT.2.AND.IP(IE(M,5)).EQ.1)GOTO 20
      QK(1,12)=1.0/(Y(IE(M,3))-Y(IE(M,1)))
      QK(12,1)=QK(1,12)
      QK(12,6)=-1.0D0
      QK(7,12)=-QK(1,12)
      QK(12,7)=QK(7,12)
      QK(6,12)=-1.0D0
   20 CALL ADDS(3,12,M,QK,Q)
      RETURN
      END
      SUBROUTINE JOINTH(QK,Q,ZZ,NBN)
      IMPLICIT REAL*8 (A-H,O-Z)
      DIMENSION QK(12,12),Q(12)
      DO 10 I=1,9
      Q(I)=0.0
      DO 10 J=1,9
   10 QK(I,J)=0.0
      QK(1,9)=-1.0/ZZ
      QK(6,9)=1.0
      QK(7,9)=-QK(1,9)
      QK(9,1)=QK(1,9)
      QK(9,6)=1.0
      QK(9,7)=QK(7,9)
      IF(NBN.LT.1)GOTO 20
      QK(1,3)=0.5
      QK(3,1)=0.5
      QK(3,4)=-1.0
      QK(3,7)=0.5
      QK(4,3)=-1.0
      QK(7,3)=0.5
   20 RETURN
      END
      SUBROUTINE JOINTV(QK,Q,ZZ,NBN)
      IMPLICIT REAL*8 (A-H,O-Z)
      DIMENSION QK(12,12),Q(12)
      DO 10 I=1,9
      Q(I)=0.0
      DO 10 J=1,9
   10 QK(I,J)=0.0
      QK(2,9)=1.0/ZZ
      QK(6,9)=1.0
      QK(8,9)=-QK(2,9)
      QK(9,2)=QK(2,9)
      QK(9,6)=1.0
      QK(9,8)=QK(8,9)
      IF(NBN.LT.1)GOTO 20
      QK(2,3)=0.5
      QK(3,2)=0.5
      QK(3,5)=-1.0
      QK(3,8)=0.5
      QK(5,3)=-1.0
      QK(8,3)=0.5
   20 RETURN
      END
      SUBROUTINE LINE(M,QK,Q,GACC)
      IMPLICIT REAL*8 (A-H,O-Z)
      COMMON/DATA/ NEL,NMAT(6),NEL1(6),NOPT,NBODY,KMAS,MODIF,NBN,NEL1
      COMMON/NODE/IE(600,5)
      COMMON/PROTY/AREN(30),E(30),PR(30),RO(30),TH(30),IP(30),IGSH
      DIMENSION QK(12,12),Q(12)
      CALL ANG(M,S,C,BL)
      SC=S*C
      S2=S**2
      C2=C**2
      IZ=IE(M,5)
      EA=E(IZ)*TH(IZ)/BL
      G=(17.28*PR(IZ))/(TH(IZ)*BL**2)
      IF(IGSH.NE.1)G=0.0
      EI=(E(IZ)*PR(IZ))/(1.0+2.0*G)
      E2=(EI*2.0/BL)*(1.0-G)
      E4=(EI*4.0/BL)*(1.0+G/2.0)
      E6=EI*6.0/BL**2
      E12=EI*12.0/BL**3
      QK(1,1)=C2*EA+S2*E12
      QK(1,2)=SC*(EA-E12)
      QK(1,3)=-S*E6
      QK(1,4)=-QK(1,1)
      QK(1,5)=-QK(1,2)
      QK(1,6)=QK(1,3)
      QK(2,2)=S2*EA+C2*E12
      QK(2,3)=C*E6
      QK(2,4)=QK(1,5)
      QK(2,5)=-QK(2,2)
      QK(2,6)=QK(2,3)
      QK(3,3)=E4
      QK(3,4)=-QK(1,3)
      QK(3,5)=-QK(2,3)
      QK(3,6)=E2
      QK(4,4)=QK(1,1)
      QK(4,5)=QK(1,2)
      QK(4,6)=QK(3,4)
      QK(5,5)=QK(2,2)
      QK(5,6)=QK(3,5)
      QK(6,6)=QK(3,3)
      DO10I=2,6
      DO10J=2,I
      K=J-1
   10 QK(I,K)=QK(K,I)
      WRITE(7)((QK(I,J),J=1,6),I=1,6)
      DO20I=1,6
   20 Q(I)=0.0D0
      IF(NBODY.EQ.0)GOTO30
      Q(1)=-RO(IZ)*TH(IZ)*BL*GACC/2.0D0
```

```
      Q(3)=Q(1)*BL*C/6.0D0
      Q(4)=Q(1)
      Q(6)=-Q(3)
   30 RETURN
      END
      SUBROUTINE ANG(M,S,C,BL)
      IMPLICIT REAL*8 (A-H,O-Z)
      COMMON/DISP/X(700),Y(700),ULX(700),VLY(700),KODE(700),NBOUN
      COMMON/NODE/IE(600,5)
      COMMON/PROTY/ALEN(30),E(30),PR(30),RO(30),TH(30),IP(30),IGSH
      XP=X(IE(M,2))-X(IE(M,1))
      YP=Y(IE(M,2))-Y(IE(M,1))
      BL=SQRT(XP**2+YP**2)
      S=YP/BL
      C=XP/BL
      BL=BL+ALEN(IE(M,5))
      RETURN
      END
      SUBROUTINE QUAD(M,AREA,QK,Q,MAXEL,MAXNP,IE,X,Y,GACC)
      IMPLICIT REAL*8 (A-H,O-Z)
      COMMON/DATA/ NEL,NMAT(6),NEL1(6),NOPT,NEQDY,KMAS,MODIF,NBN,NELT
      COMMON/PROTY/ALEN(30),E(30),PR(30),RO(30),TH(30),IP(30),IGSH
      COMMON/GAUSS/CORD(5,5),WEIGHT(5,5)
      DIMENSION IE(MAXEL,5),X(MAXNP),Y(MAXNP)
      DIMENSION XE(4,2),Q(12),QK(12,12),TQK(12,12),CB(12,12),TCB(3,12)
      I=IE(M,1)
      J=IE(M,2)
      K=IE(M,3)
      L=IE(M,4)
      MTYP=IE(M,5)
      AREA=0.0D0
      A=X(J)-X(I)
      F=X(K)-X(I)
      G=Y(J)-Y(I)
      H=Y(K)-Y(I)
      AREA1=(A*H-F*G)/2.0D0
      A=X(K)-X(I)
      F=X(L)-X(I)
      G=Y(K)-Y(I)
      H=Y(L)-Y(I)
      AREA2=(A*H-F*G)/2.0D0
      AREA=AREA1+AREA2
      DO10N=1,4
      NN=IE(M,N)
      XE(N,1)=X(NN)
      XE(N,2)=Y(NN)
   10 CONTINUE
      DO12II=1,8
   12 Q(II)=0.0D0
      DO13II=1,12
      DO13JJ=1,12
      CB(JJ,II)=0.0D0
   13 QK(II,JJ)=0.0D0
      NC=2
      DO20I2=1,NC
      ETA=CORD(I2,NC)
      WEIG1=WEIGHT(I2,NC)
      DO20J2=1,NC
      XI=CORD(J2,NC)
      WEIG2=WEIGHT(J2,NC)
      CALL FUNK(XE,XI,ETA,TQK,TCB,MTYP,M,NMAT(1),NOPT)
      FACT=WEIG1*WEIG2
      DO15I1=1,12
      DO15J1=1,12
   15 QK(I1,J1)=QK(I1,J1)+TQK(I1,J1)*FACT
   20 CONTINUE
      DO25II=1,12
      DO25JJ=1,12
   25 QK(II,JJ)=QK(II,JJ)*TH(MTYP)
      DO30L1=1,4
      IF(L1.EQ.1.OR.L1.EQ.2) ETA=-1.0D0
      IF(L1.EQ.3.OR.L1.EQ.4) ETA=1.0D0
      IF(L1.EQ.1.OR.L1.EQ.4) XI=-1.0D0
      IF(L1.EQ.2.OR.L1.EQ.3) XI=1.0D0
      CALL FUNK(XE,XI,ETA,TQK,TCB,MTYP,M,NMAT(1),NOPT)
      DO30I1=1,3
      II=I1+3*(L1-1)
      DO30J1=1,12
   30 CB(II,J1)=TCB(I1,J1)
      IF(MODIF.EQ.0) GOTO55
C
C     ELIMINATE EXTRA DEGREE OF FREEDOM ***** INCOMPATIBLE MODES *****
C
      DO50I1=1,4
      L1=12-I1
      K1=L1+1
      DO50J1=1,L1
      PIV=QK(J1,K1)/QK(K1,K1)
      DO40J2=1,12
   40 CB(J2,J1)=CB(J2,J1)-PIV*CB(J2,K1)
      DO50J2=1,L1
   50 QK(J1,J2)=QK(J1,J2)-PIV*QK(K1,J2)
   55 WRITE(7) ((QK(I1,J1),J1=1,8),I1=1,8)
      WRITE(8) M,((CB(I1,J1),J1=1,8),I1=1,12)
C
C     CALCULATE SELF WEIGHT
C
      IF(NBODY.EQ.0) GOTO99
      BODYF=GACC*AREA*RO(MTYP)*TH(MTYP)/4.0D0
      DO60I=2,8,2
      Q(I)=-BODYF
   60 CONTINUE
   99 RETURN
      END
      BLOCK DATA
      IMPLICIT REAL*8 (A-H,O-Z)
      COMMON/GAUSS/ CORD(5,5),WEIGHT(5,5)
      DATA CORD/0.0D0,0.0D0,0.0D0,0.0D0,0.0D0,
     A-0.5773502691D0,0.57735026910D0,0.0D0,0.0D0,0.0D0,
     B-0.7745966692D0,0.0D0,0.7745966692D0,0.0D0,0.0D0,
```

```
     C-0.8611363115D0,-0.3399810435D0,0.3399810435D0,0.8611363115D0,
     *0.0D0,
     D-0.9061798459D0,-0.5384693101D0,0.0D0,0.5384693101D0,0.9061798459D
     *0/
      DATA WEIGHT/0.0D0,0.0D0,0.0D0,0.0D0,0.0D0,0.0D0,
     E1.0D0,1.0D0,0.0D0,0.0D0,0.0D0,0.0D0,
     F0.555555555D0,0.888888888D0,0.555555555D0,0.0D0,0.0D0,
     G0.347854845 1D0,0.652145154 8D0,0.652145154 8D0,0.347854845 1D0,0.0D0,
     H0.236926885D0,0.478628670 4D0,0.568888888 8D0,0.478628670 4D0,0.23692
     *6885D0/
      END
      SUBROUTINE FUNK(XE,XI,ETA,TQK,TCB,MTYP,M,NMAT,NOPT)
      IMPLICIT REAL*8 (A-H,O-Z)
      COMMON/PROTY/ALEN(30), E(30),PR(30),RO(30),TH(30),IP(30),IGSH
      DIMENSION B(3,12),C(3,3),DXY(2,6),BT(12,3)
      DIMENSION XE(4,2),TQK(12,12),TCB(3,12)
      DO20I=1,3
      DO20J=1,12
   20 B(I,J)=0.0D0
      C(1,3)=0.0D0
      C(2,3)=0.0D0
      C(3,1)=0.0D0
      C(3,2)=0.0D0
      IF(NMAT.EQ.1.AND.L.GT.1) GOTO 5
      IF(NOPT.EQ.2) GOTO2
      CF=E(MTYP)/((1.0D0+PR(MTYP))*(1.0D0-2.0D0*PR(MTYP)))
      C(1,1)=CF*(1.0D0-PR(MTYP))
      C(1,2)=CF*PR(MTYP)
      C(2,1)=C(1,2)
      C(2,2)=C(1,1)
      C(3,3)=CF*(1.0D0-2.0D0*PR(MTYP))/2.0D0
      GOTO5
    2 CF=E(MTYP)/(1.0D0-PR(MTYP)**2)
      C(1,1)=CF
      C(1,2)=PR(MTYP)*CF
      C(2,1)=C(1,2)
      C(2,2)=CF
      C(3,3)=CF*(1.0D0-PR(MTYP))/2.0D0
    5 CONTINUE
      CALL JACOBI(XE,XI,ETA,DET,DXY)
      DO25I=1,6
      II=2*I-1
      B(1,II)=DXY(1,I)
      B(2,II+1)=DXY(2,I)
      B(3,II)=DXY(2,I)
      B(3,II+1)=DXY(1,I)
   25 CONTINUE
      CALL TRANS(3,12,B,BT)
      CALL MATMUL(3,3,12,C,B,TCB)
      CALL MATMUL(12,3,12,BT,TCB,TQK)
      DO30I=1,12
      DO30J=1,12
   30 TQK(I,J)=TQK(I,J)*DET
      RETURN
      END
```

```
      SUBROUTINE JACOBI(XE,XI,ETA,DET,DXY)
      IMPLICIT REAL*8 (A-H,O-Z)
      DIMENSION XE(4,2),DXY(2,6),AJ(2,2),DXE(2,4),TXE(2,6)
      DXE(1,1)=-(1.0D0-ETA)/4.0D0
      DXE(1,2)=(1.0D0-ETA)/4.0D0
      DXE(2,2)=(-1.0D0-XI)/4.0D0
      DXE(2,1)=-(1.0D0-XI)/4.0D0
      DXE(1,3)=(1.0D0+ETA)/4.0D0
      DXE(2,3)=(1.0D0+XI)/4.0D0
      DXE(1,4)=-(1.0D0+ETA)/4.0D0
      DXE(2,4)=(1.0D0-XI)/4.0D0
      CALL MATMUL(2,4,2,DXE,XE,AJ)
      DET=AJ(1,1)*AJ(2,2)-AJ(1,2)*AJ(2,1)
      TEM=AJ(1,1)
      AJ(1,1)=AJ(2,2)
      AJ(2,2)=TEM
      AJ(1,2)=-AJ(1,2)
      AJ(2,1)=-AJ(2,1)
      DO10I=1,2
      DO10J=1,2
   10 AJ(I,J)=AJ(I,J)/DET
      DO20I=1,2
      DO20J=1,4
   20 TXE(I,J)=DXE(I,J)
      TXE(1,5)=-2.0D0*XI
      TXE(1,6)=0.0D0
      TXE(2,5)=0.0D0
      TXE(2,6)=-2.0D0*ETA
      CALL MATMUL(2,2,6,AJ,TXE,DXY)
      RETURN
      END
      SUBROUTINE TRANS(K,L,AA,BB)
      IMPLICIT REAL*8 (A-H,O-Z)
      DIMENSION AA(K,L),BB(L,K)
      DO10I=1,K
      DO10J=1,L
   10 BB(J,I)=AA(I,J)
      RETURN
      END
      SUBROUTINE MATMUL(K,L,M,AA,BB,CC)
      IMPLICIT REAL*8 (A-H,O-Z)
      DIMENSION AA(K,L),BB(L,M),CC(K,M)
      DO10I=1,K
      DO10J=1,M
      CC(I,J)=0.0D0
      DO10J1=1,L
   10 CC(I,J)=CC(I,J)+AA(I,J1)*BB(J1,J)
      RETURN
      END
      SUBROUTINE ASEMAS(ISTOP,MAXNEC,MAXBW)
      IMPLICIT REAL*8 (A-H,O-Z)
      COMMON/DATA/ NEL,NMAT(6),NEL1(6),NOPT,NBODY,KMAS,MODIF,NEK,NELI
      COMMON/THREE/B(1400),AK(1400,40)
      COMMON/DISP/X(700),Y(700),ULX(700),VLY(700),KODE(700),ABCUR
      COMMON/NODE/IE(600,5)
```

```
      COMMON/PROTY/ALEN(30),E(30),PR(30),RO(30),TH(30),IP(30),IGSH
      COMMON/TWO/IBAND,NEQ
      COMMON/FRE/NT(700)
      COMMON/TEMP/IDF(700),NNP
      DIMENSION QK(8,8),LP(8),LUM(150,2),EXMAS(150),RMAS(150)
      READ(5,*) KMAS,NSEC
      WRITE(9,120) KMAS,NSEC
      IF(NSEC.LE.0) GOTO 5
      READ(5,*) ((LUM(I,J),J=1,2),EXMAS(I),RMAS(I),I=1,NSEC)
      WRITE(9,130) ((LUM(I,J),J=1,2),EXMAS(I),RMAS(I),I=1,NSEC)
    5 CONTINUE
      DO10I=1,NEQ
      DO10J=1,IBAND
   10 AK(I,J)=0.0
      M=0
      IF(NEL1(1).LE.0)GOTO 12
      DO 11 I=1,NEL1(1)
      M=M+1
      NODE1=IE(M,1)
      NODE2=IE(M,2)
      NODE3=IE(M,3)
      NODE4=IE(M,4)
      A=X(NODE2)-X(NODE1)
      F=X(NODE3)-X(NODE1)
      G=Y(NODE2)-Y(NODE1)
      H=Y(NODE3)-Y(NODE1)
      AREA1=ABS((A*H-F*G)/2.0)
      A=X(NODE3)-X(NODE1)
      F=X(NODE4)-X(NODE1)
      G=Y(NODE3)-Y(NODE1)
      H=Y(NODE4)-Y(NODE1)
      AREA2=ABS((A*H-F*G)/2.0)
      AREA=AREA1+AREA2
      MTYP=IE(M,5)
      CALL QUAMAS(QK,AREA,MTYP,RMAS)
   11 CALL ADDM(2,8,M,QK)
   12 IF(NEL1(2).LE.0)GOTO 14
      DO 13 I=1,NEL1(2)
      M=M+1
      BL=SQRT((X(IE(M,2))-X(IE(M,1)))**2+(Y(IE(M,2))-Y(IE(M,1)))**2)
      MTYP=IE(M,5)
      CALL BEAMAS(QK,MTYP,KMAS,BL)
   13 CALL ADDM(3,6,M,QK)
   14 M=M+NEL1(3)+NEL1(4)+NEL1(5)
C
C     ADDITION OF EXTERNAL MASSES
C
      IF(NSEC.LE.0) GOTO 39
      DO38I1=1,NSEC
      M1=LUM(I1,2)
      DO36J1=1,M1
      J=LUM(I1,1)+J1-1
      IF(NT(J).EQ.4) ISTOP=ISTOP+1
      NP1=IDF(J)+1
      NP2=NP1+1
      AK(NP1,1)=AK(NP1,1)+EXMAS(I1)
      AK(NP2,1)=AK(NP2,1)+EXMAS(I1)
      IF(NT(J).NE.2.AND.NT(J).NE.3)GOTO 36
      NP3=NP2+1
      AK(NP3,1)=AK(NP3,1)+RMAS(I1)
   36 CONTINUE
   38 CONTINUE
   39 CONTINUE
C
C     RESTRAINED DEGREES OF FREEDOM
C
      DO 60 MP=1,NNP
      IF(KODE(MP).GE.0.AND.KODE(MP).LE.3) GOTO 40
      ISTOP=ISTOP+1
      GOTO 60
   40 K=KODE(MP)+1
      GOTO(60,59,58,57),K
   57 CALL GEOME(0.0D0,IDF(MP)+3,3,AK,MAXNEQ,MAXBW,2)
   58 CALL GEOME(0.0D0,IDF(MP)+1,R,AK,MAXNEQ,MAXBW,2)
   59 CALL GEOME(0.0D0,IDF(MP)+2,R,AK,MAXNEQ,MAXBW,2)
   60 CONTINUE
      REWIND 2
      DO70I=1,NEQ
   70 WRITE(2) (AK(I,J),J=1,IBAND)
  120 FORMAT(//,15X,'**** KMASS ',I5,10X,'**** NSEC =',I5,//)
  130 FORMAT(//15X,27H**** EXTRA LUMPED MASS ****/5X,
     *10HSTART NODE,9X,11HTOTAL NODES,13X,4HMASS,9X,17HMOMENT OF INERTIA
     *//(8X,I4,16X,I4,12X,F12.5,8X,F12.5))
   80 RETURN
      END
      SUBROUTINE ADDM(NF,LIM,M,QK)
      IMPLICIT REAL*8 (A-H,O-Z)
      COMMON/THREE/R(1400),AK(1400,40)
      COMMON/NODE/IE(600,5)
      COMMON/TEMP/IDF(700),NNP
      DIMENSION LP(9),QK(8,8)
C
C     FINDS POSITION OF ELEMENT MASS IN MASS MATRIX
C
      DO 10 I=NF,LIM,NF
      IJ=I/NF
      J=IDF(IE(M,IJ))
      DO 10 K=1,NF
      KK=I-NF+K
      LP(KK)=J+K
   10 CONTINUE
C
C     ADDS IN ELEMENT MASS
C
      DO 20 LL=1,LIM
      I=LP(LL)
      DO 20 MM=1,LIM
      J=LP(MM)-I+1
      IF(J.LE.0)GOTO 20
      AK(I,J)=AK(I,J)+QK(LL,MM)
```

```
20 CONTINUE
   RETURN
   END
   SUBROUTINE QUAMAS(QK,AREA,MTYP,KMAS)
   IMPLICIT REAL*8 (A-H,O-Z)
   COMMON/PROTY/ALEN(30),E(30),PR(30),RO(30),TH(30),IP(30),IGSH
   DIMENSION QK(8,8)
   DO10I=1,8
   DO10J=1,8
10 QK(I,J)=0.0
   CONST=0.25*AREA*TH(MTYP)*RO(MTYP)
   IF(KMAS.EQ.0) GOTO 20
   QK(1,1)=0.44444444*CONST
   QK(1,3)=0.22222222*CONST
   QK(1,5)=0.11111111*CONST
   QK(1,7)=0.22222222*CONST
   QK(2,2)=0.44444444*CONST
   QK(2,4)=0.22222222*CONST
   QK(2,6)=0.11111111*CONST
   QK(2,8)=0.22222222*CONST
   QK(3,1)=0.22222222*CONSI
   QK(3,3)=0.44444444*CONST
   QK(3,5)=0.22222222*CONST
   QK(3,7)=0.11111111*CONST
   QK(4,2)=0.22222222*CONST
   QK(4,4)=0.44444444*CONST
   QK(4,6)=0.22222222*CONST
   QK(4,8)=0.11111111*CONST
   QK(5,1)=0.11111111*CONST
   QK(5,3)=0.22222222*CONSI
   QK(5,5)=0.44444444*CONST
   QK(5,7)=0.22222222*CONST
   QK(6,2)=0.11111111*CONST
   QK(6,4)=0.22222222*CONST
   QK(6,6)=0.44444444*CONST
   QK(6,8)=0.22222222*CONST
   QK(7,1)=0.22222222*CONST
   QK(7,3)=0.11111111*CONST
   QK(7,5)=0.22222222*CONST
   QK(7,7)=0.44444444*CONST
   QK(8,2)=0.22222222*CONST
   QK(8,4)=0.11111111*CONST
   QK(8,6)=0.22222222*CONST
   QK(8,8)=0.44444444*CONST
   GO TO 40
20 DO30I=1,8
30 QK(I,I)=CONST
40 RETURN
   END
   SUBROUTINE BEAMAS(QK,MTYP,KMAS,BL)
   IMPLICIT REAL*8 (A-H,O-Z)
   COMMON/PROTY/ALEN(30),E(30),PR(30),RO(30),TH(30),IP(30),IGSH
   DIMENSION QK(8,8)
   W=BL*TH(MTYP)*RO(MTYP)/2.0
   PHI=W*BL/6.0
```

```
      DO10I=1,6
      DO10J=1,6
   10 QK(I,J)=0.0
      QK(1,1)=W
      QK(2,2)=W
      QK(3,3)=PHI
      QK(4,4)=W
      QK(5,5)=W
      QK(6,6)=PHI
      RETURN
      END
      SUBROUTINE GEOME(U,N,RD,AKM,NDIM,MDIM,IC)
      IMPLICIT REAL*8 (A-H,O-Z)
      COMMON/TWO/IBAND,NEQ
      DIMENSION RD(NDIM),AKM(NDIM,MDIM)
      IF(IC.EQ.2) GOTO 200
C
C     STIFFNESS MATRIX
C
      DO100M=2,IBAND
      K=N-M+1
      IF(K.LE.0) GOTO 50
      RD(K)=RD(K)-AKM(K,M)*U
      AKM(K,M)=0.0
   50 K=N+M-1
      IF(K.GT.NEQ) GOTO100
      RD(K)=RD(K)-AKM(N,M)*U
      AKM(N,M)=0.0
  100 CONTINUE
      AKM(N,1)=1.0
      RD(N)=U
      GOTO 400
C
C     MASS MATRIX
C
  200 CONTINUE
      DO300MM=2,IBAND
      J=N-MM+1
      IF(J.LE.0) GOTO 250
      AKM(J,MM)=0.0
  250 J=N+MM-1
      IF(J.GT.NEQ) GOTO 300
      AKM(N,MM)=0.0
  300 CONTINUE
      AKM(N,1)=0.0
  400 RETURN
      END
      SUBROUTINE BANSOL(KKK,AK,R,NEQ,IBAND,NDIM,MDIM)
      IMPLICIT REAL*8 (A-H,O-Z)
      DIMENSION AK(NDIM,MDIM),R(NDIM)
      NBS=NEQ-1
      NB=NEQ
      IF(KKK.EQ.2) GOTO 200
      DO120N=1,NBS
      M=N-1
```

```
      NSM=NR-M
      MB=MINO(IBAND,NRM)
      PIVOT=AK(N,1)
      IF(PIVOT.EQ.0.0)WRITE(9,1000)N
 1000 FORMAT(16H PIVOT=0 ON LINE,I4)
      DO120L=2,MB
      CP=0.0
      IF(PIVOT.EQ.0.0) GOTO 100
      CF=AK(N,L)/PIVOT
  100 CONTINUE
      I=M+L
      J=0
      DO110K=L,MB
      J=J+1
  110 AK(I,J)=AK(I,J)-CF*AK(N,K)
  120 AK(N,L)=CP
      IF(KKK.EQ.1) GOTO 400
  200 DC220N=1,NBS
      M=N-1
      NBM=NR-M
      MB=MINO(IBAND,NBM)
      CF=R(M)
      R(M)=0.0
      IF(AK(N,1).EQ.0.0) GOTO 210
      R(M)=CP/AK(N,1)
  210 CONTINUE
      DC220L=2,MB
      I=M+L
  220 R(I)=R(I)-AK(N,L)*CP
      IF(AK(Nk,1).EQ.0.0) GOTO 230
      R(NR)=R(NR)/AK(NR,1)
      GCTO 240
  230 R(NR)=0.0
  240 CCNTINUE
      DO320I=1,NRS
      N=NR-I
      M=N-1
      NEM=NR-M
      MB=MINO(IBAND,NBM)
      DC320K=2,MB
      L=M+K
  320 R(M)=R(M)-AK(N,K)*R(L)
  400 RETURN
      END
      SUBROUTINE FORCE(R,IE,MAXEL,MAXNEQ,MAXNP,XFORCE,YFORCE,X,Y)
      IMPLICIT REAL*8 (A-H,O-Z)
      CCMMON/DATA/ NEL,NMAT(6),NEL1(6),NOPT,NDODY,KMAS,NODIF,NBW,NELT
      COMMON/TEMP/IDF(700),NNP
      DIMENSION R(MAXNEQ),IE(MAXEL,5),X(MAXNP),Y(MAXNP)
      DIMENSION XFORCE(MAXNP),YFORCE(MAXNP)
      DIMENSION ZDIS(8,1),QK(8,8),Q(8)
      NEXTD 7
      WRITE(9,11)
      IMDEX=0
      DO5K=1,MAXNP
      XFORCE(K)=0.0
      YFORCE(K)=0.0
    5 CONTINUE
      DC80M=1,NEL1(1)
      DC20I=1,4
      NN=IE(M,I)
      EDIS(I*2-1,1)=F(IDF(NN)+1)
   20 EDIS(2*I,1)=R(IDF(NN)+2)
      READ(7)((QK(I,J),J=1,8),I=1,8)
      CALL MATMUL(8,8,1,QK,EDIS,0)
      IF(INDEX.EQ.1) WRITE(9,100) M
      DO60II=1,4
      NN=IE(M,II)
      XFORCE(NN)=XFORCE(NN)+Q(2*II-1)
      YFORCE(NN)=YFORCE(NN)+Q(2*II)
      IF(INDEX.EQ.1) WRITE(9,110) NN,Q(2*II-1),Q(2*II)
   60 CONTINUE
   80 CONTINUE
  100 FORMAT(/25X,'ELEMENT NUMBER=',I5/,5X,'NODE',12X,'X-STRESS'
     1,12X,'Y-STRESS')
  110 FORMAT(I10,2E20.8)
      WRITE(9,120)
      DIS=0.0
      FOR=0.0
      DC90JJ=1,NNP
      J=NNP+1-JJ
      DIS=DIS+R(IDF(J)+1)
      FOR=FOR+XFORCE(J)
      WRITE(9,130) J,X(J),Y(J),R(IDF(J)+1),R(IDF(J)+2),XFORCE(J),YFORCE(
     1J)
      IF(X(J).NE.0.0) GOTO 90
      WRITE(9,22) DIS,FOR
      WRITE(9,33)
      FOR=0.0
      DIS=0.0
   90 CONTINUE
   11 FORMAT(1H1,'**** OUTPUT TABLE 2. FORCE OF EACH NODE ****'//)
   22 FORMAT(5X,'**** TOTAL VALUE AT THIS SECTION ****',F15.5,F40.5)
   33 FORMAT(5X,'**********************************************')
  120 FORMAT(5X,'NODE',9X,'X',9X,'Y',10X,'U-DISP',13X,'V-DISP',
     113X,'X-FORCE',13X,'Y-FORCE',/)
  130 FORMAT(I10,2F10.3,4F20.8)
      RETURN
      END
      SUBROUTINE ZWDFOR(R,MAXNEQ)
      IMPLICIT REAL*8 (A-H,O-Z)
      COMMON/DATA/ NEL,NMAT(6),NEL1(6),NOPT,NDODY,KMAS,NODIF,NEW,NELT
      CCMMON/NODE/IE(600,5)
      COMMON/TEMP/IDF(700),NNP
      DIMENSION R(MAXNEQ)
      DIMENSION RDIS(6,1),QK(6,6),Q(6,1),ZF(6),DUM(8,8)
      IF(NEL1(2).LE.0)RETURN
      WRITE(9,100)
      NEXTD 7
      IF(NEL1(1).LE.0)GOTO 20
```

```
      DO 10 M=1,NEL1(1)
   10 READ(7) ((DUM(I,J),J=1,8),I=1,8)
   20 IBEG=NEL1(1)+1
      IFIN=NEL1(1)+NEL1(2)
      DO 50 M=IBEG,IFIN
      DO30I=1,2
      NN=IDF(IE(M,I))
      DO30J=1,3
      IJ=I*3-3+J
   30 EDIS(IJ,1)=R(NN+J)
      READ(7) ((QK(I,J),J=1,6),I=1,6)
      CALL MATMUL(6,6,1,QK,EDIS,Q)
      CALL ANG(M,S,C,BL)
      EF(1)=C*Q(1,1)+S*Q(2,1)
      EF(2)=C*Q(2,1)-S*Q(1,1)
      EF(3)=Q(3,1)
      EF(4)=C*Q(4,1)+S*Q(5,1)
      EF(5)=C*Q(5,1)-S*Q(4,1)
      EF(6)=Q(6,1)
      WRITE(9,200)M,(EF(I),I=1,6)
   50 CONTINUE
      WRITE(9,300)
      RETURN
  100 FORMAT(///27H BEAM AND COLUMN END FORCES/27H **********************
     1*****//8H ELEMENT,11X,5HAXIAL,13X,5HSHEAR,12X,6HMOMENT,13X,5HAXIAL
     2,13X,5HSHEAR,12X,6HMOMENT//)
  200 FORMAT(1H ,I6,6E18.6)
  300 FORMAT(/1H ,25(1H*)///)
      END
      SUBROUTINE STRESS(R,IE,X,Y,XFORCE,YFORCE,MAXNEQ,MAXEL,MAXNP,ND)
      IMPLICIT REAL*8 (A-H,O-Z)
      COMMON/DATA/ NEL,NMAT(6),NEL1(6),NOPT,NBODY,KMAS,MODIF,NBN,NELT
      COMMON/FRE/NT(700)
      COMMON/TEMP/IDF(700),NNP
      DIMENSION R(MAXNEQ),IE(MAXEL,5),X(MAXNP),Y(MAXNP),ND(MAXNP)
      DIMENSION XFORCE(MAXNP),YFORCE(MAXNP),SHEAR(1250)
      DIMENSION CB(3,8),TCB(12,8),EDIS(8,1),STRES(3,1)
      REWIND 8
      DO5K=1,MAXNP
      XFORCE(K)=0.0
      YFORCE(K)=0.0
      ND(K)=0
      SHEAR(K)=0.0
    5 CONTINUE
      DO60M=1,NEL1(1)
      DC20J=1,4
      NN=IE(M,J)
      EDIS(2*J-1,1)=R(IDF(NN)+1)
      EDIS(2*J,1)=R(IDF(NN)+2)
   20 CONTINUE
      MTYP=IE(M,5)
      INDX=0
      IF(INDX.EQ.2) WRITE(9,200) M
      READ(8) MM,((TCB(I,J),J=1,8),I=1,12)
      IF(M.NE.MM) WRITE(9,1030) M,MM
      IF(M.NE.MM) RETURN
      DC30I=1,4
      NN=IE(M,I)
      DC25KK=1,3
      I1=KK+3*(I-1)
      DC25LL=1,8
   25 CB(KK,LL)=TCB(I1,LL)
      CALL MATMUL(3,8,1,CB,EDIS,STRES)
      IF(INDX.EQ.2) WRITE(9,100) NN,(STRES(J,1),J=1,3)
  100 FORMAT(10X,I5,3E20.8)
  200 FORMAT(/15X,'STRESSES IN THE ELEMENT NO.= ',I5,//11X,'NODE',
     112X,'X-STRESS',12X,'Y-STRESS',8X,'SHEAR-STRESS')
      XFORCE(NN)=XFORCE(NN)+STRES(1,1)
      YFORCE(NN)=YFORCE(NN)+STRES(2,1)
      SHEAR(NN)=SHEAR(NN)+STRES(3,1)
      ND(NN)=ND(NN)+1
   30 CONTINUE
   60 CONTINUE
      WRITE(9,300)
      NOLINE=48
      DC80K=1,NNP
      IF(NT(K).EQ.2)GOTO80
      XFORCE(K)=XFORCE(K)/ND(K)
      YFORCE(K)=YFORCE(K)/ND(K)
      SHEAR(K)=SHEAR(K)/ND(K)
      SP=(XFORCE(K)+YFORCE(K))/2.0
      SM=(XFORCE(K)-YFORCE(K))/2.0
      SQ=SM**2+SHEAR(K)**2
      DS=SQRT(SQ)
      SIG1=SP+DS
      SIG2=SP-DS
      ALFA=0.5*ATAN(SHEAR(K)/SM)
      ALFA=ALFA*180.0/3.141592654
      IF(X(K).EQ.0.AND.K.GT.1) WRITE(9,400)
      WRITE(9,1010) K,X(K),Y(K),XFORCE(K),YFORCE(K),SHEAR(K),SIG1,SIG2,
     *ALFA
      IF(NOLINE.EQ.0) WRITE(9,1000)
      IF(NOLINE.EQ.0) NOLINE=50
      NOLINE=NOLINE-1
   80 CONTINUE
      WRITE(9,400)
  300 FORMAT(1H1,//'****OUTOUT TABLE 3. STRESSES ON EACH NODE****'/
     */2X,7H  NODE ,8X,1HX,9X,1HY,6X,8HSIGMA(X),6X,8HSIGMA(Y),6X,
     28HTAU(X,Y),6X,8HSIGMA(1),6X,8HSIGMA(2),9X,5HANGLE)
  400 FORMAT(4X,'**************************************************')
 1000 FORMAT(1H1,7H  NODE ,9X,1HX,9X,1HY,6X,8HSIGMA(X),6X,8HSIGMA(Y),
     16X,8HTAU(X,Y),6X,8HSIGMA(1),6X,8HSIGMA(2),5HANGLE)
 1010 FORMAT(I8,2F10.2,6E14.6)
 1020 FORMAT(/53HOUTPUT TABLE NO 3. STRAINS AT THE ELEMENT CENTROIDS //
     *1X,7HELEMENT,7X,13HX-DIRE STRAIN,7X,13HY-DIRE STRAIN,8X,
     *12HSHEAR STRAIN)
 1030 FORMAT(//15X,'**** ELEMENT STRESS-DISPLACEMENT MATRIX ON TAPE'
     *'NO.8 WAS WRONG',5X,'XXXXM= ',I5,5X,'XXXXMM = ',I5,//)
      RETURN
      END
```

```
      SUBROUTINE DATAIN(MAXEL,MAXNP,MAXMAT,ISTOP)
      IMPLICIT REAL*8 (A-H,O-Z)
      COMMON/DISP/X(700),Y(700),ULX(700),VLY(700),KODE(700),NBOUN
      COMMON/DATA/NEL,NMAT(6),NEL1(6),NOPT,NBODY,KMAS,MODIF,NBN,NELT
      COMMON/NODE/IE(600,5)
      COMMON/PROTY/ALEN(30),E(30),PR(30),RO(30),TH(30),IP(30),IGSH
      COMMON/FRE/NT(700)
      COMMON/TEMP/IDF(700),NNP
      ISTOP=0
      READ(5,*)NNP,NBOUN,NBODY
      READ(5,*)(NEL1(I),I=1,NELT)
      READ(5,*)(NMAT(I),I=1,NELT)
      NMATS=0
      NEL=0
      DO 10 I=1,NELT
      NMATS=NMATS+NMAT(I)
   10 NEL=NEL+NEL1(I)
      IF(NNP.LE.MAXNP)GOTO 20
      ISTOP=ISTOP+1
   20 WRITE(9,1020)NNP
      IF(NEL.LE.MAXEL)GOTO30
      ISTOP=ISTOP+1
   30 WRITE(9,1030)NEL
      IF(NMATS.LE.MAXMAT)GOTO40
      ISTOP=ISTOP+1
   40 WRITE(9,1040)NMATS
      WRITE(9,1050)NBODY
C
C     NODAL POINT DATA
C
      WRITE(9,1060)
      READ(5,*)(K,X(K),Y(K),ULX(K),VLY(K),NT(K),J=1,NNP)
      WRITE(9,1080)(J,X(J),Y(J),ULX(J),VLY(J),NT(J),J=1,NNP)
C
C     ELEMENT CONFIGURATION AND TYPE
C
      M=1
C
C     QUADRILATERAL ELEMENTS
C
      IF(NEL1(1).LT.1)GOTO 70
      WRITE(9,1100)
      READ(5,*)MODIF,NOPT
      IF(MODIF.NE.0)WRITE(9,1120)
      WRITE(9,1130)NOPT
      WRITE(9,1090)
      DO 50 J=1,NEL1(1)
      READ(5,*)(IE(M,I),I=1,5)
      WRITE(9,1150)M,(IE(M,I),I=1,5)
   50 M=M+1
      WRITE(9,1160)
      DO 60 J=1,NMAT(1)
      READ(5,*)I,E(I),PR(I),RO(I),TH(I)
   60 WRITE(9,1180)I,E(I),PR(I),RO(I),TH(I)
C
C     LINE ELEMENTS
C
   70 CONTINUE
      IF(NEL1(2).LT.1)GOTO 100
      WRITE(9,1190)
      READ(5,*)IGSH
      IF(IGSH.EQ.1)WRITE(9,1140)
      WRITE(9,1090)
      DO 80 J=1,NEL1(2)
      READ(5,*)(IE(M,I),I=1,2),IE(M,5)
      WRITE(9,1200)M,(IE(M,I),I=1,2),IE(M,5)
   80 M=M+1
      WRITE(9,1210)
      DO 90 J=1,NMAT(2)
      READ(5,*)I,E(I),PR(I),RO(I),TH(I),ALEN(I)
   90 WRITE(9,1180)I,E(I),PR(I),RO(I),TH(I),ALEN(I)
C
C     JOINT CONSTRAINT ELEMENTS
C
  100 CONTINUE
      IF(NEL1(3)+NEL1(4).LE.0)GOTO 140
      READ(5,*)NBN
      IF(NEL1(3).LT.1)GOTO 120
      WRITE(9,1220)
      IF(NBN.LT.1)WRITE(9,1300)
      WRITE(9,1090)
      DO 110 J=1,NEL1(3)
      READ(5,*)(IE(M,I),I=1,3)
      WRITE(9,1230)M,(IE(M,I),I=1,3)
  110 M=M+1
  120 CONTINUE
      IF(NEL1(4).LT.1)GOTO140
      WRITE(9,1240)
      IF(NBN.LT.1)WRITE(9,1300)
      WRITE(9,1090)
      DO 130 J=1,NEL1(4)
      READ(5,*)(IE(M,I),I=1,3)
      WRITE(9,1230)M,(IE(M,I),I=1,3)
  130 M=M+1
C
C     TYPE 2 JOINT
C
  140 IF(NEL1(5).LE.0)GOTO 160
      WRITE(9,1310)
      WRITE(9,1090)
      DO 150 J=1,NEL1(5)
      READ(5,*)(IE(M,I),I=1,5)
      WRITE(9,1150)M,(IE(M,I),I=1,5)
  150 M=M+1
      WRITE(9,1340)
      DO 155 J=1,NMAT(5)
      READ(5,*)I,E(I),IP(I),PR(I)
  155 WRITE(9,1360)I,E(I),IP(I),PR(I)
C
C     RECTANGULAR BEAM ELEMENT
```

```
C
  160 IF(NEL1(6).LE.0)GOTO 190
      WRITE(9,1320)
      WRITE(9,1090)
      DO 170 J=1,NEL1(6)
      READ(5,*)(IE(M,I),I=1,5)
      WRITE(9,1150)M,(IE(M,I),I=1,5)
  170 M=M+1
      WRITE(9,1160)
      DO 180 J=1,NMAT(6)
      READ(5,*)I,E(I),PR(I),RO(I),TH(I)
  180 WRITE(9,1180)I,E(I),PR(I),RO(I),TH(I)
  190 CONTINUE
C
C     BOUNDARY CONDITIONS
C
      WRITE(9,1250)
      DO 200 J=1,KNP
  200 KODE(J)=0
      DO 210 J=1,NBOUN
      READ(5,*)I,KODE(I)
      IF(KODE(I).EQ.1)WRITE(9,1280)I
      IF(KODE(I).EQ.2)WRITE(9,1260)I
      IF(KODE(I).EQ.3)WRITE(9,1270)I
  210 CONTINUE
      RETURN
 1020 FORMAT(1H ,8X,25HNUMBER OF NODAL POINTS = ,I6/)
 1030 FORMAT(1H ,12X,21HNUMBER OF ELEMENTS = ,I6/)
 1040 FORMAT(1H ,6X,27HNUMBER OF MATERIAL TYPES = ,I6/)
 1050 FORMAT(1H ,2X,31HBODY FORCES (1=Y-DIR)(0=NONE) = ,I6/)
 1060 FORMAT(//1H ,9X,5HNODAL,8X,1HX,13X,1HY,14X,1HX,12X,1HY,4X,4HTYPE/
     1 1H ,9X,5HPOINT,6X,5HCCORD,9X,5HCOORD,10X,5HFORCE,8X,5HFORCE//)
 1080 FORMAT(1H ,10X,I3,6X,F9.2,5X,F9.2,4X,F8.2,5X,F8.2,I6)
 1090 FORMAT(/1H ,8X,7HELEMENT,20X,5HNODES/
     1 1H ,10X,3HNO.,5X,1H1,6X,1H2,6X,1H3,6X,1H4,6X,4HTYPE/)
 1100 FORMAT(////23H QUADRILATERAL ELEMENTS/)
 1120 FORMAT(17H NOM - CONFORMING/)
 1130 FORMAT(1H ,1X,32H(1PLANE STRAIN)(2PLANE STRESS) = ,I6/)
 1140 FORMAT(/' LINE ELEMENTS INCLUDE SHEAR DEFLECTIONS'/)
 1150 FORMAT(1H ,6X,5(4X,I3),3X,I3)
 1160 FORMAT(//1H ,8X,8HMATERIAL,6X,7HELASTIC,12X,8HPOISSONS/
     1 1H ,10X,3HNO.,9X,7HMODULUS,14X,5HRATIO,8X,7HDENSITY,7X,9HTHICKNES
     2S/)
 1180 FORMAT(10X,I2,5X,E14.5,4X,E14.5,6X,E9.3,7X,E9.3,7X,F8.2)
 1190 FORMAT(////14H LINE ELEMENTS/)
 1200 FORMAT(1H ,6X,3(4X,I3),17X,I3)
 1210 FORMAT(//1H ,8X,8HMATERIAL,6X,7HELASTIC ,12X,6HMOMENT,23X,9HX-SECT
     1ION,7X,5HADDED/1H ,10X,3HNO.,9X,7HMODULUS,12X,7HOF AREA,8X,7HDENSI
     2TY,9X,4HAREA,10X,6HLENGTH/)
 1220 FORMAT(////28H HORIZONTAL JOINT CONSTRAINT/)
 1230 FORMAT(1H ,6X,4(4X,I3),10X,I3)
 1240 FORMAT(////26H VERTICAL JOINT CONSTRAINT/)
 1250 FORMAT(////1H ,9X,5HNODAL,5X,6HFIXITY/1H ,9X,5HPOINT,5X,4HHORZ,2X,
     14HVERT,2X,3HROT/)
 1260 FORMAT(1H ,10X,I3,2X,2(5X,1HX))
 1270 FORMAT(1H ,10X,I3,2X,3(5X,1HX))
 1280 FORMAT(1H ,10X,I3,13X,1HX)
 1300 FORMAT(/26H NEGLECTING B-N HYPOTHESIS/)
 1310 FORMAT(////13H TYPE 2 JOINT/)
 1320 FORMAT(////25H RECTANGULAR BEAM ELEMENT/)
 1340 FORMAT(//9X,8HMATERIAL,7X,5HYIELD,8X,8HYIELDING,6X,15HC = NOT ALLC
     1WED,6X,17HPERCENT STIFFNESS/11X,3HNO.,10X,6HMOMENT,7X,7HALLOWED,7X
     2,11H1 = ALLOWED,13X,11HAFTER YIELD/)
 1360 FORMAT(10X,I2,5X,F14.2,7X,I2,35X,F4.1)
      END
      SUBROUTINE EIGEN(AA,V,NMAX,NBAND,KMAS,GACC)
      IMPLICIT REAL*8 (A-H,O-Z)
C FREE VIBRATION ANALYSIS : COMPUTE FREQUENCIES AND MODE SHAPES
      COMMON/VECTOR/VV(1400,5),FM(1400)
      COMMON/TWO/ IBAND,NEQ
      DIMENSION AA(NMAX,NBAND),V(NMAX)
      DIMENSION BN(100),FQ(10)
      NFQ=0
      IFQ=5
      WRITE(9,5)
      IF(KMAS.EQ.0) WRITE(9,20)
      IF(KMAS.GT.0) WRITE(9,30)
      READ(5,*) NEIG,NSPUM
    1 NFQ=NFQ+1
      READ(5,*) W,DW,EPS,NDEG
      WRITE(9,15) W,DW,EPS,NDEG
      CALL FOOT(W,DW,EPS,AA,BN,NMAX,NBAND)
      FREQ1=SQRT(W)
      FREQ2=FREQ1/(2.0*3.141592654)
      FQ(NFQ)=1.0/FREQ2
      WRITE(9,40) W,FREQ1,FREQ2
      CALL VECT(W,AA,V,BN,NMAX,NBAND,NEQ,IBAND,NDEG)
      DO3I=1,NEQ
    3 VV(I,NFQ)=V(I)
      IF(NFQ.LT.NEIG) GOTO 1
      IF(NSPUM.EQ.0) RETURN
      REWIND 2
      DO4I=1,NEQ
      READ(2)(BN(J),J=1,IBAND)
    4 FM(I)=BN(1)
      CALL SPTRUM(FQ,VV,FM,V,KMAX,NEQ,NFQ,IFQ,GACC)
    5 FORMAT(1H1,15X,'***** DYNAMIC PROBLEM OF FREE VIBRATION ****'//)
   15 FORMAT(//15X,'W = ',F15.3,5X,'DW = ',F10.3,5X,'EPS = ',F10.6//15X,
     *'NDEG = ',I10//)
   20 FORMAT(//16X,'**** LUMPED MASS MATRIX WAS USED ****',//)
   30 FORMAT(//16X,'***** CONSISTENT MASS MATRIX WAS USED ****',//)
   40 FORMAT(//10X,'EIGEN VALUE = ',E20.8,//12X,'FREQUENCY = ',F16.8,  5
     *X,'(RAD/SEC)',//12X,'FREQUENCY = ',F16.8,5X,' (CYCLES/SEC)'//)
      RETURN
      END
      SUBROUTINE ROOT(W,DW,EPS,AA,BN,NMAX,NBAND)
      IMPLICIT REAL*8 (A-H,O-Z)
      COMMON/TWO/ IBAND,NEQ
      DIMENSION AA(NMAX,NBAND),BN(NBAND)
      NPATH=1
```

```
      CALL FUNCT(A,W,AA,BN,NMAX,NBAND,NPATH)
    8 DW=DW+W
      CALL FUNCT(B,DW,AA,BN,NMAX,NBAND,NPATH)
      IF(A*B) 6,10,7
    7 W=W+DW
      A=B
      IF(NPATH.EQ.2)GOTO 6
      DW=DW*1.0
      GOTO 8
    6 DW=DW/2.0
      NPATH=2
      DELT=ABS(DW)
      IF(DELT-EPS) 11,11,8
   10 WRITE(9,20) A,B,W,DW
   20 FORMAT(//15X,'A= ',E20.8,'B= ',E20.8,'W= ',E20.8,'DW= ',E20.8/)
   11 CONTINUE
      RETURN
      END
      SUBROUTINE FUNCT(DET,W,AA,BN,NMAX,NBAND,NPATH)
      IMPLICIT REAL*8 (A-H,O-Z)
      COMMON/TWO/ IBAND,NEQ
      DIMENSION AA(NMAX,NBAND),BN(NBAND)
      REWIND 1
      READ(1) ((AA(I,J),J=1,IBAND),I=1,NEQ)
      REWIND 2
      DO10I=1,NEQ
      READ(2) (BN(J),J=1,IBAND)
      DO10K=1,IBAND
   10 AA(I,K)=AA(I,K)-W*BN(K)
      CALL HFDET(AA,BN,NMAX,NBAND,DET,RS)
      WRITE(6,30) W,DET,RS
   30 FORMAT(/15X,'W =',E20.8,10X,'DET =',F4.1,10X,F15.5)
      RETURN
      END
      SUBROUTINE HFDET(AA,BN,NMAX,NBAND,DET,RS)
C
C     CALCULATE THE SIGN AND APPROX VALUE OF THE DETERMINANT OF MATRIX AA
C                              METHOD
C
      IMPLICIT REAL*8 (A-H,O-Z)
      COMMON/TWO/ IBAND,NEQ
      DIMENSION AA(NMAX,NBAND),BN(NBAND)
      N=0
      DET=1.0
      RS=0.0
  100 N=N+1
      ERR=ABS(AA(N,1))
      IF(ERR.LT.1.0E-12) GOTO 600
      DET=DET*AA(N,1)
C
C     ABSOLUTE VALUE OF DET (APPROXIMATE)
C
      RS=RS+DLOG10(ERR)
C
      DET=DET/ABS(DET)
      IF(N-NEQ) 150,300,150
  150 CONTINUE
      DO200K=2,IBAND
      BN(K)=AA(N,K)
  200 AA(N,K)=AA(N,K)/AA(N,1)
      DO260L=2,IBAND
      I=N+L-1
      IF(NEQ-I) 260,240,240
  240 J=0
      DO250K=L,IBAND
      J=J+1
  250 AA(I,J)=AA(I,J)-BN(L)*AA(N,K)
  260 CONTINUE
      GOTO 100
  300 CONTINUE
      GOTO 500
  600 DET=0.0
  500 RETURN
      END
      SUBROUTINE VECT(W,AA,V,BN,NMAX,NBAND,N,NBH,NDEG)
      IMPLICIT REAL*8 (A-H,O-Z)
      COMMON/TWO/ IBAND,NEQ
      COMMON/FRE/NT(700)
      COMMON/TEMP/IDF(700),PNP
      DIMENSION AA(NMAX,NBAND),BN(NBAND),V(NMAX)
      REWIND 1
      REWIND 2
      READ(1) ((AA(I,J),J=1,IBAND),I=1,NEQ)
      DO10I=1,NEQ
      READ(2) (BN(J),J=1,IBAND)
      DO10K=1,IBAND
   10 AA(I,K)=AA(I,K)-W*BN(K)
      DO30I=1,NMAX
   30 V(I)=0.0
      IJ=NDEG
      DO40J=1,IBAND
      IJJ=IJ-IBAND+J
      IF(IJJ.LE.0) GOTO 50
      IBW=IBAND-J+1
      V(IJJ)=-AA(IJJ,IBW)
      AA(IJJ,IBW)=0.0
   50 CONTINUE
      V(IJ+J-1)=-AA(IJ,J)
   40 AA(IJ,J)=0.0
      AA(IJ,1)=1.0
      V(IJ)=1.0
      CALL BANSOL(0,AA,V,NEQ,IBAND,NMAX,NBAND)
C
C     ****NORMALISATION ****
C
C     FIND LARGEST DISPLACEMENT
C
      VMAX=V(1)
      DO60I=1,NNP
      IF(NT(I).EQ.4)GOTO 60
```

```
      DO60J=1,2
      IJ=IDF(I)+J
      IF(ABS(V(IJ)).GT.ABS(VMAX)) VMAX=V(IJ)
   60 CONTINUE
C
C     DIVIDE BY LARGEST DISPLACEMENT
C     PRINT EIGENVECTOR     (MODE SHAPE)
C
      WRITE(9,80)
      DO70I=1,NNP
      II=NNP+1-I
      L=IDF(II)+1
      VNORX=V(L)/VMAX
      VNORY=V(L+1)/VMAX
      IF(NT(II).GT.1)GOTO20
      WRITE(9,81)II,V(L),V(L+1),VNORX,VNORY
      GOTO23
   20 VNORR=V(L+2)/VMAX
      IF(NT(II).EQ.4)GOTO21
      WRITE(9,82)II,V(L),V(L+1),V(L+2),VNORX,VNORY,VNORR
      GOTO22
   21 WRITE(9,83)II,V(L),V(L+1),V(L+2),VNORX,VNORY,VNORR
   22 V(L+2)=VNORR
   23 V(L)=VNORX
      V(L+1)=VNORY
   70 CONTINUE
      WRITE(9,100)
C
C     OUTPUT MODE SHAPE TO SEPERATE FILE
C
      WRITE(10,1000)(V(I),I=1,NEQ)
 1000 FORMAT(5E15.8)
   80 FORMAT(1H1,4X,'NODE',11X,'******UNNORMALISED*****',30X,'******NORM
     *ALISED******'/)
   81 FORMAT(3X,I5,2X,2F18.8,20X,2F18.8)
   82 FORMAT(3X,I5,2X,2F18.8,F20.8,3F18.8)
   83 FORMAT(3X,I5,2X,2F18.8,' LLL',E12.5,'LLI ',2F18.8,' LLL',E12.5,'LL
     CL')
  100 FORMAT(5X,'END**************************************************')
   90 RETURN
      END
      SUBROUTINE SPTRUM(W,VV,PM,V,NMAX,NEQ,NFQ,IFQ,GACC)
      IMPLICIT REAL*8 (A-H,O-Z)
      COMMON/DISP/X(700),Y(700),ULX(700),VLY(700),KODE(700),NBOUN
      COMMON/FRE/NT(700)
      COMMON/TEMP/IDF(700),NNP
      DIMENSION VV(NMAX,IFQ),V(NMAX),PM(NMAX)
      DIMENSION W(10),TITLE(10),P(10),PP(10),SA(10),Z(10),SP(2,50)
      DIMENSION TV(10),TF(10),TQ(10),PAVE(10)
      DIMENSION YBAR(10),TFORC(10),CNT(10)
      READ(5,90) TITLE
C
C     MODE:- 0 DONT PRINT RESULTS FOR EACH MODE
C            1 DO PRINT RESULTS ...
C     NEC :- NUMBER OF DATA POINTS FOR E-Q ACCELERATION SPECTRUM
C     SF  :- SCALLING FACTOR FOR E-Q DATA
C     DAP :- DAMPING
C     SE  :- ACCELERATION SPECTUM
C
      READ(5,100) MODE,NPC,SF,DAP
      READ(5,110) (SP(1,I),SP(2,I),I=1,NPC)
      WRITE(9,120) TITLE,NPC,SF,DAP,GACC
      WRITE(9,130) (SP(1,I),SP(2,I),I=1,NPC)
      DO40N=1,NFQ
      P(N)=0.0
      PP(N)=0.0
      DO10J=1,NEQ
   10 PP(N)=PP(N)+VV(J,N)**2*PM(J)
      DO15J=1,NNP
      I=IDF(J)+1
   15 P(N)=P(N)+VV(I,N)*PM(I)
      WW=(2.0*3.141592654/W(N))**2
      T=W(N)
C
C     INTERPOLATION OF ACCELERATION SPECTRUM DATA
C
      DO20I=2,NPC
      T1=SP(1,I-1)
      T2=SP(1,I)
      SE1=SP(2,I-1)
      SE2=SP(2,I)
      IF(T.LT.T2) GO TO 30
   20 CONTINUE
   30 RT1=(T2-T)/(T2-T1)
      RT2=(T-T1)/(T2-T1)
      SA(N)=SF*GACC*(SE1*RT1+SE2*RT2)
      Z(N)=P(N)*SA(N)/(PP(N)*WW)
   40 CONTINUE
C
C     MODE   PERIOD   ACC.SPECTRA   PARTICIPATION FACTOR
C
      WRITE(9,220) (J,W(J),SA(J),P(J),J=1,NFQ)
      WRITE(9,160)
C
C     CALCULATE FORCES IN STRUCTURE
C
      NI=3
      II=NNP
      IF(NT(II).EQ.1)NI=2
      DO42K=1,NFQ
      PAVE(K)=0.0
      YBAR(K)=0.0
   42 TFORC(K)=0.0
      FORC=0.0
      SFORC=0.0
      AMONT=0.0
      DO50IK=1,NEQ
      I=NEQ+1-IK
      V(I)=0.0
      IF(NI.LT.4)GOTO25
```

```
      II=II-1
      NI=1
      IF(NT(II).EQ.1)NI=2
25    DO45N=1,NPQ
      TV(N)=Z(N)*VV(I,N)
      TF(N)=PM(I)*VV(I,N)*P(N)*SA(N)/EP(N)
45    V(I)=V(I)+TV(N)**2
      IF(MODE.NE.0) WRITE(9,170)  II,(TV(K),TF(K),K=1,NPQ)
      IF(NI.NE.3) GOTO 48
      DO46K=1,NPQ
46    FAVE(K)=FAVE(K)+TF(K)
      IF(X(II).NE.0.0) GOTO 46
      WRITE(9,200)  (FAVE(K),K=1,NPQ)
      DO47K=1,NPQ
      ONT(K)=TFORC(K)*YBAR(K)
      TFOEC(K)=TFORC(K)+FAVE(K)
47    CONTINUE
      DC 49 K=1,NPQ
      FORC=FORC+FAVE(K)**2
      SFORC=SFORC+TFORC(K)**2
      AMONT=AMONT+ONT(K)**2
      FAVE(K)=0.0
      IF(Y(II).EQ.0.0)GOTO49
      YBAR(K)=ONT(K)/TFORC(K)+Y(II)-Y(II-1)
49    CONTINUE
      FORC=SQRT(FORC)
      SFORC=SQRT(SFOEC)
      AMONT=SQRT(AMONT)
      WRITE(9,190)Y(II),FORC,SFORC,AMONT
      FCRC=0.0
      SFORC=0.0
      AMONT=0.0
46    CONTINUE
      NI=NI+1
50    V(I)=SQRT(V(I))
      Q=0.0
      DO60I=1,NPQ
      TQ(I)=P(I)**2*SA(1)/PP(I)
60    Q=Q+TQ(I)**2
      Q=SQRT(Q)
      NN=NEQ/2
      WRITE(9,140)  Q,(I,TQ(I),I=1,NPQ)
90    FORMAT(10A8)
100   FORMAT(2I5,2F10.5)
110   FORMAT(8F10.3)
120   FORMAT(1H1,10X,'**** ACCELERATION SPECTRUM ANALYSIS ****'//
     *5X,10A8//5X,'*** NUMBER OF PERIOD CARDS =',I5,5X,'**** SCALE
     *FACTOR =',F10.5,//5X,'**** DAMPING FACTOR =',F10.5,5X,'*** GROUND
     * ACC. =',F15.5 // )
130   FORMAT(5X,'****ACCELERATION SPECTRUM DATA ****',/5X,'*** PERIOD',5
     *X,'***ACCELERATION',//(5X,F10.3,6X,F15.5))
140   FORMAT(//5X,'****MAXIMUM BASE SHEAR FORCE =',F15.5,//(I10,F15.5,I10
     *,F15.5,I10,F15.5)//)
160   FORMAT(//10X,'THE DISTRIBUTION OF MAXIMUM DISPLACEMENT AND MAXIMUM
     * EFFECTIVE EARTHQUAKE FORCES IN EACH MODE',//3X,'MODE',16X,
     *'*FIRST MODE',25X,'SECOND MODE',26X,'THIRD MODE',/2X,'NUMBER',
     *10X,'DISP.',14X,'FORCES',11X,'DISP.',14X,'FORCES',11X,'SHEISP.',8X,'
     *FORCES',//)
170   FORMAT(I5,5X,(6F18.8))
190   FORMAT(//10X,'***HEIGHT =',F17.5,9X,'***SECTION FORCE =',F20.8,/
     *5X,'***TOTAL FORCE =',F20.8,5X,'***TOTAL MOMENT =',F20.8/)
200   FORMAT(2X,16HTOTAL HORIZONTAL,10X,3(F18.8,18X))
220   FORMAT(//5X,'MODE',4X,'PERIOD',3X,'ACC. SPECTRA',5X,'PARTICIPATION
     * FACTOR',//(I9,F10.5,F15.5,F20.5))
      RETURN
      END
      SUBROUTINE RESPON(MAXDCP,MAXEI,MAXNE,NEQ,IBAND,GACC,MAXDW,NDYNAM)
      IMPLICIT REAL*8 (A-H,O-Z)
C
C     !!! NEWMARK BETA INTEGRATION !!!
C
      COMMON/DAMP/C1,C2,DT,NF
      COMMON/NODE/IE(600,5)
      COMMON/DATA/ NEL,NMAT(6),NEL1(6),NCFT,NEQDX,KMAS,MODIF,MEN,NEL1
      COMMON/THREE/E(1400),AR(1400,4C)
      COMMON/DISP/X(700),ULX(7CC),VLX(733),KODE(70C),NECON
      COMMON/PROPY/ALEN(30),E(30),FR(30),FO(30),TH(30),IE(30),IGSH
      COMMON/FREE/NT(700)
      COMMON/TEMP/IDF(730),XNF
      COMMON/OUT/U1(1400),V1(1400),A1(1400)
      DIMENSION CH(700),CV(700)
      DIMENSION BN(40),E(3,350),TNEE(5,2)
      DIMENSION AMS(1400),AA(1400),BB(1400),QK(12,12),Q(12)
      DIMENSION BSV(1400),STS(50,50),EXM(53),FHS(50),SOL(50,5C)
      LOGICAL SLIP(50)
      LOGICAL REPEAT
      NX=IDF(NNP)+1
C
C     READ STIFFNESS MATRIX AND DIAGONALS OF MASS MATRIX
C
      REWIND 1
      READ(1) ((AK(I,J),J=1,IBAND),I=1,NEQ)
      REWIND 2
      DO5I=1,NEQ
      READ (2)  (BN(J),J=1,IBAND)
      AMS(I)=BN(1)
5     CONTINUE

      INT   :- 0  INITIAL CONDITIONS ALL ZERO
               1  DISPLACEMENT AND VELOCITY GIVEN
               2  ACCELERATION ALSO GIVEN
      MPRINT:- THE STEP AT WHICH RESULTS ARE PRINTED
      NSTEP :- THE TOTAL NUMBER OF STEPS
      MAXSTP:- THE STEP AT WHICH D V & A ARE STORED
      NTYP  :- 0  FORCING FUNCTION
               1  GROUND ACCELERATION
      NF    :- NUMBER OF DATA POINTS DESCRIBING FORCING FUNCTION OR ACCE

      READ(5,13) INT,NPRINT,NSTEP,MAXSTP,NTYP,NP
      READ(5,50) C1,C2,DELT,DT,TIME,SF
```

```
C
C     NFIX  :- NO. OF BASE NODES,OR = NNP TO READ IN FORCE VECTOR
C     NVEC  :- 10  HORIZONTAL FORCING
C              01  VERTICAL
C              11  BOTH
C     MSPAC :- NODAL SPACING OF PRINTED RESULTS
C     MSTRS :- 0  NO FORCES PRINTED
C              1  BEAM & COLUMN FORCES
C              2  & QUAD ELEMENT FORCES,STRESSES
C     NEED  :- NO. OF TIME INTERVALS DURING WHICH FORCES ARE PRINTED
C
      READ(5,10) NFIX,NVEC,MSPAC,MSTRS,NEED
      IF(MSTRS.EQ.0) GOTO 15
      READ(5,60) (TNED(I,1),TNED(I,2),I=1,NEED)
   15 CONTINUE
C
C     INTEGRATION PARAMETERS
C
      BITA=0.25*(1.0+DELT)**2
      GAMA=0.5+DELT
      CON1=1.0+C1*GAMA*DT
      CON2=C2*GAMA*DT
      CON3=BITA*DT**2
      CON=CON2+CON3
C            *
C     FORM [K] AND TRIANGULARISE
C
      DO 250 I=1,NNP
      M=IDF(I)+1
      N=M+1
      IF(NT(I).NE.1)N=N+1
      DO 250 J=M,N
      DO 245 L=1,IBAND
  245 AK(J,L)=CON*AK(J,L)
  250 AK(J,1)=AK(J,1)+CON1*AMS(J)
C
C      ADD CONSTRAINT EQUATIONS
C
      IF(NEL1(4).LE.0)GOTO 253
      M=NEL1(1)+NEL1(2)+NEL1(3)
      DO 252 J=1,NEL1(4)
      M=M+1
      ZZ=X(IE(M,3))-X(IE(M,1))
      CALL JOINTV(QK,Q,ZZ,NBN)
  252 CALL ADDS(3,9,M,QK,Q)
  253 IF(NEL1(5).LE.0)GOTO 257
      IS=NEL1(1)+NEL1(2)+NEL1(3)+NEL1(4)+1
      IT=IS+NEL1(5)-1
      DO 255 M=IS,IT
      CALL CONECT(M,NDYNAM)
  255 CONTINUE
  257 CONTINUE
      CALL BANSOL(1,AK,B,NEQ,IBAND,MAXDOF,MAXBW)
      REWIND 2
      WRITE (2) ((AK(I,J),J=1,IBAND),I=1,NEQ)
      IF(NEL1(5).LE.0)GOTO 258
      REWIND 1
      READ (1) ((AK(I,J),J=1,IBAND),I=1,NEQ)
      DO 254 M=IS,IT
      CALL CONECT(M,NDYNAM)
  254 CONTINUE
  258 CONTINUE
C
C *** SET UP FORCE VECTORS
C
      DO20I=1,NNP
      CH(I)=0.0
      CV(I)=0.0
      IF(I.LE.NFIX) GOTO 20
      IF(NVEC.EQ.11.OR.NVEC.EQ.10) CH(I)=1.0
      IF(NVEC.EQ.11.OR.NVEC.EQ.01) CV(I)=1.0
   20 CONTINUE
      IF(NTYP) 22,24,22
   22 DO23N=1,NNP
      I=IDF(N)+1
      CH(N)=-CH(N)*GACC*AMS(I)
   23 CV(N)=-CV(N)*GACC*AMS(I+1)
   24 CONTINUE
      IF(NFIX.LT.NNP) GO TO 26
C
C     EXTERNAL FORCE
C
      READ(5,10) NVC
      DO25I=1,NVC
   25 READ(5,90) II,CH(II),CV(II)
   26 CONTINUE
C
C     FORCE FUNCTION OR ACCELERATION
C
      DO 27 J=1,NP
      READ(5,1000)(P(I,J),I=1,3)
      P(2,J)=P(2,J)*SF
      P(3,J)=P(3,J)*SF
   27 CONTINUE
C
C     SET UP INITIAL D V & A
C
      IF(INT.EQ.0) GOTO 100
      READ(3,30) (U1(I),I=1,NEQ)
      READ(3,30) (V1(I),I=1,NEQ)
      IF(INT.EQ.1) GOTO 120
      READ(3,30) (A1(I),I=1,NEQ)
      GOTO 215
  100 DO110I=1,NEQ
      U1(I)=0.0
  110 V1(I)=0.0
C
C     CALCULATE A FROM D & V
C
  120 CONTINUE
```

```
C
C     DATA CHECKING OUTPUT
C
      WRITE(3,300)
      IF(KMAS.EQ.0) WRITE(9,335)
      IF(KMAS.GT.0) WPITE(9,310)
      IF(NTXP.EQ.0) WRITE(9,317)
      IF(NTXP.GT.0) WPITE(9,318)
      WRITE(9,315) INT,NPRINT,NSTEP,NTXP,NP
      WRITE(9,320) DT,GAMA,BITA,DELT,C1,C2,GACC
      IF(MSTRS.EQ.0)GOTC 240
      WRITE(9,335) (I,TNED(I,1),TNED(I,2),I=1,NEED)
240   WRITE(9,325) ( I,CH(I),CV(I),I=1,NNP)
      WRITE(9,330) (J,P(1,J),F(2,J),F(3,J),J=1,NP)
      WRITE(9,400) TIME
      CALL OPUT(1)
      WRITE(9,95)
      WRITE(9,340)
340   FORMAT(7X,4HSTEP,14X,4HTIME,21X,6HX-DISP,20X,6HY-DISP//)
300   FORMAT(1H1,15X,'**** THE FORCED RESPONSE PROBLEM *****',//15X,'**
     *******NEWMARK BETA METHOD ****** *',//)
305   FORMAT(///15X,'*****LUMPED MASS MATRIX WAS USED ****'//)
310   FORMAT(///15X,'**** CONSISTENT MASS MATRIX USED **** ',///)
315   FORMAT(///10X,'** INC    ** DEFINT ** NSTEP  **NTXP    **NP ****',
     * // 6X,5I10)
317   FORMAT(///15X,'**** FORCING FUNCTION RESPONSE ANALYSIS ****'//)
318   FORMAT(///15X,' **** EARTHQUAKE RESPONSE HISTORY ANALYSIS ****'//)
320   FORMAT(///20X,'  TIME INTERVAL = ',F10.6,///15X,' GAMA = ',F10.5,3X,
     *' BETA = ',F10.5,3X,' DELT = ',F10.5,///15X,' CONST1 = ',F10.5,3X,
     *' CONST2 = ',F10.5,3X,' GACC = ',F10.5)
325   FORMAT(///10X,' **** FORCE VECTOR ****',//(I10,2F15.6))
330   FORMAT(///10X,'**** FORCE FUNCTION ****',//(I10,F10.4,2F15.6))
335   FORMAT(///10X,'**** FORCES AND STRESSES CALCULATED AT FOLLOWING TIM
     *E INTERVAL',//5X,'ELEM',16X,'FACM',18X,'TO',//I8,4X,2F20.5)
400   FORMAT(///15X,' INITIAL CONDITION AT TIME = ',F8.5//)
C
C     *** NEWMARK INTEGRATION
C
C     SLIP COEFFICIENTS MA.2
C
      REWIND 2
      READ (2)  ((AK(I,J),J=1,IBAND),I=1,NEQ)
      IF(NEL1(5).LE.0)GOTO 230
      REWIND 2
      READ (2)  ((AK(I,J),J=1,IDAMD),I=1,NEQ)
      M1=IS-1
      DO 226 I=1,NEL1(5)
      M1=M1+1
      ICF1=IDF(IE(M1,4))+3
      DC 221 J=1,NEQ
221   R(J)=0.0
      F(IOF1)=-1.0
      CALL BANSOL(2,AK,F,NEQ,IBAND,MA(DOF,AADM)
      M2=IS-1
      DC 225 K=1,NEL1(5)
      M2=M2+1
      ICF2=IDF(IE(M2,4))+3
      STS(I,K)=R(IOF2)
225   CONTINUE
226   CCNTINUE
230   CONTINUE
C
C     MODIFICATION FOR BI-LINEAR YIELDING
C
      M=IS-1
      DO 259 I=1,NEL1(5)
      M=M+1
      K1=IDF(IE(M,2))+3
      PS=PR(IE(M,5))
      QM=AK(K1,1)*PS/(100.0-ES)
      STS(I,I)=STS(I,I)+QM
255   CONTINUE
C
C     FOR EACH TIME STEP
C     FCAM EFFECTIVE LOAD VECTOR [F]
C
      KK=1
      LL=1
      DO280M1=1,NSTEP
      REPEAT=.FALSE.
      TIME=TIME+DT
      DC2801=1,NEQ
      AA(I)=V1(I)*(1.0-GAMA)*DT*A1(I)
260   RR(I)=U1(I)+DT*V1(I)+(0.5-BITA)*(DT**2)*A1(I)
```

```
C      DO 620 I=1,NNP
C      IF(NT(I).NE.4)GOTO 620
C      ICF=IDF(I)+1
C      DO 610 M=IOF,IOF+2
C      AA(M)=0.0
C  610 BB(M)=0.0
C  620 CONTINUE
       MF=N1-LL*NPRINT
       CALL LOAD(AMS,P,AA,BB,CH,CV,NEQ,IBAND,TIME)
C
C      CORRECT FOR CONSTRAINT EQUATIONS
C
       DO 265 I=1,NNP
       IF(NT(I).NE.4)GOTO 265
       JC=IDF(I)+1
       IF(NEL1(5).LE.0)GOTO 266
       R(JC+2)=0.0
   266 CONTINUE
       R(JC)=0.0
       R(JC+1)=0.0
   265 CONTINUE
C
C      SAVE LOAD VECTOR
C
       DO 267 I=1,NEQ
   267 RSV(I)=R(I)
C
C      SOLVE FOR ACCELERATION
C
       REWIND 2
       READ (2) ((AK(I,J),J=1,IBAND),I=1,NEQ)
       CALL BANSOL(2,AK,R,NEQ,IBAND,MAXDOF,MAXBW)
       CALL PMOM(N1,IS,NEL1(5))
C
C *** CHECK FOR SLIP AT JOINTS ***
C
       IF(NEL1(5).LE.0)GOTO 269
       DO 256 I=1,NEL1(5)
   256 SLIP(I)=.FALSE.
C
C      CHECK FOR YIELD VALUE EXCEEDED
C
       M=IS-1
       DO 501 I=1,NEL1(5)
       M=M+1
       IF(IP(IE(M,5)).EQ.0) GOTO 501
       IOF4=IDF(IE(M,4))+3
       EXM(I)=ABS(R(IOF4))-E(IE(M,5))
       IF(EXM(I).LT.0.0) GOTO 500
       SLIP(I)=.TRUE.
       REPEAT=.TRUE.
   500 IF(R(IOF4).LT.0.0) EXM(I)=-EXE(I)
   501 CONTINUE
C
C      SOLVE FOR YIELDING
```

```
C
       IF(.NOT.REPEAT) GOTO 269
   505 IC=0
       DO 520 I=1,NEL1(5)
       IF(.NOT.SLIP(I)) GOTO 520
       IC=IC+1
       JC=0
       DO 510 J=1,NEL1(5)
       IF(.NOT.SLIP(J)) GOTO 510
       JC=JC+1
       JP=JC-IC+1
       IF(JP.LT.1) GOTO 510
       SOL(IC,JP)=STS(I,J)
   510 CONTINUE
       RHS(IC)=EXM(I)
   520 CONTINUE
       CALL BANSOL(0,SOL,RHS,IC,IC,50,50)
C
C      CHECK FOR YIELD DIRECTION
C
       IC=0
       M=IS-1
       DO 530 I=1,NEL1(5)
       M=M+1
       IF(.NOT.SLIP(I)) GOTO 530
       IOF4=IDF(IE(M,4))+3
       IC=IC+1
       OK=SOL(IC,1)*RHS(IC)*R(IOF4)
       IF(OK.GE.0.0) GOTO 530
       SLIP(I)=.FALSE.
       WRITE(6,*)' DIRECTION',I
       GOTO 505
   530 CONTINUE
C
C      CHECK FOR NEW YIELDING
C
       M=IS-1
       DO 550 I=1,NEL1(5)
       M=M+1
       IF(IP(IE(M,5)).EQ.0) GOTO 550
       IF(SLIP(I)) GOTO 550
       IOF4=IDF(IE(M,4))+3
       AMOM=0.0
       IC=0
       DO 540 J=1,NEL1(5)
       IF(.NOT.SLIP(J)) GOTO 540
       IC=IC+1
       AMOM=AMOM-STS(I,J)*PHS(IC)
   540 CONTINUE
       AMOM=AMOM+R(IOF4)
       IF(ABS(AMOM).LE.E(IE(M,5))) GOTO 550
       SLIP(I)=.TRUE.
       WRITE(6,*) 'NEW',I
       GOTO 505
   550 CONTINUE
```

```
C
C     PUT RHS IN RSV
C
      M=IS-1
      IC=0
      DO 555 I=1,NEL1(5)
      M=M+1
      IF(.NOT.SLIP(I)) GOTO 555
      IC=IC+1
      IOF4=IDF(IE(M,4))+3
      RSV(IOF4)=RHS(IC)
  555 CONTINUE
C
C     USE MODIFIED LOAD VECTOR FOR NEW SOLUTION
C
      WRITE(10,1010)
 1010 FORMAT(7H REPEAT)
      DO 570 I=1,NEQ
  570 R(I)=RSV(I)
      CALL BANSOL(2,AK,R,NEQ,IBAND,MAXDOF,MAXBW)
      CALL PMOM(N1,IS,NEL1(5))
C
C     CALCULATE NEW D  V & A
C
  269 DO270I=1,NEQ
      U1(I)=U1(I)+DT*V1(I)+(0.5-BITA)*(DT**2)*A1(I)+BITA*(DT**2)*R(I)
      V1(I)=V1(I)+(1.0-GAMA)*DT*A1(I)+GAMA*DT*R(I)
      A1(I)=R(I)
  270 R(I)=U1(I)
C     DO 600 I=1,NNP
C     IF(NT(I).NE.4)GOTO 600
C     IOF=IDF(I)+1
C     R(IOF)=A1(IOF)
C     R(IOF+1)=A1(IOF+1)
C     R(IOF+2)=A1(IOF+2)
C     U1(IOF)=A1(IOF)
C     U1(IOF+1)=A1(IOF+1)
C     U1(IOF+2)=A1(IOF+2)
C 600 CONTINUE
C
C     FIX PREVIOUSLY SLIPING JOINTS
C
      IF(NEL1(5).LE.0)GOTO 700
      M=IS-1
      DO 690 I=1,NEL1(5)
      M=M+1
      IF(.NOT.SLIP(I))GOTO 690
      IOF1=IDF(IE(M,1))+1
      IOF2=IDF(IE(M,2))+3
      IOF3=IDF(IE(M,3))+1
      D=Y(IE(M,3))-Y(IE(M,1))
      V1(IOF2)=(V1(IOF1)-V1(IOF3))/D
      A1(IOF2)=(A1(IOF1)-A1(IOF3))/D
  690 CONTINUE
  700 CONTINUE
      WRITE(9,80) N1,TIME,U1(NX),U1(NX+1)
      IF(N1.NE.MAXSTP) GOTO 275
C
C     WRITE TO FILE FOR USE AS INITIAL VALUES
C
      WRITE(9,70) N1,TIME
      CALL OPUT(1)
      WRITE(4,30) (U1(I),I=1,NEQ)
      WRITE(4,30) (V1(I),I=1,NEQ)
      WRITE(4,30) (A1(I),I=1,NEQ)
  275 CONTINUE
C
C     PRINT OUT RESULTS
C
      IF(MP.NE.0) GOTO 280
      LL=LL+1
      WRITE(9,70) N1,TIME
      CALL OPUT(MSPAC)
      WRITE(9,95)
C
C     OUTPUT FORCES AND STRESSES
C
      IF(MSTRS.EQ.0) GOTO 280
      IF(KK.GT.NEED) GOTO 280
      IF(TIME.LT.TNED(KK,1)) GOTO 280
      IF(TIME.GE.TNED(KK,2)) KK=KK+1
      CALL ENDFOR(R,MAXDOF)
      IF(MSTRS.EQ.1) GOTO 280
      CALL FORCE(R,IE,MAXEL,MAXDOF,MAXNP,ULX,VLY,X,Y)
      CALL STRESS(P,IE,X,Y,ULX,VLY,MAXDOF,MAXEL,MAXNP,KODE)
  280 CONTINUE
   10 FORMAT(6I5)
   30 FORMAT(5E15.8)
   50 FORMAT(5F10.6,F10.7)
   60 FORMAT(6F10.4)
   70 FORMAT(//10X,'*** THE NUMBER OF STEP = ',I5,5X,'*** TIME =',F12.8,
     *//5X,4HNODE,15X,12HDISPLACEMENT,24X,8HVELOCITY,27X,12HACCELERATION
     *//)
   80 FORMAT(I10,3F25.8,2F10.2)
   90 FORMAT(I5,2F10.5)
   95 FORMAT(5X,'** END LINE ****',90(1H*)/)
 1000 FORMAT(3F10.4)
      RETURN
      END
      SUBROUTINE OPUT(MSPAC)
      IMPLICIT REAL*8 (A-H,O-Z)
C
C     PRINT DISPLACEMENT VELOCITY AND ACCELERATION
C
      COMMON/FRE/NT(700)
      COMMON/IDEP/IDF(700),NNP
      COMMON/OUT/U(1400),V(1400),A(1400)
      DO 40 J=1,NNP,MSPAC
      N=NNP+1-J
      I=IDF(N)+1
```

```
      K=NT(N)
      GOTO(10,20,20,30),K
   10 WRITE(9,100)N,U(I),U(I+1),V(I),V(I+1),A(I),A(I+1)
      GOTO40
   20 WRITE(9,200)N,U(I),U(I+1),U(I+2),V(I),V(I+1),V(I+2),A(I),A(I+1),A(
     CI+2)
      GOTO40
   30 WRITE(9,300)N,U(I),U(I+1),U(I+2),V(I),V(I+1),V(I+2),A(I),A(I+1),A(
     CI+2)
   40 CONTINUE
  100 FORMAT(1H ,I5,2X,3(2F12.5,12X))
  200 FORMAT(1H ,I5,2X,9F12.5)
  300 FORMAT(1H ,I5,2X,3(2F12.5,E12.3))
      RETURN
      END
      SUBROUTINE LOAD(AMS,P,AA,BB,CH,CV,NEQ,IBAND,TIME)
      IMPLICIT REAL*8 (A-H,O-Z)
C
C     CALCULATE EFFECTIVE LOAD [P   store in r()
C
      COMMON/THREE/P(1400),AK(1400,40)
      COMMON/DAMP/C1,C2,DT,NP
      COMMON/FRE/NT(700)
      COMMON/TEMP/IDF(700),NNP
      DIMENSION AMS(NEQ)
      DIMENSION AA(NEQ),BB(NEQ),CH(700),CV(700)
      DIMENSION P(3,350)
      DO 10 I=1,NEQ
   10 R(I)=0.0
      TAU=TIME
      K=1
      IF(NP.LE.1) GOTO 40
C
C     CALCULATION OF GROUND ACCELERATION
C
C     FIND POSITION IN ACCELERATION TIME-HISTORY
C
   20 IF(TAU.GE.P(1,K).AND.TAU.LT.P(1,K+1)) GOTO 30
      K=K+1
      IF(K.LT.NP) GOTO 20
C
C     DATA FINISHED     P(T+DT)=0.0
C
      GOTO 70
C
C     INTERPOLATION OF ACCELERATION DATA
C
   30 D=P(1,K+1)-P(1,K)
      DH=P(2,K+1)-P(2,K)
      DV=P(3,K+1)-P(3,K)
      T1=TAU-P(1,K)
      FH=P(2,K)+T1*DH/D
      FV=P(3,K)+T1*DV/D
      GOTO 50
C
C     SINE FORCING-AT-FREQUENCY-I-(1,1)
C
   40 CONTINUE
      FH=P(2,1)*SIN(2.0*3.1416*P(1,1)*TAU)
      FV=P(3,1)*SIN(2.0*3.1416*P(1,1)*TAU)
C
C     CALCULATE  P(T+DT)
C
   50 DO 60 N=1,NNP
      NN=IDF(N)+1
      R(NN)=CH(N)*FH
      R(NN+1)=CV(N)*FV
   60 CONTINUE
C                          *
C     IF TIME=0 THEN [P] = P(T+DT)     RETURN
C
   70 IF(TIME) 80,130,80
C
C     CALCULATE  P(T+DT)     -C1[B][A]
C                             C2[A]+[B]
C
   80 CONTINUE
      DO 90 I=1,NNP
      IF(NT(I).GT.2)GOTO 90
      M=IDF(I)+1
      N=M+1
      IF(NT(I).EQ.2)N=N+1
      DO 85 J=M,N
      R(J)=P(J)-C1*AMS(J)*AA(J)
   85 BB(J)=BB(J)+C2*AA(J)
   90 CONTINUE
C
C     P(T+DT)-C1[M][A]   -[K]     [C2[A]+[B]]
C
      REWIND 1
      READ (1) ((AK(I,J),J=1,IBAND),I=1,NEQ)
      DO120I=1,NEQ
      K=NEQ-I+1
      K=MIN0(K,IBAND)
      DO100J=1,K
      IJ=I+J-1
  100 R(I)=R(I)-AK(I,J)*BB(IJ)
      L=MIN0(I,IBAND)-1
      IF(L.LE.0)GOTO 120
      II=I
      DO110J=1,L
      II=II-1
  110 R(I)=R(I)-AK(II,J+1)*BB(II)
  120 CONTINUE
  130 RETURN
      END
      SUBROUTINE PHOE(N1,IS,NEL5)
      IMPLICIT REAL*8 (A-H,O-Z)
      COMMON/NODE/IE(600,5)
      COMMON/THREE/P(1400),AK(1400,40)
```

```
      COMMON/TEMP/IDF(700),NNP
      COMMON/OUT/U(1400),V(1400),A1(1400)
      DIMENSION EMOM(30)
      WRITE(10,1000)N1
      M=IS
      DO 10 I=1,NEL5
      IOF4=IDF(IE(M,4))+3
      EMOM(I)=R(IOF4)
      M=M+1
   10 CONTINUE
      WRITE(10,1010)(EMOM(I),I=1,NEL5)
      WRITE(10,1020)
      RETURN
 1000 FORMAT(6H STEP ,I4)
 1010 FORMAT(10(F10.2,1X))
 1020 FORMAT(/)
      END
```